JOURNAL OF RESEARCH of the National Bureau of Standards—A. Physics and Chemistry
Vol. 78A, No. 2, March–April 1974

Proposed Secondary Wavelength Standards and Line Classifications in Thorium Spectra Between 0.9 and 3 μm

A. Giacchetti,* J. Blaise, C. H. Corliss, and R. Zalubas**

Institute for Basic Standards, National Bureau of Standards, Washington, D.C. 20234

(December 19, 1973)

The spectrum of thorium as emitted by an electrodeless lamp has been recorded by Connes and collaborators by means of Fourier Transform Spectroscopy in the region 0.9 to 3 μm. Of the 3100 lines observed, about 1900 are classified as transitions in the energy level system of Th I and 412 in Th II. Since the average deviation between the observed and calculated wave numbers is less than 0.002 cm^{-1}, the observed wavelengths are suitable for use as standard wavelengths.

Key words: Classified lines of Th I and Th II; Fourier transform spectra of Th; infrared spectra of Th; spectra of Th; Th I and Th II; thorium spectra; wavelengths of Th.

1. Introduction

The spectra of Th I and Th II have been measured in the photographic range, 2000–12 000 Å, by Zalubas. Th I is being analysed by Zalubas [1968][1] and ThII by Zalubas and Corliss [1974]. Many thorium lines have also been interferometrically measured as suggested by Meggers [1957] and a list of 1556 secondary standard thorium wavelengths has been published by Giacchetti, Stanley, and Zalubas [1970].

Both Th I and Th II contain electron configurations of each parity that lie below 8000 cm^{-1} with respect to the ground level. For the precise determination of relative energy levels in such spectra it is useful to have accurate observations of infrared wavelengths. Furthermore, when the calculated secondary standard wavelengths for Th I were prepared by Giacchetti et al. [1970], the number of high-accuracy Th II lines was insufficient to obtain an extensive energy level array of high precision. Although there are other infrared observations of thorium lines, by Steers [1967] and by Bernage, Houdart, and Niay [1971], those in the present paper are more numerous and more accurate, since better spectroscopic means were available.

2. Observations

At the present time the most precise measurements of infrared wavelengths are carried out by means of the Fourier transformation of observations made with a variable spacing interferometer of a Michelson type as developed in recent years by Pierre and Janine Connes and their colleagues. Connes et al. [1970] have reported the observation of the spectrum from a thorium iodide electrodeless lamp in the region 0.9 to 3 μm. With the observation of 10^6 data points over a mirror displacement of one meter they attained a resolution of 0.02 cm^{-1}. The Fourier transformation of the data was traced on a plotter as a chart 80 m long. Portions of the spectrum are illustrated in the paper by Connes et al. [1970]. Inspection of the tracing in comparison with the computer printout of wave numbers permitted separation of the faintest real lines from the noise in the printout. An arbitrary logarithmic intensity scale of 0 to 9 was adopted with the strongest line at 8902 cm^{-1} set equal to 9 and the intensity numbers were read from the charts. No intensity standardization as a function of wavelength was attempted. The ghost intensities are about 1/1000 of the parent line but they are clearly asymmetrical and cannot be confused with real lines. They arise from periodic errors in the advance of the carriage of the moving mirror.

The reference wavelength was provided by a He-Xe laser line at 3.5 μm, sufficiently sharp to provide useful fringes over the whole range of travel of the moving carriage. The fringes provide control for the stepwise advancement of the carriage as well as the wavelength reference with respect to which the Th wave numbers are calculated from the results of the Fourier transformation.

The xenon reference wavelength is not accurately known and no correction for the dispersion of air was

*Argonne National Laboratory, Argonne, Ill. 60439, and Laboratorie Aimé Cotton, C.N.R.S., F-91405-Orsay, France. Present address: Dept. of Scientific Affairs, Organization of American States, Washington, D.C. 20006
**Laboratoire Aimé Cotton, C.N.R.S., F-91405—Orsay, France.

[1] Literature references are at the end of this paper.

made in the wave number calculations. In consequence we plotted (fig. 1) a correction curve with reference to internal standards of Th I lines whose wave numbers were calculated from the accurately known energy level values of Th I used by Giacchetti, Stanley and Zalubas [1970] in their calculation of the secondary-standard wavelengths below 1.2 μm. This converted the relative scale of wave numbers in air obtained from the Fourier transform calculation to an absolute scale of wave numbers in vacuum that is consistent with the secondary standards. The correction curve had the same amplitude and shape as a correction curve for the dispersion of air.

3. Classification of Lines

Analysis of Th I was begun by Schuurmans [1946] at Amsterdam and has been greatly extended by Zalubas [1968] at the National Bureau of Standards. The analysis of Th II was begun by McNally, Harrison, and Park [1942] at M.I.T. and independently by de Bruin, Schuurmans and Klinkenberg [1943, 1944] at Amsterdam and has been extended by Zalubas and Corliss [1974] and others. These analyses provide energy levels that classify most of the strong lines and many of the weaker lines emitted by electrodeless lamp discharges in thorium vapor.

To classify the Th I lines we searched our list for all possible transitions with $\Delta j = \pm 1, 0$. Many of the levels were known to three decimal places from Giacchetti, Stanley, and Zalubas [1970]; and most of the remainder were determined to three places with the aid of the present line list. Finally, 1907 lines were classified as Th I transitions by using all even levels below 33 100 cm^{-1}, all odd levels below 28 000 cm^{-1}, and a tolerance of ± 0.005 cm^{-1}. Levels above the given values were not used in order to reduce the number of mere chance coincidences of observed wave numbers with calculated level differences. Less than 5 percent of the lines classified as Th I differed from the calculated wave number by more than 0.003 cm^{-1}. The average value of O−C for Th I lines is 0.0016 cm^{-1}.

The levels of Zalubas and Corliss [1974] below 32 000 cm^{-1} were used to classify the Th II lines. The values of most of the levels were determined to three decimal places with the observed interferometric wave numbers. The lines were classified using a tolerance of ± 0.005 cm^{-1}. This procedure permitted classification of 412 lines of Th II, also with an average value of O−C of ± 0.0016 cm^{-1}. There remain 792 lines unclassified from the total of 3111 lines in the Fourier transform spectrum list.

4. Results and Their Relevance to Standard Wavelengths

The wavelengths in air, wave numbers in vacuum and intensities of 3111 infrared thorium lines are listed in table 1. For the classified lines the numerical values of the lower and upper energy levels with their J values are given, the decimal parts being omitted.

The average value of O−C given for Th II suggests that calculated standards for Th II would exceed the

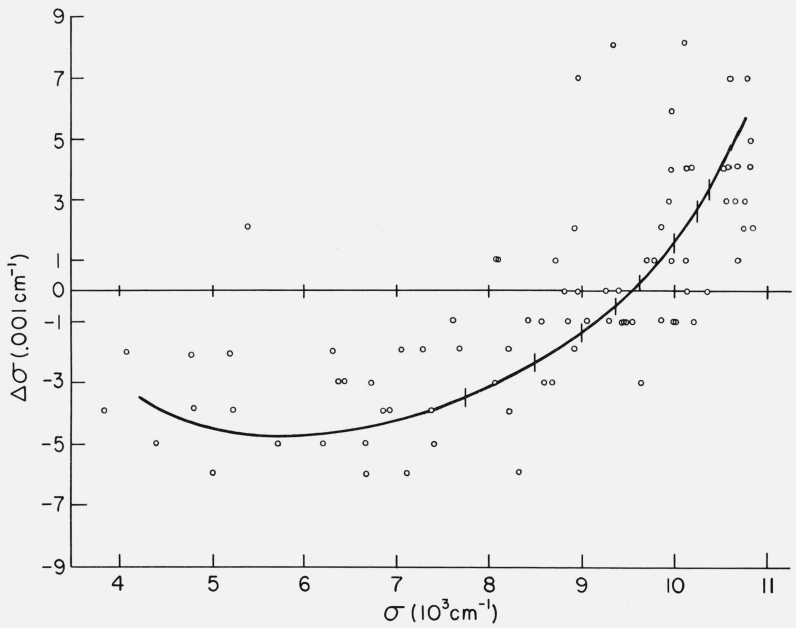

FIGURE 1. *Correction curve from relative wave numbers in air to absolute wave numbers in vacuum.*

accuracy criterion of 0.01 cm^{-1} suggested by Littlefield [1961] to Commission 14 of the I.A.U. for class B (secondary) standards. A report on this matter is now in preparation by Zalubas. Furthermore, the wavelengths in the present list themselves satisfy the criterion.

5. References

Bernage, P., Houdart, R., and Niay, P. [1971], Spectrochimica Acta **26B**, 261.

Connes, J., Delouis, H., Connes, P., Guelachvili, G., Maillard, J-P., and Michel, G. [1970], Nouv. Rev. d'Optique applique **1**, 3.

de Bruin, T. L., Schuurmans, P., and Klinkenberg, P. F. A. [1943], Z. Phys. **121**, 667.

de Bruin, T. L., Klinkenberg, P. F. A., and Schuurmans, P. [1944], Z. Phys. **122**, 23.

Giacchetti, A., Stanley, R. W., and Zalubas, R. [1970], J. Opt. Soc. Am. **69**, 474.

Littlefield, T. A. [1961], Trans. I.A.U. **11B**, 211.

McNally, J. R., Harrison, G. R., and Park, H. B., [1942], J. Opt. Soc. Am. **32**, 334.

Meggers, W. F. [1957], Trans. I.A.U. **9**, 225.

Schuurmans, P. [1946], Dissertation, Univ. Amsterdam (N.V. Noord-Hollandsche Uitgevers Maatschappij, Amsterdam).

Steers, E. B. M. [1967], Spectrochimica Acta **23B**, 135.

Zalubas, R. [1968], J. Opt. Soc. Am. **58**, 1195.

Zalubas, R., and Corliss, C. H. [1974], J. Res. Nat. Bur. Stand. (U.S.), **78A** (Phys. and Chem.) No. 2, p. 163.

(Paper 78A2–812)

TABLE 1. *Infrared spectral lines of thorium*

Wavelength Å	Wavenumber cm^{-1}	Intensity	Spectrum	Classification	Wavelength Å	Wavenumber cm^{-1}	Intensity	Spectrum	Classification
29662.822	3370.304	0	I	$9804_5 - 13175^0_4$	24007.982	4164.145	4	I	$6362_2 - 10526^0_3$
29068.481	3439.214	1	II	$10379_{4\frac{1}{2}} - 13818^0_{3\frac{1}{2}}$	23964.262	4171.742	3	II	$16818_{3\frac{1}{2}} - 20989^0_{4\frac{1}{2}}$
28574.421	3498.679	0	I	$12847_3 - 16346^0_4$	23940.033	4175.964	0	I	$24182^0_2 - 28358_3$
28477.471	3510.590	0			23907.149	4181.708	1	I	$17959_4 - 22141^0_3$
26734.663	3739.442	0	I	$7502_3 - 11241^0_3$	23865.994	4188.919	0	I	$22855^0_3 - 27044_3$
26377.115	3790.131	2	I	$10414^0_4 - 14204_5$	23850.490	4191.642	2	II	$8378^0_{3\frac{1}{2}} - 12570_{3\frac{1}{2}}$
25984.374	3847.417	1	I	$18549_2 - 22396^0_1$	23781.839	4203.742	4	I	$13297_4 - 17501^0_5$
25971.332	3849.349	0	I	$14204_5 - 18053^0_4$	23745.817	4210.119	1	II	$13250_{2\frac{1}{2}} - 17460^0_{2\frac{1}{2}}$
25913.673	3857.914	0	I	$23113^0_4 - 26971_4$	23742.146	4210.770	4	II	$6168^0_{3\frac{1}{2}} - 10379_{4\frac{1}{2}}$
25790.101	3876.399	1	I	$20522^0_2 - 24399_3$	23712.604	4216.016	0	I	$25336^0_6 - 29552_6$
25735.979	3884.551	1	I	$13962_1 - 17847^0_2$	23704.794	4217.405	1	I	$22163^0_4 - 26380_5$
25561.646	3911.044	1	I	$17166_5 - 21077^0_5$	23696.506	4218.880	1	II	$14349_{\frac{1}{2}} - 18568^0_{\frac{1}{2}}$
25401.710	3935.669	1	II	$10855_{3\frac{1}{2}} - 14790^0_{3\frac{1}{2}}$	23672.844	4223.097	1	I	$18809^0_4 - 23032_4$
25269.196	3956.308	1	I	$23015^0_5 - 26971_4$	23671.785	4223.286	1	I	$13175^0_4 - 17398_3$
25181.424	3970.098	1	II	$4490^0_{2\frac{1}{2}} - 8460_{1\frac{1}{2}}$	23663.487	4224.767	1	I	$14206^0_4 - 18431_3$
25111.575	3981.141	1	I	$22399^0_5 - 26380_5$	23621.480	4232.280	2	II	$4146_{3\frac{1}{2}} - 8378^0_{3\frac{1}{2}}$
25080.636	3986.052	2	I	$11877^0_1 - 15863_2$	23608.338	4234.636	0	I	$17411^0_3 - 21645_4$
25049.573	3990.995	2	I	$13175^0_4 - 17166_5$	23597.934	4236.503	1	II	$18118_{1\frac{1}{2}} - 22355^0_{1\frac{1}{2}}$
25032.462	3993.723	0	I	$25690^0_5 - 29684_5$	23588.463	4238.204	1	I	$18431_3 - 22669^0_3$
25000.730	3998.792	0			23551.636	4244.831	1	I	$15970_3 - 20214^0_3$
24997.523	3999.305	1	I	$13847_2 - 17847^0_2$	23514.732	4251.493	5	I	$11241^0_3 - 15493_4$
24973.732	4003.115	1	I	$26723^0_6 - 30726_7$	23504.277	4253.384	0		
24931.344	4009.921	1	I	$15493_4 - 19503^0_3$	23484.229	4257.015	1		
24926.551	4010.692	3	II	$9238^0_{4\frac{1}{2}} - 13248_{4\frac{1}{2}}$	23477.705	4258.198	0	I	$24421^0_3 - 28679_2$
24902.355	4014.589	1	I	$13945^0_3 - 17959_4$	23477.236	4258.283	1	II	$13468^0_{4\frac{1}{2}} - 17727_{5\frac{1}{2}}$
24887.997	4016.905	2	II	$14101^0_{\frac{1}{2}} - 18118_{1\frac{1}{2}}$	23458.743	4261.640	0	II	$20120^0_{2\frac{1}{2}} - 24381_{3\frac{1}{2}}$
24810.069	4029.522	0			23437.525	4265.498	5	II	$4113_{2\frac{1}{2}} - 8378^0_{3\frac{1}{2}}$
24789.343	4032.891	1	I	$21890^0_3 - 25923_4$	23403.546	4271.691	0	I	$18930^0_3 - 23201_3$
24684.317	4050.050	0	I	$19227^0_6 - 23277_5$	23381.575	4275.705	0		
24516.271	4077.811	1	I	$23113^0_4 - 27191_5$	23372.954	4277.282	0	II	$20969^0_{3\frac{1}{2}} - 25246_{4\frac{1}{2}}$
24486.763	4082.725	0	I	$24259^0_4 - 28342_5$	23330.692	4285.030	2	I	$26645^0_5 - 30930_6$
24470.262	4085.478	0	I	$23481^0_1 - 27566_2$	23316.550	4287.629	1	II	$17727_{5\frac{1}{2}} - 22014^0_{5\frac{1}{2}}$
24439.138	4090.681	1			23314.380	4288.028	1	I	$22508^0_2 - 26796_3$
24428.586	4092.448	1	I	$22163^0_4 - 26255_4$	23297.038	4291.220	0	I	$24850^0_6 - 29141_5$
24420.077	4093.874	1	I	$22877^0_5 - 26971_4$	23270.076	4296.192	2	I	$11197^0_5 - 15493_4$
24352.698	4105.201	0	II	$10379_{4\frac{1}{2}} - 14484^0_{5\frac{1}{2}}$	23222.202	4305.049	1	II	$20158_{2\frac{1}{2}} - 24463^0_{2\frac{1}{2}}$
24345.717	4106.378	0	II	$9711_{3\frac{1}{2}} - 13818^0_{3\frac{1}{2}}$	23217.661	4305.891	1	I	$18549_2 - 22855^0_3$
24329.294	4109.150	0	I	$25575^0_4 - 29684_5$	23175.469	4313.730	3	I	$16554_6 - 20867^0_7$
24301.853	4113.790	1	I	$13297_4 - 17411^0_3$	23153.597	4317.805	4	I	$15736^0_1 - 20054_2$
24291.248	4115.586	3	II	$4490^0_{2\frac{1}{2}} - 8605_{2\frac{1}{2}}$	23127.608	4322.657	1	I	$13088_3 - 17411^0_3$
24262.390	4120.481	1	I	$18549_2 - 22669^0_3$	23121.211	4323.853	0	I	$25690^0_5 - 30014_4$
24216.068	4128.363	0	I	$21575_2 - 25703^0_2$	23085.081	4330.620	0	I	$14243^0_1 - 18574_1$
24214.789	4128.581	1			23075.703	4332.380	2	II	$12485^0_{3\frac{1}{2}} - 16818_{3\frac{1}{2}}$
24185.996	4133.496	0			23007.044	4345.309	1	I	$27948^0_4 - 32293_5$
24172.879	4135.739	2	I	$13088_3 - 17224^0_2$	23003.968	4345.890	2	II	$12472^0_{2\frac{1}{2}} - 16818_{3\frac{1}{2}}$
24171.733	4135.935	0	I	$11601_1 - 15736^0_1$	22978.346	4350.736	0	I	$17224^0_2 - 21575_2$
24138.665	4141.601	0	I	$24421^0_3 - 28562_4$	22964.759	4353.310	1	I	$21902^0_4 - 26255_4$
24136.264	4142.013	3	I	$20522^0_2 - 24664_3$	22959.448	4354.317	0		
24120.715	4144.683	1	I	$17501^0_5 - 21645_4$	22937.124	4358.555	2	II	$6213_{4\frac{1}{2}} - 10572^0_{4\frac{1}{2}}$
24060.000	4155.142	1	II	$6700^0_{4\frac{1}{2}} - 10855_{3\frac{1}{2}}$	22916.350	4362.506	0		

TABLE 1. *Infrared spectral lines of thorium*—Continued

Wavelength Å	Wavenumber cm^{-1}	Intensity	Spectrum	Classification	Wavelength Å	Wavenumber cm^{-1}	Intensity	Spectrum	Classification
22911.403	4363.448	0	II	$24982^{\circ}_{3\,1/2} - 29345_{2\,1/2}$	22103.641	4522.907	4	I	$16554_{6} - 21077^{\circ}_{5}$
22900.906	4365.448	2	I	$21890^{\circ}_{3} - 26255_{4}$	22098.511	4523.957	0	II	$15786_{2\,1/2} - 20310^{\circ}_{2\,1/2}$
22900.565	4365.513	0	I	$15166^{\circ}_{3} - 19532_{4}$	22082.481	4527.241	1	I	$25321^{\circ}_{3} - 29849_{4}$
22875.089	4370.375	0	I	$17224^{\circ}_{2} - 21594_{3}$	22073.514	4529.080	1	I	$19503^{\circ}_{3} - 24032_{4}$
22864.133	4372.469	2	I	$25180^{\circ}_{7} - 29552_{6}$	22029.034	4538.225	0	I	$21575_{2} - 26113^{\circ}_{2}$
22860.040	4373.252	0	I	$24561^{\circ}_{3} - 28934_{3}$	21990.719	4546.132	2	I	$15166^{\circ}_{3} - 19713_{3}$
22855.180	4374.182	2	I	$18614^{\circ}_{1} - 22988_{2}$	21987.769	4546.742	0	I	$19713_{3} - 24259^{\circ}_{4}$
22851.632	4374.861	3	I	$8800_{4} - 13175^{\circ}_{4}$				I	$26882^{\circ}_{0} - 31429_{1}$
22843.962	4376.330	1	I	$12847_{3} - 17224^{\circ}_{2}$	21986.275	4547.051	0	I	$21143_{5} - 25690^{\circ}_{5}$
22834.596	4378.125	2	I	$3865_{1} - 8243^{\circ}_{2}$	21978.488	4548.662	1		
22829.522	4379.098	2	I	$17959_{4} - 22338^{\circ}_{3}$	21973.106	4549.776	2		
22806.940	4383.434	0	I	$21539^{\circ}_{4} - 25923_{4}$	21959.399	4552.616	1	I	$15970_{3} - 20522^{\circ}_{2}$
22785.721	4387.516	1	I	$14226_{0} - 18614^{\circ}_{1}$	21952.080	4554.134	1	I	$17847^{\circ}_{2} - 22401_{1}$
22785.383	4387.581	1	II	$10855_{3\,1/2} - 15242^{\circ}_{4\,1/2}$	21944.958	4555.612	4	I	$3687_{2} - 8243^{\circ}_{2}$
22760.862	4392.308	0	I	$20522^{\circ}_{2} - 24915_{3}$	21925.759	4559.601	2	I	$15863_{2} - 20423^{\circ}_{1}$
22750.249	4394.357	1	I	$18699_{2} - 23093^{\circ}_{2}$	21907.002	4563.505	1	II	$10673^{\circ}_{2\,1/2} - 15236_{1\,1/2}$
22733.218	4397.649	0	II	$27526_{4\,1/2} - 31924^{\circ}_{5\,1/2}$	21906.445	4563.621	1	II	$9711_{3\,1/2} - 14275^{\circ}_{4\,1/2}$
22723.153	4399.597	0	I	$14032^{\circ}_{2} - 18431_{3}$	21883.548	4568.396	0	I	$18069^{\circ}_{3} - 22637_{3}$
22710.196	4402.107	3	I	$9804_{5} - 14206^{\circ}_{4}$	21871.813	4570.847	1	II	$4490^{\circ}_{2\,1/2} - 9061_{2\,1/2}$
22646.195	4414.548	3	I	$11802_{2} - 16217^{\circ}_{2}$	21862.515	4572.791	1	I	$23655^{\circ}_{4} - 28227_{4}$
22641.743	4415.416	0			21852.069	4574.977	2	II	$7001_{1\,1/2} - 11576^{\circ}_{1\,1/2}$
22631.728	4417.370	0	II	$9400_{2\,1/2} - 13818^{\circ}_{3\,1/2}$	21830.625	4579.471	1		
22616.700	4420.305	1	I	$13962_{1} - 18382^{\circ}_{0}$	21809.793	4583.845	0	I	$18053^{\circ}_{4} - 22637_{3}$
22614.383	4420.758	4	I	$6362_{2} - 10783^{\circ}_{2}$	21765.236	4593.229	0		
22582.257	4427.047	1	II	$15453^{\circ}_{3\,1/2} - 19880_{4\,1/2}$	21756.165	4595.144	1	I	$17073_{1} - 21668^{\circ}_{1}$
22571.571	4429.143	1	II	$19880_{4\,1/2} - 24309^{\circ}_{5\,1/2}$	21749.619	4596.527	1	I	$15970_{3} - 20566^{\circ}_{4}$
22544.420	4434.477	1	I	$25321^{\circ}_{3} - 29756_{4}$	21747.329	4597.011	1	I	$17501^{\circ}_{5} - 22098_{4}$
22537.763	4435.787	3	I	$15618^{\circ}_{3} - 20054_{2}$	21743.999	4597.715	5	II	$10855_{3\,1/2} - 15453^{\circ}_{3\,1/2}$
22518.913	4439.500	0	I	$17959_{4} - 22399^{\circ}_{5}$	21743.999	4597.715	5	I	$7280_{2} - 11877^{\circ}_{1}$
22513.933	4440.482	1	I	$24701^{\circ}_{5} - 29141_{5}$	21712.571	4604.370	4	I	$8243^{\circ}_{2} - 12847_{3}$
22506.128	4442.022	4	II	$8460_{1\,1/2} - 12902^{\circ}_{1\,1/2}$	21706.674	4605.621	1	I	$14204_{5} - 18809^{\circ}_{4}$
22496.819	4443.860	2	I	$19588^{\circ}_{5} - 24032_{4}$	21706.264	4605.708	1	I	$23752^{\circ}_{2} - 28358_{3}$
22467.732	4449.613	1	II	$15144^{\circ}_{1\,1/2} - 19594_{1/2}$	21683.632	4610.515	0	I	$21143_{5} - 25753^{\circ}_{5}$
22446.273	4453.867	0	I	$21594_{3} - 26048^{\circ}_{4}$	21676.298	4612.075	0	I	$7502_{3} - 12114^{\circ}_{2}$
22445.678	4453.985	2	II	$8018_{1\,1/2} - 12472^{\circ}_{2\,1/2}$	21662.376	4615.039	0	II	$22642^{\circ}_{4\,1/2} - 27257_{3\,1/2}$
22439.688	4455.174	0	I	$15493_{4} - 19948^{\circ}_{4}$	21655.755	4616.450	2	I	$11601_{1} - 16217^{\circ}_{2}$
22437.386	4455.631	1	I	$14243^{\circ}_{1} - 18699_{2}$	21637.288	4620.390	2		
22412.467	4460.585	0			21628.998	4622.161	4	I	$11241^{\circ}_{3} - 15863_{2}$
22377.781	4467.499	1	I	$18809^{\circ}_{4} - 23277_{5}$	21605.654	4627.155	1	I	$24307^{\circ}_{2} - 28934_{3}$
22369.419	4469.169	1			21599.082	4628.563	1	I	$22637_{3} - 27266^{\circ}_{4}$
22350.905	4472.871	0	I	$23093^{\circ}_{2} - 27566_{2}$	21580.898	4632.463	0	I	$22338^{\circ}_{3} - 26971_{4}$
22344.755	4474.102	2	I	$11877^{\circ}_{1} - 16351_{0}$	21558.955	4637.178	2	II	$15242^{\circ}_{4\,1/2} - 19880_{4\,1/2}$
22343.861	4474.281	3	II	$13248_{4\,1/2} - 17722^{\circ}_{4\,1/2}$	21556.115	4637.789	0	I	$21252^{\circ}_{2} - 25890_{2}$
22323.993	4478.263	0	I	$21902^{\circ}_{4} - 26380_{5}$	21527.563	4643.940	0	I	$22877^{\circ}_{5} - 27521_{4}$
22318.327	4479.400	1	I	$19273_{2} - 23752^{\circ}_{2}$	21519.111	4645.764	0	I	$23916^{\circ}_{4} - 28562_{4}$
22283.623	4486.376	0	I	$13945^{\circ}_{3} - 18431_{3}$	21472.877	4655.767	1	I	$25355^{\circ}_{4} - 30011_{3}$
22264.353	4490.259	6	II	$0_{1\,1/2} - 4490^{\circ}_{2\,1/2}$	21442.806	4662.296	1	I	$18431_{3} - 23093^{\circ}_{2}$
22215.926	4500.047	1	I	$18549_{2} - 23049^{\circ}_{1}$	21424.751	4666.225	0	I	$22855^{\circ}_{3} - 27521_{4}$
22135.320	4516.434	0			21418.725	4667.538	0	I	$14032^{\circ}_{2} - 18699_{2}$
22115.259	4520.531	0	I	$23752^{\circ}_{2} - 28273_{2}$	21415.242	4668.297	2	I	$19713_{3} - 24381^{\circ}_{2}$

530-326 OL - 74 - 11

TABLE 1. *Infrared spectral lines of thorium*—Continued

Wavelength Å	Wavenumber cm^{-1}	Intensity	Spectrum	Classification	Wavelength Å	Wavenumber cm^{-1}	Intensity	Spectrum	Classification
21408.148	4669.844	0			20863.115	4791.840	0	I	$23481^{\circ}_{4} - 28273_{2}$
21406.777	4670.143	1	I	$19532_{4} - 24202^{\circ}_{4}$	20862.579	4791.963	2	I	$22399^{\circ}_{5} - 27191_{5}$
21387.561	4674.339	1	II	$24757^{\circ}_{4\frac{1}{2}} - 29431_{3\frac{1}{2}}$	20833.885	4798.563	1	I	$25753^{\circ}_{5} - 30552_{4}$
21375.118	4677.060	3	I	$9804_{5} - 14481^{\circ}_{6}$	20792.737	4808.059	1	I	$14465^{\circ}_{2} - 19273_{2}$
21358.737	4680.647	1			20735.100	4821.424	0	I	$18699_{2} - 23521^{\circ}_{3}$
21353.185	4681.864	3	I	$18431_{3} - 23113^{\circ}_{4}$	20730.370	4822.524	0		
21329.914	4686.972	1	II	$6168^{\circ}_{3\frac{1}{2}} - 10855_{3\frac{1}{2}}$	20717.817	4825.446	0	I	$20054_{2} - 24880^{\circ}_{1}$
21328.149	4687.360	0	I	$23655^{\circ}_{4} - 28342_{5}$	20716.744	4825.696	2	I	$22669^{\circ}_{3} - 27495_{4}$
21319.166	4689.335	1	I	$22877^{\circ}_{1} - 27566_{2}$	20715.963	4825.878	0	I	$25306^{\circ}_{2} - 30132_{2}$
21280.628	4697.827	1			20702.372	4829.046	0	I	$15493_{4} - 20322^{\circ}_{5}$
21264.265	4701.442	0	II	$14349_{\frac{1}{2}} - 19050^{\circ}_{1\frac{1}{2}}$	20692.063	4831.452	6	II	$1859_{1\frac{1}{2}} - 6691^{\circ}_{1\frac{1}{2}}$
21262.841	4701.757	1	II	$12570_{3\frac{1}{2}} - 17272^{\circ}_{4\frac{1}{2}}$	20682.889	4833.595	4	II	$9711_{3\frac{1}{2}} - 14545^{\circ}_{2\frac{1}{2}}$
21260.824	4702.203	0	I	$24850^{\circ}_{6} - 29552_{6}$	20681.631	4833.889	0	I	$24850^{\circ}_{6} - 29684_{5}$
21256.077	4703.253	0	I	$23655^{\circ}_{4} - 28358_{3}$	20680.125	4834.241	4	I	$7280_{2} - 12114^{\circ}_{2}$
21250.077	4704.581	0	I	$25306^{\circ}_{2} - 30011_{3}$	20674.386	4835.583	1		
21247.182	4705.222	0	I	$22338^{\circ}_{3} - 27044_{3}$	20661.764	4838.537	1	I	$20566^{\circ}_{4} - 25405_{4}$
21239.694	4706.881	1	I	$23521^{\circ}_{3} - 28227_{4}$	20651.478	4840.947	0	I	$21539^{\circ}_{4} - 26380_{5}$
21205.593	4714.450	0			20649.114	4841.501	1	II	$22685^{\circ}_{3\frac{1}{2}} - 27526_{4\frac{1}{2}}$
21203.367	4714.945	0	I	$20054_{2} - 24769^{\circ}_{3}$	20634.364	4844.962	6	I	$8243^{\circ}_{2} - 13088_{3}$
21199.298	4715.850	0			20618.818	4848.615	0	I	$19713_{3} - 24561^{\circ}_{3}$
21198.664	4715.991	0	I	$21539^{\circ}_{4} - 26255_{4}$	20610.588	4850.551	1	I	$17398_{3} - 22248^{\circ}_{2}$
21173.002	4721.707	1	I	$15493_{4} - 20214^{\circ}_{3}$	20609.747	4850.749	1	II	$17983^{\circ}_{2\frac{1}{2}} - 22834_{3\frac{1}{2}}$
21162.697	4724.006	5	II	$7001_{1\frac{1}{2}} - 11725^{\circ}_{\frac{1}{2}}$	20605.987	4851.634	2	I	$22669^{\circ}_{3} - 27521_{4}$
21148.510	4727.175	3	I	$23306^{\circ}_{6} - 28034_{5}$	20584.349	4856.734	0	I	$24561^{\circ}_{3} - 29418_{2}$
21143.170	4728.369	4	I	$11241^{\circ}_{3} - 15970_{3}$	20575.702	4858.775	0		
21132.654	4730.722	2	I	$19039^{\circ}_{2} - 23769_{1}$	20575.042	4858.931	0	I	$21252^{\circ}_{2} - 26111_{1}$
21123.018	4732.880	0	II	$13250_{2\frac{1}{2}} - 17983^{\circ}_{2\frac{1}{2}}$	20562.003	4862.012	0	I	$16783^{\circ}_{4} - 21645_{4}$
21121.474	4733.226	1	II	$10572^{\circ}_{4\frac{1}{2}} - 15305_{4\frac{1}{2}}$	20561.348	4862.167	2	I	$21645_{4} - 26508^{\circ}_{3}$
21117.677	4734.077	0	I	$21143_{5} - 25877^{\circ}_{4}$	20554.521	4863.782	3	II	$10379_{4\frac{1}{2}} - 15242^{\circ}_{4\frac{1}{2}}$
21108.367	4736.165	1	I	$17166_{5} - 21902^{\circ}_{4}$	20550.363	4864.766	1		
21095.446	4739.066	0	I	$15493_{4} - 20232^{\circ}_{4}$	20541.715	4866.814	1	I	$24274^{\circ}_{5} - 29141_{5}$
			I	$21645_{4} - 26384^{\circ}_{4}$	20528.880	4869.857	4	II	$8378^{\circ}_{3\frac{1}{2}} - 13248_{4\frac{1}{2}}$
21046.638	4750.056	0	II	$23187^{\circ}_{6\frac{1}{2}} - 27937_{5\frac{1}{2}}$	20521.311	4871.653	2	II	$8378^{\circ}_{3\frac{1}{2}} - 13250_{2\frac{1}{2}}$
21019.525	4756.183	2	I	$13297_{4} - 18053^{\circ}_{4}$	20513.976	4873.395	0	I	$15863_{2} - 20737^{\circ}_{1}$
21014.864	4757.238	2	II	$9061_{2\frac{1}{2}} - 13818^{\circ}_{3\frac{1}{2}}$	20489.032	4879.328	1	I	$6362_{2} - 11241^{\circ}_{3}$
21011.808	4757.930	2	I	$21165^{\circ}_{3} - 25923_{4}$	20478.858	4881.752	1	I	$24259^{\circ}_{4} - 29141_{5}$
21009.229	4758.514	1	I	$13088_{3} - 17847^{\circ}_{2}$	20468.653	4884.186	4	II	$8018_{1\frac{1}{2}} - 12902^{\circ}_{1\frac{1}{2}}$
20981.790	4764.737	0	I	$17398_{3} - 22163^{\circ}_{4}$	20468.318	4884.266	0		
20973.743	4766.565	1	I	$13847_{2} - 18614^{\circ}_{1}$	20453.217	4887.872	0	I	$15166^{\circ}_{3} - 20054_{2}$
20965.562	4768.425	1	I	$21594_{3} - 26363^{\circ}_{2}$	20450.627	4888.491	1	II	$7331^{\circ}_{2\frac{1}{2}} - 12219_{1\frac{1}{2}}$
20951.480	4771.630	1	I	$13297_{4} - 18069^{\circ}_{3}$	20450.008	4888.639	1	I	$19532_{4} - 24421^{\circ}_{3}$
20941.487	4773.907	0			20443.773	4890.130	2	II	$12570_{3\frac{1}{2}} - 17460^{\circ}_{2\frac{1}{2}}$
20936.496	4775.045	1			20430.283	4893.359	0	II	$18118_{1\frac{1}{2}} - 23012^{\circ}_{1\frac{1}{2}}$
20935.448	4775.284	0			20428.437	4893.801	1	I	$21902^{\circ}_{4} - 26796_{3}$
20934.926	4775.403	0	II	$15305_{4\frac{1}{2}} - 20080^{\circ}_{3\frac{1}{2}}$	20421.761	4895.401	3	I	$17959_{4} - 22855^{\circ}_{3}$
20920.513	4778.693	1	I	$26363^{\circ}_{2} - 31141_{3}$	20419.379	4895.972	0	I	$19503^{\circ}_{3} - 24399_{3}$
20895.196	4784.483	0			20395.738	4901.647	3	II	$12219_{1\frac{1}{2}} - 17121^{\circ}_{1\frac{1}{2}}$
20893.881	4784.784	0	I	$13175^{\circ}_{4} - 17959_{4}$	20392.064	4902.530	0	I	$26363^{\circ}_{2} - 31265_{3}$
20879.577	4788.062	1	I	$21575_{2} - 26363^{\circ}_{2}$	20391.719	4902.613	0	I	$22141^{\circ}_{3} - 27044_{3}$
20869.452	4790.385	4	I	$17847^{\circ}_{2} - 22637_{3}$	20389.710	4903.096	4	II	$6213_{4\frac{1}{2}} - 11116^{\circ}_{3\frac{1}{2}}$

TABLE 1. *Infrared spectral lines of thorium*—Continued

Wavelength Å	Wavenumber cm^{-1}	Intensity	Spectrum	Classification	Wavelength Å	Wavenumber cm^{-1}	Intensity	Spectrum	Classification
20381.309	4905.117	3	I	$21143_5 - 26048^{\circ}_4$	19768.543	5057.161	0		
20377.894	4905.939	1	I	$21890^{\circ}_3 - 26796_3$	19765.178	5058.022	3	I	$21738^{\circ}_2 - 26796_3$
20374.476	4906.762	1	I	$18574_1 - 23481^{\circ}_1$	19764.361	5058.231	0	I	$15863_2 - 20922^{\circ}_2$
20358.092	4910.711	0	II	$4490^{\circ}_{2\frac{1}{2}} - 9400_{2\frac{1}{2}}$	19762.115	5058.806	0	I	$22508^{\circ}_2 - 27566_2$
20321.907	4919.455	0	I	$18069^{\circ}_3 - 22988_2$	19758.662	5059.690	1		
20317.777	4920.455	4	I	$23113^{\circ}_4 - 28034_5$	19757.006	5060.114	0	I	$18930^{\circ}_3 - 23990_2$
20292.710	4926.533	0			19741.428	5064.107	5	I	$8111_4 - 13175^{\circ}_4$
20264.464	4933.400	0			19736.666	5065.329	0	I	$24769^{\circ}_3 - 29835_3$
20263.141	4933.722	0	I	$26995^{\circ}_3 - 31929_3$	19733.467	5066.150	1	I	$26363^{\circ}_2 - 31429_1$
20234.945	4940.597	0	I	$17398_3 - 22338^{\circ}_3$	19721.637	5069.189	0	I	$21902^{\circ}_4 - 26971_4$
20205.662	4947.757	0	I	$25703^{\circ}_2 - 30651_3$	19719.303	5069.789	1	II	$25414^{\circ}_{5\frac{1}{2}} - 30484_{5\frac{1}{2}}$
20191.383	4951.256	3	I	$19039^{\circ}_2 - 23990_2$	19717.004	5070.380	0		
20183.242	4953.253	0	I	$27087^{\circ}_1 - 32041_2$	19705.256	5073.403	0	I	$15493_4 - 20566^{\circ}_4$
20165.057	4957.720	3			19703.648	5073.817	1	II	$7828_{1\frac{1}{2}} - 12902^{\circ}_{1\frac{1}{2}}$
20158.039	4959.446	2	I	$12114^{\circ}_2 - 17073_1$	19703.283	5073.911	1	II	$10379_{4\frac{1}{2}} - 15453^{\circ}_{3\frac{1}{2}}$
20139.866	4963.921	1	II	$13250_{2\frac{1}{2}} - 18214^{\circ}_{1\frac{1}{2}}$	19701.761	5074.303	0	II	$15236_{1\frac{1}{2}} - 20310^{\circ}_{2\frac{1}{2}}$
			I	$18069^{\circ}_3 - 23032_4$	19696.195	5075.737	1	I	$23603^{\circ}_2 - 28679_2$
20128.687	4966.678	3	I	$10526^{\circ}_3 - 15493_4$	19692.738	5076.628	1	I	$13962_1 - 19039^{\circ}_2$
20122.241	4968.269	0	I	$20922^{\circ}_2 - 25890_2$	19692.319	5076.736	0		
20118.722	4969.138	1			19683.409	5079.034	5	II	$9711_{3\frac{1}{2}} - 14790^{\circ}_{3\frac{1}{2}}$
20108.593	4971.641	2	I	$18549_2 - 23521^{\circ}_3$	19683.215	5079.084	4	I	$10414^{\circ}_4 - 15493_4$
20082.971	4977.984	1			19676.823	5080.734	1	I	$10783^{\circ}_2 - 15863_2$
20077.401	4979.365	2	I	$18053^{\circ}_4 - 23032_4$	19674.535	5081.325	3	I	$21890^{\circ}_3 - 26971_4$
20061.498	4983.312	0			19669.905	5082.521	2	I	$13847_2 - 18930^{\circ}_3$
20047.945	4986.681	2	I	$24769^{\circ}_3 - 29756_4$	19668.461	5082.894	4	I	$20322^{\circ}_5 - 25405_4$
20026.106	4992.119	2			19645.360	5088.871	1		
19998.121	4999.105	1	I	$12847_3 - 17847^{\circ}_2$	19644.523	5089.088	4	II	$14790^{\circ}_{3\frac{1}{2}} - 19880_{4\frac{1}{2}}$
19984.221	5002.582	0	II	$26770^{\circ}_{5\frac{1}{2}} - 31773_{4\frac{1}{2}}$	19643.457	5089.364	1	I	$18431_3 - 23521^{\circ}_3$
19935.599	5014.783	0	I	$27948^{\circ}_4 - 32963_5$	19639.120	5090.488	1	I	$21165^{\circ}_3 - 26255_4$
19922.803	5018.004	1	I	$23916^{\circ}_4 - 28934_3$	19626.624	5093.729	0		
19919.437	5018.852	0	I	$23015^{\circ}_5 - 28034_5$	19626.212	5093.836	1		
19908.520	5021.604	0	I	$18011^{\circ}_5 - 23032_4$	19622.548	5094.787	0	I	$22248^{\circ}_2 - 27343_3$
19902.706	5023.071	4	I	$14204_5 - 19227^{\circ}_6$	19617.154	5096.188	2	I	$22399^{\circ}_5 - 27495_4$
19890.383	5026.183	2			19595.083	5101.928	3	I	$18930^{\circ}_3 - 24032_4$
19885.078	5027.524	0			19593.390	5102.369	0	II	$19880_{4\frac{1}{2}} - 24982^{\circ}_{3\frac{1}{2}}$
19882.301	5028.226	2	I	$22163^{\circ}_4 - 27191_5$	19586.250	5104.229	0	I	$22508^{\circ}_2 - 27612_3$
19862.586	5033.217	0	I	$24981^{\circ}_3 - 30014_4$	19571.602	5108.049	2	I	$19273_2 - 24381^{\circ}_2$
19857.666	5034.464	2	I	$19273_2 - 24307^{\circ}_2$	19561.688	5110.638	2	I	$24307^{\circ}_2 - 29418_2$
19852.906	5035.671	2	I	$23306^{\circ}_6 - 28342_5$	19540.414	5116.202	1	II	$10189^{\circ}_{5\frac{1}{2}} - 15305_{4\frac{1}{2}}$
19850.778	5036.211	1	I	$25336^{\circ}_6 - 30372_6$	19535.499	5117.489	0	II	$22139^{\circ}_{4\frac{1}{2}} - 27257_{3\frac{1}{2}}$
19848.224	5036.859	0						I	$26878^{\circ}_3 - 31995_4$
19847.455	5037.054	0	I	$24381^{\circ}_2 - 29418_2$	19528.833	5119.236	0		
19844.520	5037.799	0	II	$25414^{\circ}_{5\frac{1}{2}} - 30452_{4\frac{1}{2}}$	19519.076	5121.795	0	I	$27674^{\circ}_2 - 32796_3$
19840.952	5038.705	1			19505.411	5125.383	0	I	$22855^{\circ}_3 - 27980_3$
19829.520	5041.610	1	I	$23521^{\circ}_3 - 28562_4$	19503.105	5125.989	1	II	$23697^{\circ}_{3\frac{1}{2}} - 28823_{2\frac{1}{2}}$
19797.857	5049.673	0	I	$23481^{\circ}_1 - 28531_2$	19476.782	5132.917	1	I	$18069^{\circ}_3 - 23201_3$
19786.004	5052.698	5	I	$7795^{\circ}_4 - 12847_3$	19474.463	5133.528	2		
19784.595	5053.058	1	I	$18699_2 - 23752^{\circ}_2$	19473.652	5133.742	1		
19774.295	5055.690	6	II	$4146_{3\frac{1}{2}} - 9202^{\circ}_{3\frac{1}{2}}$	19449.859	5140.022	0		
19770.799	5056.584	1	I	$24084^{\circ}_6 - 29141_5$	19444.483	5141.443	1	I	$17847^{\circ}_2 - 22988_2$

TABLE 1. *Infrared spectral lines of thorium*—Continued

Wavelength Å	Wavenumber cm^{-1}	Intensity	Spectrum	Classification	Wavelength Å	Wavenumber cm^{-1}	Intensity	Spectrum	Classification
19432.597	5144.588	3	II	$9400_{2\frac{1}{2}} - 14545^{\circ}_{2\frac{1}{2}}$	19082.536	5238.963	3	II	$12488^{\circ}_{4\frac{1}{2}} - 17727_{5\frac{1}{2}}$
19430.829	5145.056	2	I	$8800_4 - 13945^{\circ}_3$	19080.012	5239.656	1	I	$24182^{\circ}_2 - 29422_1$
19420.664	5147.749	1	I	$19516^{\circ}_2 - 24664_3$	19078.887	5239.965	1	I	$25690^{\circ}_5 - 30930_6$
19418.336	5148.366	1	I	$18053^{\circ}_4 - 23201_3$	19076.390	5240.651	0	II	$12219_{1\frac{1}{2}} - 17460^{\circ}_{2\frac{1}{2}}$
19402.768	5152.497	2	II	$12570_{3\frac{1}{2}} - 17722^{\circ}_{4\frac{1}{2}}$	19074.406	5241.196	3	I	$14032^{\circ}_2 - 19273_2$
19400.479	5153.105	3	I	$20737^{\circ}_1 - 25890_2$	19073.289	5241.503	2	I	$21143_5 - 26384^{\circ}_4$
19396.794	5154.084	2	I	$21890^{\circ}_3 - 27044_3$	19050.366	5247.810	0	I	$14465^{\circ}_2 - 19713_3$
19391.319	5155.539	1	I	$18614^{\circ}_1 - 23769_1$	19042.039	5250.105	0		
19388.002	5156.421	1	I	$22877^{\circ}_5 - 28034_5$	19035.208	5251.989	0	I	$20054_2 - 25306^{\circ}_2$
19353.457	5165.625	0	II	$20080^{\circ}_{3\frac{1}{2}} - 25246_{4\frac{1}{2}}$	19033.646	5252.420	1	I	$24880^{\circ}_1 - 30132_2$
19345.173	5167.837	0	I	$22098_4 - 27266^{\circ}_4$	19018.615	5256.571	2	I	$13175^{\circ}_4 - 18431_3$
19342.209	5168.629	2	I	$19532_4 - 24701^{\circ}_5$	18984.562	5266.000	0	I	$18011^{\circ}_5 - 23277_5$
19338.976	5169.493	7	II	$1521_{2\frac{1}{2}} - 6691^{\circ}_{1\frac{1}{2}}$	18964.790	5271.490	1	I	$17398_3 - 22669^{\circ}_3$
19336.983	5170.026	0	I	$22396^{\circ}_1 - 27566_2$	18961.873	5272.301	1	II	$25607^{\circ}_{4\frac{1}{2}} - 30879_{3\frac{1}{2}}$
19321.626	5174.135	0	I	$26363^{\circ}_2 - 31537_3$	18958.367	5273.276	1	I	$22338^{\circ}_3 - 27612_3$
19320.977	5174.309	1			18957.939	5273.395	0	I	$24561^{\circ}_3 - 29835_3$
19317.885	5175.137	3	I	$17073_1 - 22248^{\circ}_2$	18942.594	5277.667	0	I	$26651^{\circ}_2 - 31929_3$
19307.868	5177.822	2	II	$10855_{3\frac{1}{2}} - 16033^{\circ}_{2\frac{1}{2}}$	18942.109	5277.802	1	I	$24274^{\circ}_5 - 29552_6$
19291.493	5182.217	1	I	$23752^{\circ}_2 - 28934_3$	18938.047	5278.934	1	I	$23603^{\circ}_2 - 28882_2$
19290.328	5182.530	0	I	$22338^{\circ}_3 - 27521_4$	18931.513	5280.756	1		
19273.916	5186.943	2	I	$10783^{\circ}_2 - 15970_3$	18925.238	5282.507	0	I	$15970_3 - 21252^{\circ}_2$
19268.474	5188.408	0			18919.776	5284.032	2	I	$12114^{\circ}_2 - 17398_3$
19264.749	5189.411	1	I	$20922^{\circ}_2 - 26111_1$	18911.609	5286.314	0		
19261.710	5190.230	0	I	$20214^{\circ}_3 - 25405_4$	18907.334	5287.509	2	I	$24561^{\circ}_3 - 29849_4$
19261.001	5190.421	0	I	$23655^{\circ}_4 - 28845_4$	18905.486	5288.026	1		
19257.450	5191.378	0	I	$13847_2 - 19039^{\circ}_2$	18904.263	5288.368	0	I	$19273_2 - 24561^{\circ}_3$
19256.382	5191.666	1	I	$18549_2 - 23741^{\circ}_1$	18893.288	5291.440	0	I	$27260^{\circ}_3 - 32551_3$
19244.968	5194.745	0	I	$24561^{\circ}_3 - 29756_4$	18892.767	5291.586	0		
19244.035	5194.997	1	I	$15970_3 - 21165^{\circ}_3$	18886.685	5293.290	6	I	$7795^{\circ}_4 - 13088_3$
19241.246	5195.750	0	I	$21594_3 - 26790^{\circ}_4$	18885.747	5293.553	0		
19240.420	5195.973	0	I	$11877^{\circ}_1 - 17073_1$	18885.154	5293.719	1	I	$24838^{\circ}_1 - 30132_2$
19204.660	5205.648	1	I	$12847_3 - 18053^{\circ}_4$	18884.038	5294.032	0		
19190.670	5209.443	2	I	$27084^{\circ}_6 - 32293_5$	18880.700	5294.968	0	II	$22642^{\circ}_{4\frac{1}{2}} - 27937_{5\frac{1}{2}}$
19188.567	5210.014	0			18872.185	5297.357	1		
19188.114	5210.137	0			18865.586	5299.210	3	I	$16346^{\circ}_4 - 21645_4$
19179.419	5212.499	3	II	$8605_{2\frac{1}{2}} - 13818^{\circ}_{3\frac{1}{2}}$	18858.490	5301.204	1	I	$15863_2 - 21165^{\circ}_3$
19178.389	5212.779	2	I	$23015^{\circ}_5 - 28227_4$	18856.508	5301.761	0		
19165.340	5216.328	1	II	$12902^{\circ}_{1\frac{1}{2}} - 18118_{1\frac{1}{2}}$	18850.731	5303.386	2	I	$21077^{\circ}_5 - 26380_5$
19162.549	5217.088	1	I	$26048^{\circ}_4 - 31265_3$	18840.854	5306.166	0	I	$21738^{\circ}_2 - 27044_3$
19158.359	5218.229	0			18824.439	5310.793	0	I	$22669^{\circ}_3 - 27980_3$
19151.815	5220.012	4	I	$5563_1 - 10783^{\circ}_2$	18811.879	5314.339	7	I	$16783^{\circ}_4 - 22098_4$
19147.846	5221.094	3	I	$12847_3 - 18069^{\circ}_3$	18802.414	5317.014	3	I	$16351_0 - 21668^{\circ}_1$
19145.601	5221.706	7	II	$4490^{\circ}_{2\frac{1}{2}} - 9711_{3\frac{1}{2}}$	18799.282	5317.900	0	I	$22248^{\circ}_2 - 27566_2$
19143.281	5222.339	1	I	$18809^{\circ}_4 - 24032_4$	18788.340	5320.997	0	I	$18431_3 - 23752^{\circ}_2$
19138.077	5223.759	1	I	$18053^{\circ}_4 - 23277_5$	18781.224	5323.013	1	I	$17073_1 - 22396^{\circ}_1$
			I	$23049^{\circ}_1 - 28273_2$	18772.446	5325.502	3	I	$14206^{\circ}_4 - 19532_4$
19113.116	5230.581	2	I	$25321^{\circ}_3 - 30552_4$	18763.740	5327.973	0	I	$13945^{\circ}_3 - 19273_2$
19108.517	5231.840	0			18737.838	5335.338	0	I	$24421^{\circ}_3 - 29756_4$
19091.898	5236.394	0	I	$23609^{\circ}_5 - 28845_4$	18730.785	5337.347	2	I	$10526^{\circ}_3 - 15863_2$
19088.610	5237.296	3	I	$19532_4 - 24769^{\circ}_3$	18689.399	5349.166	0	I	$16554_6 - 21903^{\circ}_7$

TABLE 1. *Infrared spectral lines of thorium* — Continued

Wavelength Å	Wavenumber cm^{-1}	Intensity	Spectrum	Classification	Wavelength Å	Wavenumber cm^{-1}	Intensity	Spectrum	Classification
18685.648	5350.240	0	I	$26645^{\circ}_{5} - 31995_{4}$	18228.371	5484.456	4	II	$9061_{2\frac{1}{2}} - 14545^{\circ}_{2\frac{1}{2}}$
18685.274	5350.347	1	I	$22877^{\circ}_{5} - 28227_{4}$	18225.855	5485.213	1	I	$18431_{3} - 23916^{\circ}_{4}$
18682.627	5351.105	0			18221.955	5486.387	1	I	$23655^{\circ}_{4} - 29141_{5}$
18664.162	5356.399	2	I	$20566^{\circ}_{4} - 25923_{4}$	18209.323	5490.193	0	I	$27061^{\circ}_{2} - 32551_{3}$
18663.748	5356.518	0			18192.490	5495.273	0		
18657.231	5358.389	2	I	$22163^{\circ}_{4} - 27521_{4}$	18174.187	5500.807	0		
18651.748	5359.964	0	I	$19039^{\circ}_{2} - 24399_{3}$	18173.926	5500.886	1	I	$26036^{\circ}_{3} - 31537_{3}$
18625.408	5367.544	0	I	$26645^{\circ}_{5} - 32012_{4}$	18170.303	5501.983	1	I	$21143_{5} - 26645^{\circ}_{5}$
18624.701	5367.748	0	II	$14790^{\circ}_{3\frac{1}{2}} - 20158_{2\frac{1}{2}}$	18169.715	5502.161	1	I	$7795^{\circ}_{4} - 13297_{4}$
18595.874	5376.069	3	I	$18614^{\circ}_{1} - 23990_{2}$	18166.638	5503.093	1	I	$22855^{\circ}_{3} - 28358_{3}$
18568.136	5384.100	1			18161.579	5504.626	2	I	$21539^{\circ}_{4} - 27044_{3}$
18557.981	5387.046	3	I	$18382^{\circ}_{0} - 23769_{1}$	18156.664	5506.116	0	I	$14206^{\circ}_{4} - 19713_{3}$
18557.117	5387.297	1			18141.007	5510.868	0		
18547.718	5390.027	3	II	$9400_{2\frac{1}{2}} - 14790^{\circ}_{3\frac{1}{2}}$	18135.791	5512.453	1	I	$13297_{4} - 18809^{\circ}_{4}$
18546.830	5390.285	1	I	$25336^{\circ}_{6} - 30726_{7}$	18125.969	5515.440	5	I	$6362_{2} - 11877^{\circ}_{1}$
18531.218	5394.826	1			18119.136	5517.520	1		
18520.188	5398.039	0	I	$19516^{\circ}_{2} - 24915_{3}$	18112.220	5519.627	1		
18509.757	5401.081	1	I	$23481^{\circ}_{1} - 28882_{2}$	18111.639	5519.804	0		
18490.644	5406.664	4	I	$8800_{4} - 14206^{\circ}_{4}$	18103.118	5522.402	2	I	$24850^{\circ}_{6} - 30372_{6}$
18469.362	5412.894	1	II	$12570_{3\frac{1}{2}} - 17983^{\circ}_{2\frac{1}{2}}$	18087.083	5527.298	2	I	$24307^{\circ}_{2} - 29835_{3}$
18468.454	5413.160	3	I	$17224^{\circ}_{2} - 22637_{3}$	18082.856	5528.590	4	II	$6691^{\circ}_{1\frac{1}{2}} - 12219_{1\frac{1}{2}}$
18452.242	5417.916	0	I	$22855^{\circ}_{3} - 28273_{2}$	18075.163	5530.943	1	II	$9711_{3\frac{1}{2}} - 15242^{\circ}_{4\frac{1}{2}}$
18440.493	5421.368	4	I	$11802_{2} - 17224^{\circ}_{2}$	18072.340	5531.807	4	I	$17501^{\circ}_{5} - 23032_{4}$
18427.858	5425.085	0	I	$27674^{\circ}_{2} - 33099_{3}$	18070.540	5532.358	1	I	$23609^{\circ}_{5} - 29141_{5}$
18402.093	5432.681	0			18060.792	5535.344	1		
18396.840	5434.232	0	I	$17073_{1} - 22508^{\circ}_{2}$	18049.109	5538.927	0		
18381.291	5438.829	3	II	$4146_{3\frac{1}{2}} - 9585^{\circ}_{2\frac{1}{2}}$	18034.646	5543.369	0		
18380.568	5439.043	0			18029.644	5544.907	2		
18353.121	5447.177	0			18025.092	5546.307	2		
18348.035	5448.687	1	I	$19532_{4} - 24981^{\circ}_{3}$	18023.692	5546.738	1	I	$25180^{\circ}_{7} - 30726_{7}$
18339.435	5451.242	0	I	$25306^{\circ}_{2} - 30758_{2}$	18007.579	5551.701	2	I	$11802_{2} - 17354^{\circ}_{1}$
18335.284	5452.476	2	I	$4961_{4} - 10414^{\circ}_{4}$	18000.660	5553.835	1	I	$24202^{\circ}_{4} - 29756_{4}$
18334.595	5452.681	0	I	$24561^{\circ}_{3} - 30014_{4}$	17993.769	5555.962	3	I	$10414^{\circ}_{4} - 15970_{3}$
18331.495	5453.603	1	I	$21890^{\circ}_{3} - 27343_{3}$	17991.742	5556.588	0	I	$26645^{\circ}_{5} - 32202_{5}$
18331.136	5453.710	0	I	$24381^{\circ}_{2} - 29835_{3}$	17987.035	5558.042	1	I	$22669^{\circ}_{3} - 28227_{4}$
18320.410	5456.903	0	I	$17398_{3} - 22855^{\circ}_{3}$	17976.979	5561.151	4	I	$17959_{4} - 23521^{\circ}_{3}$
18301.976	5462.399	1	I	$26995^{\circ}_{3} - 32458_{4}$	17969.554	5563.449	0	I	$24981^{\circ}_{3} - 30544_{2}$
18293.755	5464.854	1	II	$21297^{\circ}_{2\frac{1}{2}} - 26762_{1\frac{1}{2}}$	17964.920	5564.884	6	I	$4961_{4} - 10526^{\circ}_{3}$
18293.550	5464.915	1	I	$22877^{\circ}_{5} - 28342_{5}$	17962.477	5565.641	0	I	$19273_{2} - 24838^{\circ}_{1}$
18286.901	5466.902	1	I	$20423^{\circ}_{1} - 25890_{2}$	17960.037	5566.397	0	I	$26363^{\circ}_{2} - 31929_{3}$
18281.471	5468.526	1	I	$24182^{\circ}_{2} - 29650_{2}$	17955.860	5567.692	2	I	$20543^{\circ}_{0} - 26111_{1}$
18280.488	5468.820	0	I	$18930^{\circ}_{3} - 24399_{3}$	17945.777	5570.820	3		
18278.904	5469.294	0			17938.774	5572.995	0		
18274.319	5470.666	0	I	$22141^{\circ}_{3} - 27612_{3}$	17936.434	5573.722	7	II	$4146_{3\frac{1}{2}} - 9720^{\circ}_{3\frac{1}{2}}$
18271.367	5471.550	5	II	$1859_{1\frac{1}{2}} - 7331^{\circ}_{2\frac{1}{2}}$	17900.307	5584.971	4	II	$9720^{\circ}_{3\frac{1}{2}} - 15305_{4\frac{1}{2}}$
18269.704	5472.048	3	II	$4113_{2\frac{1}{2}} - 9585^{\circ}_{2\frac{1}{2}}$	17893.451	5587.111	0	I	$13945^{\circ}_{3} - 19532_{4}$
18247.402	5478.736	0			17890.207	5588.124	0		
18239.409	5481.137	5	II	$6244_{1\frac{1}{2}} - 11725^{\circ}_{1\frac{1}{2}}$	17887.982	5588.819	3	I	$20522^{\circ}_{2} - 26111_{1}$
18236.594	5481.983	1			17886.677	5589.227	2	I	$18809^{\circ}_{4} - 24399_{3}$
18233.507	5482.911	0			17886.181	5589.382	0	I	$24259^{\circ}_{4} - 29849_{4}$

TABLE 1. *Infrared spectral lines of thorium*—Continued

Wavelength Å	Wavenumber cm^{-1}	Intensity	Spectrum	Classification	Wavelength Å	Wavenumber cm^{-1}	Intensity	Spectrum	Classification
17883.051	5590.360	2	I	$14226_0 - 19817^\circ_1$	17620.591	5673.629	0		
17877.768	5592.012	0			17614.900	5675.462	1	I	$20214^\circ_3 - 25890_2$
17873.738	5593.273	2	I	$24421^\circ_3 - 30014_4$	17614.015	5675.747	1	I	$22855^\circ_3 - 28531_2$
17873.620	5593.310	1	I	$21902^\circ_4 - 27495_4$	17597.889	5680.948	1	I	$14032^\circ_2 - 19713_3$
17872.284	5593.728	1	I	$19713_3 - 25306^\circ_2$	17595.542	5681.706	1	I	$18699_2 - 24381^\circ_2$
17854.649	5599.253	2	I	$24084^\circ_6 - 29684_5$	17584.517	5685.268	7	I	$9804_5 - 15490^\circ_5$
17849.848	5600.759	1	I	$20322^\circ_5 - 25923_4$	17578.779	5687.124	1		
17838.977	5604.172	1	I	$8243^\circ_2 - 13847_2$	17575.945	5688.041	1	I	$20423^\circ_1 - 26111_1$
17837.933	5604.500	1	II	$14275^\circ_{4\frac{1}{2}} - 19880_{4\frac{1}{2}}$	17573.115	5688.957	3	I	$20566^\circ_4 - 26255_4$
17834.907	5605.451	1	I	$21890^\circ_3 - 27495_4$	17568.106	5690.579	0		
17830.167	5606.941	5	II	$4113_{2\frac{1}{2}} - 9720^\circ_{3\frac{1}{2}}$	17553.728	5695.240	1	I	$17959_4 - 23655^\circ_4$
17827.385	5607.816	1	I	$18574_1 - 24182^\circ_2$	17552.671	5695.583	4	I	$17398_3 - 23093^\circ_2$
17826.416	5608.121	0	I	$18699_2 - 24307^\circ_2$	17551.531	5695.953	1	I	$25575^\circ_4 - 31271_5$
17825.875	5608.291	5	I	$11802_2 - 17411^\circ_3$	17549.205	5696.708	0	I	$26096^\circ_3 - 31793_4$
17823.987	5608.885	1	I	$19713_3 - 25321^\circ_3$	17547.178	5697.366	0	I	$27266^\circ_4 - 32963_5$
17795.604	5617.831	3	II	$12219_{1\frac{1}{2}} - 17837^\circ_{1\frac{1}{2}}$	17535.679	5701.102	1		
17788.214	5620.165	2	I	$21645_4 - 27266^\circ_4$	17535.396	5701.194	0	II	$23730^\circ_{4\frac{1}{2}} - 29431_{3\frac{1}{2}}$
17783.170	5621.759	4	I	$17411^\circ_3 - 23032_4$	17534.504	5701.484	5	II	$11116^\circ_{3\frac{1}{2}} - 16818_{3\frac{1}{2}}$
17778.391	5623.270	1	I	$11601_1 - 17224^\circ_2$	17528.629	5703.395	0		
17763.368	5628.026	0	I	$26384^\circ_4 - 32012_4$	17521.738	5705.638	2	I	$24838^\circ_1 - 30544_2$
17757.108	5630.010	2	I	$24381^\circ_2 - 30011_3$	17516.448	5707.361	0	I	$22855^\circ_3 - 28562_4$
17753.195	5631.251	0			17508.350	5710.001	2	I	$21902^\circ_4 - 27612_3$
17752.753	5631.391	1	I	$21890^\circ_3 - 27521_4$	17507.525	5710.270	0	II	$25246_{4\frac{1}{2}} - 30956^\circ_{4\frac{1}{2}}$
17744.898	5633.884	5	I	$17354^\circ_1 - 22988_2$	17503.828	5711.476	1	I	$17166_5 - 22877^\circ_5$
17742.618	5634.608	0	I	$22399^\circ_5 - 28034_5$	17492.573	5715.151	2	I	$17398_3 - 23113^\circ_4$
17721.115	5641.445	4	II	$8460_{1\frac{1}{2}} - 14101^\circ_{1\frac{1}{2}}$	17492.364	5715.219	0		
17720.358	5641.686	2	I	$22338^\circ_3 - 27980_3$	17490.072	5715.968	0		
17717.673	5642.541	0	I	$19713_3 - 25355^\circ_4$	17481.041	5718.921	7	I	$8243^\circ_2 - 13962_1$
17705.162	5646.528	3	II	$12472^\circ_{2\frac{1}{2}} - 18118_{1\frac{1}{2}}$	17473.699	5721.324	2	I	$13088_3 - 18809^\circ_4$
17703.673	5647.003	3	I	$21143_5 - 26790^\circ_4$	17468.689	5722.965	1		
17699.808	5648.236	0	II	$23697^\circ_{3\frac{1}{2}} - 29345_{2\frac{1}{2}}$	17462.260	5725.072	3	II	$13248_{4\frac{1}{2}} - 18973^\circ_{3\frac{1}{2}}$
17696.443	5649.310	2			17461.866	5725.201	0		
17689.714	5651.459	0			17456.286	5727.031	0	II	$19880_{4\frac{1}{2}} - 25607^\circ_{4\frac{1}{2}}$
17688.744	5651.769	2	I	$21539^\circ_4 - 27191_5$	17455.753	5727.206	0	II	$24757^\circ_{4\frac{1}{2}} - 30484_{5\frac{1}{2}}$
17683.810	5653.346	3	I	$15490^\circ_5 - 21143_5$	17447.564	5729.894	3	II	$9061_{2\frac{1}{2}} - 14790^\circ_{3\frac{1}{2}}$
17683.237	5653.529	0	I	$22877^\circ_1 - 28531_2$	17441.114	5732.013	0	I	$23113^\circ_4 - 28845_4$
17677.815	5655.263	0			17437.704	5733.134	1	I	$18574_1 - 24307^\circ_2$
17677.481	5655.370	3	I	$13847_2 - 19503^\circ_3$	17413.587	5741.074	2	II	$9711_{3\frac{1}{2}} - 15453^\circ_{3\frac{1}{2}}$
17670.229	5657.691	1	I	$24850^\circ_6 - 30508_5$	17405.417	5743.769	3	II	$9400_{2\frac{1}{2}} - 15144^\circ_{1\frac{1}{2}}$
17669.614	5657.888	3	I	$25306^\circ_2 - 30964_3$	17404.332	5744.127	4	I	$14204_5 - 19948^\circ_4$
17663.853	5659.733	0	I	$25877^\circ_4 - 31537_3$	17401.230	5745.151	1	I	$26048^\circ_4 - 31793_4$
17658.896	5661.322	0	I	$26113^\circ_2 - 31774_3$	17388.612	5749.320	0	I	$25877^\circ_4 - 31626_5$
17649.490	5664.339	2	I	$24880^\circ_1 - 30544_2$	17385.370	5750.392	4	I	$25180^\circ_7 - 30930_6$
17645.848	5665.508	0			17381.909	5751.537	7	I	$16346^\circ_4 - 22098_4$
17634.332	5669.208	4	I	$13847_2 - 19516^\circ_2$	17380.610	5751.967	5	I	$6362_2 - 12114^\circ_2$
17633.725	5669.403	0	I	$23752^\circ_2 - 29422_1$	17375.665	5753.604	1	I	$11601_1 - 17354^\circ_1$
17629.891	5670.636	0			17372.868	5754.530	1	I	$20054_2 - 25809^\circ_1$
17627.118	5671.528	0	I	$21645_4 - 27317^\circ_3$	17346.089	5763.414	1	II	$12219_{1\frac{1}{2}} - 17983^\circ_{2\frac{1}{2}}$
17626.046	5671.873	3	I	$15493_4 - 21165^\circ_3$	17334.404	5767.299	1	I	$23916^\circ_4 - 29684_5$
17623.094	5672.823	6	I	$7502_3 - 13175^\circ_4$	17333.121	5767.726	1	I	$13945^\circ_3 - 19713_3$

TABLE 1. *Infrared spectral lines of thorium*—Continued

Wavelength Å	Wavenumber cm^{-1}	Intensity	Spectrum	Classification	Wavelength Å	Wavenumber cm^{-1}	Intensity	Spectrum	Classification
17323.648	5770.880	0	I	$18431_3 - 24202^\circ_4$	17103.520	5845.153	1	I	$16554_6 - 22399^\circ_5$
17323.507	5770.927	0			17088.335	5850.347	2	I	$22508^\circ_2 - 28358_3$
17311.753	5774.845	1	I	$24769^\circ_3 - 30544_2$	17085.097	5851.456	0	I	$24701^\circ_5 - 30552_4$
17307.662	5776.210	7	I	$17501^\circ_5 - 23277_5$	17083.605	5851.967	0		
17304.463	5777.278	0			17078.798	5853.614	3	I	$16783^\circ_4 - 22637_3$
17295.913	5780.134	0			17075.750	5854.659	3	I	$13962_1 - 19817^\circ_1$
17294.865	5780.484	0			17069.452	5856.819	1		
17290.627	5781.901	1	I	$14204_5 - 19986^\circ_6$	17054.299	5862.023	0	I	$18699_2 - 24561^\circ_3$
17277.735	5786.215	0	I	$25355^\circ_4 - 31141_3$	17030.220	5870.311	3	II	$6700^\circ_{4\frac{1}{2}} - 12570_{3\frac{1}{2}}$
17271.005	5788.470	0	I	$23093^\circ_2 - 28882_2$	17028.599	5870.870	1	I	$22163^\circ_4 - 28034_5$
17267.932	5789.500	3	I	$19532_4 - 25321^\circ_3$	17026.334	5871.651	1	I	$18549_2 - 24421^\circ_3$
17264.172	5790.761	3	I	$17411^\circ_3 - 23201_3$	17020.168	5873.778	1		
17261.632	5791.613	0	I	$21252^\circ_2 - 27044_3$	17019.670	5873.950	0	I	$20922^\circ_2 - 26796_3$
17244.366	5797.412	1	II	$22139^\circ_{4\frac{1}{2}} - 27937_{5\frac{1}{2}}$	17018.885	5874.221	2	I	$21738^\circ_2 - 27612_3$
17235.699	5800.327	1	II	$13250_{2\frac{1}{2}} - 19050^\circ_{1\frac{1}{2}}$	17014.224	5875.830	1		
17229.251	5802.498	0	II	$20686^\circ_{2\frac{1}{2}} - 26488_{2\frac{1}{2}}$	17014.114	5875.868	1	I	$19039^\circ_2 - 24915_3$
17227.152	5803.205	0	I	$25442^\circ_3 - 31245_2$	17013.556	5876.061	0	I	$18431_3 - 24307^\circ_2$
17225.670	5803.704	3	I	$17073_1 - 22877^\circ_1$	17012.360	5876.474	0	I	$24850^\circ_6 - 30726_7$
17221.632	5805.065	1	I	$15863_2 - 21668^\circ_1$	17008.982	5877.641	0		
17217.782	5806.363	2	I	$21165^\circ_3 - 26971_4$	17008.562	5877.786	2	I	$24880^\circ_1 - 30758_2$
17216.726	5806.719	0	I	$18574_1 - 24381^\circ_2$	17008.100	5877.946	0		
17208.215	5809.591	8	II	$1521_{2\frac{1}{2}} - 7331^\circ_{2\frac{1}{2}}$	17005.290	5878.917	2	I	$27084^\circ_6 - 32963_5$
17198.807	5812.769	0	I	$26645^\circ_5 - 32458_4$	17004.697	5879.122	3	I	$21165^\circ_3 - 27044_3$
17195.420	5813.914	0	I	$20566^\circ_3 - 26380_5$	16997.972	5881.448	0	I	$24769^\circ_3 - 30651_3$
17192.605	5814.866	1	I	$23603^\circ_2 - 29418_2$	16992.702	5883.272	0		
17186.894	5816.798	2	I	$19588^\circ_5 - 25405_4$	16989.777	5884.285	1	I	$25442^\circ_3 - 31326_4$
17182.265	5818.365	0			16976.362	5888.935	0	I	$22338^\circ_3 - 28227_4$
17173.440	5821.355	0	I	$23113^\circ_4 - 28934_3$	16964.222	5893.149	0	I	$26036^\circ_3 - 31929_3$
17168.126	5823.157	0	I	$19532_4 - 25355^\circ_4$	16960.892	5894.306	1	I	$21077^\circ_5 - 26971_4$
17165.765	5823.958	2	I	$22855^\circ_3 - 28679_2$	16958.427	5895.163	1		
17163.009	5824.893	1	I	$24307^\circ_2 - 30132_2$	16956.701	5895.763	2	II	$15786_{2\frac{1}{2}} - 21682^\circ_{3\frac{1}{2}}$
17155.413	5827.472	1	II	$23518^\circ_{3\frac{1}{2}} - 29345_{2\frac{1}{2}}$	16954.783	5896.430	0		
17153.591	5828.091	2	I	$18431_3 - 24259^\circ_4$	16952.178	5897.336	0	I	$23521^\circ_3 - 29418_2$
17152.876	5828.334	1			16949.485	5898.273	0	I	$23752^\circ_2 - 29650_2$
17152.288	5828.534	1	I	$22399^\circ_5 - 28227_4$	16947.451	5898.981	0		
17151.508	5828.799	1	I	$21738^\circ_2 - 27566_2$	16945.150	5899.782	0	I	$26651^\circ_2 - 32551_3$
17151.178	5828.911	0	I	$24182^\circ_2 - 30011_3$	16941.790	5900.952	0	II	$7001_{1\frac{1}{2}} - 12902^\circ_{1\frac{1}{2}}$
17146.766	5830.411	0	I	$23015^\circ_5 - 28845_4$	16938.730	5902.018	3	I	$19503^\circ_3 - 25405_4$
17143.105	5831.656	2			16918.744	5908.990	0	I	$26384^\circ_4 - 32293_5$
17135.330	5834.302	4	I	$8111_4 - 13945^\circ_3$	16915.692	5910.056	0	I	$25355^\circ_4 - 31265_3$
17134.167	5834.698	4	I	$23306^\circ_6 - 29141_5$	16915.097	5910.264	1	I	$19532_4 - 25442^\circ_3$
17133.189	5835.031	1	I	$25306^\circ_2 - 31141_3$	16912.370	5911.217	1	II	$21682^\circ_{3\frac{1}{2}} - 27593_{2\frac{1}{2}}$
17124.268	5838.071	1	I	$15736^\circ_1 - 21575_2$	16911.655	5911.467	0		
17121.318	5839.077	3	I	$22141^\circ_3 - 27980_3$	16906.064	5913.422	0	II	$23518^\circ_{3\frac{1}{2}} - 29431_{3\frac{1}{2}}$
17120.840	5839.240	0	I	$27260^\circ_3 - 33099_3$	16900.345	5915.423	1	I	$25355^\circ_4 - 31271_5$
17120.083	5839.498	1	I	$23916^\circ_4 - 29756_4$	16890.066	5919.023	5	II	$7331^\circ_{2\frac{1}{2}} - 13250_{2\frac{1}{2}}$
17113.767	5841.653	1			16887.173	5920.037	1	I	$15970_3 - 21890^\circ_3$
17113.542	5841.730	2	I	$13088_3 - 18930^\circ_3$	16883.454	5921.341	0	I	$18069^\circ_3 - 23990_2$
17111.210	5842.526	0			16879.312	5922.794	2	I	$17847^\circ_2 - 23769_1$
17105.103	5844.612	1			16875.970	5923.967	0	I	$25321^\circ_3 - 31245_2$

TABLE 1. *Infrared spectral lines of thorium*—Continued

Wavelength Å	Wavenumber cm^{-1}	Intensity	Spectrum	Classification	Wavelength Å	Wavenumber cm^{-1}	Intensity	Spectrum	Classification
16852.625	5932.173	2	I	$15970_3 - 21902^\circ_4$	16588.332	6026.687	0		
16849.382	5933.315	0	I	$20322^\circ_5 - 26255_4$	16587.815	6026.875	3	I	$15618^\circ_3 - 21645_4$
16846.815	5934.219	0	I	$22338^\circ_3 - 28273_2$	16587.044	6027.155	0	I	$22855^\circ_3 - 28882_2$
16846.017	5934.500	0	I	$25336^\circ_6 - 31271_5$	16578.581	6030.232	1		
16840.767	5936.350	0	I	$25690^\circ_5 - 31626_5$	16578.017	6030.437	0		
16832.896	5939.126	0	I	$25306^\circ_2 - 31245_2$	16569.667	6033.476	0	I	$19273_2 - 25306^\circ_2$
16827.445	5941.050	0			16540.424	6044.143	5	I	$11802_2 - 17847^\circ_2$
16823.435	5942.466	1			16538.399	6044.883	3	I	$16351_0 - 22396^\circ_1$
16820.947	5943.345	1	I	$23609^\circ_5 - 29552_6$	16534.332	6046.370	2	I	$15493_4 - 21539^\circ_4$
16818.657	5944.154	0			16531.417	6047.436	1	I	$23603^\circ_2 - 29650_2$
16811.787	5946.583	0	I	$26790^\circ_4 - 32737_5$	16522.232	6050.798	0		
16806.361	5948.503	1			16521.658	6051.008	1	I	$24838^\circ_1 - 30889_1$
16804.426	5949.188	0			16520.919	6051.279	3	II	$10855_{3\frac{1}{2}} - 16906^\circ_{3\frac{1}{2}}$
16801.531	5950.213	0	I	$24182^\circ_2 - 30132_2$	16518.765	6052.068	3	II	$9400_{2\frac{1}{2}} - 15453^\circ_{3\frac{1}{2}}$
16800.478	5950.586	1	I	$13088_3 - 19039^\circ_2$	16503.791	6057.559	4	I	$18614^\circ_1 - 24671_2$
16797.452	5951.658	1			16501.244	6058.494	0	I	$20054_2 - 26113^\circ_2$
16785.229	5955.992	2	I	$21539^\circ_4 - 27495_4$	16495.017	6060.781	0	II	$15236_{1\frac{1}{2}} - 21297^\circ_{2\frac{1}{2}}$
16785.046	5956.057	2	I	$15618^\circ_3 - 21575_2$	16492.394	6061.745	2	II	$13818^\circ_{3\frac{1}{2}} - 19880_{4\frac{1}{2}}$
16782.389	5957.000	1	I	$17959_4 - 23916^\circ_4$	16477.433	6067.249	2	II	$9238^\circ_{4\frac{1}{2}} - 15305_{4\frac{1}{2}}$
16771.639	5960.818	1			16461.254	6073.212	1	I	$19817^\circ_1 - 25890_2$
16768.550	5961.916	6	I	$12847_3 - 18809^\circ_4$	16453.368	6076.123	0	II	$20686^\circ_{2\frac{1}{2}} - 26762_{1\frac{1}{2}}$
16761.533	5964.412	0	I	$26048^\circ_4 - 32012_4$	16452.932	6076.284	0	I	$21594_3 - 27670^\circ_3$
16750.771	5968.244	0			16447.180	6078.409	0	I	$21902^\circ_4 - 27980_3$
16748.433	5969.077	5	I	$11197^\circ_5 - 17166_5$	16443.836	6079.645	0		
16747.499	5969.410	2	I	$13847_2 - 19817^\circ_1$	16436.507	6082.356	2		
16746.683	5969.701	1			16436.339	6082.418	3		
16741.938	5971.393	0	I	$25355^\circ_4 - 31326_4$	16433.049	6083.636	2	II	$9061_{2\frac{1}{2}} - 15144^\circ_{1\frac{1}{2}}$
16730.028	5975.644	3	I	$17073_1 - 23049^\circ_1$	16428.820	6085.202	2	II	$8460_{1\frac{1}{2}} - 14545^\circ_{2\frac{1}{2}}$
16725.712	5977.186	0			16420.336	6088.346	0		
16724.318	5977.684	1	I	$17224^\circ_2 - 23201_3$	16414.399	6090.548	1	I	$21890^\circ_3 - 27980_3$
16720.218	5979.150	0	I	$24307^\circ_2 - 30286_1$	16412.823	6091.133	3	I	$21252^\circ_2 - 27343_3$
16718.081	5979.914	1			16403.906	6094.444	0	I	$23916^\circ_4 - 30011_3$
16712.444	5981.931	3	I	$21539^\circ_4 - 27521_4$	16394.343	6097.999	1	I	$24274^\circ_5 - 30372_6$
16707.945	5983.542	0	I	$24981^\circ_3 - 30964_3$	16390.870	6099.291	0	I	$21575_2 - 27674^\circ_2$
16704.639	5984.726	3	I	$18930^\circ_3 - 24915_3$	16380.898	6103.004	6	II	$9202^\circ_{3\frac{1}{2}} - 15305_{4\frac{1}{2}}$
16694.697	5988.290	0	I	$24769^\circ_3 - 30758_2$	16377.984	6104.090	0		
16691.676	5989.374	1	I	$18431_3 - 24421^\circ_3$	16375.188	6105.132	1	I	$18809^\circ_4 - 24915_3$
16688.906	5990.368	1	I	$19713_3 - 25703^\circ_2$	16367.427	6108.027	1		
16687.560	5990.851	0	I	$24561^\circ_3 - 30552_4$	16363.631	6109.444	2	I	$22248^\circ_2 - 28358_3$
16686.678	5991.168	1	I	$26790^\circ_4 - 32781_4$	16349.247	6114.819	1		
16634.036	6010.128	0			16343.137	6117.105	0		
16630.351	6011.460	0			16340.749	6117.999	2	I	$14204_5 - 20322^\circ_5$
16624.607	6013.537	2	I	$18614^\circ_1 - 24627_1$	16329.816	6122.095	2	I	$20922^\circ_2 - 27044_3$
16612.968	6017.750	0			16326.067	6123.501	2	I	$24421^\circ_3 - 30544_2$
16606.290	6020.170	1	I	$17073_1 - 23093^\circ_2$	16316.903	6126.940	0		
16604.436	6020.842	1	I	$18011^\circ_5 - 24032_4$	16310.703	6129.269	3	I	$20867^\circ_7 - 26997_6$
16599.350	6022.687	3	I	$14032^\circ_2 - 20054_2$	16308.851	6129.965	2	I	$18431_3 - 24561^\circ_3$
16594.999	6024.266	0	I	$22248^\circ_2 - 28273_2$	16308.606	6130.057	2		
16592.118	6025.312	2			16305.893	6131.077	0		
16589.555	6026.243	1	I	$15863_2 - 21890^\circ_3$	16304.920	6131.443	0	I	$24421^\circ_3 - 30552_4$

TABLE 1. *Infrared spectral lines of thorium*—Continued

Wavelength Å	Wavenumber cm^{-1}	Intensity	Spectrum	Classification	Wavelength Å	Wavenumber cm^{-1}	Intensity	Spectrum	Classification
16304.149	6131.733	3	I	$21902^{\circ}_{4} - 28034_{5}$	16006.680	6245.685	0	I	$23306^{\circ}_{6} - 29552_{6}$
16297.533	6134.222	0	I	$22396^{\circ}_{1} - 28531_{2}$	16005.763	6246.043	4	I	$11601_{1} - 17847^{\circ}_{2}$
16284.058	6139.298	1	I	$18699_{2} - 24838^{\circ}_{1}$	15997.841	6249.136	2	I	$16783^{\circ}_{4} - 23032_{4}$
16280.282	6140.722	3	I	$17166_{5} - 23306^{\circ}_{6}$	15981.974	6255.340	0		
16273.373	6143.329	0	I	$17847^{\circ}_{2} - 23990_{2}$	15978.393	6256.742	2	I	$17398_{3} - 23655^{\circ}_{4}$
16270.823	6144.292	0	I	$26651^{\circ}_{2} - 32796_{3}$	15973.502	6258.658	1	I	$23752^{\circ}_{2} - 30011_{3}$
16269.133	6144.930	3	II	$10673^{\circ}_{2\frac{1}{2}} - 16818_{3\frac{1}{2}}$	15972.593	6259.014	0	I	$25753^{\circ}_{5} - 32012_{4}$
16263.051	6147.228	1	I	$23609^{\circ}_{5} - 29756_{4}$	15963.355	6262.636	0		
16250.275	6152.061	1			15960.024	6263.943	2	I	$22877^{\circ}_{5} - 29141_{5}$
16240.450	6155.783	2	I	$15490^{\circ}_{5} - 21645_{4}$	15954.449	6266.132	4	I	$11802_{2} - 18069^{\circ}_{3}$
16238.115	6156.668	3	I	$11241^{\circ}_{3} - 17398_{3}$	15951.379	6267.338	0	II	$20989^{\circ}_{4\frac{1}{2}} - 27257_{3\frac{1}{2}}$
16234.453	6158.057	0	I	$19532_{4} - 25690^{\circ}_{5}$	15944.136	6270.185	0		
16224.530	6161.823	0			15941.439	6271.246	0	I	$25355^{\circ}_{4} - 31626_{5}$
16220.740	6163.263	3	I	$22399^{\circ}_{5} - 28562_{4}$	15939.011	6272.201	1	II	$6213_{4\frac{1}{2}} - 12485^{\circ}_{3\frac{1}{2}}$
16217.564	6164.470	0	I	$19713_{3} - 25877^{\circ}_{4}$	15936.374	6273.239	4	II	$7828_{2\frac{1}{2}} - 14101^{\circ}_{1\frac{1}{2}}$
16212.890	6166.247	1			15936.069	6273.359	3	I	$20522^{\circ}_{2} - 26796_{3}$
16211.744	6166.683	0	I	$26384^{\circ}_{4} - 32551_{3}$	15932.409	6274.800	6	II	$6213_{4\frac{1}{2}} - 12488^{\circ}_{4\frac{1}{2}}$
16204.728	6169.353	0			15927.216	6276.846	0	II	$24982^{\circ}_{3\frac{1}{2}} - 31259_{2\frac{1}{2}}$
16204.604	6169.400	1	I	$19273_{2} - 25442^{\circ}_{3}$	15925.011	6277.715	1	I	$15863_{2} - 22141^{\circ}_{3}$
16195.248	6172.964	1	I	$26790^{\circ}_{4} - 32963_{5}$	15924.829	6277.787	0	I	$24274^{\circ}_{5} - 30552_{4}$
16188.147	6175.672	0	I	$22669^{\circ}_{3} - 28845_{4}$	15922.130	6278.851	4	I	$15970_{3} - 22248^{\circ}_{2}$
16182.835	6177.699	0	II	$20310^{\circ}_{2\frac{1}{2}} - 26488_{2\frac{1}{2}}$	15920.010	6279.687	0		
16180.368	6178.641	0	I	$21165^{\circ}_{3} - 27343_{3}$	15919.042	6280.069	1	I	$4961_{4} - 11241^{\circ}_{3}$
16178.472	6179.365	2	I	$22163^{\circ}_{4} - 28342_{5}$	15915.448	6281.487	1	I	$18699_{2} - 24981^{\circ}_{3}$
16172.466	6181.660	1	I	$25355^{\circ}_{4} - 31537_{3}$	15913.906	6282.096	0	I	$22248^{\circ}_{2} - 28531_{2}$
16163.327	6185.155	3	II	$8605_{2\frac{1}{2}} - 14790^{\circ}_{3\frac{1}{2}}$	15899.553	6287.767	3	I	$24084^{\circ}_{6} - 30372_{6}$
16147.600	6191.179	3	I	$12847_{3} - 19039^{\circ}_{2}$	15898.637	6288.129	1	II	$20969^{\circ}_{3\frac{1}{2}} - 27257_{3\frac{1}{2}}$
16145.326	6192.051	1	I	$22338^{\circ}_{3} - 28531_{2}$	15895.139	6289.513	1	I	$18549_{2} - 24838^{\circ}_{1}$
16142.758	6193.036	2	I	$15970_{3} - 22163^{\circ}_{4}$	15893.090	6290.324	1	I	$25336^{\circ}_{6} - 31626_{5}$
16140.194	6194.020	0	I	$23655^{\circ}_{4} - 29849_{4}$	15891.854	6290.813	3	I	$16346^{\circ}_{4} - 22637_{3}$
16137.810	6194.935	0	I	$24769^{\circ}_{3} - 30964_{3}$	15891.564	6290.928	4	I	$13297_{4} - 19588^{\circ}_{5}$
16125.805	6199.547	0	I	$25575^{\circ}_{4} - 31774_{3}$	15887.023	6292.726	1	I	$24259^{\circ}_{4} - 30552_{4}$
16120.565	6201.562	0			15880.810	6295.188	1		
16109.798	6205.707	5	I	$13297_{4} - 19503^{\circ}_{3}$	15877.380	6296.548	0	II	$21297^{\circ}_{2\frac{1}{2}} - 27593_{2\frac{1}{2}}$
16100.958	6209.114	0	I	$23752^{\circ}_{2} - 29961_{1}$	15871.650	6298.821	0		
16084.899	6215.313	0	I	$25321^{\circ}_{3} - 31537_{3}$	15868.987	6299.878	2	I	$17959_{4} - 24259^{\circ}_{4}$
16081.086	6216.787	1	I	$22141^{\circ}_{3} - 28358_{3}$	15861.758	6302.749	1	I	$21645_{4} - 27948^{\circ}_{4}$
16072.590	6220.073	3			15854.989	6305.440	1	I	$24202^{\circ}_{4} - 30508_{5}$
16071.988	6220.306	1	I	$18549_{2} - 24769^{\circ}_{3}$	15853.227	6306.141	0		
16070.913	6220.722	0	I	$23741^{\circ}_{1} - 29961_{1}$	15851.771	6306.720	0		
16068.852	6221.520	1	I	$19532_{4} - 25753^{\circ}_{5}$	15847.733	6308.327	3	I	$20054_{2} - 26363^{\circ}_{2}$
16056.201	6226.422	0	I	$22877^{\circ}_{5} - 29104_{4}$	15843.848	6309.874	0	II	$9400_{2\frac{1}{2}} - 15710^{\circ}_{1\frac{1}{2}}$
16048.543	6229.393	1	I	$24701^{\circ}_{5} - 30930_{6}$	15835.343	6313.263	1		
16047.145	6229.936	0			15833.507	6313.995	0	I	$23521^{\circ}_{3} - 29835_{3}$
16045.762	6230.473	0	I	$25306^{\circ}_{2} - 31537_{3}$	15832.882	6314.244	0	I	$21252^{\circ}_{2} - 27566_{2}$
16042.116	6231.889	0			15831.752	6314.695	7	I	$5563_{1} - 11877^{\circ}_{1}$
16038.518	6233.287	3	I	$24274^{\circ}_{5} - 30508_{5}$	15825.176	6317.319	2	I	$12114^{\circ}_{2} - 18431_{3}$
16033.162	6235.369	2	I	$4961_{4} - 11197^{\circ}_{5}$	15815.492	6321.187	6	II	$9711_{3\frac{1}{2}} - 16033^{\circ}_{2\frac{1}{2}}$
16014.426	6242.664	2	I	$17959_{4} - 24202^{\circ}_{4}$	15810.170	6323.315	1	I	$19713_{3} - 26036^{\circ}_{3}$
16008.311	6245.049	3	I	$18382^{\circ}_{0} - 24627_{1}$	15807.445	6324.405	0	I	$23093^{\circ}_{2} - 29418_{2}$

TABLE 1. *Infrared spectral lines of thorium*—Continued

Wavelength Å	Wavenumber cm^{-1}	Intensity	Spectrum	Classification	Wavelength Å	Wavenumber cm^{-1}	Intensity	Spectrum	Classification
15804.308	6325.660	1	I	$21902^{\circ}_{4} - 28227_{4}$	15602.299	6407.561	0	I	$17073_{1} - 23481^{\circ}_{1}$
15794.600	6329.548	0			15598.808	6408.995	4	I	$7795^{\circ}_{4} - 14204_{5}$
15793.353	6330.048	0	I	$18069^{\circ}_{3} - 24399_{3}$	15598.676	6409.049	4	I	$15493_{4} - 21902^{\circ}_{4}$
15792.250	6330.490	0	I	$21165^{\circ}_{3} - 27495_{4}$	15597.528	6409.521	0		
15791.447	6330.812	1	I	$18549_{2} - 24880^{\circ}_{1}$	15593.649	6411.115	1	II	$13468^{\circ}_{4\frac{1}{2}} - 19880_{4\frac{1}{2}}$
15788.721	6331.905	0	I	$25442^{\circ}_{3} - 31774_{3}$	15585.229	6414.579	3	I	$13088_{3} - 19503^{\circ}_{3}$
15781.849	6334.662	1	I	$19588^{\circ}_{5} - 25923_{4}$	15583.635	6415.235	2	I	$17354^{\circ}_{1} - 23769_{1}$
15767.555	6340.405	3	II	$13818^{\circ}_{3\frac{1}{2}} - 20158_{2\frac{1}{2}}$	15576.584	6418.139	6	I	$16783^{\circ}_{4} - 23201_{3}$
15754.904	6345.496	1	I	$18053^{\circ}_{4} - 24399_{3}$	15575.870	6418.433	1	I	$21077^{\circ}_{5} - 27495_{4}$
15747.955	6348.296	1	II	$12219_{1\frac{1}{2}} - 18568^{\circ}_{\frac{1}{2}}$	15574.463	6419.013	1	I	$25355^{\circ}_{4} - 31774_{3}$
15745.306	6349.364	0			15572.352	6419.883	2	I	$19503^{\circ}_{3} - 25923_{4}$
15743.881	6349.939	2	I	$24202^{\circ}_{4} - 30552_{4}$	15572.117	6419.980	4	I	$16217^{\circ}_{2} - 22637_{3}$
15733.987	6353.932	0	I	$21594_{3} - 27948^{\circ}_{4}$	15569.510	6421.055	3	I	$22141^{\circ}_{3} - 28562_{4}$
15732.702	6354.451	0	I	$25575^{\circ}_{4} - 31929_{3}$	15568.155	6421.614	0	I	$20922^{\circ}_{2} - 27343_{3}$
15728.365	6356.203	0	I	$23655^{\circ}_{4} - 30011_{3}$	15565.585	6422.674	0	I	$26645^{\circ}_{5} - 33068_{6}$
15727.808	6356.428	0	I	$21165^{\circ}_{3} - 27521_{4}$	15559.575	6425.155	2		
15720.977	6359.190	1	I	$23655^{\circ}_{4} - 30014_{4}$	15558.814	6425.469	2	II	$4146_{3\frac{1}{2}} - 10572^{\circ}_{4\frac{1}{2}}$
15719.798	6359.667	1	I	$21252^{\circ}_{2} - 27612_{3}$	15553.233	6427.775	2	I	$15166^{\circ}_{3} - 21594_{3}$
15716.044	6361.186	1			15551.679	6428.417	4	I	$13088_{3} - 19516^{\circ}_{2}$
15713.149	6362.358	4	I	$14204_{5} - 20566^{\circ}_{4}$	15547.561	6430.120	1	I	$19273_{2} - 25703^{\circ}_{2}$
15706.454	6365.070	2	II	$4490^{\circ}_{2\frac{1}{2}} - 10855_{3\frac{1}{2}}$	15542.668	6432.144	2	I	$19948^{\circ}_{4} - 26380_{5}$
15703.035	6366.456	0			15537.904	6434.116	0	I	$22669^{\circ}_{3} - 29104_{4}$
15702.559	6366.649	1	I	$8800_{4} - 15166^{\circ}_{3}$	15523.156	6440.229	1	I	$21902^{\circ}_{4} - 28342_{5}$
15701.306	6367.157	3	I	$13847_{2} - 20214^{\circ}_{3}$	15516.436	6443.018	6	I	$7502_{3} - 13945^{\circ}_{3}$
15698.032	6368.485	0	II	$20120^{\circ}_{2\frac{1}{2}} - 26488_{2\frac{1}{2}}$	15513.174	6444.373	1	I	$21077^{\circ}_{5} - 27521_{4}$
15697.541	6368.684	0			15508.866	6446.163	1	I	$22399^{\circ}_{5} - 28845_{4}$
15697.019	6368.896	1	I	$15970_{3} - 22338^{\circ}_{3}$	15505.455	6447.581	0	I	$26651^{\circ}_{2} - 33099_{3}$
15696.943	6368.927	1	I	$23049^{\circ}_{1} - 29418_{2}$	15503.005	6448.600	0	I	$24202^{\circ}_{4} - 30651_{3}$
15690.237	6371.649	1			15499.015	6450.260	1	I	$24307^{\circ}_{2} - 30758_{2}$
15676.166	6377.368	3	I	$23306^{\circ}_{6} - 29684_{5}$	15485.384	6455.938	0		
15671.451	6379.287	0			15479.404	6458.432	1		
15662.128	6383.084	0	I	$21890^{\circ}_{3} - 28273_{2}$	15475.060	6460.245	1	I	$12114^{\circ}_{2} - 18574_{1}$
15647.283	6389.140	1			15473.472	6460.908	1	I	$16554_{6} - 23015^{\circ}_{5}$
15641.777	6391.389	0	I	$24259^{\circ}_{4} - 30651_{3}$	15473.326	6460.969	1	I	$13962_{1} - 20423^{\circ}_{1}$
15641.596	6391.463	1			15472.864	6461.162	3	I	$17959_{4} - 24421^{\circ}_{3}$
15641.344	6391.566	3	I	$23741^{\circ}_{1} - 30132_{2}$	15467.501	6463.402	1		
15640.438	6391.936	5	II	$9061_{2\frac{1}{2}} - 15453^{\circ}_{3\frac{1}{2}}$	15461.432	6465.939	0		
15637.160	6393.276	3	II	$11725^{\circ}_{\frac{1}{2}} - 18118_{1\frac{1}{2}}$	15456.917	6467.828	1	I	$25306^{\circ}_{2} - 31774_{3}$
15634.482	6394.371	2	I	$19986^{\circ}_{6} - 26380_{5}$	15455.882	6468.261	0	I	$21890^{\circ}_{3} - 28358_{3}$
15631.483	6395.598	1	II	$15710^{\circ}_{1\frac{1}{2}} - 22106_{2\frac{1}{2}}$	15454.759	6468.731	0	I	$24182^{\circ}_{2} - 30651_{3}$
15628.272	6396.912	3	I	$15493_{4} - 21890^{\circ}_{3}$	15447.452	6471.791	1		
15624.606	6398.413	1	II	$17983^{\circ}_{2\frac{1}{2}} - 24381_{3\frac{1}{2}}$	15440.113	6474.867	4	I	$18930^{\circ}_{3} - 25405_{4}$
15621.888	6399.526	0	I	$22163^{\circ}_{4} - 28562_{4}$	15439.546	6475.105	2	I	$15863_{2} - 22338^{\circ}_{3}$
15620.165	6400.232	2	I	$19713_{3} - 26113^{\circ}_{2}$	15429.783	6479.202	7	I	$15618^{\circ}_{3} - 22098_{4}$
15616.447	6401.756	1	I	$21165^{\circ}_{3} - 27566_{2}$	15425.673	6480.928	2	II	$22106_{2\frac{1}{2}} - 28587^{\circ}_{2\frac{1}{2}}$
15615.505	6402.142	1	II	$6168^{\circ}_{3\frac{1}{2}} - 12570_{3\frac{1}{2}}$	15400.599	6491.480	0		
15613.859	6402.817	0			15395.715	6493.539	2	I	$16783^{\circ}_{4} - 23277_{5}$
15612.710	6403.288	0	II	$12570_{3\frac{1}{2}} - 18973^{\circ}_{3\frac{1}{2}}$	15392.243	6495.004	0		
15608.939	6404.835	2	I	$20566^{\circ}_{4} - 26971_{4}$	15390.079	6495.917	0	I	$24769^{\circ}_{3} - 31265_{3}$
15608.145	6405.161	1	I	$23609^{\circ}_{5} - 30014_{4}$	15373.158	6503.067	0	I	$26048^{\circ}_{4} - 32551_{3}$

TABLE 1. *Infrared spectral lines of thorium*—Continued

Wavelength Å	Wavenumber cm^{-1}	Intensity	Spectrum	Classification
15372.295	6503.432	0		
15364.893	6506.565	1	I	$22338^{\circ}_{3} - 28845_{4}$
15355.694	6510.463	5	I	$14226_{0} - 20737^{\circ}_{1}$
15342.358	6516.122	1	I	$19532_{4} - 26048^{\circ}_{4}$
15336.766	6518.498	0	I	$17398_{3} - 23916^{\circ}_{4}$
15320.133	6525.575	0	I	$16351_{0} - 22877^{\circ}_{1}$
15317.814	6526.563	3	II	$4146_{3\frac{1}{2}} - 10673^{\circ}_{2\frac{1}{2}}$
15315.929	6527.366	5	II	$8018_{1\frac{1}{2}} - 14545^{\circ}_{2\frac{1}{2}}$
15315.660	6527.481	2	II	$10379_{4\frac{1}{2}} - 16906^{\circ}_{3\frac{1}{2}}$
15309.803	6529.978	0		
15307.300	6531.046	6	I	$17501^{\circ}_{5} - 24032_{4}$
15299.948	6534.184	2		
15297.656	6535.163	0	I	$21738^{\circ}_{2} - 28273_{2}$
15296.303	6535.741	0		
15295.651	6536.020	0	I	$19273_{2} - 25809^{\circ}_{1}$
15293.025	6537.142	0	II	$20989^{\circ}_{4\frac{1}{2}} - 27526_{4\frac{1}{2}}$
15292.511	6537.362	1	I	$23015^{\circ}_{5} - 29552_{6}$
15291.203	6537.921	2	I	$13175^{\circ}_{4} - 19713_{3}$
15288.921	6538.897	4	II	$8605_{2\frac{1}{2}} - 15144^{\circ}_{1\frac{1}{2}}$
15285.339	6540.429	1		
15284.311	6540.869	0	I	$22877^{\circ}_{1} - 29418_{2}$
15282.038	6541.842	2	I	$9804_{5} - 16346^{\circ}_{4}$
15280.959	6542.304	2	II	$11576^{\circ}_{1\frac{1}{2}} - 18118_{1\frac{1}{2}}$
15278.264	6543.458	1	I	$22338^{\circ}_{3} - 28882_{2}$
15273.332	6545.571	2	I	$17224^{\circ}_{2} - 23769_{1}$
15266.440	6548.526	4	II	$6700^{\circ}_{4\frac{1}{2}} - 13248_{4\frac{1}{2}}$
15265.258	6549.033	0	I	$24880^{\circ}_{1} - 31429_{1}$
15264.344	6549.425	2	I	$18431_{3} - 24981^{\circ}_{3}$
15260.157	6551.222	2	I	$5563_{1} - 12114^{\circ}_{2}$
15246.115	6557.256	1	I	$24769^{\circ}_{3} - 31326_{4}$
15242.228	6558.928	0		
15241.775	6559.123	1	II	$6691^{\circ}_{1\frac{1}{2}} - 13250_{2\frac{1}{2}}$
15240.242	6559.783	7	II	$4113_{2\frac{1}{2}} - 10673^{\circ}_{2\frac{1}{2}}$
15239.289	6560.193	4	I	$13962_{1} - 20522^{\circ}_{2}$
15230.042	6564.176	2		
15226.150	6565.854	0		
15218.677	6569.078	1		
15218.580	6569.120	0		
15215.038	6570.649	0	I	$23113^{\circ}_{4} - 29684_{5}$
15214.240	6570.994	1	II	$20686^{\circ}_{2\frac{1}{2}} - 27257_{3\frac{1}{2}}$
15212.582	6571.710	0		
15203.638	6575.576	0	I	$24182^{\circ}_{2} - 30758_{2}$
15195.303	6579.183	0	I	$17411^{\circ}_{3} - 23990_{2}$
15190.777	6581.143	3	I	$20214^{\circ}_{3} - 26796_{3}$
15190.369	6581.320	2	I	$13962_{1} - 20543^{\circ}_{0}$
15188.855	6581.976	5	II	$17727_{5\frac{1}{2}} - 24309^{\circ}_{5\frac{1}{2}}$
15180.335	6585.670	0		
15171.406	6589.546	1		
15168.869	6590.648	0		
15167.182	6591.381	0	I	$26508^{\circ}_{3} - 33099_{3}$
15158.232	6595.273	1	I	$18809^{\circ}_{4} - 25405_{4}$
15157.340	6595.661	0	I	$18069^{\circ}_{3} - 24664_{3}$
15156.775	6595.907	1	I	$22338^{\circ}_{3} - 28934_{3}$
15143.355	6601.752	2	I	$17959_{4} - 24561^{\circ}_{3}$
15137.607	6604.259	0	I	$21668^{\circ}_{1} - 28273_{2}$
15135.223	6605.299	0	II	$10855_{3\frac{1}{2}} - 17460^{\circ}_{2\frac{1}{2}}$
15128.735	6608.132	1		
15112.474	6615.242	2	I	$10783^{\circ}_{2} - 17398_{3}$
15100.835	6620.341	2	I	$21738^{\circ}_{2} - 28358_{3}$
15099.336	6620.998	4	I	$17411^{\circ}_{3} - 24032_{4}$
15096.026	6622.450	2		
15095.376	6622.735	1	I	$25306^{\circ}_{2} - 31929_{3}$
15090.817	6624.736	2	I	$20566^{\circ}_{4} - 27191_{5}$
15084.090	6627.690	1		
15077.746	6630.479	0		
15073.742	6632.240	0		
15065.723	6635.770	1	I	$17354^{\circ}_{1} - 23990_{2}$
15060.159	6638.222	1		
15059.008	6638.729	0		
15051.950	6641.842	2	I	$24084^{\circ}_{6} - 30726_{7}$
15049.671	6642.848	2	I	$23113^{\circ}_{4} - 29756_{4}$
15045.413	6644.728	3	I	$20922^{\circ}_{2} - 27566_{2}$
15037.137	6648.385	0	I	$15493_{4} - 22141^{\circ}_{3}$
15035.312	6649.192	0	I	$20322^{\circ}_{5} - 26971_{4}$
15034.068	6649.742	3	II	$9061_{2\frac{1}{2}} - 15710^{\circ}_{1\frac{1}{2}}$
15033.345	6650.062	0		
15031.317	6650.959	1	I	$13297_{4} - 19948^{\circ}_{4}$
15021.804	6655.171	3	I	$12847_{3} - 19503^{\circ}_{3}$
15017.893	6656.904	0	I	$24307^{\circ}_{2} - 30964_{3}$
15015.230	6658.085	2	II	$6244_{1/2} - 12902^{\circ}_{1\frac{1}{2}}$
15013.595	6658.810	0	II	$17722^{\circ}_{4\frac{1}{2}} - 24381_{3\frac{1}{2}}$
15010.031	6660.391	3	I	$21902^{\circ}_{4} - 28562_{4}$
15009.909	6660.445	2	II	$22685^{\circ}_{3\frac{1}{2}} - 29345_{2\frac{1}{2}}$
15007.406	6661.556	0	I	$14481^{\circ}_{6} - 21143_{5}$
14994.654	6667.221	3	I	$19588^{\circ}_{5} - 26255_{4}$
14994.569	6667.259	2	I	$17073_{1} - 23741^{\circ}_{1}$
14990.632	6669.010	1	I	$12847_{3} - 19516^{\circ}_{2}$
14988.603	6669.913	4	I	$15493_{4} - 22163^{\circ}_{4}$
14984.882	6671.569	4	I	$11877^{\circ}_{1} - 18549_{2}$
14982.726	6672.529	1	I	$21890^{\circ}_{3} - 28562_{4}$
14980.034	6673.728	0	I	$25321^{\circ}_{3} - 31995_{4}$
14977.689	6674.773	0		
14977.332	6674.932	3	I	$22877^{\circ}_{5} - 29552_{6}$
14976.848	6675.148	0		
14970.942	6677.781	1		
14970.770	6677.858	1		
14969.772	6678.303	1	II	$25246_{4\frac{1}{2}} - 31924^{\circ}_{5\frac{1}{2}}$
14968.497	6678.872	2	I	$17073_{1} - 23752^{\circ}_{2}$
14960.529	6682.429	0	I	$22163^{\circ}_{4} - 28845_{4}$
14956.476	6684.240	2	I	$24561^{\circ}_{3} - 31245_{2}$

TABLE 1. *Infrared spectral lines of thorium*—Continued

Wavelength Å	Wavenumber cm^{-1}	Intensity	Spectrum	Classification	Wavelength Å	Wavenumber cm^{-1}	Intensity	Spectrum	Classification
14955.641	6684.613	1	I	$26096^{\circ}_{3} - 32781_{4}$	14740.403	6782.221	0	I	$24182^{\circ}_{2} - 30964_{3}$
14951.792	6686.334	1	I	$16346^{\circ}_{4} - 23032_{4}$	14739.988	6782.412	0		
14947.310	6688.339	2	I	$21539^{\circ}_{4} - 28227_{4}$	14736.470	6784.031	0	I	$17398_{3} - 24182^{\circ}_{2}$
14947.021	6688.468	1	I	$26048^{\circ}_{4} - 32737_{5}$	14719.449	6791.876	1	I	$23752^{\circ}_{2} - 30544_{2}$
14943.987	6689.826	6	I	$8800_{4} - 15490^{\circ}_{5}$	14718.799	6792.176	5	I	$19588^{\circ}_{5} - 26380_{5}$
14940.492	6691.391	7	II	$0_{1\,1/2} - 6691^{\circ}_{1\nu/2}$	14716.370	6793.297	2	I	$22141^{\circ}_{3} - 28934_{3}$
14939.197	6691.971	1	II	$12902^{\circ}_{1\nu/2} - 19594_{\nu/2}$	14714.650	6794.091	1		
14929.051	6696.519	3			14711.400	6795.592	1		
14928.485	6696.773	4	I	$11877^{\circ}_{1} - 18574_{1}$	14710.285	6796.107	1		
14925.498	6698.113	1			14702.750	6799.590	0		
14921.758	6699.792	0	I	$15970_{3} - 22669^{\circ}_{3}$	14699.723	6800.990	2	II	$16033^{\circ}_{2\nu/2} - 22834_{3\nu/2}$
14920.495	6700.359	3	II	$16818_{3\nu/2} - 23518^{\circ}_{3\nu/2}$	14695.579	6802.908	3	I	$21539^{\circ}_{4} - 28342_{5}$
14911.028	6704.613	2	I	$22399^{\circ}_{5} - 29104_{4}$	14690.666	6805.183	0	I	$21143_{5} - 27948^{\circ}_{4}$
14910.459	6704.869	2			14689.932	6805.523	0	I	$23481^{\circ}_{1} - 30286_{1}$
14899.905	6709.618	2	II	$15305_{4\nu/2} - 22014^{\circ}_{5\nu/2}$	14688.909	6805.997	0	I	$15863_{2} - 22669^{\circ}_{3}$
14889.079	6714.497	0			14687.576	6806.615	0	I	$22877^{\circ}_{5} - 29684_{5}$
14880.943	6718.168	0	I	$11241^{\circ}_{3} - 17959_{4}$	14680.667	6809.818	0	I	$17959_{4} - 24769^{\circ}_{3}$
14875.259	6720.735	1	I	$24421^{\circ}_{3} - 31141_{3}$	14677.249	6811.404	5	I	$11802_{2} - 18614^{\circ}_{1}$
14873.575	6721.496	1	I	$23113^{\circ}_{4} - 29835_{3}$	14672.400	6813.655	0	II	$18568^{\circ}_{\nu/2} - 25381_{1\nu/2}$
14866.776	6724.570	0			14665.680	6816.777	0		
14850.034	6732.151	0	I	$18574_{1} - 25306^{\circ}_{2}$	14661.334	6818.798	0	I	$21539^{\circ}_{4} - 28358_{3}$
14842.404	6735.612	0	I	$23113^{\circ}_{4} - 29849_{4}$	14654.914	6821.785	7	I	$11877^{\circ}_{1} - 18699_{2}$
14830.215	6741.148	3	I	$17959_{4} - 24701^{\circ}_{5}$	14651.482	6823.383	3	I	$20054_{2} - 26878^{\circ}_{3}$
14830.001	6741.245	1	I	$23015^{\circ}_{5} - 29756_{4}$	14644.393	6826.686	1	I	$18699_{2} - 25526^{\circ}_{1}$
14809.031	6750.791	2	I	$17166_{5} - 23916^{\circ}_{4}$	14638.811	6829.289	0	I	$20214^{\circ}_{3} - 27044_{3}$
14806.456	6751.965	5	I	$7280_{2} - 14032^{\circ}_{2}$	14638.217	6829.566	1	I	$20737^{\circ}_{1} - 27566_{2}$
14805.415	6752.440	3	I	$19503^{\circ}_{3} - 26255_{4}$	14633.086	6831.961	3	II	$13248_{4\nu/2} - 20080^{\circ}_{3\nu/2}$
14805.099	6752.584	1	I	$16554_{6} - 23306^{\circ}_{6}$	14628.703	6834.008	2	I	$23015^{\circ}_{5} - 29849_{4}$
14804.483	6752.865	0			14627.874	6834.395	4	II	$15305_{4\nu/2} - 22139^{\circ}_{4\nu/2}$
14797.874	6755.881	2			14624.891	6835.789	1		
14797.624	6755.995	0			14618.976	6838.555	7	I	$3687_{2} - 10526^{\circ}_{3}$
14796.452	6756.530	0	I	$20214^{\circ}_{3} - 26971_{4}$	14615.924	6839.983	1	I	$19273_{2} - 26113^{\circ}_{2}$
14795.403	6757.009	0			14609.166	6843.147	0		
14789.356	6759.772	1	I	$26036^{\circ}_{3} - 32796_{3}$	14604.155	6845.495	2	I	$24084^{\circ}_{6} - 30930_{6}$
14784.758	6761.874	1	I	$13962_{1} - 20724^{\circ}_{0}$	14603.558	6845.775	3	I	$15493_{4} - 22338^{\circ}_{3}$
14781.114	6763.541	0	I	$23609^{\circ}_{5} - 30372_{6}$	14603.174	6845.955	0	I	$18069^{\circ}_{3} - 24915_{3}$
14780.863	6763.656	0			14599.499	6847.678	1	I	$19948^{\circ}_{4} - 26796_{3}$
14777.907	6765.009	1	I	$22338^{\circ}_{3} - 29104_{4}$	14591.907	6851.241	1	I	$19039^{\circ}_{2} - 25890_{2}$
14777.230	6765.319	1	I	$24561^{\circ}_{3} - 31326_{4}$	14582.663	6855.584	1		
14772.419	6767.522	0	I	$24769^{\circ}_{3} - 31537_{3}$	14579.735	6856.961	6	II	$1521_{2\nu/2} - 8378^{\circ}_{3\nu/2}$
14772.031	6767.700	3	I	$25690^{\circ}_{5} - 32458_{4}$	14573.635	6859.831	2	I	$13088_{3} - 19948^{\circ}_{4}$
14769.918	6768.668	0			14570.349	6861.378	3	I	$17398_{3} - 24259^{\circ}_{4}$
14769.355	6768.926	1			14565.023	6863.887	0	II	$8460_{1\nu/2} - 15324^{\circ}_{\nu/2}$
14764.746	6771.039	2	I	$16217^{\circ}_{2} - 22988_{2}$	14563.856	6864.437	0		
14757.373	6774.422	0			14563.603	6864.556	0	I	$24381^{\circ}_{2} - 31245_{2}$
14756.630	6774.763	3	I	$13962_{1} - 20737^{\circ}_{1}$	14561.641	6865.481	1		
14751.515	6777.112	0	I	$20566^{\circ}_{4} - 27343_{3}$	14560.886	6865.837	0		
14747.581	6778.920	0			14557.004	6867.668	4	II	$10855_{3\nu/2} - 17722^{\circ}_{4\nu/2}$
14741.842	6781.559	0			14553.980	6869.095	1	I	$20322^{\circ}_{5} - 27191_{5}$
14741.329	6781.795	5	I	$11601_{1} - 18382^{\circ}_{0}$	14551.849	6870.101	0		

TABLE 1. *Infrared spectral lines of thorium*—Continued

Wavelength Å	Wavenumber cm^{-1}	Intensity	Spectrum	Classification	Wavelength Å	Wavenumber cm^{-1}	Intensity	Spectrum	Classification
14548.134	6871.855	2	I	$10526^{\circ}_{3} - 17398_{3}$	14343.260	6970.010	6	II	$4146_{3\frac{1}{2}} - 11116^{\circ}_{3\frac{1}{2}}$
14545.954	6872.885	2	I	$14204_{5} - 21077^{\circ}_{5}$	14340.036	6971.577	0	I	$22877^{\circ}_{5} - 29849_{4}$
14541.314	6875.078	1	I	$18431_{3} - 25306^{\circ}_{2}$	14339.066	6972.049	2	II	$9061_{2\frac{1}{2}} - 16033^{\circ}_{2\frac{1}{2}}$
14533.419	6878.813	4	I	$22877^{\circ}_{5} - 29756_{4}$	14326.032	6978.392	1	I	$22163^{\circ}_{4} - 29141_{5}$
14519.935	6885.201	2	I	$15970_{3} - 22855^{\circ}_{3}$	14324.702	6979.040	0	I	$9804_{5} - 16783^{\circ}_{4}$
14510.851	6889.511	0	I	$13847_{2} - 20737^{\circ}_{1}$	14323.255	6979.745	1	I	$22855^{\circ}_{3} - 29835_{3}$
14508.948	6890.415	1	II	$19880_{4\frac{1}{2}} - 26770^{\circ}_{5\frac{1}{2}}$	14322.367	6980.178	1		
14503.235	6893.129	6	II	$10379_{4\frac{1}{2}} - 17272^{\circ}_{4\frac{1}{2}}$	14313.992	6984.262	4	I	$10414^{\circ}_{4} - 17398_{3}$
14502.932	6893.273	1	I	$18549_{2} - 25442^{\circ}_{3}$	14306.560	6987.890	2	I	$17411^{\circ}_{3} - 24399_{3}$
14501.117	6894.136	0			14297.496	6992.320	0	I	$21890^{\circ}_{3} - 28882_{2}$
14500.307	6894.521	1			14296.656	6992.731	2	I	$18930^{\circ}_{3} - 25923_{4}$
14493.424	6897.795	2	I	$23113^{\circ}_{4} - 30011_{3}$	14294.346	6993.861	0	I	$22855^{\circ}_{3} - 29849_{4}$
14491.248	6898.831	1	I	$23609^{\circ}_{5} - 30508_{5}$	14289.338	6996.312	1		
14487.168	6900.774	0			14287.043	6997.436	0		
14482.670	6902.917	0			14283.487	6999.178	1	I	$23015^{\circ}_{5} - 30014_{4}$
14476.391	6905.911	0	I	$24421^{\circ}_{3} - 31326_{4}$	14281.708	7000.050	0		
14475.836	6906.176	4	I	$15493_{4} - 22399^{\circ}_{5}$	14275.223	7003.230	0	II	$4113_{2\frac{1}{2}} - 11116^{\circ}_{3\frac{1}{2}}$
14472.395	6907.818	1	II	$20686^{\circ}_{2\frac{1}{2}} - 27593_{2\frac{1}{2}}$	14271.876	7004.872	1	I	$24769^{\circ}_{3} - 31774_{3}$
14469.188	6909.349	2	I	$17398_{3} - 24307^{\circ}_{2}$	14270.962	7005.321	1	I	$23752^{\circ}_{2} - 30758_{2}$
14467.109	6910.342	0	I	$22508^{\circ}_{2} - 29418_{2}$	14266.229	7007.645	1		
14462.402	6912.591	0	II	$16818_{3\frac{1}{2}} - 23730^{\circ}_{4\frac{1}{2}}$	14262.156	7009.646	0		
14461.502	6913.021	0			14259.243	7011.078	5	I	$19986^{\circ}_{6} - 26997_{6}$
14452.427	6917.362	0	I	$23093^{\circ}_{2} - 30011_{3}$	14254.713	7013.306	5	I	$11601_{1} - 18614^{\circ}_{1}$
14452.147	6917.496	2	I	$13297_{4} - 20214^{\circ}_{3}$	14254.065	7013.625	0	I	$15863_{2} - 22877^{\circ}_{1}$
14451.758	6917.682	4	I	$3865_{1} - 10783^{\circ}_{2}$	14253.783	7013.764	1	I	$19273_{2} - 26287^{\circ}_{1}$
14449.799	6918.620	1	I	$25877^{\circ}_{4} - 32796_{3}$	14249.904	7015.673	0		
14449.350	6918.835	2	I	$17166_{5} - 24084^{\circ}_{6}$	14247.867	7016.676	0		
14441.112	6922.782	0			14244.211	7018.477	2	I	$15618^{\circ}_{3} - 22637_{3}$
14438.799	6923.891	3	I	$18431_{3} - 25355^{\circ}_{4}$	14239.881	7020.611	1	I	$21252^{\circ}_{2} - 28273_{2}$
14433.541	6926.413	1	II	$8378^{\circ}_{3\frac{1}{2}} - 15305_{4\frac{1}{2}}$	14238.660	7021.213	2	I	$17959_{4} - 24981^{\circ}_{3}$
14424.537	6930.737	7	I	$16346^{\circ}_{4} - 23277_{5}$	14237.955	7021.561	1	I	$22396^{\circ}_{1} - 29418_{2}$
14423.392	6931.287	2	I	$15166^{\circ}_{3} - 22098_{4}$	14235.729	7022.659	2	I	$17398_{3} - 24421^{\circ}_{3}$
14412.536	6936.508	4	I	$14206^{\circ}_{4} - 21143_{5}$	14234.902	7023.067	2	I	$19948^{\circ}_{4} - 26971_{4}$
14407.785	6938.795	1	I	$19713_{3} - 26651^{\circ}_{2}$				I	$21539^{\circ}_{4} - 28562_{4}$
14403.474	6940.872	1	I	$22163^{\circ}_{4} - 29104_{4}$	14233.051	7023.980	0	I	$24769^{\circ}_{3} - 31793_{4}$
14403.132	6941.037	0	I	$23603^{\circ}_{2} - 30544_{2}$	14231.327	7024.831	4	I	$13297_{4} - 20322^{\circ}_{5}$
14398.454	6943.292	2	I	$21902^{\circ}_{4} - 28845_{4}$	14230.620	7025.180	0	I	$20566^{\circ}_{4} - 27591_{5}$
14393.566	6945.650	0			14230.460	7025.259	0	I	$22396^{\circ}_{1} - 29422_{1}$
14382.181	6951.148	1			14224.305	7028.299	0		
14374.424	6954.899	2	I	$20566^{\circ}_{4} - 27521_{4}$	14220.096	7030.379	1		
14373.329	6955.429	1	I	$21890^{\circ}_{3} - 28845_{4}$	14217.138	7031.842	1	I	$24981^{\circ}_{3} - 32012_{4}$
14370.393	6956.850	0	I	$21077^{\circ}_{5} - 28034_{5}$	14214.389	7033.202	0	I	$20054_{2} - 27087^{\circ}_{1}$
14368.039	6957.990	0			14209.924	7035.412	1		
14367.834	6958.089	0			14202.775	7038.953	0		
14364.711	6959.602	2	I	$13962_{1} - 20922^{\circ}_{2}$	14192.323	7044.137	4	I	$20522^{\circ}_{2} - 27566_{2}$
14363.687	6960.098	2	I	$18930^{\circ}_{3} - 25890_{2}$	14191.050	7044.769	2	I	$21890^{\circ}_{3} - 28934_{3}$
14360.388	6961.697	0	II	$15144^{\circ}_{1\frac{1}{2}} - 22106_{2\frac{1}{2}}$	14189.283	7045.646	0	I	$20566^{\circ}_{4} - 27612_{3}$
14358.938	6962.400	2	I	$22141^{\circ}_{3} - 29104_{4}$	14188.681	7045.945	0		
14357.839	6962.933	3	I	$7502_{3} - 14465^{\circ}_{2}$	14187.489	7046.537	2	I	$25690^{\circ}_{5} - 32737_{5}$
14355.909	6963.869	0	I	$7280_{2} - 14243^{\circ}_{1}$	14170.625	7054.923	0	I	$16554_{6} - 23609^{\circ}_{5}$

TABLE 1. *Infrared spectral lines of thorium*—Continued

Wavelength Å	Wavenumber cm^{-1}	Intensity	Spectrum	Classification	Wavelength Å	Wavenumber cm^{-1}	Intensity	Spectrum	Classification
14168.671	7055.896	7	I	$8111_4 - 15166^{\circ}_3$	13904.491	7189.955	6	I	$11241^{\circ}_3 - 18431_3$
14160.194	7060.120	1	I	$24981^{\circ}_3 - 32041_2$	13898.031	7193.297	1	I	$21165^{\circ}_3 - 28358_3$
14159.556	7060.438	0	II	$13250_{2\frac{1}{2}} - 20310^{\circ}_{2\frac{1}{2}}$	13895.433	7194.642	3	II	$9711_{3\frac{1}{2}} - 16906^{\circ}_{3\frac{1}{2}}$
14154.750	7062.835	0	I	$21165^{\circ}_3 - 28227_4$	13891.459	7196.700	0		
14148.646	7065.882	2	I	$23306^{\circ}_6 - 30372_6$	13886.527	7199.256	4	I	$20322^{\circ}_5 - 27521_4$
14113.635	7083.410	0			13882.834	7201.171	1	I	$23306^{\circ}_6 - 30508_5$
14107.467	7086.507	1	I	$22669^{\circ}_3 - 29756_4$	13872.468	7206.552	0	I	$25575^{\circ}_4 - 32781_4$
14101.396	7089.558	3	I	$20522^{\circ}_2 - 27612_3$	13862.050	7211.968	0	I	$23752^{\circ}_2 - 30964_3$
14100.879	7089.818	2	I	$19273_2 - 26363^{\circ}_2$	13861.889	7212.052	0		
14095.249	7092.650	1	I	$24701^{\circ}_5 - 31793_4$	13859.106	7213.500	1	I	$21668^{\circ}_1 - 28882_2$
14090.246	7095.168	7	I	$3687_2 - 10783^{\circ}_2$	13844.566	7221.076	0	I	$25575^{\circ}_4 - 32796_3$
14083.851	7098.390	0			13836.909	7225.072	0	II	$15786_{2\frac{1}{2}} - 23012^{\circ}_{1\frac{1}{2}}$
14079.818	7100.423	5	I	$12847_3 - 19948^{\circ}_4$	13828.453	7229.490	1	I	$24307^{\circ}_2 - 31537_3$
14073.329	7103.697	2			13828.057	7229.697	1		
14070.742	7105.003	5	II	$8605_{2\frac{1}{2}} - 15710^{\circ}_{1\frac{1}{2}}$	13827.979	7229.738	1		
14070.200	7105.277	3			13822.377	7232.668	0	II	$9585^{\circ}_{2\frac{1}{2}} - 16818_{3\frac{1}{2}}$
14063.614	7108.604	2	I	$17166_5 - 24274^{\circ}_5$	13818.508	7234.693	1	I	$18574_1 - 25809^{\circ}_1$
14061.486	7109.680	0	I	$18699_2 - 25809^{\circ}_1$	13815.598	7236.217	1	I	$11802_2 - 19039^{\circ}_2$
14061.215	7109.817	1	I	$14465^{\circ}_2 - 21575_2$	13814.181	7236.959	0	I	$23521^{\circ}_3 - 30758_2$
14054.652	7113.137	1	I	$18809^{\circ}_4 - 25923_4$	13813.983	7237.063	0		
14054.140	7113.396	2			13813.265	7237.439	0	I	$23049^{\circ}_1 - 30286_1$
14053.546	7113.697	1			13811.481	7238.374	4	II	$20288^{\circ}_{5\frac{1}{2}} - 27526_{4\frac{1}{2}}$
14052.066	7114.446	0			13809.796	7239.257	1	I	$21902^{\circ}_4 - 29141_5$
14043.929	7118.568	1	II	$15236_{1\frac{1}{2}} - 22355^{\circ}_{1\frac{1}{2}}$	13799.139	7244.848	0	I	$25306^{\circ}_2 - 32551_3$
14038.143	7121.502	0	I	$24307^{\circ}_2 - 31429_1$	13795.378	7246.823	1	I	$24182^{\circ}_2 - 31429_1$
14032.419	7124.407	1	I	$24202^{\circ}_4 - 31326_4$	13792.422	7248.376	5	I	$16783^{\circ}_4 - 24032_4$
14030.586	7125.338	0			13788.405	7250.488	1	II	$8460_{1\frac{1}{2}} - 15710^{\circ}_{1\frac{1}{2}}$
14028.560	7126.367	4	I	$13088_3 - 20214^{\circ}_3$	13787.653	7250.883	1		
14028.205	7126.547	3	II	$8018_{1\frac{1}{2}} - 15144^{\circ}_{1\frac{1}{2}}$	13786.380	7251.553	1	I	$15736^{\circ}_1 - 22988_2$
14027.270	7127.022	0			13779.592	7255.125	1	I	$22877^{\circ}_1 - 30132_2$
14026.605	7127.360	5	I	$11802_2 - 18930^{\circ}_3$	13778.916	7255.481	6	II	$6213_{4\frac{1}{2}} - 13468^{\circ}_{4\frac{1}{2}}$
14025.216	7128.066	2	II	$10855_{3\frac{1}{2}} - 17983^{\circ}_{2\frac{1}{2}}$	13777.235	7255.366	1	II	$12902^{\circ}_{1\frac{1}{2}} - 20158_{2\frac{1}{2}}$
14022.503	7129.445	0			13774.118	7258.008	1	I	$19532_4 - 26790^{\circ}_4$
14008.158	7136.746	0	I	$22877^{\circ}_5 - 30014_4$	13760.203	7265.348	2	I	$21077^{\circ}_5 - 28342_5$
14007.683	7136.988	1	II	$20120^{\circ}_{2\frac{1}{2}} - 27257_{3\frac{1}{2}}$	13757.224	7266.921	0		
14007.173	7137.248	0	I	$23752^{\circ}_2 - 30889_1$	13756.558	7267.273	2		
13995.011	7143.450	0	I	$15970_3 - 23113^{\circ}_4$	13752.928	7269.191	2	I	$13297_4 - 20566^{\circ}_4$
13993.145	7144.403	1	I	$21738^{\circ}_2 - 28882_2$	13752.277	7269.535	0	I	$20322^{\circ}_5 - 27591_5$
13976.090	7153.121	2	I	$22399^{\circ}_5 - 29552_6$	13748.535	7271.514	0	I	$24769^{\circ}_3 - 32041_2$
13975.932	7153.202	4	I	$19227^{\circ}_6 - 26380_5$	13748.149	7271.718	2	I	$18431_3 - 25703^{\circ}_2$
13974.383	7153.995	1	I	$18549_2 - 25703^{\circ}_2$	13746.311	7272.690	0		
13972.014	7155.208	1	II	$10572^{\circ}_{4\frac{1}{2}} - 17727_{5\frac{1}{2}}$	13745.894	7272.911	0	I	$25690^{\circ}_5 - 32963_5$
13970.381	7156.044	2	I	$22855^{\circ}_3 - 30011_3$	13739.956	7276.054	5	I	$18614^{\circ}_1 - 25890_2$
13964.777	7158.916	2	I	$12114^{\circ}_2 - 19273_2$	13738.583	7276.781	3	I	$22141^{\circ}_3 - 29418_2$
13957.824	7162.482	0			13735.446	7278.443	2	I	$21252^{\circ}_2 - 28531_2$
13950.984	7165.994	0			13734.218	7279.094	2	I	$19516^{\circ}_2 - 26796_3$
13936.736	7173.320	5	I	$20322^{\circ}_5 - 27495_4$	13731.271	7280.656	2	I	$20214^{\circ}_3 - 27495_4$
13930.234	7176.668	3	I	$15493_4 - 22669^{\circ}_3$	13729.372	7281.663	2		
13928.452	7177.586	1			13728.599	7282.073	0		
13927.042	7178.313	0			13727.340	7282.741	1	I	$19713_3 - 26995^{\circ}_3$

TABLE 1. *Infrared spectral lines of thorium*—Continued

Wavelength Å	Wavenumber cm^{-1}	Intensity	Spectrum	Classification
13723.460	7284.800	0	I	$22399^{\circ}_{5} - 29684_{5}$
13719.712	7286.790	2		
13709.552	7292.190	1	II	$22139^{\circ}_{4\frac{1}{2}} - 29431_{3\frac{1}{2}}$
13699.211	7297.695	3	II	$23187^{\circ}_{6\frac{1}{2}} - 30484_{5\frac{1}{2}}$
13680.790	7307.521	0	I	$17073_{1} - 24381^{\circ}_{2}$
13680.494	7307.679	1	I	$11241^{\circ}_{3} - 18549_{2}$
13677.064	7309.512	2	I	$23655^{\circ}_{4} - 30964_{3}$
13672.580	7311.909	0	I	$24701^{\circ}_{5} - 32012_{4}$
13672.490	7311.957	0	I	$22338^{\circ}_{3} - 29650_{2}$
13668.402	7314.144	0	I	$25753^{\circ}_{5} - 33068_{6}$
13665.979	7315.441	0	II	$14790^{\circ}_{3\frac{1}{2}} - 22106_{2\frac{1}{2}}$
13664.755	7316.096	1		
13664.604	7316.177	3	II	$7828_{\frac{1}{2}} - 15144^{\circ}_{1\frac{1}{2}}$
13662.574	7317.264	2	I	$17354^{\circ}_{1} - 24671_{2}$
13662.466	7317.322	1	I	$13847_{2} - 21165^{\circ}_{3}$
13654.606	7321.534	0	II	$18118_{1\frac{1}{2}} - 25440^{\circ}_{2\frac{1}{2}}$
13647.606	7325.289	5	I	$18930^{\circ}_{3} - 26255_{4}$
13636.063	7331.490	5	II	$0_{1\,1/2} - 7331^{\circ}_{2\frac{1}{2}}$
13630.233	7334.626	2		
13628.932	7335.326	1	I	$14204_{5} - 21539^{\circ}_{4}$
13626.318	7336.733	1		
13626.116	7336.842	4	II	$15305_{4\frac{1}{2}} - 22642^{\circ}_{4\frac{1}{2}}$
13618.580	7340.902	0		
13612.012	7344.444	0	I	$22669^{\circ}_{3} - 30014_{4}$
13609.614	7345.738	2	I	$19532_{4} - 26878^{\circ}_{3}$
13603.594	7348.989	1		
13602.938	7349.343	0		
13599.702	7351.092	3	I	$20922^{\circ}_{2} - 28273_{2}$
13598.599	7351.688	3	I	$24850^{\circ}_{6} - 32202_{5}$
13598.305	7351.847	1		
13598.167	7351.922	2	I	$20214^{\circ}_{3} - 27566_{2}$
13597.830	7352.104	1	I	$24274^{\circ}_{5} - 31626_{5}$
13595.363	7353.438	0	I	$25442^{\circ}_{3} - 32796_{3}$
13592.829	7354.809	0	I	$24182^{\circ}_{2} - 31537_{3}$
13589.496	7356.613	0		
13588.783	7356.999	4	I	$22399^{\circ}_{5} - 29756_{4}$
13587.748	7357.559	0	I	$23015^{\circ}_{5} - 30372_{6}$
13584.089	7359.541	0		
13582.026	7360.659	0	II	$22513^{\circ}_{2\frac{1}{2}} - 29873_{3\frac{1}{2}}$
13579.485	7362.036	2		
13579.410	7362.077	4	I	$15493_{4} - 22855^{\circ}_{3}$
13579.201	7362.190	0		
13572.266	7365.952	0	I	$21165^{\circ}_{3} - 28531_{2}$
13570.411	7366.959	3	I	$12847_{3} - 20214^{\circ}_{3}$
13565.665	7369.536	7	I	$15618^{\circ}_{3} - 22988_{2}$
13562.388	7371.317	2	I	$17398_{3} - 24769^{\circ}_{3}$
13553.046	7376.398	0		
13551.673	7377.145	0		
13549.102	7378.545	2	I	$19273_{2} - 26651^{\circ}_{2}$
13544.406	7381.103	1	II	$15453^{\circ}_{3\frac{1}{2}} - 22834_{3\frac{1}{2}}$
13540.748	7383.097	3	I	$19588^{\circ}_{5} - 26971_{4}$
13538.429	7384.362	2	I	$15493_{4} - 22877^{\circ}_{5}$
13532.204	7387.759	2	I	$14206^{\circ}_{4} - 21594_{3}$
13529.689	7389.132	1	I	$16351_{0} - 23741^{\circ}_{1}$
13524.811	7391.797	1	II	$12488^{\circ}_{4\frac{1}{2}} - 19880_{4\frac{1}{2}}$
13520.057	7394.396	1	II	$12485^{\circ}_{3\frac{1}{2}} - 19880_{4\frac{1}{2}}$
13518.143	7395.443	6	I	$11877^{\circ}_{1} - 19273_{2}$
13517.712	7395.679	2	I	$17959_{4} - 25355^{\circ}_{4}$
13514.671	7397.343	1	I	$20214^{\circ}_{3} - 27612_{3}$
13508.886	7400.511	0	I	$25336^{\circ}_{6} - 32737_{5}$
13503.654	7403.378	0		
13501.001	7404.833	4	I	$13847_{2} - 21252^{\circ}_{2}$
13498.256	7406.339	0		
13494.985	7408.134	0	II	$8378^{\circ}_{3\frac{1}{2}} - 15786_{2\frac{1}{2}}$
13493.439	7408.983	4		
13491.454	7410.073	1	I	$23916^{\circ}_{4} - 31326_{4}$
13487.329	7412.339	0		
13484.963	7413.640	1	I	$18699_{2} - 26113^{\circ}_{2}$
13484.304	7414.002	3	I	$15618^{\circ}_{3} - 23032_{4}$
13483.659	7414.357	3		
13478.127	7417.400	0	I	$22338^{\circ}_{3} - 29756_{4}$
13468.267	7422.830	0		
13465.671	7424.261	0	I	$24202^{\circ}_{4} - 31626_{5}$
13461.947	7426.315	0		
13460.761	7426.969	1		
13460.143	7427.310	3	II	$8605_{2\frac{1}{2}} - 16033^{\circ}_{2\frac{1}{2}}$
13449.197	7433.355	4	I	$10526^{\circ}_{3} - 17959_{4}$
13448.036	7433.997	1	I	$24561^{\circ}_{3} - 31995_{4}$
13447.755	7434.152	4	I	$13088_{3} - 20522^{\circ}_{2}$
13447.160	7434.481	0		
13445.057	7435.644	0	II	$13250_{2\frac{1}{2}} - 20686^{\circ}_{2\frac{1}{2}}$
13443.925	7436.270	4	I	$20922^{\circ}_{2} - 28358_{3}$
13440.583	7438.119	4	I	$11601_{1} - 19039^{\circ}_{2}$
13439.085	7438.948	1	I	$14206^{\circ}_{4} - 21645_{4}$
13436.414	7440.427	0	I	$17224^{\circ}_{2} - 24664_{3}$
13433.332	7442.134	3	I	$14226_{0} - 21668^{\circ}_{1}$
13429.635	7444.183	1		
13427.136	7445.568	3	II	$10673^{\circ}_{2\frac{1}{2}} - 18118_{1\frac{1}{2}}$
13426.907	7445.695	3	I	$18809^{\circ}_{4} - 26255_{4}$
13426.686	7445.818	2	I	$18431_{3} - 25877^{\circ}_{4}$
13425.849	7446.282	0	II	$20080^{\circ}_{3\frac{1}{2}} - 27526_{4\frac{1}{2}}$
13423.480	7447.596	2	I	$17224^{\circ}_{2} - 24671_{2}$
13421.280	7448.817	0		
13419.576	7449.763	4	I	$22399^{\circ}_{5} - 29849_{4}$
13418.102	7450.581	0	I	$23093^{\circ}_{2} - 30544_{2}$
13404.943	7457.895	4	I	$11241^{\circ}_{3} - 18699_{2}$
13400.553	7460.338	0		
13395.691	7463.046	4	II	$4113_{2\frac{1}{2}} - 11576^{\circ}_{1\frac{1}{2}}$
13395.136	7463.355	1	I	$19532_{4} - 26995^{\circ}_{3}$
13391.987	7465.110	0		

TABLE 1. *Infrared spectral lines of thorium*—Continued

Wavelength Å	Wavenumber cm^{-1}	Intensity	Spectrum	Classification	Wavelength Å	Wavenumber cm^{-1}	Intensity	Spectrum	Classification
13387.914	7467.381	0	I	$20566^{\circ}_{4} - 28034_{5}$	13247.730	7546.399	4	I	$8800_{4} - 16346^{\circ}_{4}$
13386.236	7468.317	2	I	$19503^{\circ}_{3} - 26971_{4}$	13246.336	7547.193	0	I	$19948^{\circ}_{4} - 27495_{4}$
13382.214	7470.562	4	I	$15166^{\circ}_{3} - 22637_{3}$	13245.664	7547.576	2	I	$18549_{2} - 26096^{\circ}_{3}$
13376.396	7473.811	0	II	$20120^{\circ}_{2\frac{1}{2}} - 27593_{2\frac{1}{2}}$	13241.997	7549.666	0	II	$12570_{3\frac{1}{2}} - 20120^{\circ}_{2\frac{1}{2}}$
13373.859	7475.229	3			13239.744	7550.951	4	I	$15970_{3} - 23521^{\circ}_{3}$
13370.573	7477.066	1	I	$24981^{\circ}_{3} - 32458_{4}$	13236.164	7552.993	3	I	$19713_{3} - 27266^{\circ}_{4}$
13370.190	7477.280	2	II	$19880_{4\frac{1}{2}} - 27357^{\circ}_{4\frac{1}{2}}$	13234.852	7553.742	2	I	$3687_{2} - 11241^{\circ}_{3}$
13368.792	7478.062	6	I	$13088_{3} - 20566^{\circ}_{4}$	13230.970	7555.958	0		
13367.083	7479.018	1			13223.385	7560.292	3	II	$9711_{3\frac{1}{2}} - 17272^{\circ}_{4\frac{1}{2}}$
13360.349	7482.788	0	I	$17959_{4} - 25442^{\circ}_{3}$	13222.361	7560.878	0	II	$14545^{\circ}_{2\frac{1}{2}} - 22106_{2\frac{1}{2}}$
13355.490	7485.510	0	I	$21077^{\circ}_{5} - 28562_{4}$	13219.366	7562.591	0	I	$14032^{\circ}_{2} - 21594_{3}$
13353.446	7486.656	0	I	$23655^{\circ}_{4} - 31141_{3}$	13217.149	7563.859	0	I	$18549_{2} - 26113^{\circ}_{2}$
13352.939	7486.940	0	I	$18549_{2} - 26036^{\circ}_{3}$	13216.178	7564.415	1	I	$21539^{\circ}_{4} - 29104_{4}$
13350.017	7488.579	1			13215.207	7564.971	0	I	$22396^{\circ}_{1} - 29961_{1}$
13348.625	7489.360	1	I	$25306^{\circ}_{2} - 32796_{3}$	13205.290	7570.652	6	I	$18809^{\circ}_{4} - 26380_{5}$
13342.411	7492.848	1	I	$23015^{\circ}_{5} - 30508_{5}$	13202.889	7572.029	1	I	$24202^{\circ}_{4} - 31774_{3}$
13336.712	7496.050	3	I	$22338^{\circ}_{3} - 29835_{3}$	13200.969	7573.130	1	I	$19948^{\circ}_{4} - 27521_{4}$
13334.671	7497.197	1	I	$18614^{\circ}_{1} - 26111_{1}$	13199.517	7573.963	0		
13322.946	7503.795	0	I	$17411^{\circ}_{3} - 24915_{3}$	13198.322	7574.649	0		
13319.676	7505.637	1	II	$9400_{2\frac{1}{2}} - 16906^{\circ}_{3\frac{1}{2}}$	13188.919	7580.049	2	II	$9238^{\circ}_{4\frac{1}{2}} - 16818_{3\frac{1}{2}}$
13315.518	7507.981	1	I	$8111_{4} - 15618^{\circ}_{3}$	13185.440	7582.049	0		
13314.704	7508.440	1	I	$24421^{\circ}_{3} - 31929_{3}$	13184.286	7582.713	2	I	$17398_{3} - 24981^{\circ}_{3}$
13311.623	7510.178	2	II	$12570_{3\frac{1}{2}} - 20080^{\circ}_{3\frac{1}{2}}$	13183.941	7582.911	3	I	$6362_{2} - 13945^{\circ}_{3}$
13310.052	7511.064	1	II	$20120^{\circ}_{2\frac{1}{2}} - 27631_{1\frac{1}{2}}$	13183.783	7583.002	3	I	$15618^{\circ}_{3} - 23201_{3}$
13306.095	7513.298	2	II	$20080^{\circ}_{3\frac{1}{2}} - 27593_{2\frac{1}{2}}$	13179.568	7585.427	0		
13304.846	7514.003	2	II	$19248^{\circ}_{2\frac{1}{2}} - 26762_{1\frac{1}{2}}$	13179.277	7585.595	0	II	$15786_{2\frac{1}{2}} - 23372^{\circ}_{1\frac{1}{2}}$
13303.409	7514.815	1	I	$24259^{\circ}_{4} - 31774_{3}$	13176.103	7587.422	2	I	$18699_{2} - 26287^{\circ}_{1}$
13296.036	7518.982	1	I	$24274^{\circ}_{5} - 31793_{4}$	13171.565	7590.036	0		
13292.355	7521.064	0	I	$22163^{\circ}_{4} - 29684_{5}$	13169.665	7591.131	0	I	$24202^{\circ}_{4} - 31793_{4}$
13290.823	7521.931	1	I	$15493_{4} - 23015^{\circ}_{5}$	13168.345	7591.892	0	I	$24421^{\circ}_{3} - 32012_{4}$
13289.735	7522.547	0			13167.879	7592.161	0	I	$24182^{\circ}_{2} - 31774_{3}$
13288.387	7523.310	1	II	$17722^{\circ}_{4\frac{1}{2}} - 25246_{4\frac{1}{2}}$	13156.601	7598.669	1	I	$12114^{\circ}_{2} - 19713_{3}$
13286.526	7524.364	0	I	$25575^{\circ}_{4} - 33099_{3}$	13150.947	7601.936	1	I	$21539^{\circ}_{4} - 29141_{5}$
13283.226	7526.233	1	II	$21297^{\circ}_{2\frac{1}{2}} - 28823_{2\frac{1}{2}}$	13146.765	7604.354	1	I	$19713_{3} - 27317^{\circ}_{3}$
13281.453	7527.238	4	I	$19516^{\circ}_{2} - 27044_{3}$	13146.229	7604.664	1	I	$18431_{3} - 26036^{\circ}_{3}$
13279.662	7528.253	0	I	$21890^{\circ}_{3} - 29418_{2}$	13145.904	7604.852	7	II	$6213_{4\frac{1}{2}} - 13818^{\circ}_{3\frac{1}{2}}$
13278.433	7528.950	0			13144.547	7605.637	1	I	$19986^{\circ}_{6} - 27591_{5}$
13275.351	7530.698	5	I	$16554_{6} - 24084^{\circ}_{6}$	13142.940	7606.567	2		
13271.329	7532.980	0			13136.162	7610.492	0	I	$23655^{\circ}_{4} - 31265_{3}$
13269.677	7533.918	1	I	$24259^{\circ}_{4} - 31793_{4}$	13130.308	7613.885	1	II	$22106_{2\frac{1}{2}} - 29720^{\circ}_{1\frac{1}{2}}$
13268.368	7534.661	0			13128.501	7614.933	2	I	$22399^{\circ}_{5} - 30014_{4}$
13267.880	7534.938	2	I	$17166_{5} - 24701^{\circ}_{5}$	13127.923	7615.268	5	I	$16783^{\circ}_{4} - 24399_{3}$
13263.633	7537.351	2	I	$23015^{\circ}_{5} - 30552_{4}$	13126.998	7615.805	1	II	$9202^{\circ}_{3\frac{1}{2}} - 16818_{3\frac{1}{2}}$
13262.164	7538.186	2	II	$10189^{\circ}_{5\frac{1}{2}} - 17727_{5\frac{1}{2}}$	13126.337	7616.188	0	I	$20054_{2} - 27670^{\circ}_{3}$
13261.338	7538.655	0	I	$18574_{1} - 26113^{\circ}_{2}$	13124.108	7617.482	1	I	$15863_{2} - 23481^{\circ}_{1}$
13257.081	7541.076	3	I	$19503^{\circ}_{3} - 27044_{3}$	13120.544	7619.551	1	I	$20054_{2} - 27674^{\circ}_{2}$
13253.863	7542.907	5	I	$15490^{\circ}_{5} - 23032_{4}$	13119.476	7620.171	1	I	$24421^{\circ}_{3} - 32041_{2}$
13251.713	7544.131	2	II	$7001_{1\frac{1}{2}} - 14545^{\circ}_{2\frac{1}{2}}$	13116.755	7621.752	1	I	$24307^{\circ}_{2} - 31929_{3}$
13250.406	7544.875	1	I	$2869_{3} - 10414^{\circ}_{4}$	13115.845	7622.281	0		
13248.848	7545.762	2	I	$10414^{\circ}_{4} - 17959_{4}$	13111.862	7624.596	0	I	$22508^{\circ}_{2} - 30132_{2}$

TABLE 1. *Infrared spectral lines of thorium*—Continued

Wavelength Å	Wavenumber cm^{-1}	Intensity	Spectrum	Classification	Wavelength Å	Wavenumber cm^{-1}	Intensity	Spectrum	Classification
13107.912	7626.894	1	I	$25336^{\circ}_{6} - 32963_{5}$	12949.037	7720.470	1	I	$16554_{6} - 24274^{\circ}_{5}$
13103.036	7629.732	0	I	$13945^{\circ}_{3} - 21575_{2}$	12948.255	7720.936	0	I	$24274^{\circ}_{5} - 31995_{4}$
13102.832	7629.851	1	I	$21252^{\circ}_{2} - 28882_{2}$	12940.934	7725.304	2		
13101.858	7630.418	1	I	$22877^{\circ}_{5} - 30508_{5}$	12940.654	7725.471	7	II	$1859_{1\frac{1}{2}} - 9585^{\circ}_{2\frac{1}{2}}$
13101.123	7630.846	2			12939.572	7726.117	1		
13092.193	7636.051	1			12938.933	7726.499	2	I	$8243^{\circ}_{2} - 15970_{3}$
13079.586	7643.411	1	I	$19948^{\circ}_{4} - 27591_{5}$	12936.840	7727.749	1	I	$19532_{4} - 27260^{\circ}_{3}$
13070.834	7648.529	6	I	$10783^{\circ}_{2} - 18431_{3}$	12935.233	7728.709	3	I	$18382^{\circ}_{0} - 26111_{1}$
13069.399	7649.369	3	I	$13945^{\circ}_{3} - 21594_{3}$	12934.697	7729.029	0		
13063.724	7652.692	0			12933.760	7729.589	1	I	$20054_{2} - 27784^{\circ}_{2}$
13062.628	7653.334	1			12933.539	7729.721	5	II	$4490^{\circ}_{2\frac{1}{2}} - 12219_{1\frac{1}{2}}$
13058.026	7656.031	0			12932.107	7730.577	2	I	$17959_{4} - 25690^{\circ}_{5}$
13056.097	7657.162	2	I	$15863_{2} - 23521^{\circ}_{3}$	12930.664	7731.440	1	II	$15786_{2\frac{1}{2}} - 23518^{\circ}_{3\frac{1}{2}}$
13055.889	7657.284	6	I	$2869_{3} - 10526^{\circ}_{3}$	12930.425	7731.583	1	I	$25336^{\circ}_{6} - 33068_{6}$
13049.034	7661.307	2	I	$20566^{\circ}_{4} - 28227_{4}$	12925.892	7734.294	3		
13048.139	7661.832	1	I	$23609^{\circ}_{5} - 31271_{5}$	12925.197	7734.710	1	I	$19713_{3} - 27447^{\circ}_{2}$
13045.340	7663.476	1	I	$18699_{2} - 26363^{\circ}_{2}$	12924.885	7734.897	0		
13044.181	7664.157	1			12923.256	7735.872	0	I	$24259^{\circ}_{4} - 31995_{4}$
13043.407	7664.612	4	I	$7502_{3} - 15166^{\circ}_{3}$	12921.032	7737.203	3		
13042.243	7665.296	0			12920.304	7737.639	0	I	$18549_{2} - 26287^{\circ}_{1}$
13034.773	7669.689	2	I	$6362_{2} - 14032^{\circ}_{2}$	12919.299	7738.241	3	I	$24274^{\circ}_{5} - 32012_{4}$
13031.133	7671.831	3	I	$23655^{\circ}_{4} - 31326_{4}$	12916.981	7739.630	4	I	$15863_{2} - 23603^{\circ}_{2}$
13030.257	7672.347	0	I	$22338^{\circ}_{3} - 30011_{3}$	12911.946	7742.648	1		
13029.053	7673.056	0	II	$12485^{\circ}_{3\frac{1}{2}} - 20158_{2\frac{1}{2}}$	12901.919	7748.665	2	II	$9711_{3\frac{1}{2}} - 17460^{\circ}_{2\frac{1}{2}}$
13026.187	7674.744	6	I	$12847_{3} - 20522^{\circ}_{2}$	12900.246	7749.670	2	I	$19817^{\circ}_{1} - 27566_{2}$
13023.092	7676.568	1	I	$23752^{\circ}_{2} - 31429_{1}$	12898.865	7750.500	4	I	$20522^{\circ}_{2} - 28273_{2}$
13016.640	7680.373	5	II	$1521_{2\frac{1}{2}} - 9202^{\circ}_{3\frac{1}{2}}$	12888.182	7756.924	2	I	$19039^{\circ}_{2} - 26796_{3}$
13013.722	7682.095	1			12881.709	7760.822	0	I	$21890^{\circ}_{3} - 29650_{2}$
13010.439	7684.034	1	I	$21738^{\circ}_{2} - 29422_{1}$	12880.819	7761.358	0		
13010.154	7684.202	3	I	$17166_{5} - 24850^{\circ}_{6}$	12874.595	7765.110	1	I	$17073_{1} - 24838^{\circ}_{1}$
13008.873	7684.959	0			12873.533	7765.751	1	I	$20214^{\circ}_{3} - 27980_{3}$
13008.742	7685.036	0	I	$15970_{3} - 23655^{\circ}_{4}$	12872.702	7766.252	3	I	$10783^{\circ}_{2} - 18549_{2}$
13007.832	7685.574	5	I	$16346^{\circ}_{4} - 24032_{4}$	12866.644	7769.909	7	I	$19227^{\circ}_{6} - 26997_{6}$
13006.151	7686.567	2	II	$12472^{\circ}_{2\frac{1}{2}} - 20158_{2\frac{1}{2}}$	12861.651	7772.925	4	I	$16217^{\circ}_{2} - 23990_{2}$
13004.273	7687.677	4			12854.102	7777.490	1	I	$25321^{\circ}_{3} - 33099_{3}$
12994.532	7693.440	3	I	$22141^{\circ}_{3} - 29835_{3}$	12846.823	7781.897	1	I	$24769^{\circ}_{3} - 32551_{3}$
12990.876	7695.605	0			12845.690	7782.583	1	I	$15970_{3} - 23752^{\circ}_{2}$
12989.585	7696.370	1	I	$9804_{5} - 17501^{\circ}_{5}$	12841.750	7784.971	2	I	$19532_{4} - 27317^{\circ}_{3}$
12988.177	7697.204	1	I	$22855^{\circ}_{5} - 30552_{4}$	12837.894	7787.309	2	I	$15490^{\circ}_{3} - 23277_{5}$
12986.920	7697.949	4	I	$7795^{\circ}_{4} - 15493_{4}$	12836.536	7788.133	1	I	$19273_{2} - 27061^{\circ}_{2}$
12983.105	7700.211	0	I	$11802_{2} - 19503^{\circ}_{3}$	12834.733	7789.227	2		
12982.529	7700.553	1	I	$13945^{\circ}_{3} - 21645_{4}$	12831.063	7791.455	0	I	$10783^{\circ}_{2} - 18574_{1}$
12974.600	7705.259	0			12830.547	7791.768	3	I	$20566^{\circ}_{4} - 28358_{3}$
12970.735	7707.555	2	I	$22141^{\circ}_{3} - 29849_{4}$	12828.909	7792.763	0		
12966.746	7709.926	0	I	$23916^{\circ}_{4} - 31626_{5}$	12828.379	7793.085	1	I	$24202^{\circ}_{4} - 31995_{4}$
12964.195	7711.443	2	II	$19050^{\circ}_{1\frac{1}{2}} - 26762_{1\frac{1}{2}}$	12827.456	7793.646	0	I	$22338^{\circ}_{3} - 30132_{2}$
12963.697	7711.739	2	I	$20322^{\circ}_{5} - 28034_{5}$	12826.806	7794.041	3	I	$17959_{4} - 25753^{\circ}_{5}$
12961.197	7713.227	1			12799.956	7810.390	2	I	$24202^{\circ}_{4} - 32012_{4}$
12959.819	7714.047	7	I	$11802_{2} - 19516^{\circ}_{2}$	12798.586	7811.226	0		
12952.082	7718.655	5	I	$12847_{3} - 20566^{\circ}_{4}$	12796.262	7812.645	0		

530-326 OL - 74 - 12

TABLE 1. *Infrared spectral lines of thorium*—Continued

Wavelength Å	Wavenumber cm^{-1}	Intensity	Spectrum	Classification	Wavelength Å	Wavenumber cm^{-1}	Intensity	Spectrum	Classification
12782.294	7821.182	1	I	$13847_2 - 21668^\circ_1$	12604.640	7931.416	2	I	$18431_3 - 26363^\circ_2$
12782.059	7821.326	2	I	$18069^\circ_3 - 25890_2$	12591.895	7939.444	1	II	$16818_{3\frac{1}{2}} - 24757^\circ_{4\frac{1}{2}}$
12781.578	7821.620	4	I	$15166^\circ_3 - 22988_2$	12590.688	7940.205	0		
12776.786	7824.554	1			12587.889	7941.971	4	I	$20737^\circ_1 - 28679_2$
12773.189	7826.757	1	I	$19516^\circ_2 - 27343_3$	12583.229	7944.912	1	I	$21890^\circ_3 - 29835_3$
12762.096	7833.560	6	I	$13088_3 - 20922^\circ_2$	12582.855	7945.148	1		
12760.142	7834.760	0			12580.239	7946.800	1	I	$15970_3 - 23916^\circ_4$
12756.360	7837.083	1			12580.100	7946.888	1	I	$21902^\circ_4 - 29849_4$
12752.448	7839.487	0			12571.690	7952.204	2	I	$18699_2 - 26651^\circ_2$
12750.649	7840.593	0	I	$19503^\circ_3 - 27343_3$	12568.412	7954.278	2		
12743.510	7844.985	2			12563.833	7957.177	0	I	$17398_3 - 25355^\circ_4$
12742.669	7845.503	1	II	$9061_{2\frac{1}{2}} - 16906^\circ_{3\frac{1}{2}}$	12562.651	7957.926	2	I	$19713_3 - 27670^\circ_3$
12738.275	7848.209	0	I	$22163^\circ_4 - 30011_3$	12561.555	7958.620	3	I	$18549_2 - 26508^\circ_3$
12733.582	7851.102	3	I	$23113^\circ_4 - 30964_3$	12561.165	7958.867	1	I	$14204_5 - 22163^\circ_4$
12722.917	7857.683	2			12558.855	7960.331	1	I	$20922^\circ_2 - 28882_2$
12720.812	7858.983	1			12553.032	7964.024	5	I	$19227^\circ_6 - 27191_5$
12710.230	7865.526	1			12552.801	7964.170	4	I	$23306^\circ_6 - 31271_5$
12709.820	7865.780	4	I	$18930^\circ_3 - 26796_3$	12540.971	7971.683	2	I	$23655^\circ_4 - 31626_5$
12709.330	7866.083	5	I	$15166^\circ_3 - 23032_4$	12527.232	7980.426	2		
12703.962	7869.407	0	I	$18053^\circ_4 - 25923_4$	12522.256	7983.597	1	I	$8800_4 - 16783^\circ_4$
12703.428	7869.738	1	I	$22141^\circ_3 - 30011_3$	12519.264	7985.505	0		
12691.421	7877.183	4	I	$15863_2 - 23741^\circ_1$	12518.195	7986.187	3	I	$18809^\circ_4 - 26796_3$
12690.790	7877.575	0			12512.531	7989.802	0		
12690.055	7878.031	2			12510.096	7991.357	1		
12687.216	7879.794	0			12508.396	7992.443	2	I	$19503^\circ_3 - 27495_4$
12685.466	7880.881	1	I	$16783^\circ_4 - 24664_3$	12507.967	7992.717	0		
12684.798	7881.296	3			12502.990	7995.899	0		
12684.317	7881.595	0	I	$6362_2 - 14243^\circ_1$	12502.774	7996.037	2	I	$20566^\circ_4 - 28562_4$
12683.507	7882.098	1	I	$23655^\circ_4 - 31537_3$	12499.696	7998.006	2		
12683.213	7882.281	4	II	$7828_{\frac{1}{2}} - 15710^\circ_{1\frac{1}{2}}$	12488.669	8005.068	1	I	$19039^\circ_2 - 27044_3$
12682.679	7882.613	0	I	$22669^\circ_3 - 30552_4$	12479.376	8011.029	1	II	$9711_{3\frac{1}{2}} - 17722^\circ_{4\frac{1}{2}}$
12680.944	7883.691	1	I	$22248^\circ_2 - 30132_2$	12477.297	8012.364	7	I	$3865_1 - 11877^\circ_1$
12673.959	7888.036	2	I	$25180^\circ_7 - 33068_6$	12476.305	8013.001	3	I	$20214^\circ_3 - 28227_4$
12670.936	7889.918	2			12474.364	8014.248	2	I	$11802_2 - 19817^\circ_1$
12670.355	7890.280	1	I	$13847_2 - 21738^\circ_2$	12473.069	8015.080	0		
12668.767	7891.269	2	I	$14206^\circ_4 - 22098_4$	12471.346	8016.187	1	I	$23521^\circ_3 - 31537_3$
12649.241	7903.450	1			12470.867	8016.495	0		
12648.388	7903.983	1	I	$17501^\circ_5 - 25405_4$	12469.228	8017.549	4	I	$10414^\circ_4 - 18431_3$
12646.536	7905.141	8	I	$10526^\circ_3 - 18431_3$	12468.606	8017.949	1	II	$11576^\circ_{1\frac{1}{2}} - 19594_{\frac{1}{2}}$
12645.697	7905.665	4	I	$20322^\circ_5 - 28227_4$	12466.651	8019.206	0	I	$24274^\circ_5 - 32293_5$
12642.339	7907.765	3			12465.206	8020.136	1		
12641.383	7908.363	3	I	$17398_3 - 25306^\circ_2$	12465.053	8020.234	3	I	$20322^\circ_5 - 28342_5$
12636.142	7911.643	5	I	$18011^\circ_5 - 25923_4$	12460.967	8022.864	4	I	$10526^\circ_3 - 18549_2$
12633.943	7913.020	0			12458.068	8024.731	1	II	$19912^\circ_{6\frac{1}{2}} - 27937_{5\frac{1}{2}}$
12632.545	7913.896	3	I	$2869_3 - 10783^\circ_2$	12455.465	8026.408	0	I	$24769^\circ_3 - 32796_3$
12629.269	7915.949	0	I	$11601_1 - 19516^\circ_2$	12454.517	8027.019	2		
12617.523	7923.318	1			12453.262	8027.828	3	I	$15493_4 - 23521^\circ_3$
12617.200	7923.521	1	I	$17398_3 - 25321^\circ_3$	12447.488	8031.552	5	I	$11241^\circ_3 - 19273_2$
12611.214	7927.282	0	I	$24274^\circ_5 - 32202_5$	12446.347	8032.288	1	I	$19948^\circ_4 - 27980_3$
12610.394	7927.797	2			12445.393	8032.904	3	I	$15736^\circ_1 - 23769_1$

TABLE 1. *Infrared spectral lines of thorium*—Continued

Wavelength Å	Wavenumber cm^{-1}	Intensity	Spectrum	Classification	Wavelength Å	Wavenumber cm^{-1}	Intensity	Spectrum	Classification
12442.013	8035.086	5	I	$15166^{\circ}_{3} - 23201_{3}$	12325.069	8111.325	0		
12440.650	8035.966	2	I	$24701^{\circ}_{5} - 32737_{5}$	12323.962	8112.054	0	I	$21902^{\circ}_{4} - 30014_{4}$
12440.364	8036.151	1			12322.400	8113.082	1	I	$24850^{\circ}_{6} - 32963_{5}$
12437.583	8037.948	0	I	$22248^{\circ}_{2} - 30286_{1}$	12321.120	8113.925	3	I	$18930^{\circ}_{3} - 27044_{3}$
12433.627	8040.505	1			12318.487	8115.659	1	II	$12570_{3\frac{1}{2}} - 20686^{\circ}_{2\frac{1}{2}}$
12430.756	8042.362	1	I	$13847_{2} - 21890^{\circ}_{3}$	12318.050	8115.947	3	I	$15493_{4} - 23609^{\circ}_{5}$
12430.591	8042.469	1			12316.913	8116.696	2	I	$7502_{3} - 15618^{\circ}_{3}$
12429.285	8043.314	1	I	$17847^{\circ}_{2} - 25890_{2}$	12316.372	8117.053	1	I	$24084^{\circ}_{6} - 32202_{5}$
12424.510	8046.405	0			12314.487	8118.295	0		
12423.210	8047.247	0			12312.736	8119.450	2	I	$23655^{\circ}_{4} - 31774_{3}$
12422.300	8047.837	4	I	$19986^{\circ}_{6} - 28034_{5}$	12310.069	8121.209	3	I	$21890^{\circ}_{3} - 30011_{3}$
12421.310	8048.478	1	II	$21297^{\circ}_{2\frac{1}{2}} - 29345_{2\frac{1}{2}}$	12303.742	8125.385	1		
12419.161	8049.871	2	I	$19516^{\circ}_{2} - 27566_{2}$	12295.924	8130.551	0	I	$24421^{\circ}_{3} - 32551_{3}$
12417.933	8050.667	0			12294.985	8131.172	1	I	$16783^{\circ}_{4} - 24915_{3}$
12415.160	8052.465	5	I	$16346^{\circ}_{4} - 24399_{3}$	12292.964	8132.509	0		
12414.206	8053.084	1			12285.424	8137.500	1	II	$20686^{\circ}_{2\frac{1}{2}} - 28823_{2\frac{1}{2}}$
12406.195	8058.284	1	I	$20214^{\circ}_{3} - 28273_{2}$	12283.851	8138.542	1	I	$19532_{4} - 27670^{\circ}_{3}$
12402.749	8060.523	1	II	$9061_{2\frac{1}{2}} - 17121^{\circ}_{1\frac{1}{2}}$	12277.781	8142.566	0		
12400.331	8062.095	3	II	$6213_{4\frac{1}{2}} - 14275^{\circ}_{4\frac{1}{2}}$	12276.652	8143.315	1	II	$7001_{1\frac{1}{2}} - 15144^{\circ}_{1\frac{1}{2}}$
12398.153	8063.511	2	II	$1521_{2\frac{1}{2}} - 9585^{\circ}_{2\frac{1}{2}}$	12276.430	8143.462	0	I	$20214^{\circ}_{3} - 28358_{3}$
12397.849	8063.709	4	I	$19503^{\circ}_{3} - 27566_{2}$	12273.859	8145.168	2	I	$20737^{\circ}_{1} - 28882_{2}$
12396.828	8064.373	0	I	$21077^{\circ}_{5} - 29141_{5}$	12271.398	8146.801	2	I	$16554_{6} - 24701^{\circ}_{5}$
12384.580	8072.348	2			12263.449	8152.082	1	I	$23113^{\circ}_{4} - 31265_{3}$
12381.813	8074.152	3	I	$12847_{3} - 20922^{\circ}_{2}$	12262.250	8152.879	1	I	$13945^{\circ}_{3} - 22098_{4}$
12379.808	8075.460	0			12261.910	8153.105	2	I	$22399^{\circ}_{5} - 30552_{4}$
12378.451	8076.345	1	I	$18431_{3} - 26508^{\circ}_{3}$	12256.743	8156.542	2	I	$20522^{\circ}_{2} - 28679_{2}$
12378.290	8076.450	2	I	$17959_{4} - 26036^{\circ}_{3}$	12251.360	8160.126	0	II	$22834_{3\frac{1}{2}} - 30994^{\circ}_{3\frac{1}{2}}$
12377.115	8077.217	0	I	$18574_{1} - 26651^{\circ}_{2}$	12249.188	8161.573	4	I	$18809^{\circ}_{4} - 26971_{4}$
12372.881	8079.981	0			12246.140	8163.604	0		
12372.484	8080.240	4	II	$4490^{\circ}_{2\frac{1}{2}} - 12570_{3\frac{1}{2}}$	12245.483	8164.042	3	I	$13088_{3} - 21252^{\circ}_{2}$
12372.007	8080.552	2	I	$24701^{\circ}_{5} - 32781_{4}$	12244.970	8164.384	3	II	$16818_{3\frac{1}{2}} - 24982^{\circ}_{3\frac{1}{2}}$
12364.267	8085.610	1	I	$19948^{\circ}_{4} - 28034_{5}$	12244.077	8164.980	1		
12362.538	8086.741	0			12242.874	8165.782	0	I	$21252^{\circ}_{2} - 29418_{2}$
12361.433	8087.464	0			12237.332	8169.480	1	I	$21252^{\circ}_{2} - 29422_{1}$
12359.625	8088.647	2	I	$17959_{4} - 26048^{\circ}_{4}$	12236.549	8170.003	2	I	$14226_{0} - 22396^{\circ}_{1}$
12356.076	8090.970	2	II	$12219_{1\frac{1}{2}} - 20310^{\circ}_{2\frac{1}{2}}$	12234.949	8171.071	1	I	$23603^{\circ}_{2} - 31774_{3}$
12355.491	8091.353	0	I	$24202^{\circ}_{4} - 32293_{5}$	12233.199	8172.240	5	I	$14465^{\circ}_{2} - 22637_{3}$
12351.988	8093.648	3			12231.942	8173.080	8	I	$10526^{\circ}_{3} - 18699_{2}$
12349.478	8095.293	2	I	$19516^{\circ}_{2} - 27612_{3}$	12229.332	8174.824	1	I	$7795^{\circ}_{4} - 15970_{3}$
12348.314	8096.056	0	I	$23916^{\circ}_{4} - 32012_{4}$	12228.284	8175.525	1		
12348.094	8096.200	0			12226.604	8176.648	1	I	$17398_{3} - 25575^{\circ}_{4}$
12346.884	8096.994	0	I	$21738^{\circ}_{2} - 29835_{3}$	12226.177	8176.934	4	I	$11877^{\circ}_{1} - 20054_{2}$
12344.348	8098.657	0			12223.788	8178.532	2	I	$18699_{2} - 26878^{\circ}_{3}$
12341.497	8100.528	0			12219.156	8181.632	0	I	$16217^{\circ}_{2} - 24399_{3}$
12338.612	8102.422	0	I	$18549_{2} - 26651^{\circ}_{2}$	12216.424	8183.462	1	I	$24274^{\circ}_{5} - 32458_{4}$
12337.998	8102.825	7	I	$6362_{2} - 14465^{\circ}_{2}$	12211.865	8186.517	2	I	$18069^{\circ}_{3} - 26255_{4}$
12330.800	8107.555	1	I	$20423^{\circ}_{1} - 28531_{2}$	12206.894	8189.851	7	I	$3687_{2} - 11877^{\circ}_{1}$
12329.207	8108.603	2	I	$22399^{\circ}_{5} - 30508_{5}$	12202.844	8192.569	1		
12328.492	8109.073	1	I	$21902^{\circ}_{4} - 30011_{3}$	12200.702	8194.007	1	II	$18568^{\circ}_{1\frac{1}{2}} - 26762_{1\frac{1}{2}}$
12328.408	8109.128	0	I	$19503^{\circ}_{3} - 27612_{3}$	12194.157	8198.405	8	II	$1521_{2\frac{1}{2}} - 9720^{\circ}_{3\frac{1}{2}}$

TABLE 1. *Infrared spectral lines of thorium*—Continued

Wavelength Å	Wavenumber cm^{-1}	Intensity	Spectrum	Classification	Wavelength Å	Wavenumber cm^{-1}	Intensity	Spectrum	Classification
12188.866	8201.964	1	I	$18053^{\circ}_{4} - 26255_{4}$	12055.291	8292.843	0	I	$21668^{\circ}_{1} - 29961_{1}$
12188.576	8202.159	0			12051.267	8295.612	1	I	$22248^{\circ}_{2} - 30544_{2}$
12182.019	8206.574	3	I	$9804_{5} - 18011^{\circ}_{5}$	12050.486	8296.150	0	I	$18699_{2} - 26995^{\circ}_{3}$
12178.456	8208.975	2	I	$24084^{\circ}_{6} - 32293_{5}$	12043.786	8300.765	1	II	$8605_{2\frac{1}{2}} - 16906^{\circ}_{3\frac{1}{2}}$
12178.009	8209.276	0			12042.947	8301.343	0		
12177.607	8209.547	2			12038.242	8304.588	1	I	$19039^{\circ}_{2} - 27343_{3}$
12171.815	8213.454	4	I	$4961_{4} - 13175^{\circ}_{4}$	12037.639	8305.004	4	I	$17398_{3} - 25703^{\circ}_{2}$
12171.754	8213.495	2			12020.095	8317.125	1	I	$12847_{3} - 21165^{\circ}_{3}$
12171.023	8213.988	0			12018.718	8318.078	7	I	$16346^{\circ}_{4} - 24664_{3}$
12170.869	8214.092	0			12018.054	8318.538	4	I	$15863_{2} - 24182^{\circ}_{2}$
12167.821	8216.150	3	I	$11601_{1} - 19817^{\circ}_{1}$	12015.950	8319.994	4	I	$23306^{\circ}_{6} - 31626_{5}$
12166.851	8216.805	0	I	$21539^{\circ}_{4} - 29756_{4}$	12015.478	8320.321	1	I	$19532_{4} - 27852^{\circ}_{5}$
12162.431	8219.791	3			12011.883	8322.811	0	II	$7001_{1\frac{1}{2}} - 15324^{\circ}{}_{1\frac{1}{2}}$
12161.908	8220.144	0	I	$18431_{3} - 26651^{\circ}_{2}$	12007.854	8325.604	5	II	$4146_{3\frac{1}{2}} - 12472^{\circ}_{2\frac{1}{2}}$
12149.443	8228.578	2			12007.313	8325.979	0	I	$23603^{\circ}_{2} - 31929_{3}$
12146.324	8230.691	2			12005.953	8326.922	1	I	$18053^{\circ}_{4} - 26380_{5}$
12143.705	8232.466	0	I	$15970_{3} - 24202^{\circ}_{4}$	12004.504	8327.927	1		
12140.955	8234.331	3	I	$18809^{\circ}_{4} - 27044_{3}$	11999.611	8331.323	0		
12140.751	8234.469	1	I	$24561^{\circ}_{3} - 32796_{3}$	11986.392	8340.511	0	I	$23655^{\circ}_{4} - 31995_{4}$
12139.017	8235.645	1	I	$8111_{4} - 16346^{\circ}_{4}$	11984.664	8341.714	8	II	$4146_{3\frac{1}{2}} - 12488^{\circ}_{4\frac{1}{2}}$
12136.565	8237.309	1	II	$22642^{\circ}_{4\frac{1}{2}} - 30879_{3\frac{1}{2}}$	11980.135	8344.867	1	I	$22163^{\circ}_{4} - 30508_{5}$
12132.020	8240.395	3	I	$20322^{\circ}_{5} - 28562_{4}$	11979.873	8345.050	2	II	$15786_{2\frac{1}{2}} - 24132^{\circ}_{1\frac{1}{2}}$
12129.427	8242.157	5	I	$13297_{4} - 21539^{\circ}_{4}$	11976.025	8347.731	1	I	$20214^{\circ}_{3} - 28562_{4}$
12128.913	8242.506	1	I	$21890^{\circ}_{3} - 30132_{2}$	11974.695	8348.658	1	II	$16033^{\circ}_{2\frac{1}{2}} - 24381_{3\frac{1}{2}}$
12127.302	8243.601	8	I	$0_{2} - 8243^{\circ}_{2}$	11974.134	8349.049	1	I	$24202^{\circ}_{4} - 32551_{3}$
12126.918	8243.862	1	I	$24307^{\circ}_{2} - 32551_{3}$	11961.578	8357.813	1	I	$23655^{\circ}_{4} - 32012_{4}$
12126.419	8244.201	5	I	$18011^{\circ}_{5} - 26255_{4}$	11960.136	8358.821	3	II	$4113_{2\frac{1}{2}} - 12472^{\circ}_{2\frac{1}{2}}$
12124.024	8245.830	0			11956.759	8361.182	0	I	$22396^{\circ}_{1} - 30758_{2}$
12119.644	8248.810	3	I	$9804_{5} - 18053^{\circ}_{4}$	11955.885	8361.793	0	I	$18699_{2} - 27061^{\circ}_{2}$
12117.950	8249.963	0	I	$22508^{\circ}_{2} - 30758_{2}$	11952.411	8364.223	0		
12113.062	8253.292	0	I	$21165^{\circ}_{3} - 29418_{2}$	11952.063	8364.467	4	I	$19227^{\circ}_{6} - 27591_{5}$
12109.655	8255.614	0	I	$24202^{\circ}_{4} - 32458_{4}$	11946.618	8368.279	1	I	$20566^{\circ}_{4} - 28934_{3}$
12109.434	8255.765	3	I	$20423^{\circ}_{1} - 28679_{2}$	11945.362	8369.159	6	I	$18011^{\circ}_{5} - 26380_{5}$
12109.313	8255.847	1	I	$23015^{\circ}_{5} - 31271_{5}$	11942.130	8371.424	5	I	$15618^{\circ}_{3} - 23990_{2}$
12102.779	8260.304	1	II	$17121^{\circ}_{1\frac{1}{2}} - 25381_{1\frac{1}{2}}$	11940.834	8372.333	2	II	$4113_{2\frac{1}{2}} - 12485^{\circ}_{3\frac{1}{2}}$
12099.785	8262.348	2	I	$24701^{\circ}_{5} - 32963_{5}$	11940.638	8372.470	7	I	$2869_{3} - 11241^{\circ}_{3}$
12093.304	8266.776	1			11934.349	8376.882	1	II	$20969^{\circ}_{3\frac{1}{2}} - 29345_{2\frac{1}{2}}$
12087.362	8270.840	2	II	$6213_{4\frac{1}{2}} - 14484^{\circ}_{5\frac{1}{2}}$	11927.809	8381.475	0	I	$18809^{\circ}_{4} - 27191_{5}$
12086.503	8271.428	3	II	$9711_{3\frac{1}{2}} - 17983^{\circ}_{2\frac{1}{2}}$	11925.197	8383.311	1		
12086.289	8271.574	0			11919.113	8387.590	0		
12083.777	8273.294	0	I	$21738^{\circ}_{2} - 30011_{3}$	11916.586	8389.369	3	I	$22163^{\circ}_{4} - 30552_{4}$
12082.221	8274.359	2	I	$23655^{\circ}_{4} - 31929_{3}$	11911.501	8392.950	4		
12075.537	8278.939	1	I	$20566^{\circ}_{4} - 28845_{4}$	11910.840	8393.416	0	I	$22877^{\circ}_{5} - 31271_{5}$
12074.667	8279.536	2	I	$19948^{\circ}_{4} - 28227_{4}$	11910.542	8393.626	0		
12066.559	8285.099	0	I	$23916^{\circ}_{4} - 32202_{5}$	11909.862	8394.105	1	I	$19948^{\circ}_{4} - 28342_{5}$
12061.506	8288.570	2			11904.795	8397.678	2	I	$19273_{2} - 27670^{\circ}_{3}$
12060.198	8289.469	2			11903.594	8398.525	0		
12059.895	8289.677	0	I	$15970_{3} - 24259^{\circ}_{4}$	11899.837	8401.177	4	I	$13847_{2} - 22248^{\circ}_{2}$
12058.422	8290.690	0	I	$11241^{\circ}_{3} - 19532_{4}$	11894.942	8404.634	3	I	$12847_{3} - 21252^{\circ}_{2}$
12055.394	8292.772	0			11888.825	8408.958	1		

TABLE 1. *Infrared spectral lines of thorium*—Continued

Wavelength Å	Wavenumber cm^{-1}	Intensity	Spectrum	Classification	Wavelength Å	Wavenumber cm^{-1}	Intensity	Spectrum	Classification
11887.357	8409.997	1	I	$19948^{\circ}_{4} - 28358_{3}$	11777.121	8488.716	0		
11886.085	8410.897	2	I	$22141^{\circ}_{3} - 30552_{4}$	11776.403	8489.233	5	II	$9238^{\circ}_{4\frac{1}{2}} - 17727_{5\frac{1}{2}}$
11884.530	8411.997	5	I	$11802_{2} - 20214^{\circ}_{3}$	11775.163	8490.127	4	I	$10783^{\circ}_{2} - 19273_{2}$
11882.776	8413.239	2	I	$15618^{\circ}_{3} - 24032_{4}$	11773.211	8491.535	0		
11879.545	8415.527	0			11772.698	8491.905	1	I	$23521^{\circ}_{3} - 32012_{4}$
11878.611	8416.189	2	I	$19532_{4} - 27948^{\circ}_{4}$	11761.537	8499.963	1	I	$20922^{\circ}_{2} - 29422_{1}$
11874.629	8419.011	2	I	$22338^{\circ}_{3} - 30758_{2}$	11757.273	8503.046	1		
11874.199	8419.316	3	II	$12570_{3\frac{1}{2}} - 20989^{\circ}_{4\frac{1}{2}}$	11746.350	8510.953	0		
11873.851	8419.563	2	I	$13175^{\circ}_{4} - 21594_{3}$	11746.174	8511.080	1	I	$19273_{2} - 27784^{\circ}_{2}$
11870.629	8421.848	1	I	$17501^{\circ}_{5} - 25923_{4}$	11739.687	8515.783	2	II	$8605_{2\frac{1}{2}} - 17121^{\circ}_{1\frac{1}{2}}$
11868.373	8423.449	3			11737.416	8517.431	1		
11868.045	8423.682	0	I	$15493_{4} - 23916^{\circ}_{4}$	11736.880	8517.820	0		
11867.085	8424.363	1			11729.339	8523.296	1	I	$14465^{\circ}_{2} - 22988_{2}$
11865.636	8425.392	4	II	$15305_{4\frac{1}{2}} - 23730^{\circ}_{4\frac{1}{2}}$				I	$20322^{\circ}_{5} - 28845_{4}$
11864.247	8426.378	7	I	$3687_{2} - 12114^{\circ}_{2}$	11729.109	8523.463	0		
11862.597	8427.550	1			11724.039	8527.149	0		
11862.198	8427.834	1			11723.279	8527.702	2	I	$19039^{\circ}_{2} - 27566_{2}$
11858.382	8430.546	4	I	$14206^{\circ}_{4} - 22637_{3}$	11722.487	8528.278	1	I	$16351_{0} - 24880^{\circ}_{1}$
11853.098	8434.304	1	I	$13962_{1} - 22396^{\circ}_{1}$	11720.628	8529.631	3		
11848.313	8437.710	1	I	$23603^{\circ}_{2} - 32041_{2}$	11715.587	8533.301	1	II	$9585^{\circ}_{2\frac{1}{2}} - 18118_{1\frac{1}{2}}$
11846.202	8439.214	2	II	$8378^{\circ}_{3\frac{1}{2}} - 16818_{3\frac{1}{2}}$	11713.893	8534.535	2		
11842.232	8442.043	0			11712.220	8535.754	3	I	$17354^{\circ}_{1} - 25890_{2}$
11840.529	8443.257	0	I	$23093^{\circ}_{2} - 31537_{3}$	11712.007	8535.909	1		
11839.689	8443.856	1	I	$15863_{2} - 24307^{\circ}_{2}$	11709.471	8537.758	0	I	$24561^{\circ}_{3} - 33099_{3}$
11837.186	8445.642	2	I	$19588^{\circ}_{5} - 28034_{5}$	11704.645	8541.278	1	I	$23916^{\circ}_{4} - 32458_{4}$
11836.168	8446.368	0	I	$18549_{2} - 26995^{\circ}_{3}$	11703.457	8542.145	7	I	$15490^{\circ}_{5} - 24032_{4}$
11834.938	8447.246	1	I	$16217^{\circ}_{2} - 24664_{3}$	11698.831	8545.523	3	I	$13962_{1} - 22508^{\circ}_{2}$
11831.941	8449.386	0	I	$22877^{\circ}_{5} - 31326_{4}$	11695.652	8547.846	0	II	$18214^{\circ}_{1\frac{1}{2}} - 26762_{1\frac{1}{2}}$
11829.730	8450.965	4	I	$15970_{3} - 24421^{\circ}_{3}$	11695.263	8548.130	2	I	$17959_{4} - 26508^{\circ}_{3}$
11829.640	8451.029	5	I	$13088_{3} - 21539^{\circ}_{4}$	11694.285	8548.845	3	I	$21738^{\circ}_{2} - 30286_{1}$
11827.583	8452.499	4	I	$17073_{1} - 25526^{\circ}_{1}$	11694.000	8549.053	2	I	$13847_{2} - 22396^{\circ}_{1}$
11824.901	8454.416	1	I	$16217^{\circ}_{2} - 24671_{2}$	11690.334	8551.734	0	I	$22877^{\circ}_{1} - 31429_{1}$
11822.640	8456.033	4	I	$19817^{\circ}_{1} - 28273_{2}$	11682.909	8557.169	1	I	$15863_{2} - 24421^{\circ}_{3}$
11821.839	8456.606	1	I	$22508^{\circ}_{2} - 30964_{3}$	11680.650	8558.824	1		
11821.500	8456.848	0	I	$7280_{2} - 15736^{\circ}_{1}$	11678.305	8560.543	1	I	$18699_{2} - 27260^{\circ}_{3}$
11819.155	8458.526	0			11675.696	8562.456	0		
11818.546	8458.962	1	I	$20423^{\circ}_{1} - 28882_{2}$	11673.465	8564.092	1	I	$18431_{3} - 26995^{\circ}_{3}$
11811.926	8463.703	2	I	$19516^{\circ}_{2} - 27980_{3}$	11671.783	8565.326	1		
11811.172	8464.243	0			11667.638	8568.369	5	I	$16346^{\circ}_{4} - 24915_{3}$
11811.055	8464.327	0	I	$20214^{\circ}_{3} - 28679_{2}$	11666.014	8569.562	1		
11808.476	8466.176	0	II	$12219_{1\frac{1}{2}} - 20686^{\circ}_{2\frac{1}{2}}$	11662.923	8571.833	2		
11804.617	8468.943	6	I	$5563_{1} - 14032^{\circ}_{2}$	11661.167	8573.124	3	I	$19039^{\circ}_{2} - 27612_{3}$
11804.116	8469.303	3	I	$21903^{\circ}_{7} - 30372_{6}$	11658.782	8574.878	2		
11802.102	8470.748	1	I	$13175^{\circ}_{4} - 21645_{4}$	11657.259	8575.998	1	I	$22669^{\circ}_{3} - 31245_{2}$
11801.327	8471.304	0	I	$11241^{\circ}_{3} - 19713_{3}$	11655.207	8577.508	1	II	$6213_{4\frac{1}{2}} - 14790^{\circ}_{3\frac{1}{2}}$
11793.069	8477.236	1	I	$24259^{\circ}_{4} - 32737_{5}$	11653.134	8579.034	1	I	$24202^{\circ}_{4} - 32781_{4}$
11792.645	8477.541	1	I	$19503^{\circ}_{3} - 27980_{3}$	11648.639	8582.344	1	II	$11576^{\circ}_{1\frac{1}{2}} - 20158_{2\frac{1}{2}}$
11790.463	8479.110	0			11648.509	8582.440	1	I	$21252^{\circ}_{2} - 29835_{3}$
11790.382	8479.168	1	I	$17411^{\circ}_{3} - 25890_{2}$	11641.195	8587.832	1	I	$17166_{5} - 25753^{\circ}_{5}$
11779.528	8486.981	2	I	$16351_{0} - 24838^{\circ}_{1}$	11636.590	8591.231	2	I	$18930^{\circ}_{3} - 27521_{4}$

TABLE 1. *Infrared spectral lines of thorium*—Continued

Wavelength Å	Wavenumber cm^{-1}	Intensity	Spectrum	Classification	Wavelength Å	Wavenumber cm^{-1}	Intensity	Spectrum	Classification
11636.496	8591.300	1	I	$21165^{\circ}_{3} - 29756_{4}$	11526.904	8672.982	5		
11636.155	8591.552	3	I	$15970_{3} - 24561^{\circ}_{3}$	11526.460	8673.316	4	I	$14204_{5} - 22877^{\circ}_{5}$
11634.601	8592.699	4	I	$13297_{4} - 21890^{\circ}_{3}$	11525.422	8674.097	1		
11632.343	8594.367	2			11521.827	8676.804	2	II	$15786_{2^1/_2} - 24463^{\circ}_{2^1/_2}$
11631.948	8594.659	3	II	$10379_{4^1/_2} - 18973^{\circ}_{3^1/_2}$	11517.393	8680.144	1	I	$23113^{\circ}_{4} - 31793_{4}$
11630.479	8595.745	0	I	$22669^{\circ}_{3} - 31265_{3}$	11516.800	8680.591	0		
11629.776	8596.264	1			11516.456	8680.850	5	I	$5563_{1} - 14243^{\circ}_{1}$
11627.313	8598.085	0			11516.297	8680.970	1		
11621.783	8602.177	2			11515.375	8681.665	0	II	$16564^{\circ}_{5^1/_2} - 25246_{4^1/_2}$
11621.209	8602.602	0			11514.959	8681.979	4	I	$18930^{\circ}_{3} - 27612_{3}$
11618.190	8604.837	3	I	$13297_{4} - 21902^{\circ}_{4}$	11512.800	8683.607	0		
11617.462	8605.376	5	I	$14032^{\circ}_{2} - 22637_{3}$	11512.063	8684.163	3	I	$5563_{1} - 14247^{\circ}_{0}$
11615.211	8607.044	1	I	$21077^{\circ}_{5} - 29684_{5}$	11511.566	8684.538	6	I	$20867^{\circ}_{7} - 29552_{6}$
11613.318	8608.447	3			11511.286	8684.749	1	I	$23609^{\circ}_{5} - 32293_{5}$
11609.914	8610.971	2	I	$8800_{4} - 17411^{\circ}_{3}$	11510.028	8685.698	3	I	$18809^{\circ}_{4} - 27495_{4}$
11606.246	8613.692	1	I	$24182^{\circ}_{2} - 32796_{3}$	11506.079	8688.679	1	I	$24274^{\circ}_{5} - 32963_{5}$
11605.473	8614.266	3	I	$19948^{\circ}_{4} - 28562_{4}$	11502.185	8691.621	3	I	$12847_{3} - 21539^{\circ}_{4}$
11602.596	8616.402	0	I	$22141^{\circ}_{3} - 30758_{2}$	11501.478	8692.155	4	I	$13945^{\circ}_{3} - 22637_{3}$
11600.761	8617.765	0	I	$18699_{2} - 27317^{\circ}_{3}$	11494.068	8697.759	2	I	$15863_{2} - 24561^{\circ}_{3}$
11600.523	8617.942	0	I	$21668^{\circ}_{1} - 30286_{1}$	11489.885	8700.925	5	I	$8800_{4} - 17501^{\circ}_{5}$
11597.002	8620.558	1	I	$11802_{2} - 20423^{\circ}_{1}$	11483.227	8705.970	0		
11595.985	8621.314	6	I	$16783^{\circ}_{4} - 25405_{4}$	11481.957	8706.933	0		
11594.834	8622.170	0	II	$16818_{3^1/_2} - 25440^{\circ}_{2^1/_2}$	11478.781	8709.342	1	I	$15493_{4} - 24202^{\circ}_{4}$
11589.953	8625.801	4	I	$16554_{6} - 25180^{\circ}_{7}$	11478.678	8709.420	2	II	$7001_{1^1/_2} - 15710^{\circ}_{1^1/_2}$
11588.544	8626.850	2			11476.910	8710.762	0	I	$18549_{2} - 27260^{\circ}_{3}$
11584.866	8629.589	0	I	$17073_{1} - 25703^{\circ}_{2}$	11476.074	8711.396	1	I	$17166_{5} - 25877^{\circ}_{4}$
11584.675	8629.731	1	I	$18431_{3} - 27061^{\circ}_{2}$	11475.757	8711.637	3	I	$18809^{\circ}_{4} - 27521_{4}$
11583.465	8630.633	0	I	$20214^{\circ}_{3} - 28845_{4}$	11472.823	8713.865	2	I	$19817^{\circ}_{1} - 28531_{2}$
11582.709	8631.196	1			11471.073	8715.194	0	I	$7502_{3} - 16217^{\circ}_{2}$
11581.313	8632.236	1			11468.598	8717.075	3		
11579.846	8633.330	2			11465.039	8719.781	5	I	$11802_{2} - 20522^{\circ}_{2}$
11578.263	8634.510	2			11464.786	8719.973	2	I	$20214^{\circ}_{3} - 28934_{3}$
11577.991	8634.713	1	I	$23916^{\circ}_{4} - 32551_{3}$	11458.461	8724.787	1	I	$19503^{\circ}_{3} - 28227_{4}$
11575.518	8636.558	4	I	$18930^{\circ}_{5} - 27566_{2}$	11456.776	8726.070	0		
11573.652	8637.950	1	I	$17398_{3} - 26036^{\circ}_{3}$	11455.648	8726.929	1	II	$12570_{3^1/_2} - 21297^{\circ}_{2^1/_2}$
11571.485	8639.568	5	I	$19588^{\circ}_{5} - 28227_{4}$	11455.545	8727.008	1	I	$18069^{\circ}_{3} - 26796_{3}$
11565.916	8643.728	0			11454.332	8727.932	0		
11563.750	8645.347	0			11448.044	8732.726	0		
11558.214	8649.488	3	I	$13088_{3} - 21738^{\circ}_{2}$	11444.419	8735.492	2	I	$17073_{1} - 25809^{\circ}_{1}$
11557.337	8650.144	3	I	$17398_{3} - 26048^{\circ}_{4}$	11442.751	8736.765	1	I	$14465^{\circ}_{2} - 23201_{3}$
11557.225	8650.228	0	I	$21902^{\circ}_{4} - 30552_{4}$	11441.097	8738.028	0		
11554.767	8652.068	0	I	$24084^{\circ}_{6} - 32737_{5}$	11436.956	8741.192	0		
11551.616	8654.428	0	I	$21890^{\circ}_{3} - 30544_{2}$	11432.844	8744.336	2		
11543.905	8660.209	2			11432.593	8744.528	4	I	$14243^{\circ}_{1} - 22988_{2}$
11543.824	8660.270	2	I	$13847_{2} - 22508^{\circ}_{2}$	11429.704	8746.738	6	I	$10526^{\circ}_{3} - 19273_{2}$
11543.157	8660.770	0			11427.901	8748.118	1	I	$18699_{2} - 27447^{\circ}_{2}$
11542.494	8661.268	3	II	$8460_{1^1/_2} - 17121^{\circ}_{1^1/_2}$	11426.433	8749.242	0	I	$22877^{\circ}_{5} - 31626_{5}$
11541.028	8662.368	0	I	$21890^{\circ}_{3} - 30552_{4}$	11423.611	8751.403	1		
11536.071	8666.090	2	I	$17224^{\circ}_{2} - 25890_{2}$	11420.044	8754.137	1	I	$19588^{\circ}_{5} - 28342_{5}$
11530.938	8669.948	3	I	$21165^{\circ}_{3} - 29835_{3}$	11419.693	8754.406	1	I	$17501^{\circ}_{5} - 26255_{4}$

TABLE 1. *Infrared spectral lines of thorium*—Continued

Wavelength Å	Wavenumber cm^{-1}	Intensity	Spectrum	Classification	Wavelength Å	Wavenumber cm^{-1}	Intensity	Spectrum	Classification
11417.309	8756.234	3	I	$19516^{\circ}_{2} - 28273_{2}$	11306.901	8841.735	0		
11416.708	8756.695	0			11303.787	8844.171	5	I	$13297_{4} - 22141^{\circ}_{3}$
11415.542	8757.589	1	I	$22508^{\circ}_{2} - 31265_{3}$	11303.544	8844.361	4	I	$7502_{3} - 16346^{\circ}_{4}$
11412.071	8760.253	2	II	$4490^{\circ}_{2\frac{1}{2}} - 13250_{2\frac{1}{2}}$				I	$17411^{\circ}_{3} - 26255_{4}$
11411.321	8760.829	1	I	$24202^{\circ}_{4} - 32963_{5}$	11301.136	8846.246	1	I	$21165^{\circ}_{3} - 30011_{3}$
11408.167	8763.251	0			11300.160	8847.010	0		
11406.101	8764.838	0			11297.608	8849.008	1	I	$23609^{\circ}_{5} - 32458_{4}$
11403.120	8767.129	0			11297.490	8849.101	0		
11402.009	8767.984	0	I	$18549_{2} - 27317^{\circ}_{3}$	11296.103	8850.187	0		
11398.870	8770.398	0			11292.744	8852.820	0		
11397.100	8771.760	0			11292.585	8852.944	0		
11387.846	8778.888	1	II	$17983^{\circ}_{2\frac{1}{2}} - 26762_{1\frac{1}{2}}$	11290.238	8854.785	0	II	$8605_{2\frac{1}{2}} - 17460^{\circ}_{2\frac{1}{2}}$
11386.235	8780.130	5	I	$15618^{\circ}_{3} - 24399_{3}$	11289.645	8855.250	2	I	$19503^{\circ}_{3} - 28358_{3}$
11384.471	8781.491	3	I	$15493_{4} - 24274^{\circ}_{5}$	11288.321	8856.288	0		
11383.920	8781.916	3	I	$18809^{\circ}_{4} - 27591_{5}$	11285.357	8858.614	2		
11383.489	8782.248	0			11277.612	8864.698	0	I	$23916^{\circ}_{4} - 32781_{4}$
11374.713	8789.024	6	II	$4113_{2\frac{1}{2}} - 12902^{\circ}_{1\frac{1}{2}}$	11276.818	8865.322	4	I	$15166^{\circ}_{3} - 24032_{4}$
11371.299	8791.663	1	I	$24307^{\circ}_{2} - 33099_{3}$	11276.338	8865.700	2	I	$13297_{4} - 22163^{\circ}_{4}$
11369.091	8793.370	2	I	$24274^{\circ}_{5} - 33068_{6}$	11273.574	8867.873	4	I	$21890^{\circ}_{3} - 30758_{2}$
11366.315	8795.518	2	I	$14481^{\circ}_{6} - 23277_{5}$	11264.063	8875.361	0		
11361.606	8799.163	0			11262.936	8876.249	2		
11360.181	8800.267	0			11260.143	8878.451	1	I	$24084^{\circ}_{6} - 32963_{5}$
11358.564	8801.520	1	I	$22163^{\circ}_{4} - 30964_{3}$	11258.986	8879.363	4	I	$17501^{\circ}_{5} - 26380_{5}$
11358.499	8801.570	3	I	$13088_{3} - 21890^{\circ}_{3}$	11258.130	8880.038	3	I	$21252^{\circ}_{2} - 30132_{2}$
11357.450	8802.383	0	I	$18809^{\circ}_{4} - 27612_{3}$	11255.513	8882.103	0	I	$23113^{\circ}_{4} - 31995_{4}$
11356.910	8802.802	0	I	$22338^{\circ}_{3} - 31141_{3}$	11255.092	8882.435	3	I	$17166_{5} - 26048^{\circ}_{4}$
11356.608	8803.036	1	I	$23655^{\circ}_{4} - 32458_{4}$	11252.925	8884.146	1		
11354.715	8804.503	8	I	$6362_{2} - 15166^{\circ}_{3}$	11249.018	8887.231	0	I	$17224^{\circ}_{2} - 26111_{1}$
11352.128	8806.510	2	I	$21738^{\circ}_{2} - 30544_{2}$	11246.685	8889.075	1	I	$20214^{\circ}_{3} - 29104_{4}$
11351.924	8806.668	6	I	$19227^{\circ}_{6} - 28034_{5}$	11245.412	8890.081	2	I	$12847_{3} - 21738^{\circ}_{2}$
11350.081	8808.098	1			11244.356	8890.916	1		
11346.494	8810.883	1	I	$14204_{5} - 23015^{\circ}_{5}$	11244.310	8890.952	2	II	$13248_{4\frac{1}{2}} - 22139^{\circ}_{4\frac{1}{2}}$
11344.334	8812.560	1			11238.982	8895.167	2	I	$23306^{\circ}_{6} - 32202_{5}$
11343.709	8813.046	4	I	$11241^{\circ}_{3} - 20054_{2}$	11238.344	8895.672	0	I	$20522^{\circ}_{2} - 29418_{2}$
11343.167	8813.467	0			11236.858	8896.849	1	I	$24202^{\circ}_{4} - 33099_{3}$
11342.857	8813.708	3	I	$13088_{3} - 21902^{\circ}_{4}$	11233.671	8899.373	2	I	$20522^{\circ}_{2} - 29422_{1}$
11338.588	8817.026	0			11232.320	8900.443	2	II	$6244_{1\frac{1}{2}} - 15144^{\circ}_{1\frac{1}{2}}$
11335.713	8819.262	0	I	$20322^{\circ}_{5} - 29141_{5}$	11230.255	8902.080	9	I	$5563_{1} - 14465^{\circ}_{2}$
11332.045	8822.117	4	I	$13847_{2} - 22669^{\circ}_{3}$	11225.532	8905.825	3	I	$15863_{2} - 24769^{\circ}_{3}$
11331.384	8822.632	1	I	$14226_{0} - 23049^{\circ}_{1}$	11221.176	8909.282	1	I	$14204_{5} - 23113^{\circ}_{4}$
11330.428	8823.376	5			11215.651	8913.671	2	I	$20737^{\circ}_{1} - 29650_{2}$
11327.681	8825.516	0			11212.583	8916.110	1	I	$22877^{\circ}_{5} - 31793_{4}$
11326.973	8826.067	3	I	$14206^{\circ}_{4} - 23032_{4}$	11211.484	8916.984	0	I	$24182^{\circ}_{2} - 33099_{3}$
11326.400	8826.514	1			11208.602	8919.277	1		
11323.876	8828.481	0	I	$18431_{3} - 27260^{\circ}_{3}$	11205.579	8921.683	4	I	$11601_{1} - 20522^{\circ}_{2}$
11322.408	8829.626	1			11204.818	8922.289	2	II	$9061_{2\frac{1}{2}} - 17983^{\circ}_{2\frac{1}{2}}$
11321.659	8830.210	2	I	$8243^{\circ}_{2} - 17073_{1}$	11203.831	8923.075	1	I	$13175^{\circ}_{4} - 22098_{4}$
11321.249	8830.530	2	I	$17959_{4} - 26790^{\circ}_{4}$	11202.078	8924.471	1	II	$17837^{\circ}_{1\frac{1}{2}} - 26762_{1\frac{1}{2}}$
11311.417	8838.205	1			11195.293	8929.880	1	I	$10783^{\circ}_{2} - 19713_{3}$
11307.314	8841.412	3	I	$19516^{\circ}_{2} - 28358_{3}$	11190.716	8933.532	3		

TABLE 1. *Infrared spectral lines of thorium*—Continued

Wavelength Å	Wavenumber cm^{-1}	Intensity	Spectrum	Classification	Wavelength Å	Wavenumber cm^{-1}	Intensity	Spectrum	Classification
11189.689	8934.352	2	I	$11802_2 - 20737^\circ_1$	11043.146	9052.911	3	I	$15618^\circ_3 - 24671_2$
11186.716	8936.727	0	II	$20158_{2\frac{1}{2}} - 29095^\circ_{2\frac{1}{2}}$	11042.986	9053.042	2	I	$13088_3 - 22141^\circ_3$
11185.925	8937.359	5	I	$7280_2 - 16217^\circ_2$	11038.296	9056.889	2		
11184.628	8938.395	0	I	$22855^\circ_3 - 31793_4$	11036.319	9058.511	4	I	$16346^\circ_4 - 25405_4$
11182.846	8939.819	2			11035.091	9059.519	0	I	$19503^\circ_3 - 28562_4$
11179.105	8942.811	3	I	$11601_1 - 20543^\circ_0$	11031.608	9062.380	1	I	$21902^\circ_4 - 30964_3$
11171.377	8948.997	1	I	$17847^\circ_2 - 26796_3$	11031.091	9062.804	0		
11165.579	8953.644	1			11028.089	9065.271	1	I	$19817^\circ_1 - 28882_2$
11162.099	8956.436	3	I	$14032^\circ_2 - 22988_2$	11026.975	9066.187	1		
11159.387	8958.612	1			11023.604	9068.960	1		
11157.560	8960.079	1	I	$18011^\circ_5 - 26971_4$	11021.768	9070.470	3	I	$14206^\circ_4 - 23277_5$
11155.405	8961.810	0			11021.045	9071.065	0		
11151.802	8964.706	0	I	$17398_3 - 26363^\circ_2$	11017.161	9074.263	0		
11148.272	8967.544	0	I	$21165^\circ_3 - 30132_2$	11016.787	9074.571	4	I	$13088_3 - 22163^\circ_4$
11148.078	8967.700	0			11016.018	9075.205	1		
11147.197	8968.409	0	I	$21539^\circ_4 - 30508_5$	11013.293	9077.450	1		
11139.881	8974.299	3	I	$19588^\circ_5 - 28562_4$	11010.266	9079.946	1	II	$6244_{1/2} - 15324^\circ_{1/2}$
11139.415	8974.674	0			11001.800	9086.933	3	I	$13962_1 - 23049^\circ_1$
11138.971	8975.032	1	I	$15863_2 - 24838^\circ_1$	11000.900	9087.676	1	I	$13945^\circ_3 - 23032_4$
11138.821	8975.153	4	I	$18069^\circ_3 - 27044_3$	10999.236	9089.051	0	I	$21668^\circ_1 - 30758_2$
11134.469	8978.661	1	I	$22163^\circ_4 - 31141_3$	10990.207	9096.518	2		
11128.287	8983.649	5	I	$4961_4 - 13945^\circ_3$	10986.695	9099.426	0		
11126.995	8984.692	1			10983.633	9101.963	5	I	$13297_4 - 22399^\circ_5$
11125.541	8985.866	4	I	$18011^\circ_5 - 26997_6$	10983.207	9102.316	2		
11124.745	8986.509	2	I	$19948^\circ_4 - 28934_3$	10982.982	9102.502	3	I	$22163^\circ_4 - 31265_3$
11124.026	8987.090	3	I	$23306^\circ_6 - 32293_5$	10982.910	9102.562	4	I	$14204_5 - 23306^\circ_6$
11114.372	8994.896	0	I	$20423^\circ_1 - 29418_2$	10982.260	9103.101	0		
11114.157	8995.070	3	I	$14206^\circ_4 - 23201_3$	10981.861	9103.431	1	II	$8018_{1/2} - 17121^\circ_{1/2}$
11107.735	9000.271	0	II	$8460_{1/2} - 17460^\circ_{2\frac{1}{2}}$	10976.518	9107.863	0	I	$22163^\circ_4 - 31271_5$
11106.476	9001.291	0			10974.389	9109.630	1	I	$17398_3 - 26508^\circ_3$
11101.804	9005.079	5	I	$9804_5 - 18809^\circ_4$	10965.252	9117.220	1	I	$15863_2 - 24981^\circ_3$
11098.788	9007.526	2	I	$13847_2 - 22855^\circ_3$	10964.829	9117.572	1	I	$20566^\circ_4 - 29684_5$
11094.494	9011.012	2	I	$15970_3 - 24981^\circ_3$	10963.975	9118.282	1	I	$10414^\circ_4 - 19532_4$
11092.159	9012.909	1	I	$21539^\circ_4 - 30552_4$	10962.885	9119.189	5	I	$11802_2 - 20922^\circ_2$
11090.735	9014.066	3	I	$19516^\circ_2 - 28531_2$	10956.004	9124.916	1	I	$18549_2 - 27674^\circ_2$
11087.646	9016.578	1			10955.633	9125.225	1		
11074.809	9027.029	5			10954.915	9125.823	0		
11073.735	9027.904	3	I	$19503^\circ_3 - 28531_2$	10948.154	9131.459	4	I	$13962_1 - 23093^\circ_2$
11071.877	9029.419	1	II	$6213_{4\frac{1}{2}} - 15242^\circ_{4\frac{1}{2}}$	10946.696	9132.675	1		
11071.478	9029.745	1	I	$13847_2 - 22877^\circ_1$	10942.432	9136.234	3	I	$16554_6 - 25690^\circ_5$
11069.049	9031.726	3	II	$7001_{1\frac{1}{2}} - 16033^\circ_{2\frac{1}{2}}$	10942.244	9136.391	8	II	$6213_{4\frac{1}{2}} - 15349^\circ_{5\frac{1}{2}}$
11065.025	9035.011	0			10941.617	9136.914	4	II	$6168^\circ_{3\frac{1}{2}} - 15305_{4\frac{1}{2}}$
11062.840	9036.795	1			10938.909	9139.176	1	I	$16783^\circ_4 - 25923_4$
11060.720	9038.527	0			10934.177	9143.131	0		
11057.009	9041.561	4	I	$13297_4 - 22338^\circ_3$	10933.859	9143.397	1		
11054.989	9043.213	4	I	$13945^\circ_3 - 22988_2$	10927.204	9148.966	1		
11054.133	9043.913	1			10924.483	9151.245	4	II	$1521_{2\frac{1}{2}} - 10673^\circ_{2\frac{1}{2}}$
11051.898	9045.742	7	I	$15618^\circ_3 - 24664_3$	10923.725	9151.880	2	I	$21738^\circ_2 - 30889_1$
11050.978	9046.495	1	I	$23916^\circ_4 - 32963_5$	10915.734	9158.579	0		
11046.224	9050.389	4	I	$18930^\circ_3 - 27980_3$	10913.581	9160.386	3	I	$13088_3 - 22248^\circ_2$

TABLE 1. *Infrared spectral lines of thorium*—Continued

Wavelength Å	Wavenumber cm^{-1}	Intensity	Spectrum	Classification	Wavelength Å	Wavenumber cm^{-1}	Intensity	Spectrum	Classification
10911.329	9162.277	2	I	$19516^{\circ}_{2} - 28679_{2}$	10759.049	9291.956	1	I	$21252^{\circ}_{2} - 30544_{2}$
10907.689	9165.334	1			10757.771	9293.060	0	II	$7828_{1/2} - 17121^{\circ}_{1/2}$
10901.193	9170.796	4	I	$18809^{\circ}_{4} - 27980_{3}$	10754.878	9295.560	0	I	$21077^{\circ}_{5} - 30372_{6}$
10894.875	9176.114	1	I	$19503^{\circ}_{3} - 28679_{2}$	10754.328	9296.035	4	I	$15618^{\circ}_{3} - 24915_{3}$
10892.630	9178.005	0	II	$15236_{1/2} - 24414^{\circ}_{1/2}$	10752.475	9297.637	2	I	$18930^{\circ}_{3} - 28227_{4}$
10890.287	9179.980	4	I	$18011^{\circ}_{5} - 27191_{5}$	10751.857	9298.172	1		
10887.285	9182.511	0	I	$23916^{\circ}_{4} - 33099_{3}$	10749.481	9300.227	2		
10883.902	9185.365	1	I	$22141^{\circ}_{3} - 31326_{4}$	10749.434	9300.268	3	I	$17959_{4} - 27260^{\circ}_{3}$
10883.233	9185.930	0	I	$22855^{\circ}_{3} - 32041_{2}$	10744.370	9304.651	2	I	$14465^{\circ}_{2} - 23769_{1}$
10882.569	9186.490	1	I	$10526^{\circ}_{3} - 19713_{3}$	10741.809	9306.869	2		
10882.153	9186.842	0	I	$23015^{\circ}_{5} - 32202_{5}$	10741.603	9307.048	0		
10869.967	9197.141	4	I	$17847^{\circ}_{2} - 27044_{3}$	10740.457	9308.041	1	II	$10572^{\circ}_{4\frac{1}{2}} - 19880_{4\frac{1}{2}}$
10866.949	9199.695	1	I	$16554_{6} - 25753^{\circ}_{5}$	10732.245	9315.163	5	I	$12847_{3} - 22163^{\circ}_{4}$
10865.480	9200.939	0			10726.926	9319.782	8	I	$2558_{0} - 11877^{\circ}_{1}$
10864.601	9201.683	2	I	$13847_{2} - 23049^{\circ}_{1}$	10725.418	9321.092	6	I	$11601_{1} - 20922^{\circ}_{2}$
10862.508	9203.456	4	I	$20214^{\circ}_{3} - 29418_{2}$	10723.921	9322.394	7	II	$4146_{3\frac{1}{2}} - 13468^{\circ}_{4\frac{1}{2}}$
10861.797	9204.059	1	II	$12902^{\circ}_{1\frac{1}{2}} - 22106_{2\frac{1}{2}}$	10720.051	9325.759	0	I	$22669^{\circ}_{3} - 31995_{4}$
10857.355	9207.824	1	I	$15493_{4} - 24701^{\circ}_{5}$	10715.361	9329.841	2		
10853.458	9211.130	3	I	$8800_{4} - 18011^{\circ}_{5}$	10707.531	9336.663	1	I	$15970_{3} - 25306^{\circ}_{2}$
10845.004	9218.311	1			10700.359	9342.921	1	I	$18930^{\circ}_{3} - 28273_{2}$
10844.405	9218.820	4	I	$17166_{5} - 26384^{\circ}_{4}$	10700.194	9343.065	0	I	$22669^{\circ}_{3} - 32012_{4}$
10843.465	9219.619	1			10690.175	9351.822	1	I	$15970_{3} - 25321^{\circ}_{3}$
10837.713	9224.512	0	I	$20737^{\circ}_{3} - 29961_{1}$	10678.631	9361.931	1	I	$20322^{\circ}_{5} - 29684_{5}$
10835.309	9226.559	2	II	$20288^{\circ}_{5\frac{1}{2}} - 29515_{4\frac{1}{2}}$	10678.369	9362.161	3	I	$11802_{2} - 21165^{\circ}_{3}$
10834.611	9227.153	2	II	$15236_{1\frac{1}{2}} - 24463^{\circ}_{2\frac{1}{2}}$	10668.486	9370.834	2	I	$7795^{\circ}_{4} - 17166_{5}$
10834.179	9227.521	3			10666.640	9372.456	0	I	$13297_{4} - 22669^{\circ}_{3}$
10832.716	9228.767	0			10665.735	9373.251	0		
10826.499	9234.067	0	I	$19039^{\circ}_{2} - 28273_{2}$	10664.767	9374.102	0	I	$22163^{\circ}_{4} - 31537_{3}$
10826.144	9234.370	0			10664.234	9374.570	5	I	$6362_{2} - 15736^{\circ}_{1}$
10820.075	9239.549	5	II	$6213_{4\frac{1}{2}} - 15453^{\circ}_{3\frac{1}{2}}$	10663.178	9375.499	1	I	$21890^{\circ}_{3} - 31265_{3}$
10819.530	9240.015	1			10660.847	9377.549	3	II	$8605_{2\frac{1}{2}} - 17983^{\circ}_{2\frac{1}{2}}$
10813.573	9245.105	4	I	$2869_{3} - 12114^{\circ}_{2}$	10658.585	9379.539	1	II	$18214^{\circ}_{1\frac{1}{2}} - 27593_{2\frac{1}{2}}$
10813.395	9245.257	6	I	$4961_{4} - 14206^{\circ}_{4}$	10656.144	9381.687	0		
10812.281	9246.209	5	I	$13847_{2} - 23093^{\circ}_{2}$	10654.499	9383.136	1		
10807.344	9250.433	3	I	$13088_{3} - 22338^{\circ}_{3}$	10651.842	9385.476	0	I	$15970_{3} - 25355^{\circ}_{4}$
10804.527	9252.845	2			10649.651	9387.407	1	I	$21165^{\circ}_{3} - 30552_{4}$
10803.918	9253.367	4	I	$8800_{4} - 18053^{\circ}_{4}$	10646.516	9390.171	2	I	$8111_{4} - 17501^{\circ}_{5}$
10802.535	9254.551	1	I	$14226_{0} - 23481^{\circ}_{1}$	10644.118	9392.287	0		
10800.157	9256.589	4	I	$6362_{2} - 15618^{\circ}_{3}$	10642.859	9393.398	1	II	$13248_{4\frac{1}{2}} - 22642^{\circ}_{4\frac{1}{2}}$
10800.053	9256.678	5	I	$13945^{\circ}_{3} - 23201_{3}$	10640.329	9395.631	1	I	$22141^{\circ}_{3} - 31537_{3}$
10794.056	9261.821	3	II	$9711_{3\frac{1}{2}} - 18973^{\circ}_{3\frac{1}{2}}$	10629.842	9404.901	2	I	$14204_{5} - 23609^{\circ}_{5}$
10790.541	9264.838	0	II	$10855_{3\frac{1}{2}} - 20120^{\circ}_{2\frac{1}{2}}$	10624.881	9409.292	1		
10788.554	9266.544	1	I	$22508^{\circ}_{2} - 31774_{3}$	10624.279	9409.825	1		
10786.371	9268.420	3	I	$20566^{\circ}_{4} - 29835_{3}$	10623.608	9410.420	1		
10785.912	9268.814	4	I	$8800_{4} - 18069^{\circ}_{3}$	10622.548	9411.359	2		
10779.100	9274.672	2	I	$18069^{\circ}_{3} - 27343_{3}$	10615.008	9418.044	4	I	$18809^{\circ}_{4} - 28227_{4}$
10778.635	9275.072	1	I	$23521^{\circ}_{3} - 32796_{3}$	10613.388	9419.481	4	I	$13088_{3} - 22508^{\circ}_{2}$
10776.984	9276.493	4	I	$15493_{4} - 24769^{\circ}_{3}$	10609.955	9422.529	1	I	$9804_{5} - 19227^{\circ}_{6}$
10774.344	9278.766	1	I	$23015^{\circ}_{5} - 32293_{5}$	10608.458	9423.859	0		
10772.436	9280.409	2			10607.807	9424.437	0		

TABLE 1. *Infrared spectral lines of thorium*—Continued

Wavelength Å	Wavenumber cm^{-1}	Intensity	Spectrum	Classification	Wavelength Å	Wavenumber cm^{-1}	Intensity	Spectrum	Classification
10607.108	9425.058	1	I	$21539^{\circ}_{4} - 30964_{3}$	10509.543	9512.555	1		
10605.464	9426.519	4	I	$18069^{\circ}_{3} - 27495_{4}$	10503.182	9518.316	1		
10601.345	9430.182	2	I	$23306^{\circ}_{6} - 32737_{5}$	10502.592	9518.851	4	I	$13962_{1} - 23481^{\circ}_{1}$
10600.597	9430.847	1	I	$21077^{\circ}_{5} - 30508_{5}$	10498.496	9522.565	5	I	$14247^{\circ}_{0} - 23769_{1}$
10596.909	9434.129	1	I	$20322^{\circ}_{5} - 29756_{4}$	10495.610	9525.183	1	I	$14465^{\circ}_{2} - 23990_{2}$
10595.992	9434.946	0	II	$13250_{2\frac{1}{2}} - 22685^{\circ}_{3\frac{1}{2}}$	10494.843	9525.879	6	I	$14243^{\circ}_{1} - 23769_{1}$
10595.264	9435.594	1	I	$22338^{\circ}_{3} - 31774_{3}$	10492.255	9528.229	6	I	$10526^{\circ}_{3} - 20054_{2}$
10594.780	9436.025	1	I	$20214^{\circ}_{3} - 29650_{2}$	10487.427	9532.615	1	I	$18809^{\circ}_{4} - 28342_{5}$
10592.495	9438.061	0	I	$23113^{\circ}_{4} - 32551_{3}$	10483.360	9536.313	4		
10591.350	9439.081	2	I	$20522^{\circ}_{2} - 29961_{1}$	10481.173	9538.303	0	I	$20423^{\circ}_{1} - 29961_{1}$
10589.207	9440.991	0			10479.584	9539.749	1		
10587.588	9442.435	1	II	$8018_{1\frac{1}{2}} - 17460^{\circ}_{2\frac{1}{2}}$	10478.801	9540.462	1		
10587.100	9442.870	3	I	$15863_{2} - 25306^{\circ}_{2}$	10477.700	9541.465	1	I	$20214^{\circ}_{3} - 29756_{4}$
10586.930	9443.022	1	I	$23015^{\circ}_{5} - 32458_{4}$	10477.082	9542.028	2		
10585.524	9444.276	0	I	$23655^{\circ}_{4} - 33099_{3}$	10469.974	9548.506	1	I	$18809^{\circ}_{4} - 28358_{3}$
10585.028	9444.718	2	I	$20566^{\circ}_{4} - 30011_{3}$	10467.587	9550.683	0		
10583.191	9446.358	0			10466.685	9551.506	3		
10581.711	9447.679	1	I	$13962_{1} - 23410^{\circ}_{0}$	10459.723	9557.864	4	I	$13297_{4} - 22855^{\circ}_{3}$
10580.518	9448.744	0			10452.445	9564.519	0		
10579.481	9449.670	1	I	$11802_{2} - 21252^{\circ}_{2}$	10450.448	9566.346	3	I	$19986^{\circ}_{6} - 29552_{6}$
10578.136	9450.872	1	I	$14204_{5} - 23655^{\circ}_{4}$	10448.996	9567.676	0		
10576.600	9452.244	1	II	$15305_{4\frac{1}{2}} - 24757^{\circ}_{4\frac{1}{2}}$	10439.505	9576.374	3	I	$16346^{\circ}_{4} - 25923_{4}$
10576.362	9452.457	2	I	$18069^{\circ}_{3} - 27521_{4}$	10436.870	9578.792	2	I	$15863_{2} - 25442^{\circ}_{3}$
10572.824	9455.620	1	II	$10855_{3\frac{1}{2}} - 20310^{\circ}_{2\frac{1}{2}}$	10435.094	9580.422	3	I	$18011^{\circ}_{5} - 27591_{5}$
10570.129	9458.031	0	I	$15863_{2} - 25321^{\circ}_{3}$	10434.890	9580.609	2		
10569.146	9458.911	0	I	$23609^{\circ}_{5} - 33068_{6}$	10434.109	9581.326	1	I	$13088_{3} - 22669^{\circ}_{3}$
10567.177	9460.673	1	I	$12114^{\circ}_{2} - 21575_{2}$	10429.665	9585.409	6	II	$0_{1\frac{1}{2}} - 9585^{\circ}_{2\frac{1}{2}}$
10565.306	9462.349	6	I	$13175^{\circ}_{4} - 22637_{3}$	10424.885	9589.804	0		
10563.181	9464.252	1			10424.126	9590.502	1	I	$22338^{\circ}_{3} - 31929_{3}$
10560.617	9466.550	1	II	$6244_{1\frac{1}{2}} - 15710^{\circ}_{1\frac{1}{2}}$	10423.795	9590.807	2	II	$14790^{\circ}_{3\frac{1}{2}} - 24381_{3\frac{1}{2}}$
10559.107	9467.904	0	I	$18053^{\circ}_{4} - 27521_{4}$	10421.511	9592.909	0	I	$21165^{\circ}_{3} - 30758_{2}$
10556.454	9470.283	7	I	$17501^{\circ}_{5} - 26971_{4}$	10419.574	9594.692	7	II	$1521_{2\frac{1}{2}} - 11116^{\circ}_{3\frac{1}{2}}$
10554.837	9471.734	4	I	$16783^{\circ}_{4} - 26255_{4}$	10417.881	9596.251	1	I	$22399^{\circ}_{5} - 31995_{4}$
10553.890	9472.584	1	I	$15970_{3} - 25442^{\circ}_{3}$	10417.087	9596.983	1		
10545.902	9479.759	1	I	$17398_{3} - 26878^{\circ}_{3}$	10412.996	9600.753	4	I	$18930^{\circ}_{3} - 28531_{2}$
10545.290	9480.309	2	I	$12114^{\circ}_{2} - 21594_{3}$	10412.507	9601.204	0	I	$19817^{\circ}_{1} - 29418_{2}$
10543.947	9481.517	0			10410.424	9603.125	2	I	$7795^{\circ}_{4} - 17398_{3}$
10542.787	9482.560	1			10408.497	9604.903	1	I	$19817^{\circ}_{1} - 29422_{1}$
10540.958	9484.205	5	I	$18011^{\circ}_{5} - 27495_{4}$	10404.502	9608.591	3		
10540.219	9484.870	2			10403.056	9609.927	1	I	$20522^{\circ}_{2} - 30132_{2}$
10539.400	9485.607	1	II	$10673^{\circ}_{2\frac{1}{2}} - 20158_{2\frac{1}{2}}$	10402.349	9610.580	1	II	$17983^{\circ}_{2\frac{1}{2}} - 27593_{2\frac{1}{2}}$
10538.316	9486.583	2	II	$7331^{\circ}_{2\frac{1}{2}} - 16818_{3\frac{1}{2}}$	10401.401	9611.456	1	I	$22163^{\circ}_{4} - 31774_{3}$
10536.866	9487.888	2	I	$15493_{4} - 24981^{\circ}_{3}$	10392.041	9620.113	0	I	$20214^{\circ}_{3} - 29835_{3}$
10533.385	9491.024	3	I	$12847_{3} - 22338^{\circ}_{3}$	10391.352	9620.750	0	II	$12485^{\circ}_{3\frac{1}{2}} - 22106_{2\frac{1}{2}}$
10532.567	9491.761	2			10387.498	9624.320	1	I	$17166_{5} - 26790^{\circ}_{4}$
10527.789	9496.069	5	I	$17501^{\circ}_{5} - 26997_{6}$	10386.273	9625.455	0		
10527.134	9496.660	1	I	$17847^{\circ}_{2} - 27343_{3}$	10378.821	9632.366	1	I	$18930^{\circ}_{3} - 28562_{4}$
10525.841	9497.826	4			10378.146	9632.993	1	I	$17411^{\circ}_{3} - 27044_{3}$
10518.190	9504.735	2	I	$20867^{\circ}_{7} - 30372_{6}$	10377.490	9633.601	2	I	$13847_{2} - 23481^{\circ}_{1}$
10512.209	9510.143	5	I	$18011^{\circ}_{5} - 27521_{4}$	10376.812	9634.231	0	I	$20214^{\circ}_{3} - 29849_{4}$

TABLE 1. *Infrared spectral lines of thorium* — Continued

Wavelength Å	Wavenumber cm^{-1}	Intensity	Spectrum	Classification
10376.020	9634.966	1	I	$21902^{\circ}_{4} - 31537_{3}$
10373.462	9637.342	0	II	$15236_{1\frac{1}{2}} - 24873^{\circ}_{2\frac{1}{2}}$
10369.528	9640.998	4	I	$13962_{1} - 23603^{\circ}_{2}$
10362.966	9647.103	1	I	$21890^{\circ}_{3} - 31537_{3}$
10359.998	9649.867	3	II	$9400_{2\frac{1}{2}} - 19050^{\circ}_{1\frac{1}{2}}$
10358.167	9651.573	3	I	$11601_{1} - 21252^{\circ}_{2}$
10357.832	9651.885	0		
10357.615	9652.087	0	I	$22141^{\circ}_{3} - 31793_{4}$
10356.372	9653.246	2	II	$15786_{2\frac{1}{2}} - 25440^{\circ}_{2\frac{1}{2}}$
10355.806	9653.773	1		
10350.334	9658.877	1	I	$18614^{\circ}_{1} - 28273_{2}$
10349.051	9660.074	5	I	$12847_{3} - 22508^{\circ}_{2}$
10346.944	9662.041	0		
10346.540	9662.419	3	I	$15863_{2} - 25526^{\circ}_{1}$
10345.899	9663.017	0	I	$17398_{3} - 27061^{\circ}_{2}$
10344.287	9664.523	1		
10335.840	9672.422	1		
10334.926	9673.277	3	I	$13847_{2} - 23521^{\circ}_{3}$
10327.838	9679.916	0		
10326.442	9681.224	0		
10317.951	9689.191	1		
10317.364	9689.743	1		
10316.894	9690.184	4	I	$17501^{\circ}_{5} - 27191_{5}$
10316.006	9691.018	1	II	$10189^{\circ}_{5\frac{1}{2}} - 19880_{4\frac{1}{2}}$
10314.894	9692.063	2	I	$20322^{\circ}_{5} - 30014_{4}$
10309.821	9696.832	0		
10308.549	9698.028	5	I	$19986^{\circ}_{6} - 29684_{5}$
10307.509	9699.007	1		
10304.810	9701.547	2	II	$10379_{4\frac{1}{2}} - 20080^{\circ}_{3\frac{1}{2}}$
10304.082	9702.233	2	I	$22338^{\circ}_{3} - 32041_{2}$
10301.391	9704.767	1		
10301.161	9704.984	6	II	$4113_{2\frac{1}{2}} - 13818^{\circ}_{3\frac{1}{2}}$
10299.876	9706.195	1		
10298.388	9707.597	1		
10294.714	9711.062	0	I	$17959_{4} - 27670^{\circ}_{3}$
10293.052	9712.630	4	I	$14204_{5} - 23916^{\circ}_{4}$
10288.987	9716.467	4	II	$1859_{1\frac{1}{2}} - 11576^{\circ}_{1\frac{1}{2}}$
10285.485	9719.775	0	I	$17847^{\circ}_{2} - 27566_{2}$
10283.118	9722.012	4	I	$7502_{3} - 17224^{\circ}_{2}$
10278.860	9726.040	1	I	$21539^{\circ}_{4} - 31265_{3}$
10278.350	9726.522	1		
10278.263	9726.605	0		
10276.804	9727.985	1		
10275.694	9729.036	0	I	$20922^{\circ}_{2} - 30651_{3}$
10272.063	9732.475	2		
10271.191	9733.302	2	I	$15970_{3} - 25703^{\circ}_{2}$
10268.554	9735.801	1	I	$19948^{\circ}_{4} - 29684_{5}$
10260 162	9743.764	0		
10257.374	9746.413	5	I	$14243^{\circ}_{1} - 23990_{2}$
10255.580	9748.118	2	I	$15166^{\circ}_{3} - 24915_{3}$
10250.684	9752.773	4	I	$18809^{\circ}_{4} - 28562_{4}$
10249.314	9754.077	1		
10247.561	9755.746	4	I	$13847_{2} - 23603^{\circ}_{2}$
10247.419	9755.881	1		
10244.986	9758.198	1	II	$22014^{\circ}_{3\frac{1}{2}} - 31773_{4\frac{1}{2}}$
10241.779	9761.253	2	I	$22306^{\circ}_{6} - 33068_{6}$
10241.463	9761.555	2	II	$13250_{2\frac{1}{2}} - 23012^{\circ}_{1\frac{1}{2}}$
10236.031	9766.735	4	I	$13088_{3} - 22855^{\circ}_{3}$
10229.541	9772.931	1		
10223.662	9778.551	3	I	$13962_{1} - 23741^{\circ}_{1}$
10220.712	9781.373	2		
10219.382	9782.646	2	II	$14349_{1/2} - 24132^{\circ}_{1\frac{1}{2}}$
10218.434	9783.554	5	I	$9804_{5} - 19588^{\circ}_{5}$
10214.957	9786.884	0		
10214.676	9787.153	1		
10214.442	9787.377	1	I	$21539^{\circ}_{4} - 31326_{4}$
10213.806	9787.987	0		
10211.538	9790.161	2	I	$13962_{1} - 23752^{\circ}_{2}$
10208.285	9793.281	0	II	$20080^{\circ}_{3\frac{1}{2}} - 29873_{3\frac{1}{2}}$
10205.020	9796.414	1	I	$20214^{\circ}_{3} - 30011_{3}$
10203.228	9798.134	0		
10202.133	9799.186	1	I	$21738^{\circ}_{2} - 31537_{3}$
10197.163	9803.962	0	II	$17722^{\circ}_{4\frac{1}{2}} - 27526_{4\frac{1}{2}}$
10194.906	9806.132	1		
10193.720	9807.273	0	I	$20737^{\circ}_{1} - 30544_{2}$
10192.965	9808.000	0	I	$19948^{\circ}_{4} - 29756_{4}$
10188.418	9812.377	3		
10184.539	9816.114	2	I	$13297_{4} - 23113^{\circ}_{4}$
10180.909	9819.614	0	II	$8018_{1\frac{1}{2}} - 17837^{\circ}_{1/2}$
10180.596	9819.916	2	I	$17224^{\circ}_{2} - 27044_{3}$
10179.844	9820.641	0		
10178.522	9821.917	5	I	$12847_{3} - 22669^{\circ}_{3}$
10177.086	9823.303	1		
10175.012	9825.305	4	I	$14206^{\circ}_{4} - 24032_{4}$
10169.296	9830.828	2	II	$10855_{3\frac{1}{2}} - 20686^{\circ}_{2\frac{1}{2}}$
10160.324	9839.509	0	I	$15863_{2} - 25703^{\circ}_{2}$
10156.406	9843.305	0	I	$19039^{\circ}_{2} - 28882_{2}$
10145.521	9853.865	0		
10144.266	9855.084	4	I	$6362_{2} - 16217^{\circ}_{2}$
10141.399	9857.870	6	I	$13175^{\circ}_{4} - 23032_{4}$
10140.434	9858.808	4	I	$20867^{\circ}_{7} - 30726_{7}$
10137.390	9861.769	2	I	$17398_{3} - 27260^{\circ}_{3}$
10136.787	9862.355	0	I	$15493_{4} - 25355^{\circ}_{4}$
10133.559	9865.497	7	II	$1859_{1\frac{1}{2}} - 11725^{\circ}_{1/2}$
10131.371	9867.628	2	I	$17398_{3} - 27266^{\circ}_{4}$
10127.552	9871.349	0	I	$22141^{\circ}_{3} - 32012_{4}$
10126.557	9872.318	1	I	$21902^{\circ}_{4} - 31774_{3}$
10123.103	9875.687	0		
10120.661	9878.070	1		
10118.774	9879.912	1		

TABLE 1. *Infrared spectral lines of thorium* — Continued

Wavelength Å	Wavenumber cm^{-1}	Intensity	Spectrum	Classification	Wavelength Å	Wavenumber cm^{-1}	Intensity	Spectrum	Classification
10118.187	9880.485	1			9998.963	9998.296	2	I	$14204_5 - 24202^{\circ}_4$
10117.993	9880.675	2	I	$14204_5 - 24084^{\circ}_6$	9998.513	9998.746	2		
10114.788	9883.805	1			9993.866	10003.395	2	II	$15242^{\circ}_{4\,1/2} - 25246_{4\,1/2}$
10113.985	9884.590	0			9993.364	10003.898	0		
10111.877	9886.651	1	I	$19948^{\circ}_4 - 29835_3$	9992.656	10004.607	3	I	$18930^{\circ}_3 - 28934_3$
10107.000	9891.421	0	I	$21902^{\circ}_4 - 31793_4$	9991.846	10005.418	0	I	$13088_3 - 23093^{\circ}_2$
10105.549	9892.842	0	I	$17959_4 - 27852^{\circ}_5$	9989.939	10007.327	2	I	$12847_3 - 22855^{\circ}_3$
10105.080	9893.301	2	I	$13847_2 - 23741^{\circ}_1$	9988.024	10009.246	2	II	$7828_{1/2} - 17837^{\circ}_{1/2}$
10104.307	9894.058	1	I	$16217^{\circ}_2 - 26111_1$	9987.636	10009.635	6	I	$8800_4 - 18809^{\circ}_4$
10103.176	9895.165	0			9985.052	10012.225	5	I	$16783^{\circ}_4 - 26796_3$
10102.579	9895.750	2	I	$19039^{\circ}_2 - 28934_3$	9974.693	10022.623	3	I	$18011^{\circ}_5 - 28034_5$
10098.624	9899.625	1	I	$22141^{\circ}_3 - 32041_2$	9973.365	10023.958	0		
10097.463	9900.764	1	I	$19948^{\circ}_4 - 29849_4$	9973.092	10024.232	1		
10092.535	9905.598	0			9970.467	10026.872	4	I	$13175^{\circ}_4 - 23201_3$
10091.483	9906.631	2			9963.495	10033.888	3	I	$16346^{\circ}_4 - 26380_5$
10089.136	9908.935	7	I	$7502_3 - 17411^{\circ}_3$	9958.059	10039.365	1	I	$21890^{\circ}_3 - 31929_3$
			I	$16346^{\circ}_4 - 26255_4$	9957.528	10039.900	1		
10086.406	9911.617	2	I	$18069^{\circ}_3 - 27980_3$	9957.181	10040.250	0		
10085.323	9912.681	1	II	$9061_{2\,1/2} - 18973^{\circ}_{3\,1/2}$	9956.844	10040.590	1		
10083.788	9914.190	5	I	$19227^{\circ}_6 - 29141_5$	9955.781	10041.662	1		
10082.880	9915.083	4	I	$15490^{\circ}_5 - 25405_4$	9952.375	10045.099	3	I	$13945^{\circ}_3 - 23990_2$
10082.719	9915.242	1	I	$19503^{\circ}_3 - 29418_2$	9948.171	10049.344	1	I	$17398_3 - 27447^{\circ}_2$
10081.227	9916.709	1	I	$18614^{\circ}_1 - 28531_2$	9947.082	10050.444	1	I	$20322^{\circ}_5 - 30372_6$
10079.542	9918.367	2			9943.061	10054.508	6	II	$1521_{2\,1/2} - 11576^{\circ}_{1\,1/2}$
10079.413	9918.494	0			9939.967	10057.638	1		
10078.906	9918.993	1	I	$17398_3 - 27317^{\circ}_3$	9938.839	10058.779	1	I	$22399^{\circ}_5 - 32458_4$
10065.187	9932.512	1	I	$17411^{\circ}_3 - 27343_3$	9935.203	10062.461	2	I	$20867^{\circ}_7 - 30930_6$
10058.937	9938.684	1			9934.723	10062.947	1	I	$19948^{\circ}_4 - 30011_3$
10056.214	9941.375	2	I	$20566^{\circ}_4 - 30508_5$	9932.777	10064.918	0	I	$18614^{\circ}_1 - 28679_2$
10055.842	9941.743	2			9930.047	10067.685	2		
10054.960	9942.615	1	I	$8111_4 - 18053^{\circ}_4$	9929.814	10067.922	3	I	$11601_1 - 21668^{\circ}_1$
10054.189	9943.377	0			9927.326	10070.445	2	I	$14204_5 - 24274^{\circ}_5$
10053.375	9944.182	0	I	$7280_2 - 17224^{\circ}_2$	9926.172	10071.616	0	II	$12570_{3\,1/2} - 22642^{\circ}_{4\,1/2}$
10051.735	9945.805	1			9923.310	10074.520	1		
10048.041	9949.461	3	I	$15493_4 - 25442^{\circ}_3$	9919.448	10078.443	0	I	$15970_3 - 26048^{\circ}_4$
10045.996	9951.486	0	II	$15236_{1\,1/2} - 25188^{\circ}_{1\,1/2}$	9916.122	10081.823	1	I	$15493_4 - 25575^{\circ}_4$
10045.316	9952.160	2	I	$18930^{\circ}_3 - 28882_2$	9913.628	10084.360	1	I	$17411^{\circ}_3 - 27495_4$
10044.021	9953.443	0			9912.205	10085.807	2	I	$22877^{\circ}_5 - 32963_5$
10041.807	9955.638	0			9911.116	10086.915	4	I	$13945^{\circ}_3 - 24032_4$
10039.364	9958.060	7	I	$8111_4 - 18069^{\circ}_3$	9910.837	10087.199	2	I	$11802_2 - 21890^{\circ}_3$
10039.101	9958.321	2	I	$14032^{\circ}_2 - 23990_2$	9907.464	10090.634	1	I	$17501^{\circ}_5 - 27591_5$
10037.115	9960.292	1			9906.948	10091.159	1	I	$16554_6 - 26645^{\circ}_5$
10036.377	9961.024	0			9904.771	10093.377	1	I	$21902^{\circ}_4 - 31995_4$
10033.226	9964.152	2	I	$19588^{\circ}_5 - 29552_6$	9902.362	10095.833	4	I	$19588^{\circ}_5 - 29684_5$
10032.967	9964.410	1			9898.356	10099.918	2	I	$17166_5 - 27266^{\circ}_4$
10032.174	9965.197	1	II	$8018_{1\,1/2} - 17983^{\circ}_{2\,1/2}$	9896.050	10102.272	3	I	$13175^{\circ}_4 - 23277_5$
10029.545	9967.809	1	I	$20922^{\circ}_2 - 30889_1$	9892.286	10106.116	0		
10011.398	9985.877	3	I	$20566^{\circ}_4 - 30552_4$	9892.187	10106.217	0	II	$14275^{\circ}_{4\,1/2} - 24381_{3\,1/2}$
9999.614	9997.645	0	I	$21539^{\circ}_4 - 31537_3$	9890.522	10107.918	1	II	$8460_{1\,1/2} - 18568^{\circ}_{1/2}$
9999.430	9997.829	1			9888.819	10109.659	0	II	$15305_{4\,1/2} - 25414^{\circ}_{5\,1/2}$

TABLE 1. *Infrared spectral lines of thorium*—Continued

Wavelength Å	Wavenumber cm^{-1}	Intensity	Spectrum	Classification	Wavelength Å	Wavenumber cm^{-1}	Intensity	Spectrum	Classification
9880.782	10117.882	2	II	$6700^{\circ}_{4 1/2} - 16818_{3 1/2}$	9736.216	10268.115	1	I	$18614^{\circ}_{1} - 28882_{2}$
9878.520	10120.199	2	II	$7001_{1 1/2} - 17121^{\circ}_{1 1/2}$	9734.696	10269.718	1	II	$13248_{4 1/2} - 23518^{\circ}_{3 1/2}$
9876.688	10122.076	0	II	$13250_{2 1/2} - 23372^{\circ}_{1 1/2}$	9718.665	10286.658	0		
9874.790	10124.022	0			9718.489	10286.844	2		
9873.821	10125.015	3	I	$18809^{\circ}_{4} - 28934_{3}$	9716.146	10289.325	2	I	$18069^{\circ}_{3} - 28358_{3}$
9872.635	10126.231	1	I	$22669^{\circ}_{3} - 32796_{3}$	9702.272	10304.038	3	I	$15618^{\circ}_{3} - 25923_{4}$
9872.185	10126.693	0			9701.580	10304.773	1	I	$18053^{\circ}_{4} - 28358_{3}$
9871.998	10126.885	2	I	$15970_{3} - 26096^{\circ}_{3}$	9700.564	10305.852	7	I	$2869_{3} - 13175^{\circ}_{4}$
9869.929	10129.008	0	II	$4146_{3 1/2} - 14275^{\circ}_{4 1/2}$	9695.033	10311.732	2	I	$13297_{4} - 23609^{\circ}_{5}$
9868.922	10130.041	2	I	$8800_{4} - 18930^{\circ}_{3}$	9684.806	10322.621	1		
9867.890	10131.101	2	I	$7280_{2} - 17411^{\circ}_{3}$	9679.111	10328.695	0		
9865.451	10133.605	1	I	$17847^{\circ}_{2} - 27980_{3}$	9678.235	10329.629	0	I	$20214^{\circ}_{3} - 30544_{2}$
9864.226	10134.864	3			9676.940	10331.012	0	I	$8243^{\circ}_{2} - 18574_{1}$
9864.094	10135.000	1			9676.840	10331.118	3	I	$18011^{\circ}_{5} - 28342_{5}$
9863.866	10135.234	1	II	$12219_{1 1/2} - 22355^{\circ}_{1/2}$	9676.107	10331.901	2	I	$19503^{\circ}_{3} - 29835_{3}$
9862.127	10137.021	0	I	$11601_{1} - 21738^{\circ}_{2}$	9674.790	10333.308	2	I	$11241^{\circ}_{3} - 21575_{2}$
9855.745	10143.585	3	I	$9804_{5} - 19948^{\circ}_{4}$	9670.794	10337.577	1		
9845.690	10153.944	2			9666.379	10342.299	0		
9840.923	10158.863	1	I	$18069^{\circ}_{3} - 28227_{4}$	9664.700	10344.096	6	I	$3687_{2} - 14032^{\circ}_{2}$
9838.008	10161.873	1	I	$21165^{\circ}_{3} - 31326_{4}$	9663.647	10345.223	1	I	$13962_{1} - 24307^{\circ}_{2}$
9837.258	10162.648	0	I	$14465^{\circ}_{2} - 24627_{1}$	9663.062	10345.849	0	II	$12488^{\circ}_{4 1/2} - 22834_{3 1/2}$
9834.008	10166.006	3			9656.439	10352.945	1	I	$11241^{\circ}_{3} - 21594_{3}$
9833.424	10166.610	8	I	$3865_{1} - 14032^{\circ}_{2}$	9652.004	10357.702	0	I	$13297_{4} - 23655^{\circ}_{4}$
9831.676	10168.418	2			9643.649	10366.676	0		
9826.452	10173.823	7	I	$5563_{1} - 15736^{\circ}_{1}$	9643.322	10367.027	1	I	$14032^{\circ}_{2} - 24399_{3}$
9819.178	10181.360	1	I	$9804_{5} - 19986^{\circ}_{6}$	9643.147	10367.215	0	I	$20522^{\circ}_{2} - 30889_{1}$
9814.962	10185.733	1	I	$20322^{\circ}_{5} - 30508_{5}$	9642.471	10367.942	4	II	$8605_{2 1/2} - 18973^{\circ}_{3 1/2}$
9813.153	10187.611	0	I	$16783^{\circ}_{4} - 26971_{4}$	9636.906	10373.929	1	I	$17073_{1} - 27447^{\circ}_{2}$
9812.698	10188.083	7	I	$8243^{\circ}_{2} - 18431_{3}$	9632.647	10378.516	6	I	$3865_{1} - 14243^{\circ}_{1}$
9801.710	10199.505	0	I	$14465^{\circ}_{2} - 24664_{3}$	9630.745	10380.565	1	I	$14247^{\circ}_{0} - 24627_{1}$
9800.586	10200.674	0			9629.572	10381.830	6	I	$3865_{1} - 14247^{\circ}_{0}$
9800.366	10200.903	1			9629.231	10382.198	0	I	$22399^{\circ}_{5} - 32781_{4}$
9797.252	10204.145	1	I	$18069^{\circ}_{3} - 28273_{2}$	9627.672	10383.879	1	I	$14243^{\circ}_{1} - 24627_{1}$
9796.200	10205.241	5	I	$4961_{4} - 15166^{\circ}_{3}$	9627.058	10384.541	0		
9795.646	10205.819	0			9625.740	10385.963	1		
9789.508	10212.218	2	I	$17354^{\circ}_{1} - 27566_{2}$	9625.204	10386.541	3	I	$19986^{\circ}_{6} - 30372_{6}$
9785.356	10216.551	0	I	$18011^{\circ}_{5} - 28227_{4}$	9623.414	10388.473	0	I	$22163^{\circ}_{4} - 32551_{3}$
9782.141	10219.908	0	I	$13962_{1} - 24182^{\circ}_{2}$	9619.222	10393.001	1	I	$15970_{3} - 26363^{\circ}_{2}$
9781.891	10220.170	2			9613.689	10398.982	5	II	$4146_{3 1/2} - 14545^{\circ}_{2 1/2}$
9779.461	10222.709	1			9608.933	10404.129	1	I	$11241^{\circ}_{3} - 21645_{4}$
9778.427	10223.790	0			9608.494	10404.605	2		
9769.538	10233.092	2	I	$15863_{2} - 26096^{\circ}_{3}$	9607.535	10405.643	0		
9764.606	10238.261	0	I	$15166^{\circ}_{3} - 25405_{4}$	9605.809	10407.513	0	I	$16783^{\circ}_{4} - 27191_{5}$
9757.222	10246.009	1	I	$12847_{3} - 23093^{\circ}_{2}$	9595.395	10418.808	4	I	$13962_{1} - 24381^{\circ}_{2}$
9757.159	10246.075	0			9593.115	10421.284	0		
9754.019	10249.374	1	I	$15863_{2} - 26113^{\circ}_{2}$	9590.348	10424.291	1		
9753.597	10249.817	2	I	$21077^{\circ}_{5} - 31326_{4}$	9588.809	10425.964	0	I	$19588^{\circ}_{5} - 30014_{4}$
9746.464	10257.318	7	I	$3687_{2} - 13945^{\circ}_{3}$	9587.027	10427.902	1	I	$14243^{\circ}_{1} - 24671_{2}$
9743.565	10260.370	4	I	$16783^{\circ}_{4} - 27044_{3}$	9583.076	10432.201	3	II	$4113_{2 1/2} - 14545^{\circ}_{2 1/2}$
9738.624	10265.576	1	I	$12847_{3} - 23113^{\circ}_{4}$	9582.816	10432.484	4	I	$13088_{3} - 23521^{\circ}_{3}$

TABLE 1. *Infrared spectral lines of thorium*—Continued

Wavelength Å	Wavenumber cm^{-1}	Intensity	Spectrum	Classification	Wavelength Å	Wavenumber cm^{-1}	Intensity	Spectrum	Classification
9577.344	10438.445	3	II	$9720^{\circ}_{3\frac{1}{2}} - 20158_{2\frac{1}{2}}$	9432.589	10598.635	0		
9571.505	10444.813	1	I	$19516^{\circ}_{2} - 29961_{1}$	9432.280	10598.983	3	II	$9711_{3\frac{1}{2}} - 20310^{\circ}_{2\frac{1}{2}}$
9570.405	10446.013	1	I	$11802_{2} - 22248^{\circ}_{2}$	9431.600	10599.747	5	I	$3865_{1} - 14465^{\circ}_{2}$
9567.826	10448.829	2	I	$11197^{\circ}_{5} - 21645_{4}$	9430.921	10600.510	0	I	$17073_{1} - 27674^{\circ}_{2}$
9567.283	10449.422	1	I	$16346^{\circ}_{4} - 26796_{3}$	9423.850	10608.464	0		
9565.567	10451.297	1			9422.317	10610.190	0	I	$18069^{\circ}_{3} - 28679_{2}$
9563.778	10453.251	0			9420.621	10612.100	2	I	$14226_{0} - 24838^{\circ}_{1}$
9563.709	10453.327	1			9420.493	10612.244	2	II	$1859_{1\frac{1}{2}} - 12472^{\circ}_{2\frac{1}{2}}$
9563.307	10453.767	1			9417.463	10615.659	0	I	$19516^{\circ}_{2} - 30132_{2}$
9563.177	10453.909	0			9414.090	10619.462	2	I	$13297_{4} - 23916^{\circ}_{4}$
9561.736	10455.484	1			9413.682	10619.922	1		
9561.245	10456.021	5	I	$8243^{\circ}_{2} - 18699_{2}$	9413.135	10620.540	1		
9559.932	10457.457	0			9409.353	10624.808	4	I	$16346^{\circ}_{4} - 26971_{4}$
9553.984	10463.967	1			9406.896	10627.583	1		
9548.028	10470.495	1			9405.282	10629.407	1		
9536.411	10483.250	1			9399.091	10636.408	7	I	$7795^{\circ}_{4} - 18431_{3}$
9521.958	10499.162	1			9396.673	10639.145	0		
9514.025	10507.916	0			9394.096	10642.064	0	II	$9238^{\circ}_{4\frac{1}{2}} - 19880_{4\frac{1}{2}}$
9510.950	10511.313	0	I	$17847^{\circ}_{2} - 28358_{3}$	9393.770	10642.433	1		
9507.656	10514.955	2	I	$13088_{3} - 23603^{\circ}_{2}$	9392.268	10644.135	0	I	$15863_{2} - 26508^{\circ}_{3}$
9505.395	10517.456	5	I	$9804_{5} - 20322^{\circ}_{5}$	9392.016	10644.421	1	II	$4146_{3\frac{1}{2}} - 14790^{\circ}_{3\frac{1}{2}}$
9501.443	10521.831	0	I	$19986^{\circ}_{6} - 30508_{5}$	9390.723	10645.886	0		
9500.302	10523.095	2	I	$12114^{\circ}_{2} - 22637_{3}$	9390.588	10646.040	2	I	$14204_{5} - 24850^{\circ}_{6}$
9500.053	10523.370	0			9388.933	10647.916	4	I	$11601_{1} - 22248^{\circ}_{2}$
9498.244	10525.375	0			9384.103	10653.397	0	I	$14226_{0} - 24880^{\circ}_{1}$
9497.191	10526.541	7	I	$0_{2} - 10526^{\circ}_{3}$	9383.275	10654.337	5	I	$5563_{1} - 16217^{\circ}_{2}$
9495.500	10528.416	7	I	$4961_{4} - 15490^{\circ}_{5}$	9380.642	10657.327	0	I	$4961_{4} - 15618^{\circ}_{3}$
9494.041	10530.034	1	II	$11576^{\circ}_{1\frac{1}{2}} - 22106_{2\frac{1}{2}}$	9379.736	10658.357	1		
9486.929	10537.928	3	I	$15970_{3} - 26508^{\circ}_{3}$	9374.051	10664.821	0	II	$17272^{\circ}_{4\frac{1}{2}} - 27937_{5\frac{1}{2}}$
9483.850	10541.349	0	II	$18973^{\circ}_{3\frac{1}{2}} - 29515_{4\frac{1}{2}}$	9366.797	10673.079	0	I	$12847_{3} - 23521^{\circ}_{3}$
9482.290	10543.084	1			9366.743	10673.141	0	II	$0_{1\,1/2} - 10673^{\circ}_{2\frac{1}{2}}$
9482.271	10543.105	1			9362.794	10677.643	0	II	$4113_{2\frac{1}{2}} - 14790^{\circ}_{3\frac{1}{2}}$
9474.882	10551.327	7	I	$7502_{3} - 18053^{\circ}_{4}$	9362.640	10677.819	1	II	$9202^{\circ}_{3\frac{1}{2}} - 19880_{4\frac{1}{2}}$
9470.684	10556.003	6	I	$3687_{2} - 14243^{\circ}_{1}$	9360.989	10679.702	2	II	$9400_{2\frac{1}{2}} - 20080^{\circ}_{3\frac{1}{2}}$
9467.200	10559.888	5	I	$16783^{\circ}_{4} - 27343_{3}$	9357.253	10683.966	0	I	$17847^{\circ}_{2} - 28531_{2}$
9462.907	10564.679	1			9357.055	10684.192	0		
9461.905	10565.798	0			9355.995	10685.402	0		
9461.208	10566.576	3	I	$13088_{3} - 23655^{\circ}_{4}$	9349.246	10693.116	1	II	$6213_{4\frac{1}{2}} - 16906^{\circ}_{3\frac{1}{2}}$
9461.031	10566.774	6	I	$7502_{3} - 18069^{\circ}_{3}$	9344.207	10698.882	1	I	$8111_{4} - 18809^{\circ}_{4}$
9460.871	10566.952	2	I	$7280_{2} - 17847^{\circ}_{2}$	9344.096	10699.009	1	I	$20566^{\circ}_{4} - 31265_{3}$
9458.783	10569.285	0			9340.708	10702.890	4	I	$8800_{4} - 19503^{\circ}_{3}$
9458.629	10569.457	0	I	$17411^{\circ}_{3} - 27980_{3}$	9336.161	10708.102	1	I	$14206^{\circ}_{4} - 24915_{3}$
9456.023	10572.370	0	II	$19912^{\circ}_{5\frac{1}{2}} - 30484_{5\frac{1}{2}}$	9327.252	10718.330	0		
9455.205	10573.284	2	I	$13847_{2} - 24421^{\circ}_{3}$	9320.071	10726.589	0	I	$13945^{\circ}_{3} - 24671_{2}$
9452.674	10576.116	1			9317.727	10729.287	3	I	$10414^{\circ}_{4} - 21143_{5}$
9450.464	10578.589	1	I	$16217^{\circ}_{2} - 26796_{3}$	9310.448	10737.675	2	I	$16783^{\circ}_{4} - 27521_{4}$
9448.890	10580.351	0			9307.899	10740.616	4	I	$19986^{\circ}_{6} - 30726_{7}$
9446.992	10582.477	0			9300.018	10749.718	1	I	$20214^{\circ}_{3} - 30964_{3}$
9439.854	10590.479	0	II	$8460_{1\frac{1}{2}} - 19050^{\circ}_{1\frac{1}{2}}$	9294.976	10755.549	1	I	$12847_{3} - 23603^{\circ}_{2}$
9436.815	10593.889	2	I	$11802_{2} - 22396^{\circ}_{1}$	9294.782	10755.773	2		

TABLE 1. *Infrared spectral lines of thorium* — Continued

Wavelength Å	Wavenumber cm^{-1}	Intensity	Spectrum	Classification	Wavelength Å	Wavenumber cm^{-1}	Intensity	Spectrum	Classification
9289.564	10761.815	5	I	$9804_5 - 20566^\circ_4$	9266.208	10788.941	6	I	$7280_2 - 18069^\circ_3$
9287.583	10764.110	0			9263.682	10791.882	0	I	$10783^\circ_2 - 21575_2$
9277.170	10776.192	0			9260.327	10795.792	2	I	$11601_1 - 22396^\circ_1$
9276.273	10777.234	5	I	$3687_2 - 14465^\circ_2$	9252.860	10804.504	0		
9272.832	10781.234	0			9250.579	10807.168	0	I	$12847_3 - 23655^\circ_4$
9271.181	10783.153	1	I	$0_2 - 10783^\circ_2$	9248.125	10810.036	1		
9270.155	10784.347	2	I	$19588^\circ_5 - 30372_6$	9245.257	10813.389	1	I	$18069^\circ_3 - 28882_2$
9267.686	10787.220	2	II	$7331^\circ_{2\frac{1}{2}} - 18118_{1\frac{1}{2}}$	9243.767	10815.133	1		
9267.082	10787.923	3			9239.328	10820.329	1	I	$15970_3 - 26790^\circ_4$
9266.920	10788.111	4	I	$8800_4 - 19588^\circ_5$					

JOURNAL OF RESEARCH of the National Bureau of Standards — A. Physics and Chemistry
Vol. 78A, No. 2, March-April 1974

Publications of the National Bureau of Standards*

Citations with Selected Abstracts

J. Res. Nat. Bur. Stand. (U.S.), **78A** *(Phys. and Chem.)*, No. 1, (Jan.-Feb. 1974), SD Catalog No. C13.22/sec.A:78/1.

Thermophysical measurements on iron above 1500 K using a transient (subsecond) technique, A. Cezairliyan and J. L. McClure.

Measurement of melting point, normal spectral emittance (at melting point) and electrical resistivity (near melting point) of some refractory alloys, A. Cezairliyan.

Comparative density measurements for solid specimens weighing a few milligrams, A. D. Franklin and J. R. Donaldson.

A density scale based on solid objects, H. A. Bowman, R. M. Schoonover, and C. L. Carroll.

Geometrical considerations in the measurement of the volume of an approximate sphere, D. P. Johnson.

Note on diffusion of vapor into flowing gas, D. P. Johnson.

Theoretical analysis of miscibility gaps in the alkali-borates, P. B. Macedo and J. H. Simmons.

J. Res. Nat. Bur. Stand. (U.S.), **78B** *(Math. Sci.)*, Nos. 1 and 2, SD Catalog No. C13.22/sec.B:78/1&2.

A class of positive stable matrices, D. Carlson.

The Smith normal form of a partitioned matrix, M. Newman.

A Lyapunov theorem for angular cones, C. R. Johnson.

Second, third, and fourth order *D*-stability, C. R. Johnson.

Comparison of some FORTRAN programs for matrix inversion, K. E. Fitzgerald.

On characters of subgroups, R. Merris.

Integer arithmetic determination of polynomial real roots, G. W. Reitwiesner.

Monogr. 132. **A compilation and evaluation of mechanical, thermal, and electrical properties of selected polymers,** R. E. Schramm, A. F. Clark, and R. P. Reed, Nat. Bur. Stand. (U.S.), Monogr. 132, 848 pages (Sept. 1973) $10.25, SD Catalog No. C13.44:132.

Key words: Compilation; electrical properties; mechanical properties; plastics; polymers; thermal properties.

This compilation abstracts original experimental data on the mechanical, thermal, and electrical properties of six commercially available polymers. After an extensive review of the open literature, all available data were collected together in graphical and tabular form along with material characterization, experimental method, and reference to the original publication. The data are also summarized and a brief description of each polymer is included.

Monogr. 136. **Graphical recoupling of angular momenta,** D. R. Lehman and J. S. O'Connell, Nat. Bur. Stand. (U.S.), Monogr. 136, 18 pages (Oct. 1973) 50 cents, SD Catalog No. C13.44:136.

Key words: Angular momentum; diagrams; graphs; quantum theory; recoupling; transformation theory.

A diagrammatic method for solving angular momentum recoupling problems is presented. It is shown that a few graphical elements with a set of rules for their use lead to the solution of many types of recoupling problems in an intuitive and systematic way. Several examples are given together with exercise to develop the reader's facility with the method.

Monogr. 137. **Applications of waveguide and circuit theory to the development of accurate microwave measurement methods and standards,** R. W. Beatty, Nat. Bur. Stand. (U.S.), Monogr. 137, 322 pages (Aug. 1973) $5.20, SD Catalog No. C13.44:137.

Key words: Attenuation definitions; attenuation measurement; barretter mount efficiency; coaxial connectors; impedance measurement; microwave network theory; mismatch errors; phase shift-measurement; power measurement; reflectometers; waveguide joints; waveguide theory.

The basic theory and analytical methods used in the development of accurate microwave measurement methods and standards are presented.

Developments at the U.S. National Bureau of Standards during 1948-1968 are described in which the above theory and analytical methods were applied.

These developments were in the fields of power, impedance, attenuation and phase shift, and led to the establishment of National Standards and calibration methods at frequencies from about 300 MHz to 30 GHz.

SP260-32. **Standard reference materials: Standard quartz cuvettes for high accuracy spectrophotometry,** R. Mavrodineanu and J. W. Lazar, Nat. Bur. Stand. (U.S.), Spec. Publ. 260-32, 27 pages (Dec. 1973) 55 cents, SD Catalog No. C13.10:260-32.

Key words: Cuvette, spectrophotometry; lightpath; pathlength; quartz, cuvette; radiation pathlength.

Accurate knowledge of lightpath and parallelism of cuvettes used in spectrophotometry is one of the indispensable parameters which must be determined when accurate transmittance measurements of liquid materials is considered. A description is given of the design and techniques developed at NBS for the production of quartz cuvettes having a nominal radiation pathlength of 10 mm $\pm$ 0.03 mm and a parallelism certified both with an uncertainty of $\pm$ 0.0005 mm. The method and instrumentation used to determine these parameters is also described in the paper.

SP300. Volume 10. **Precision measurement and calibration.** Selected NBS papers on image optics, C. S. McCamy, Editor, Nat. Bur. Stand. (U.S.), Spec. Publ. 300, Vol. 10, 953 pages (Nov. 1972) $11.10, SD Catalog No. C13.10:300, Vol. 10.

Key words: Camera calibration; image evaluation; image optics; image stability; interferometry; lens testing; light filters; light sources; photography.

This volume is one of an extended series which brings together the previously published papers, monographs, abstracts, and bibilographies by NBS authors dealing with precision measurement of specific

530-326 OL - 74 - 13

physical quantities and the calibration of the related metrology equipment. The contents have been selected as being useful to the standards laboratories of the United States in tracing to NBS standards the accuracies of measurement needed for research work, factory production, or field evaluation.

Volume 10 deals with image optics, including photography. It contains 57 reprints assembled in 4 sections: (1) Refractometry and Optical Homogeneity; (2) Interferometry in Image Optics; (3) Optical Image Evaluation; (4) Photography. Each section is introduced by an interpretive foreword, including in some instances, pertinent references.

SP305. Supplement 4. **Publications of the National Bureau of Standards 1972 catalog. A compilation of abstracts and key word and author indexes,** B. L. Oberholtzer, Nat. Bur. Stand. (U.S.), Spec. Publ. 305 Suppl. 4, 449 pages (July 1973) $3.75, SD Catalog No. C13.10:305 Suppl. 4.

Key words: Abstracts, NBS publications; key words; publications.

This supplement to Special Publication 305 Supplements 1, 2, and 3 of the National Bureau of Standards lists the publications of the Bureau issued between January 1, 1972 and December 31, 1972. It includes an abstract of each publication (plus some earlier papers omitted from Special Publication 305 Supplement 3), key-word and author indexes; and general information and instructions about NBS publications.

Miscellaneous Publication 240 (covering the period July 1, 1957 through June 30, 1960) and its supplement (covering the period July 1, 1960 through June 30, 1966), Special Publication 305 (covering the period July 1966 through December 1967) and Special Publication 305 Supplement 1 (covering the period 1968-1969), Special Publication 305 Supplement 2 (covering the period 1970), and Special Publication 305 Supplement 3 (covering the period 1971) remain in effect. Two earlier lists, Circular 460 (Publications of the National Bureau of Standards, 1901 to June 1947) and its supplement (Supplementary List of Publications of the National Bureau of Standards, July 1, 1947 to June 30, 1957) are also still in effect.

SP320. Supplement 2. **Bibliography on atomic transition probabilities July 1971 through June 1973,** J. R. Fuhr and W. L. Wiese, Nat. Bur. Stand. (U.S.), Spec. Publ. 320 Suppl. 2, 63 pages (Nov. 1973) 95 cents, SD Catalog No. C13.10:320.

Key words: Allowed; atomic; discrete; forbidden; transition probability.

This is the second supplement to the NBS Special Publication 320, "Bibliography on Atomic Transition Probabilities," and it covers the most recent literature on the subject from July 1971 through June 1973. The papers are arranged according to elements and stages of ionization, and the method employed and classification of transitions are indicated for each reference. Only articles on discrete transitions, both allowed and forbidden, are listed. Papers containing data for many elements within isoelectronic sequences are collected separately in front of the list in order to keep this bibliography to a reasonable size. Also included is a selected list of new papers dealing with the subject of atomic transition probabilities from a general point of view.

SP381. **Bibliography of ion-molecule reaction rate data (January 1950-October 1971),** G. A. Sinnott, Nat. Bur. Stand. (U.S.), Spec. Publ. 381, 73 pages (Oct. 1973) $1.00, SD Catalog No. C13.10:381.

Key words: Atoms; bibliography; cross-sections; ions; molecules; rate coefficients; reactions.

A bibliography is presented of papers in the open literature that contain original experimental data on ion-molecule reaction rates or cross sections. Positive and negative ion-molecule and ion-ion reactions are included but not electron impact processes. For papers to be included, the reactants must have been identified and data for kinetic energies below 10 electron volts must have been presented.

SP387. **Laser induced damage in optical materials: 1973.** Proceedings of a symposium sponsored by Office of Naval Research, The American Society for Testing and Materials and by the National Bureau of Standards, Boulder, Colo. May 15-16, 1973, A. J. Glass and A. H. Guenther, Editors, Nat. Bur. Stand. (U.S.), Spec. Publ. 387, 285 pages (Dec. 1973) $2.65, SD Catalog No. C13.10:387.

Key words: IR windows and mirrors; laser damage; laser materials; self-focusing; thin films.

The Fifth ASTM-ONR-NBS Symposium on Laser Induced Damage in Optical Materials was held at the National Bureau of Standards in Boulder, Colo. on May 15 and 16 of this year. These Symposia are held as part of the activities of Subcommittee II on Lasers and Laser Materials, of the ASTM. Subcommittee II is charged with the responsibilities of formulating standards and test procedures for laser materials, components, and devices. The chairman of Subcommittee II is Haynes Lee, of Owens-Illinois, Inc. Co-chairmen for the Damage Symposia are Dr. Arthur H. Guenther, Scientific Director, Technology Division of the Air Force Weapons Laboratory, and Dr. Alexander J. Glass, Head, Basic Studies, Y Division, Lawrence Livermore Laboratory.

Approximately 135 attendees at the Symposium heard 25 papers on topics relating to laser induced damage in crystalline and nonlinear optical materials, at dielectric surfaces, and in thin film coatings as well as discussions of damage problems in the infrared region due both to cw and pulsed irradiation. In addition, several reports on the theoretical analysis of laser-materials interaction, relative to the damage process were given, along with tabulations of fundamental materials properties of importance in evaluation of optical material response to high power laser radiation. Several papers presented by title only are included within the proceedings for completeness.

The proceedings of these Symposia represent the major sources of information in the field of laser induced damage in optical materials. The Symposia themselves, along with the periodic meetings of Subcommittee II, provide a unique forum for the exchange of information regarding laser materials specifications among the manufacturers and users of laser devices, components, and systems. The Symposia also serve as a mechanism of information gathering to enable the Subcommittee to write informed and realistic specifications.

SP389. **Some references on metric information with charts on all you need to know about metric and metric conversion factors,** W. R. Tilley, Editor, Nat. Bur. Stand. (U.S.), Spec. Publ. 389, 8 pages (Dec. 1973) 25 cents, SD Catalog No. C13.10:389.

Key words: Metric charts; metric information sources; metric publications.

A bibliography of metric publications issued by NBS along with a list of organizations that market metric publications, lists, and films for educators. Also includes two metric charts "All you need to know about metric" and "Metric conversion factors."

NSRDS-NBS45. **Radiation chemistry of nitrous oxide gas. Primary processes, elementary reactions, and yields,** G. R. A. Johnson, Nat. Stand. Ref. Data Ser., Nat. Bur. Stand. (U.S.), 45, 27 pages (Dec. 1973) 60 cents, SD Catalog No. C13.48:45.

Key words: Chemical kinetics; data compilation; dosimetry; G; gas; nitrous oxide; radiation chemistry; rates; review.

Data on the radiation yields from nitrous oxide gas, and the effects of variables, including dose-rate, total dose, pressure, temperature, applied fields and scavengers are reviewed and tabulated. The use of N_2O as a gas-phase, chemical dosimeter is discussed. Primary

processes in irradiated N_2O are discussed and elementary reactions, relevant to the system, are listed.

PS56-73. **Structural glued laminated timber,** *(ANS A190. 1-1973),* K. G. Newell, Jr., Technical Standards Coordinator, Nat. Bur. Stand. (U.S.), Prod. Stand. 56-73, 12 pages (Oct. 1973) 45 cents, SD Catalog No. C13.20/2:56-73.

Key words: Glued laminated timber; laminated timber; structural glued laminated timber; timber, structural glued laminated.

This Voluntary Product Standard covers requirements for the dimensions, grade combinations, lumber for laminating, appearance grades, adhesive, and laminating of structural glued laminated timber as well as inspection and test procedures, marking, and the certification by a qualified inspection and testing agency. Definitions of the trade terms used are given, and guides for ordering and information on inspection practices are provided in the appendices.

TN392. (Revised September 1973). **Thermodynamic properties of compressed gaseous and liquid fluorine,** R. Prydz and G. C. Straty, Nat. Bur. Stand. (U.S.), Tech. Note 392, 197 pages (Sept. 1974) $1.50, SD Catalog No. C13.46:392 (Rev. 1973).

Key words: Density; enthalpy; entropy; fixed points (PVT); fluorine; Joule-Thomson; latent heat; melting curve; PVT measurements; saturation densities; specific heats; vapor pressure; velocity of sound; virial coefficients.

An apparatus has been constructed and used successfully to measure vapor pressure and PVT data of fluorine from the triple point to 300 K at pressures to about 24 MN/m^2. Material problems caused by the toxic and corrosive nature of fluorine were solved. A network of isotherm and isochore polynomials and a truncated virial equation were used to represent all PVT data. These equations represent the data with an average standard deviation of about 0.02 percent in density, the corresponding accuracy being estimated at 0.1 percent. Equations for the saturated liquid and vapor densities, the vapor pressure curve, the melting line, and the ideal gas properties are also presented. Comparisons are given to published values of the second virial coefficients, vapor pressures, and saturation densities. Additional comparisons are also made to measured specific heats and latent heats of vaporization. New values are reported for the triple point and critical point parameters together with the temperature and saturation densities at the normal boiling point. Finally, extensive tables of thermodynamic properties of fluorine are given which include pressure, temperature, density, isotherm and isochore derivatives, internal energy, enthalpy, entropy, specific heats at constant pressure and volume and velocity of sound. Some erroneous values for the internal energy and enthalpy of the compressed liquid below 135 K, published previously, have been corrected in this revision.

TN641. **Survey of the properties of the hydrogen isotopes below their critical temperatures,** H. M. Roder, G. E. Childs, R. D. McCarty, and P. E. Angerhofer, Nat. Bur. Stand. (U.S.), Tech. Note 641, 122 pages (Oct. 1973) $1.25, SD Catalog No. C13.46:641.

Key words: Compilation; density; deuterium; electrical properties; enthalpy; entropy; fixed points; hydrogen; mechanical properties; optical properties; specific heat; thermophysical properties; transport properties; tritium; vapor pressure.

The survey covers PVT, thermodynamic, thermal, transport, electrical radiative and mechanical properties. All isotopic as well as ortho-para modifications of hydrogen have been included. Temperatures are limited to those below the respective critical points, in general below 40 K. The pressure range is not restricted, that is solid, liquid, and gas phases are covered. However, with the exception of hydrogen, very little data exists at pressures other than saturation. The literature surveyed includes all references available to the Cryogenic Data Center up to June of 1972, and for several subjects, through March of 1973. The total number of documents considered was nearly 1500 of which about 10 percent contain pertinent information and are referenced in this report. The various properties are presented in the form of tables of graphs; if extensive tables have been published elsewhere, the reader is referred to the original sources.

TN642. **Summary of WR15 flange evaluation at 60 GHz,** B. C. Yates and G. J. Counas, Nat. Bur. Stand. (U.S.), Tech. Note 642, 32 pages (Oct. 1973) 40 cents, SD Catalog No. C13.46:642.

Key words: Attenuation; flange measurements; reflection coefficients; VSWR.

The measurement results of flange loss and reflection coefficient magnitude at 60 GHz (WR15 waveguide) of various flange configurations are presented. Included are the effects of alignment pins, surface finish, metallic contact surface, contact area, and flange bolt torque.

TN644. **Application of a non-ideal sliding short to two-port loss measurement,** M. P. Weidman and G. F. Engen, Nat. Bur. Stand. (U.S.), Tech. Note 644, 40 pages (Oct. 1973) 50 cents, SD Catalog No. C13.46:644.

Key words: Efficiency; loss; reflectometer; sliding short; two-port.

A detailed, applications-oriented, description of a method for measuring two-port losses is given. The technique involved uses a non-ideal sliding short circuit and a tuned four-arm reflectometer. Most, if not all, of the components used in this technique can be put together using commercially available items. It is the intent of this discussion to provide enough detail and explanation so that a technician with some working knowledge of microwave measurements can set up and make loss measurements.

The reference made to two-ports implies a broad range of devices from a simple flange or connector to waveguide coaxial adaptors and even more elaborate configurations with a definable input and output connection.

TN645. **Time and frequency broadcast experiments from the ATS-3 satellite,** D. W. Hanson and W. F. Hamilton, Nat. Bur. Stand. (U.S.), Tech. Note 645, 115 pages (Nov. 1973) $1.00, SD Catalog No. C13.46:645.

Key words: Dissemination; frequency; satellites; synchronization; time.

An experiment designed to reveal the advantages and special problems associated with the broadcasting of time and frequency information from geostationary satellites is discussed. Included are discussions concerning satellite motion, time delay variation, doppler shift due to the motion, and calculation of delay. Receiver or ground station equipment requirements, time recovery techniques, timing resolution and accuracy, and special advantages of satellite broadcasts for time and frequency dissemination are also discussed. Specially equipped sites in North and South America gathered data from the experimental satellite broadcast which in turn were used to determine the potential accuracy of satellite dissemination, the results of which are presented. Delay computation aids for the user were designed to provide a simple and inexpensive means of computing free space delays between the master clock and the user via a geostationary satellite. The aids, delay overlays on an earth map and a circular slide rule, are discussed with examples. Qualitative discussions of the signals and broadcast format are given. Final comments are made concerning the results of the experiment and how they might reflect upon a final system design for a permanent service using one or more geostationary satellites.

TN740. **SETAB: An edit insert program for automatic typesetting of spectroscopic and other computerized tables,** R. C. Thompson and J. Hilsenrath, Nat. Bur. Stand. (U.S.),

Tech. Note 740, 30 pages (Dec. 1973) 55 cents, SD Catalog No. C13.46:740.

Key words: Automatic typesetting; computer-assisted typesetting; edit insertion program; FORTRAN program; phototypesetting of spectroscopic tables; typesetting of tables.

SETAB is a FORTRAN program which accepts a card deck or FORTRAN records on magnetic tape and inserts the appropriate flags and shift symbols required by many programs associated with phototypesetting devices. The program is specialized to the particular application, the phototypesetter and typography programs, and to the desired typefaces by means of parameter cards supplied at run time. Examples are shown of spectroscopic tables typeset on the Linofilm phototypesetter at the Government Printing Office using the Autoset Typography Program. The program has also been used for tables of other types of data. The program can handle any records which can be read by a FORTRAN "READ" statement under "A" format control. The original record can be divided into as many as 40 fields and these fields can be combined in any order with any of 26 strings in front of or between the pieces. The program will, on a signal, replace a field by another field or by a combination of fields and strings. The output lines are blocked and paged via the insertion of the required strings between blocks and pages.

TN794. **NBS corridor fire tests: Energy and radiation models,** F. C. W. Fung, R. Suchomel, and P. L. Oglesby, Nat. Bur. Stand. (U.S.), Tech. Note 794, 127 pages (Oct. 1973) $1.40, SD Catalog No. C13.46:794.

Key words: Ceiling radiation; corridor fires; critical energy input; flame spread, calculation, and observations; floor covering evaluations; heat balances; heat transfer mechanisms; models, energy balance, radiation, and scaling.

The NBS corridor fire program is a continuing program to investigate the growth and spread of fire and smoke through a corridor when fire is initiated in an adjoining room. Due to recent fires involving floor coverings [1], and controversies over current floor covering flammability test methods, floor coverings have received special attention during the first phase of the corridor fire program. Results of the NBS program on corridor fires are presented under the unifying concepts of energy and radiation models. The major findings are: (1) One type of carpet fire hazard has been identified as the rapid flame spread over pile surface; (2) The dominant mechanism that causes this flame spread is energy transfer from ceiling radiation. This is substantiated by measurements and calculations; (3) Carpet evaluation by critical cumulative energy input into the corridor has been found to be feasible and informative in terms of heat transfer mechanisms; (4) Finally, a radiant panel test appears to be a promising approach to simulate the corridor environment for second generation flooring tests.

TN798. **Collaborative research program between NBS and Indian Scientific Institutions. Special foreign currency program 1973 status,** H. S. Peiser, M. B. McNeil, and D. M. Bluebond, Editors, Nat. Bur. Stand. (U.S.), Tech. Note 798, 139 pages (Nov. 1973) $1.50, SD Catalog No. C13.46:798.

Key words: Binational research cooperation; international scientific cooperation; India science and technology; physical science research administration; research planning; scientific research abstracts; Special Foreign Currency.

An overview is given of grants awarded by the National Bureau of Standards under the Special Foreign Currency Program in India, authorized by Public Law 480 and its amendments. Each grant is identified by title, principal investigator, institution in India, NBS monitor charged with working in close technical touch with the project in India, and the monitor's organizational unit within NBS. The relevant work is then described briefly under the three headings "Summary Description of Project Goals," "Results and Implications to Date," and "List of Publications that Resulted from the Project." To demonstrate the wide use of such grants over the entire Program Structure of NBS, the grant descriptions are ordered by the elements of that Program Structure. Editorial comment on the significance and purpose of the NBS/SFCP grant program is confined to a Foreword and Introduction. The editors judge this grant program to have had a high benefit to cost ratio from the viewpoint of NBS.

TN799. **User procedures standardization for network access,** A. J. Neumann, Nat. Bur. Stand. (U.S.), Tech. Note 799, 43 pages (Oct. 1973) 70 cents, SD Catalog No. C13.46:799.

Key words: Network access procedures; networking; standardization; user protocols.

User access procedures to information systems have become of crucial importance with the advent of computer networks, which have opened new types of resources to a broad spectrum of users. This report surveys user access protocols of six representative systems. Functional access requirements are outlined, and implementation of access procedures is analyzed by means of a common methodology.

Qualitative assessment of standardization possibilities identify standardization candidates such as: system and user signals, on-line user entries, system requests, and network wide categories of message content.

TN802. **Network user information support,** A. J. Neumann, Nat. Bur. Stand. (U.S.), Tech. Note 802, 27 pages (Dec. 1973) 60 cents, SD Catalog No. C13.46:802.

Key words: Computers; consultation; documentation; information support; networks; on-line support; user needs; user support.

With increasing interest in the development of computer networks and the proliferation of remote entry capability from user terminals, user support takes on new dimensions. Some user characteristics are outlined as they affect user support. User support requirements are identified for training, terminal operation, and general information to aid in network operations. Support capabilities include on-line aids, information available on request, and tutorial information available at the terminal. User support also includes pertinent documentation and human consultation. Areas of future research are identified as: interactive language design, tutorial design, integration of hard-copy and on-line capabilities, and further development of user feedback capability.

TN806. **Methods of measurement for semiconductor materials, process control, and devices. Quarterly report, April 1 to June 30, 1973,** W. M. Bullis, Editor, Nat. Bur. Stand. (U.S.), Tech. Note 806, 77 pages (Nov. 1973) $1.00, SD Catalog No. C13.46:806.

Key words: Beam leads; carrier lifetime; delay time; die attachment; electrical properties; electronics; epitaxial silicon; generation centers; gold-doped silicon; methods of measurement; microelectronics; microwave diodes; mobility; pull test; recombination centers; resistivity; resistivity standards; scanning electron microscopy; semiconductor devices; semiconductor materials; semiconductor process control; silicon; S-parameters; spreading resistance; thermal resistance; thermally stimulated properties; trapping centers; wire bonds.

This quarterly progress report, twentieth of a series, describes NBS activities directed toward the development of methods of measurement for semiconductor materials, process control, and devices. Significant accomplishments during this reporting period include (1) completion of an initial identification of the more important problems in process control for integrated circuit fabrication and assembly as a basis for and expanded effort to be conducted in cooperation with ARPA, (2) completion of preparations for making silicon bulk re-

sistivity wafer standards available to the industry, and (3) undertaking of new work to establish the relationship between carrier mobility and impurity density in silicon and to investigate test patterns for use in process control and evaluation. Because of the general applicability of the first of these, a summary of the findings is presented in a separate appendix. Work is continuing on measurement of resistivity of semiconductor crystals; characterization of generation-recombination-trapping centers, including gold, in silicon; evaluation of wire bonds and die attachment; study of scanning electron microscopy for wafer inspection and test; measurement of thermal properties of semiconductor devices; determination of S-parameters and delay time in junction devices; and characterization of noise and conversion loss of microwave detector diodes. Supplementary data concerning staff, standards committee activities, technical services, and publications are also included as appendices. This is the last report in this form; future reports in this series will appear under the title, Semiconductor Measurement Technology.

TN807. **Building performance in the 1972 Managua earthquake,** R. N. Wright and S. Kramer, Nat. Bur. Stand. (U.S.), Tech. Note 807, 155 pages (Nov. 1973) $1.60, SD Catalog No. C13.36:807.

Key words: Building codes; buildings; earthquakes; hazards; natural disasters; structures.

Following the Managua, Nicaragua, earthquake of Dec. 23, 1972, a team of engineers representing the U.S. Department of Commerce's National Bureau of Standards (NBS) and the National Academy of Engineering (NAE) performed field investigations in Managua, Nicaragua, from Dec. 26, 1972, to Jan. 4, 1973. The objectives were to assist the Nicaraguan government in surveying major buildings to determine whether each was suitable for emergency use, repairable, or appropriate for clearance. The team also viewed the patterns of successful performance and damage to identify needs for improvements in building practices for mitigation of earthquake hazards and opportunities for more detailed investigations which could provide information for future improvements in practices. In general, the damages cannot be attributed to unusual intensities of ground shaking or severity of surface faulting. Most damages appeared to result from deficiencies in building practices; deficiencies which had been exhibited many times before in previous earthquakes, deficiencies which would be avoided by implementation of up-to-date provisions for earthquake resistant design and construction. However, Managua did not employ a building code with seismic design requirements appropriate to its earthquake risk, and furthermore, did not have a building regulatory system capable of effective implementation of its building code provisions. This report documents the observations of damages by the NBS/NAE team and points out relationships to inadequacies in the building practices employed. Most of these inadequacies have been well known; however, the Managuan experience may serve as an incentive to improvement of building practices in many other areas which are subject to substantial earthquake risks and have not consistently accounted for these risks in their building codes and building regulatory system.

TN808. **Potential systems for lead hazard elimination: Evaluations and recommendations for use,** D. Waksman, J. B. Ferguson, M. Godette, and T. Reichard, Nat. Bur. Stand. (U.S.), Tech. Note 808, 192 pages (Dec. 1973) $1.95, SD Catalog No. C13.46:808.

Key words: Abrasion; adhesion; colorfastness; covering; materials; flash point; flame spread; impact resistance; lead paint poisoning; materials; performance; properties; scratch resistance; smoke generation; toxic combustion products; toxicity; washability; water vapor permeance.

The National Bureau of Standards is providing technical support to the Department of Housing and Urban Development which is required by Public Law 91-695 (the Lead Paint Poisoning Prevention Act) to carry out a research program to evaluate and make recommendations regarding technology for the removal of the lead based paint hazard from the Nation's housing.

Potential hazard elimination methods have been identified by means of a survey of available technology. This report describes testing and evaluation methodologies used to determine (1) the suitability for use of a series of removal and lead barrier systems, (2) the results of this evaluation, and (3) recommendations concerning the use of said systems.

Paint removal systems were evaluated in terms of the hazards that they present in the course of their use. Both the flammability and the toxicity of the solvents found in removers were considered. Covering systems were evaluated for their suitability for use as barrier layers over lead bearing paints in housing. The effectiveness of covering systems in protecting children from leaded paint, their fire hazard properties and functional properties which are related to their serviceability were considered in making this evaluation. The properties of the systems were assessed in terms of minimum acceptable performance levels and recommendations are given for their use in a field evaluation program.

TN810. **Fire incidents involving sleepwear worn by children ages 6-12,** J. A. Slater, Nat. Bur. Stand. (U.S.), Tech. Note 810, 23 pages (Dec. 1973) 50 cents, SD Catalog No. C13.46:810.

Key words: Accidents; burns; children; clothing fires; deaths; FFACTS; fire; flammable fabrics; injury; sleepwear; standards; statistics.

Sleepwear was the first fabric item ignited more frequently than any other item in over 1,900 fire incidents reported to the National Bureau of Standards Flammable Fabrics Accident Case and Testing System (FFACTS). Information acquired since promulgation of the current sleepwear flammability standard protecting children of ages 0-5 indicates a problem of comparable magnitude exists for children of ages 6-12. Of 316 incidents involving non-contaminated sleepwear that was first to ignite, about one-fourth involved children 0-5 years old and one-fourth involved children 6-12 years old. For the 6-12 group, sleepwear ignited first more often than all other garment items combined. Females outnumbered males 4-to-1 in the 6-12 group, due mostly to the involvement of nightgowns and kitchen ranges, the most common ignition source for this age group. Five of the 6-12 year old children died and 52 of 74 victims were hospitalized. Almost all of the first-to-ignite sleepwear in this group was cotton. Data from Shriners Burns Institute and the National Burn Information Exchange provide further evidence of the involvement of children ages 6-12 in garment fires. It is recommended that a new standard be issued covering sleepwear sizes 7 through 14 to effectively protect 6-12 year old children.

This column lists all outside publications by the NBS staff, as soon after issurance as practical. For completeness, earlier references not previously reported may be included from time to time.

Abrams, M. D., Hudson, J. A., Meissner, P., Pyke, T. N., Jr., Rosenthal, R. M., Ulmer, F. H., **Use of computer networks in support of interactive graphics for computer-aided design and engineering,** *NBSIR 73-217*, 47 pages (June 30, 1972). (Available as COM 74–10470 from the National Technical Information Service, Springfield, Va. 22151.)

Key words: Computer-aided design; computer networks; interactive graphics, performance measurement; remote computer utilization.

This report covers work performed between 1 July 1971 and 30 June 1972 as part of a long-term study of interactive computer-aided techniques. The primary emphasis during this period has been on investigating the feasibility of using computer networks in support of interactive graphics for computer-aided design and engineering. Alternative means for providing remote computer service have been studied. An experimental configuration has been devised taking ad-

vantage of the fact that there is located at the National Bureau of Standards a node of the ARPA Computer Network. Arrangements were made via this configuration for users at the Electronics Command to utilize a structural design program, NASTRAN, at a remote computer site. Emphasis has been placed on the evaluation of performance of interactive design techniques using displays supported by local and remote computers in a hierarchical arrangement. A variety of problems are identified which must be considered in order to support interactive graphics via a computer network; these are compounded where the network itself is in an evolving state of development. The report includes an outline of a synchronous communication protocol which was developed for use between ECOM and NBS.

Abrams, M. D., **Remote computing: The administrative side,** *Comput. Decisions*, pp. 42-46 (Oct. 1973).

Key words: Administration; batch; computing; documentation; remote; service; users.

The administration and management of remote computing services are discussed with the objective of making both users and administrators aware of the potential problems. Likely difficulties are anticipated and coupled with discussions of assistance, operation, documentation and other features which make it more possible to utilize the technical services. The response to technical questions is covered in terms of written, on-line, and direct contact assistance. A question and answer organization is employed.

Andrews, J. R., **Random sampling oscilloscope time base,** *NBSIR 73-309*, 86 pages (June 1973). (Available as COM 73-11981 from the National Technical Information Service, Springfield, Va. 22151.)

Key words: Mercury switch; oscilloscope; picosecond; pulse; random sampling; risetime; sampling; time base; transition time.

With the advent of new miniaturized mercury (Hg) switches with reputed transition times of the order of 10 picoseconds, interest has been rekindled in their use in high speed pulse measurements. Since there is no pre-trigger signal available from a Hg switch, normal sequential sampling techniques are not usable to measure the fast Hg switch transition time. For this reason a new random sampling time base unit was designed to perform these measurements at the low repetition rate of Hg switches (< 100 Hz). The time base may be used with commercial sampling oscilloscope systems through suitable interconnection terminals or possible interface equipment. It features three selectable time windows of 1 μs, 100 ns, and 10 ns. Using its time magnifier, the fastest sweep rate is 10 ps/cm. A variable trigger lead time control is provided. The trigger sensitivity is 10 mV. The long term timing stability of the time base is excellent with less than 15 ps/h drift.

Baker, M. A., **Observing porcelain enamels with a scanning electron microscope,** *Proc. Porcelain Enamel Institute Technical Forum, The Ohio State University, Columbus, Ohio, Oct. 6-8, 1971*, **33,** 84-90 (Porcelain Enamel Institute, Inc., Washington, D.C., 1971).

Key words: Corrosion; pinhole-type defects; porcelain enamel; scanning electron microscope; weathering tests; non-dispersive x-ray spectrometer.

Porcelain enamel surfaces and enamel-metal interfaces have been observed with a scanning electron microscope. The increased depth of field and the extended range of magnifications of the scanning electron microscope were utilized in studies of the enamel-metal interface and of weathering test specimens that corroded after relatively short periods of exposure. The nondispersive x-ray spectrometer accessory for the scanning electron microscope was used to determine the elements present in the enamel surface and to obtain qualitative distributions of these elements.

Baker, M. A., **Weathering tests of porcelain enamels on steel and aluminum,** *Proc. Porcelain Enamel Institute Technical Forum, The University of Illinois, Urbana, Ill., Oct. 11-13, 1972*, **34,** 186-198 (Porcelain Enamel Institute, Inc., Washington, D.C., 1972).

Key words: Accelerated tests; acid resistance; aluminum; color; gloss; porcelain enamel; steel; weather resistance.

The Porcelain Enamel Institute and the National Bureau of Standards have been conducting weathering tests of porcelain enamels since 1939. The four tests now in progress contain matte and glossy porcelain enamels on both steel and aluminum. When the data obtained from these weathering tests were compared with accelerated test data on laboratory specimens, an excellent correlation was found. It was also found that the enamels in all four tests changed gloss and color in practically the same manner.

Ballantyne, J. P., Yakowitz, H., Nixon, W. C., **Simultaneous x-ray microanalysis and resistance measurement of electron beam induced direct metallic deposition,** (Proc. 6th Int. Conf. on X-Ray Optics and Microanalysis, Osaka, Japan, Sept. 1971), Paper in *Proceedings of the Sixth International Conference on X-Ray Optics and Microanalysis*, G. Shinoda, K. Kohra and T. Ichinokawa, Eds., pp. 219-227 (University of Tokyo Press, Tokyo, Japan, 1972).

Key words: Deposited thin film; electron beam metal deposition; scanning electron microscopy; x-ray microanalysis.

The decomposition of thin film AgCl, vapor deposited onto an oxidized silicon substrate, was caused by electron bombardment in a scanning electron microscope operating at a pressure of 10^{-8} torr. This decomposition was monitored by nondispersive x-ray analysis techniques. At the same time, the resistance of the film was also recorded.

The curves of chlorine concentration and resistance as a function of exposure are very similar in shape. The chlorine content of the film reaches a level that does not alter with increasing exposure. At this point, film resistance is about 1000 Ω and remains essentially constant with increasing exposure. The residual chlorine can be removed by chemical treatment after which the resistance values drop to less than 50Ω.

The quantitation of the x-ray results must await new correction procedures presently under study. However, a simple correction procedure has been employed in order to illustrate important trends in the direct metallic deposition process.

Ballard, L. D., Edelman, S., Epstein, W. S., Smith, E. R., **A suggestion for determining g by a two interferometer technique,** *SPIE J.* **9,** No. 5, 166-168 (June/July 1971).

Key words: Acceleration; counter; filter; g; gravity; interferometer; laser.

A method for determining the acceleration due to gravity is suggested. Two falling interferometer reflectors illuminated by a laser are used. The falling reflectors are separated by a ΔT and thus have a constant velocity differential, this generates a frequency linearly proportional to acceleration ($g = kf = \Delta V/\Delta T$).

Thus, the metrology of measuring g is simplified by having g linearly proportional to frequency.

Barber, W. C., Hayward, E., Sazama, J., **Nuclear scattering of plane-polarized photons,** (Proc. Int. Conf. on Nuclear Structure Studies using Electron Scattering and Photoreaction, Sendai, Japan, Sept. 12-15, 1972), Paper in *Nuclear Structure Studies Using Electron Scattering and Photoreaction*, Supplement to *Research Report of Laboratory of Nuclear Science*, K. Shoda and H. Ui, Eds., **5,** 313-317 (Tohoku University, Tomizawa, Sendai, Japan, 1972).

Key words: Dynamic collective model; giant resonance; photon scattering; polarized photons.

A beam of plane-polarized, monochromatic photons has been produced by the resonance fluorescence of the well-known 1^+ state in ^{12}C. These have been scattered a second time from targets of cadmium, tin, tantalum, gold, and bismuth. A measurement of the number of photons scattered along and perpendicular to the polarization vector in the incident 15.1 MeV beam allows a determination of the relative contribution of incoherent and coherent scattering to the total scattering cross section. These results can be compared to the predictions of the dynamic collective model.

Barnes, J. D., **Inelastic neutron scattering study of the "rotator" phase transition in *n*-nonadecane,** *J. Phys. Chem.* **58,** No. 12, 5193-5201 (June 15, 1973).

Key words: Molecular dynamics; *n*-alkanes; *n*-nonadecane; neutron scattering; paraffin; rotator phase.

A simple kinematic model for rotational jump diffusion of a normal alkane about its long axis (circular random walk model) is developed. Inelastic neutron scattering data obtained on the Fermi chopper time-of-flight instrument at the National Bureau of Standards reactor using an incident neutron wavelength of 2.47 Å ($\Delta\lambda/\lambda \simeq 3.8$ %) are compared with the predictions of the model. Data taken below the temperature of the "rotator" phase transition in *n*-nonadecane (295 °K) show no quasielastic scattering due to diffusive motions. Data taken in *n*-nonadecane in its disordered solid phase show quasielastic scattering consistent with the circular random walk model. Estimates for values of the model parameters of 3.5 psec. for τ_1 and $N \geq 8$ are obtained.

Barton, J. A., Jr., Burns, C. L., Chandler, H. H., Bowen, R. L., **An experimental radiopaque composite material,** *J. Dent. Res.* **52,** No. 4, 731-739 (1973).

Key words: Barium glass; dental composites; dental reinforcements; physical properties; resins; silica; x-ray opacity.

Physical properties of a composite material, developed for use as a temporary posterior restorative material, have been investigated. The material is based on isomeric phthalate esters of 2-hydroxyethyl methacrylate and reinforcing fillers consisting of particles of vitreous silica and an x-ray-opaque glass. Properties investigated include hardening time, tensile and compressive strengths, indentation and recovery, hardness, water sorption, solubility, polymerization shrinkage, optical and x-ray opacity, color stability and thermal expansion. All properties were studied using 3 different powder-liquid rations: 1.10, 1.35 and 1.45 Gm of powder to 0.4 ml of monomer, under wet and dry storage conditions. The powder-liquid ratio had little effect on compressive strength; e.g., 1.45 ratios, respectively. The tensile strength of the 1.10 ratio specimens was lower than those of the 1.35 and 1.45 ratio specimens (at six hours, 25.5 as compared to 30.4 MN/m^2). Water sorption at one week was 0.2 to 0.3 mg/cm^2.

Becker, D. A., LaFleur, P. D., **Neutron activation analysis: Application to trace element analysis in biological and environmental materials,** *Proc. 5th Annual Conf. on Trace Substances in Environmental Health, University of Missouri, Columbia, Mo., 1971*, pp. 447-453 (1972).

Key words: Biological samples; biological standards; chemical separations; environmental samples; neutron activation analysis (NAA); nondestructive; reagent blanks; trace element analysis.

Neutron activation analysis (NAA) has been found useful for trace element analysis of biological and environmental samples. The favorable characteristics of this technique include high sensitivity, wide applicability, great specificity, and reduced contamination and reagent blank problems. The utilization of this technique for the analysis of several elements (Mn, Na, Cu, Zn, U) in the recently certified NBS Biological Standard Reference Material: Orchard Leaves, is described. Techniques used include both nondestructive analysis and destructive analysis using radiochemical separations. In addition, the analytical results obtained by NAA on the Orchard Leaves, is compared to that obtained by other analytical techniques.

Bellet, J., Lafferty, W. J., Steenbeckeliers, G., **Microwave spectra of $D_2{}^{17}O$ and $D_2{}^{18}O$,** *J. Mol. Spectrosc.* **47,** No. 3, 388-402 (Sept. 1973).

Key words: Centrifugal distortion constants; $D_2{}^{17}O$; $D_2{}^{18}O$; quadrupole coupling constants; rotational constants; rotational spectra.

Forty lines of the microwave spectra of $D_2{}^{17}O$ and $D_2{}^{18}O$ have been measured in the region from 8 to 400 GHz and analyzed according to Watson's centrifugal distortion theory. Comparison of the results obtained for $D_2{}^{16}O$, $D_2{}^{17}O$, and $D_2{}^{18}O$ demonstrates their internal consistency. The transferability of the parameters according to the isotopic substitution rules is evidence for the validity of the model chosen for the study of the ground state of heavy water.

The effective rotational constants deduced from the observed spectra are very close to the values calculated using Oka's second order theory. The values obtained in MHz are:

$$A = 456766.9, B = 218041.0, C = 144701.5 \ (D_2{}^{17}O);$$

$$A = 451891.9, B = 218045.2, C = 144201.7 \ (D_2{}^{18}O).$$

The hyperfine structure of the $D_2{}^{17}O$ lines has been analyzed using as a reference the corresponding quadrupole coupling tensor of $HD^{17}O$ with the appropriate rotation. The values of χ_{gg} in MHz used for the analysis are:

$$\chi_{xx} = -1.2104, \chi_{yy} = 10.1068, \chi_{zz} = -8.8964.$$

Benzinger, M., Benzinger, T. H., **Tympanic clinical temperature,** (Proc. 5th Symp. on Temperature, Its Measurement and Control in Science and Industry, Washington, D.C., June 21-24, 1971), Paper in *Temperature, Its Measurement and Control in Science and Industry*, H. H. Plumb, Editor-in-Chief, **4,** Part 3, 2089-2102 (Instrument Society of America, Pittsburgh, Pa., 1972).

Key words: Anesthesiology; brain temperature; carotid artery; clinical medicine; cold stress (diver); disposable thermometry; esophageal thermometer; fever; fulminant hyperpyrexia; heart temperature; hypothalamus heat stress; hypothermia; obstetrics; ovulation-detection; open heart surgery; pediatric surgery; pyrogens; sweating; temperature, central body; thermocouple disconnect; thermoelectric thermometry; thermometer; vasodilation; warm sensitive neurons.

Tympanic thermometry, first introduced in physiology where it was instrumental in finding the mechanisms of human temperature regulation, has passed the test of application to clinical medicine. In the clinical situations thus far tested, which included anesthesia of various types, hypothermia for surgery, extreme heat and cold stress, extracorporeal circulation for open heart procedure and one case of terminal cooling toward exitum after stroke, tympanic and esophageal patterns were found identical for practical purposes. Rectal tracings deviated grossly from the significant central patterns which monitor the temperature of the heart, the brain and the centers of thermoregulation. These central patterns can now be conveniently obtained, by way of the tympanic approach, with clean disposable probes on awake patients, and without embarrassment, discomfort or airway interference, in hospitals or at home. For hospital use, instruments are commercially available. For home use, small and inexpensive readout instruments have yet to be developed.

Benzinger, T. H., **A new concept in thermodynamics and its implication in molecular biology and pharmacology,** Chapter 14 in *Methods in Pharmacology* **2,** Part 2, 481-488 (Appleton-Century Crofts, New York, N.Y., 1972).

Key words: Characteristic function (Planck); chemical bonding energy; double helix; heat integrals; molecular biology; thermal free energy; thermodynamics.

An extended statement of chemical equilibrium of the integral $\int_0^T (\Delta Cp/T)\, dT (= T\Delta S_T^\circ)$ and ΔH_T° – the classical terms of the equation $-RTlnK = \Delta H_T^\circ - T\Delta S_T^\circ$. The integral $\int_0^T \Delta CpdT$ is not negligible for macromolecules and particularly biopolymers, and its direct experimental determination at all temperatures down to 0 K is therefore indispensable for thermodynamic understanding of the objects of molecular biology.

Blomquist, D. S., **An experimental investigation of foam windscreens,** (Proc. 1973 International Noise Control Engineering Conference, Copenhagen, Denmark, Aug. 22-24, 1973), Paper in *Inter-Noise 73 Proceedings*, O. J. Pedersen, Ed., pp. 589-593 (Inter-Noise 73, Technical University, Lyngby, Denmark, 1973).

Key words: Acoustic attenuation; foam windscreens; wind-generated noise.

The amount of reduction in wind-generated noise and the amount of acoustic attenuation of the signal as a function of frequency for four different pore sizes and various diameters of open-cell polyurethane foam windscreens is presented.

Blomquist, D. S., Leasure, W. A., Jr., **An hourly noise exposure meter,** (Proc. 1973 International Noise Control Engineering Conference, Copenhagen, Denmark, Aug. 22-24, 1973), Paper in *Inter-Noise 73 Proceedings*, O. J. Pedersen, Ed., pp. 67-69 (Inter-Noise 73, Technical University, Lyngby, Denmark, 1973).

Key words: Acoustics (sound); environmental acoustics; instrumentation; noise exposure.

An instrument has been designed which provides information regarding the average noise exposure over each hour rather than simply a singly measure of noise exposure over an 8-hour work period. The theory of operation and examples of practical measurements utilizing this device will be discussed in the verbal presentation.

Boone, T. H., Ray, T. R., Street, W. G., **Pilot demonstration of lead based paint hazard elimination methods,** *NBSIR 73-242*, 38 pages (June 1973). (Available as PB 224654 from the National Technical Information Service, Springfield, Va. 22151.)

Key words: Cost analysis; hazard elimination; housing; lead based paint; materials; surface preparation; surface refinishing.

This report describes the elimination of the hazard of lead bearing paints in a one bedroom apartment using materials and procedures that are undergoing laboratory and field evaluation by the National Bureau of Standards (NBS). Paint removal was used to eliminate the hazard from some surfaces and two nonhazardous membrane type coverings were installed as barrier materials over the residual leaded paint on other surfaces. The preparation and refinishing of the interior surfaces are described and work rates and cost data are presented.

This pilot demonstration is the first of a series of studies that will be used to determine the merits of various lead based paint hazard elimination methods when applied to actual housing conditions.

Final recommendations for further use of materials and systems, described in this report, are not presented due to the preliminary nature of this work. The completion of the projected series of demonstrations and the long term evaluation of the in-use performance of the materials and systems will be required before final recommendations can be made.

Bowen, B. E., Cram, S. P., Leitner, J. E., Wade, R. L., **High precision sampling for chromatographic separations,** *Anal. Chem.* **45,** No. 13, 2185-2191 (Nov. 1973).

Key words: Computer-based data acquisition; gas chromatography.

The precision of several chromatographic sampling valves of original design is shown to approach 0.05 percent for unretained solutes. Hybrid-fluidic, high pressure, and commercial valves have been characterized by measuring the precision of their column input profiles and statistical moments. A computer-based data acquisition and control system was developed for use with high precision algorithms.

Bowen, R. L., Argentar, H., **A method for determining the optimum peroxide-to-amine ratio for self-curing resins,** *J. Appl. Polym. Sci.* **17,** 2213-2222 (1973).

Key words: Accelerators; amines; dental materials; initiators; peroxides; polymerization.

The rate of polymerization of a methacrylate monomer was influenced by the molar ratio of benzoyl peroxide to an aromatic tertiary amine accelerator when the product of the concentrations of these was kept constant. The maximum rate, measured as the minimum gel time, occurred in monomer solutions containing about 1.5 moles of peroxide per mole of amine.

Bowen, R. L., Chandler, H. H., **Metal-filled resin composites,** *J. Dental Res.* **52,** No. 3, 522-532 (May-June 1973).

Key words: Aluminum; composites; coupling agents gold; mercaptan; methacrylates; polymers; resin; silane; tantalum; zirconium.

Certain physical properties of metal-filled resin composite materials can be improved if properly selected and applied coupling agents are used in treating the surfaces of the metal particles.

Brauer, G. M., Termini, D. J., **Grafting of acrylates and vinyl chains onto collagen with ceric initiator,** *J. Appl. Polym. Sci.* **17,** 2557-2568 (1973).

Key words: Acrylate copolymers; ceric ion initiated; grafting collagen; graft polymerization; modification of collagenous surfaces.

To determine the scope of the grafting reaction, over 30 monomers were grafted to steer hide collagen and collagen films using ceric ammonium nitrate as initiator. High yields of apparent graft polymer were obtained with most acrylate and methacrylate esters. Yields were not changed greatly by employing the higher homologues. Moreover, monomers containing such diverse substituents as hydroxy, cyano, chloro, trifluoroethyl, or glycidyl groups may be grafted onto collagen. The presence of these functional groups in the products provides potential reaction centers to further modify the collagenous surface. Presence of vinyl polymer was confirmed by IR spectra. The large number of monomers of varying polarity which were found to undergo apparent grafting makes it possible to vary widely the surface properties of collagen. It was shown that certain monomers impart water and oil repellency to collagenous surfaces, whereas others increased the hydrophilicity or oleophilicity of the substrate. Thus, by proper selection of monomers, the desired degree of hydrophilic to hydrophobic or oleophilic to oleophobic balance of the collagen surface to suit specific applications can be obtained.

Brenner, F. C., Kondo, A., Cohen, G. B., **Research for a uniform quality grading system for tires V. Effect of environment on tread wear rate,** *Rubber Chem. Technol.* **44,** No. 4, 952-959 (Sept. 1971).

Key words: Automobile tires; environmental effects; test method; tread wear.

This paper is a continuation of work reported in *Rubber Chem. Tech.* **44,** (1971). The results of an additional tread wear test are re-

ported. This and the earlier data are analyzed to determine environmental effects on rate of tread wear.

For all types of commercial passenger car tires our test results support the thesis that the rate of wear on the tire is independent of the extent of wear. Our results also indicated that the rate of tread wear is greater on wet pavements than on dry. An explanation for this phenomenon is discussed.

Broadhurst, M. G., **Fluctuation-barrier model for rotational relaxation,** (Proc. Conf. Electrical Insulation and Dielectric Phenomena, Buck Hill Falls, Pa., Oct. 20-22, 1969), Chapter in *1969 Annual Report of the Conference Electrical Insulation and Dielectric Phenomena,* pp. 48-54 (National Research Council, National Academy of Sciences, Washington, D.C., 1970).

Key words: Elastic barrier; lattice; molecular rotation; relaxation; temperature dependence.

A model is presented where the barrier to molecular rotation in solids is taken to be the work to elastically expand the lattice around the molecule. This barrier is shown to increase with pressure and decrease with temperature. The model calculations are compared to data on long chain paraffin-like solids for the dielectrically active relaxation involving rotation of the entire molecule around its chain axis (analogous to the α relaxation in polymers). The model accurately predicts the temperature dependence of the relaxation time (the activation entropy in the Eyring Theory), and the Eyring activation energy (the activation energy does not equal the elastic barrier height). The predicted pressure dependence of the relaxation time is in error by a factor of 2 indicating the need for further refinement of the model. This paper reports the current status of this problem.

Broadhurst, M. G., Malmberg, C. G., Mopsik, F. I., Harris, W. P., **Piezo- and pyroelectricity in polymer electrets,** (Proc. Conf. on Electrets, Charge Storage and Transport in Dielectrics, Miami Beach, Fla., Oct. 8-13, 1972), Paper in *Electrets, Charge Storage and Transport in Dielectrics,* M. M. Perlman, Ed., pp. 492-504 (The Electrochemical Society, Inc., Princeton, N.J., 1973). (Available as AD 758730 from the National Technical Information Service, Springfield, Va. 22151).

Key words: Electret; piezoelectric; polymer electret; poly(vinyl chloride); pyroelectric.

A model for a polymer electret, based on an elastically isotropic solid with orientationally frozen molecular dipoles, was developed and tested experimentally. This electret is shown to be both piezoelectric and pyroelectric. The polarization is shown to change with mechanically and thermally induced strains in the polarization direction. The currents generated by the electret will be proportional to the strain rate and, for thin contact electrodes and uniform strains, unaffected by the presence of real charges. Poly(vinyl chloride) films were poled at 80 °C, just above their glass transition temperature. The pressure- and temperature-induced short-circuit currents in the polarization direction equalled 0.15 (pA/cm²)/(bar/min) and 2.2 (pA/cm²)/(K/min) respectively for a specimen poled at 320 kV/cm. These currents were 1) reversible and proportional to the rate of temperature or pressure change, 2) proportional to poling voltage up to 320 kV/cm, 3) in the direction corresponding to increasing polarization with increasing pressure and decreasing temperature, 4) stable with time without special storage conditions, 5) about 1.6 times as great for temperature induced strains as for equivalent pressure induced strains and 6) about 2-4 times as great in magnitude as expected from dielectric constant measurements. The apparent polarization from temperature measurements for the 320 kV/cm specimen was about 1.7 μC/cm², or about 1/3 the value expected for maximum alignment of dipoles. In the same specimen the pyroelectric coefficient was found to be $p_3 = -0.39$ nC/cm² K and, assuming elastic isotropy, the piezoelectric strain coefficients were found to be $d_{31} = d_{32} = d_{33} = -0.89$ pC/N.

Broadhurst, M. G., Mopsik, F. I., **Vibrational frequency spectrum for polymers,** *J. Chem. Phys.* **55,** No. 8, 3708-3711 (Oct. 15, 1971).

Key words: Frequency spectrum; linear chains; *n*-alkanes; polyethylene; polymer.

A method is given for calculating the vibrational frequency spectrum of a model linear polymer. The model is a chain of N masses having bending and stretching force constants. Each mass is quasiharmonically coupled to a Debye lattice which has a cutoff frequency ω_L. Each of the $3N$ free chain eigenfrequencies ω_j becomes a band with a low frequency cutoff $\omega_{jmin}^2 = \omega_j^2$, a high frequency cutoff $\omega_{jmax}^2 = \omega_j^2 + \omega_L^2$, and a pseudo-$n$-dimensional Debye distribution $g_j(\omega) = n\omega^{n-1}/(\omega_{jmax}^n - \omega_{jmin}^n)$ for $\omega_{jmin} < \omega < \omega_{jmax}$. The total frequency distribution agrees closely with the results by Genensky and Newell for the Stockmayer and Hecht lattice using their force constants and compares reasonably well with results of GF matrix calculations for polyethylene.

Bur, A. J., **Dielectric properties of fluorine-containing polymers,** Chapter 15 in *Fluoropolymers,* L. A. Wall, Ed., **25,** 475-505 (John Wiley-Interscience, New York, N.Y., 1972).

Key words: Dielectric constant; dielectric loss; fluoropolymer; relaxation phenomena; review.

The dielectric properties of polytetrafluorethylene, polychorotrifluoroethylene, polyvinylidene fluoride, and fluorinated ethylene propylene copolymer are reviewed. Relaxation phenomena as a function of temperature and crystallinity is emphasized. Molecular interpretations of the data are discussed. The effects of humidity changes on the dielectric properties of polytetrafluoroethylene and fluorinated ethylene-propylene copolymer show that these polymers are insensitive to humidity changes. Eighty references are cited.

Burnett, E. F. P., Somes, N. F., Leyendecker, E. V., **Residential buildings and gas-related explosions,** *NBSIR 73-208,* 31 pages (June 1973). (Available as COM 74-10127 from the National Technical Information Service, Springfield, Va. 22151.)

Key words: Building; explosion; frequency; gas; gas industry; progressive collapse; risk; statistics; structure.

The findings of an analysis of available statistics concerning the frequency of gas-related explosions in residential buildings are presented. The study was confined to incidents involving piped gas systems as they affect residential and commercial buildings. Though due regard has to be taken of the limitations inherent in the available statistics, it is concluded that in the USA the probability of occurrence of an explosion capable of causing significant structural damage could be 2.2 per million housing units per year.

Bussey, H. E., **Wavelength of a slotted rectangular line containing two dielectrics,** *NBSIR 73-326,* 17 pages (July 1973). (Available as COM 73-11465-AS from the National Technical Information Service, Springfield, Va. 22151.)

Key words: Capacitance; dielectric measurement; slab line; slotted line.

The titled electromagnetic wave property is obtained approximately for a rectangular slab line with two dielectrics. The perturbing dielectric is a thin sheet set on the center conductor and slotted to permit travel of the probe when the line is used as a slotted line. The purpose is to measure an unknown dielectric filling most of the line, but perturbed by the thin sheet.

Candela, G. A., Kahn, A. H., Negas, T., **Magnetic susceptibility of $Co^{4+}(d^5)$ in octahedral and tetrahedral environments,** *J. Solid State Chem.* **7,** No. 4, 360-369 (1973).

Key words: Co^{4+} compounds; crystal fields; magnetic susceptibility; theory of magnetic susceptibility.

Measurements of magnetic susceptibility on compounds containing stoichiometric Co^{4+} are reported. The compound Ba_2CoO_4 has the $Co^{4+}(d^5)$ ion at a tetrahedral site and displays a susceptibility of the expected magnitude for $S=5/2$. The compounds $Ba_3Co_2CO_9$ and $BaCoO_3$ have the Co^{4+} at an octahedral site and show a susceptibility expected for low spin, $S=1/2$. For the low spin case significant deviations from Kotani's calculated susceptibility were observed. Improvement of the theory was made through incorporation of the effects of distortion from perfect octahedral symmetry and the inclusion of higher electronic configurations above t_2^5 in the $^2T_2$ ground state. A case of low spin Ni in octahedral environment is also reported.

Carpenter, B. S., Samuel, D., Wasserman, I., **Quantitative applications of ^{17}O tracer,** *Radiat. Eff. Short Commun.* **19,** 59 (1973).

Key words: Alpha tracks; alumina; cellulose acetate; citric acid; image analyzing system; nuclear track technique; oxygen tracer; thermal neutrons.

We describe the use of alpha tracks from the $^{17}O(n, \alpha)^{14}C$ as a means of oxygen determination and distribution in biological material. A determination of oxygen in alumina and citric acid using enriched tracer was made.

Chertok, B. T., Sheffield, C., Lightbody, J. W., Jr., Penner, S., Blum, D., **Low-q^2 electron scattering from the 15.109-MeV state of ^{12}C and the conserved-vector-current test,** *Phys. Rev. C* **8,** No. 1, 23-36 (July 1973).

Key words: Electron scattering; extrapolation, Γ_γ; low q^2; 1^+ state; 15.11 MeV.

High-precision electron scattering measurements from the 15.109-MeV 1^+ state in ^{12}C are made at $\theta=75$ and $110°$ with $35 \leq E \leq 55$ MeV. From the measurements B ($M1$) is extrapolated to the photon point and the radiative width is determined, $\Gamma_\gamma=37.0\pm1.1$ eV. The corresponding weak magnetism results for β decay and μ capture are given.

Chesler, S. N., Cram, S. P., **Iterative curve fitting of chromatographic peaks,** *Anal. Chem.* **45,** No. 8, 1354-1359 (July 1973).

Key words: Chromatography; curve fittings; moment analysis.

Iterative curve fitting of an eight parameter function to chromatographic peak profiles by nonlinear residual least squares is reported. Gaussian, exponential, and hyperbolic tangent functions are convoluted and iteratively fit to any experimental chromatographic peak shape and integrated to give total statistical moments with errors as small as 1 percent, even for the higher order moments. Exponential and band broadening operators are deconvolved for measurement of physicochemical and analytical studies. The models and calculations may be extended to the resolution of overlapping peaks and complex elution profiles for the measurement of the rate of on-column chemical reactions.

Chignell, C. F., Benzinger, T. H., **Heatburst microcalorimetry,** Chapter 14 in *Methods in Pharmacology* **2,** Part 1, 465-489 (Appleton-Century Crofts, New York, N.Y., 1972).

Key words: Adenosinetriphosphate-thermodynamics; chemical bond energy; coiled helix thermopiles; drug receptor complexing; entropy; enzyme detection + analysis; equilibrium; free energy; free entropy concept; heat of reaction; heatburst principle; hydrogen bonding; immunoreaction calorimetry; microcalorimetry; molecular biology; pharmacology; protein calorimetry; polynucleotide calorimetry; purity assay; reaction coupling; thermodynamics; warfarin.

In this chapter the heatburst principle will be briefly discussed followed by a description of the construction and operation of the heatburst microcalorimeter. In the next section, it will be shown how heat can not only be used as an indicator for chemical or biochemical change but can also be used to derive thermodynamic data for the system under study. In a third section, some further possible applications of heatburst microcalorimetry to current problems in molecular biology and pharmacology will be suggested. In a separate section, following this article, the classical determination of the laws of chemical equilibrium and the driving energies of chemical change will be re-examined, and a new determination, more suited to the objects of molecular biology and pharmacology, will be derived.

Christ, B. W., **Effects of misalignment on the pre-macroyield region of the uniaxial stress-strain curve,** *Met. Trans.* **4,** 1961-1965 (Aug. 1973).

Key words: Bending; capacitance strain gage; tensile; Ti-6Al-4V; uniaxial loading; 4340 steel.

Some bending usually occurs in uniaxial testing systems due to small unavoidable misalignment. The resulting elastic strain gradient can lead to significant differences between axial strain and extreme surface bending strains, especially at small strains. A three-point microstrain measurement around a cylindrical sample permits evaluation of the extreme strains and of the precision of alignment. A three-point, parallel-plate capacitance strain gage having a linear output with displacement was designed to evaluate bending of tensile samples in the microstrain range. The resolution of the gage was 3 parts in 10,000 at plate separations of 0.010 in. Varying misalignment resulted in extreme elastic bending strains at the sample surface of the order of tens to hundreds of micro-in. per in. larger than the axial strain. Analysis of the mechanics of bending in uniaxial loading demonstrated that: 1) the average applied stress divided by the average elastic strain always gives a unique number, Young's modulus, and 2) the average microplastic strain is not uniquely related to the average applied stress, but rather depends upon precision of alignment. The influence of bending on the determination of the average stress at which microplastic flow initiates is discussed, and a method for making meaningful comparisons of plastic microstrain data generated with significant misalignment is suggested.

Clifton, J. R., Beeghly, H. F., Mathey, R. G., **Interim Report No. 7. Chemical resistance and physical durability testing of coating materials,** *NBSIR 73-295*, 22 pages (Aug. 1973). (Available as COM 74-10471 from the National Technical Information Service, Springfield, Va. 22151.)

Key words: Bridge decks; corrosion; creep testing; epoxy coatings; polyvinylchloride coatings; steel reinforcing bars.

The possibilities of protecting steel reinforcing bars embedded in concrete of bridge decks from corrosion by using organic barrier-type coatings are being investigated in this project. This corrosion is accelerated by the chloride ions of the two most commonly applied deicing materials, sodium chloride and calcium chloride.

In this report, physiochemical studies performed on coatings and coated bars are discussed, including: immersion studies of coatings in corrosive solutions; impact and embedded in concrete.

Cohen, E. R., Taylor, B. N., **A reevaluation of the fundamental physical constants,** (Proc. 4th Int. Conference on Atomic Masses and Fundamental Constants, Teddington, England, Sept. 3-7, 1971), Paper in *Atomic Masses and Fundamental Constants*, J. H. Sanders and A. H. Wapstra, Eds., Part 13, 543-563 (Plenum Publishing Co., New York, N.Y., 1972).

Key words: Data analysis; fundamental constants; least-squares adjustments.

This paper is a progress report on our current efforts to revise and update the comprehensive review of the fundamental physical constants by Taylor, Parker, and Langenberg (1), including their set of best or recommended values. That such an updating is necessary just two years after their review appeared is due to the extraordinary amount of new experimental and theoretical work which has since been completed. Here, we very briefly summarize the experimental

and theoretical evidence, with emphasis on the new results which have become available within the last two years, and discuss various treatments of the data. However, no new set of recommended constants is given since such a set will necessarily require the inclusion of the new data which has become available at this Conference.

Collier, R. S., Ellerbruch, D., Cruz, J. E., Stokes, R. W., Luft, P. E., Peterson, R. G., Hiester, A. E., **Mass quantity gauging by rf mode analysis,** *NBSIR 73-318*, 196 pages (June 1973). (Available as N73-27390 from the National Technical Information Service, Springfield, Va. 22151.)

Key words: Gauging; hydrogen; nitrogen; radio frequency; total mass.

This is a summary report of work done to date on NASA (Johnson Space Center) purchase order T-1738B concerning Radio Frequency (RF) Mass Quantity Gauging. Experimental apparatus has been designed and tested which measures the resonant frequencies of a tank in the "time domain." These frequencies correspond to the total mass of fluid within the tank. Experimental results are discussed for nitrogen and hydrogen in normal gravity both in the supercritical state and also in the two phase (liquid-gas) region. Theoretical discussions for more general cases are given.

Collins, R. C., Haller, W., **Protein-sodium dodecyl sulfate complexes: Determination of molecular weight, size and shape by controlled pore glass chromatography,** *Anal. Biochem.* **54,** 47-53 (1973).

Key words: Chromatography; controlled pore glass; molecular size; porous glass chromatography; protein; protein-sodium dodecyl sulfate complexes; sodium dodecyl sulfate-complexes.

The peak position vs log molecular weight curves of protein-SDS complexes chromatographed on controlled pore glass of narrow pore size distribution is linear over a molecular weight range of 17,000-385,000. A glass with a pore size of approximately 500 Å allows the inclusion of all complexes in this range. Peak position curves on glasses with broad pore distributions show decreased resolution and deviate from linearity at low elution coefficients.

Exclusion size analysis of the elution coefficients of individual complexes from different columns with pore diameters ranging from 197 to 650 Å gives from 120 to 423 Å as their longest dimension. Assuming constant hydration and SDS-to-protein ration, the found dimension suggests the shape of a football, rather than a sphere or rigid rod.

Comeford, J. J., Birky, M., **A method for the measurement of smoke and HCl evolution from poly(vinyl chloride),** *Fire Technol.* **8,** No. 2, 85-90 (May 1972).

Key words: HCl: He-Ne laser; poly(vinyl chloride); pyrolysis; smoke; thermal decomposition.

As poly(vinyl chloride) becomes more popular as a building material and electrical insulation, it becomes more important to life safety to determine its smoke and hydrogen chloride evolution characteristics during pyrolysis. The authors have devised a method of measuring the two simultaneously.

Coriell, S. R., Sekerka, R. F., **Morphological stability near a grain boundary groove in a solid-liquid interface during solidification of a binary alloy,** *J. Cryst. Growth* **19,** 285-293 (1973).

Key words: Alloy; grain boundary; morphology; solidification; stability.

In order to further explore the influence of grain boundaries on the phenomenon of morphological stability, we have extended our previous treatment for a pure substance to a binary alloy. For unidirectional solidification at constant velocity, the shape, $y = W(x,t)$, of a nearly planar interface, intersected perpendicularly by a grain boundary, is calculated. The stability-instability criterion is identical to that for an interface without a grain boundary. If the interface is unstable, the main influence of the grain boundary is to provide an initial perturbation and the time evolution of the interface shape can be treated by approximate analytical methods. For times sufficiently large that initial transients have decayed but sufficiently small that linear theory is applicable, $W(x,t)$ is proportional to $\exp(t/\tau) \cos(\omega_0 \chi) \exp(-x^2/4\mathscr{D}t)$, where ω_0, τ, and $\mathscr{D}$ are constants that depend on experimental conditions. After initial transients have decayed, a stable interface attains a time-independent shape. For this case, $W(\chi,t \leftarrow \infty)$ is evaluated numerically; it is found that $W(\chi,t \leftarrow \infty)$ can be an oscillatory function of χ. The size of the oscillations and the depth of the grain boundary groove increase as the stability-instability demarcation is approached, giving the specious appearance of premature instability.

Coriell, S. R., Sekerka, R. F., **Morphological stability near a grain boundary groove in a solid-liquid interface during solidification of a pure substance,** *J. Cryst. Growth* **19,** 90-104 (1972).

Key words: Crystal growth; grain boundary; morphological stability; solidification.

In order to explore the influence of a specific type of defect on the phenomenon of morphological instability, we have calculated the time-dependent shape of a nearly planar interface, intersected perpendicularly by a grain boundary, during solidification of a pure substance at constant velocity. The calculational methods and principal assumptions are similar to those employed in previous theories of morphological stability except that the slope of the interface is maintained at a finite and constant value, s, in the immediate vicinity of the grain boundary groove. The position of the solid-liquid interface is described by the equation $y = W(\chi,t)$ where t is the time and $W(\chi, 0) \rightarrow 0$ as $|\chi| \rightarrow \infty$ (all quantities are assumed independent of z). Whereas the stability-instability criterion is found to be identical to that for an interface without a grain boundary, the boundary is found to be an effective initial perturbation. Under conditions for instability the depth of the grain boundary groove increases exponentially with time and an oscillatory instability propagates laterally from the boundary. Under conditions for stability, the interface eventually attains a time-independent shape given by $W(\chi,t \rightarrow \infty) = (-s/a)\exp(-a\chi)$, where $a^2 = (\mathscr{G}_S + \mathscr{G}_L)/2T_M\Gamma$, $\mathscr{G}_S$ and $\mathscr{G}_L$ are conductivity-weighted temperature gradients in solid and liquid, respectively, T_M is the melting temperature and Γ is a capillary constant. For conditions corresponding to the demarcation between stability and instability, a mode of thermal grooving, similar to that previously described by Mullins, is found. A meaningful criterion for instability is shown to be the exponential growth of perturbations while, conversely, stability entails their exponential decay; phenomena such as the algebraic increase of amplitude characteristic of thermal grooving are shown to be manifestations of constraints. Finally, the situation where the interface shape is allowed to depend on z is shown to be describable by a superposition of $W(\chi,t)$ with a function $W_0(\chi,z,t)$ that corresponds to the conventional case where the grain boundary is absent.

Creitz, E. C., **Extinction of fires by halogenated compounds—a suggested mechanism,** *Fire Technol.* **8,** No. 2, 131-141 (May 1972).

Key words: Extinguishment; flame inhibition; inhibition mechanisms.

It is suggested that halogenated compounds extinguish diffusion flames by promoting recombination of reactive oxygen atoms to form less reactive molecular oxygen. Oxygen atoms are important in the branching steps of the hydrogen-oxygen chain reaction. For a fuel containing carbon, CO is an intermediate product which appears in the region in which inhibition takes place. Inhibition of its oxidation

appears to take place because of the paucity of hydroxyl radicals which are a product of the hydrogen-oxygen chain reaction. The mechanism is suggested in an attempt to rationalize a number of apparently disparate observations reported in the literature of both normal and inhibited flames. Data in support of the suggested mechanism are discussed.

Creitz, E. C., **Gas chromatographic determination of composition profiles of stable species around a propane diffusion flame,** *J. Chromatogr. Sci.* **10,** 168-173 (Mar. 1972).

Key words: Flame gases; flame inhibition; gas analysis; gas chromatographic techniques.

An analytical method was developed for determining, quantitatively, with a GC, the gases present around a 2.4 cm high propane diffusion flame burning in air. The method gives quantitative results on samples having some constituents which may not be eluted from the column. Outside the yellow mantle the only fuel species found were carbon, hydrogen and carbon monoxide. The oxygen concentration dropped to zero at a distance of 0.57 mm from the yellow mantle indicating that pyrolysis of the fuel was essentially without O_2. The absence of other fuel species implicates the hydrogen-oxygen chain reaction as having a part in the mechanism of inhibition. When CF_3Br was added to the air, its decomposition was complete at a distance of 2.56 mm from the yellow mantle. The decomposition appeared to be chemical rather than thermal.

Creswell, R. A., Lafferty, W. J., **Microwave spectrum, dipole moment, and conformation of 3,6-dioxabicyclo[3.1.0]hexane,** *J. Mol. Spectrosc.* **46,** No. 3, 371-380 (June 1973).

Key words: Boat conformation; dipole moment; microwave spectrum; ring conformation; rotational constants; 3,6-Dioxabicyclo[3.1.0]hexane.

The microwave spectrum of 3,6-dioxabicyclo[3.1.0]hexane has been obtained. The rotational lines of one ring conformation only have been observed and assigned. Ground state rotational constants are $A_0 = 6287.302 \pm 0.011$ MHa, $B_0 = 4683.546 \pm 0.008$ MHz, and $C_0 = 3358.517 \pm 0.089$ MHz. The dipole moment components obtained from Stark effect measurements are $\mu_a = 0.276 \pm 0.010$ D and $\mu_c = 2.47 \pm 0.04$ giving $\mu = 2.485 \pm 0.040$ for the dipole moment of the molecule. The rotational constants and dipole moment components obtained experimentally can be satisfactorily explained only if the boat form is the most stable ring conformation.

Currie, L. A., **On the use of small calculators having stacked registers,** *Anal. Lett.* **6,** No. 9, 847-864 (1973).

Key words: Instruction list; iteration; memory register; operational stack; pop-up; Polish notation; push-down; radioactivity and isotopic calculations; recursion; statistical calculations.

The incorporation of an operational stack considerably enhances the potential of the small calculator. Full use of the stack permits calculations involving a stored constant or two or more intermediate results, but it requires careful planning and execution. Regardless of whether the calculator is "programmable," an explicit instruction list, preferably written down, may contribute greatly to the rapidity and accuracy of such calculations. The "pop-up" feature of the stack is of particular interest, for it can be utilized to increase the permanent storage capacity. A comparison between conventional (memory) storage and stack storage is given, and examples are presented for the application of a calculator having a 4-register stack (plus 1-memory register) to problems involving 2 parameters and/or summations, iterative solution of a transcendental equation, and recursion.

Currie, L. A., **The limit of precision in nuclear and analytical chemistry,** *Nucl. Instrum. Methods* **100,** 387-395 (1972).

Key words: Counting precision; excess variability; limiting precision; photonuclear chemistry; Poisson statistics; single and multiple parameter nuclear analyses; statistical weights; 14 MeV neutron activation.

The precision associated with an experiment in nuclear chemistry or activation analysis is commonly estimated by means of Poisson counting statistics. Such an estimate, as well as the conclusion that the precision may be indefinitely improved by increasing the number of counts obtained, is necessarily wrong when additional sources of random error are operating. Knowledge of the additional, non-Poisson component of random error is required for reliable estimates of parameters and their standard errors, to detect model errors, to plan counting experiments efficiently, and to establish the limit of precision when the Poisson counting error becomes negligible. For these purposes, an iterative computation program—XESS—has been developed to take into account the additional variance and unequal statistical weights. The significance and detectability of excess variance is illustrated with data from studies of photonuclear reactions and activation analysis.

Danielson, S. L., Howe, D. A., **Use of the television vertical interval to broadcast time for everyone and program captions for the deaf,** *Commun. Soc.* **11,** No. 5, 3-6 (Nov. 1973).

Key words: Digital code; integrated circuit chip; program captioning; television; time and frequency dissemination; TvTime.

This paper describes the events leading to the development of the NBS TvTime System for both time and frequency dissemination and program captioning for the deaf. It explains how the system works, its advantages over other systems, and its cost. Finally, it discusses the possible implications of such a system for future communication applications. The text is written in laymen's language to suit the publication.

Davis, G. T., Eby, R. K., **Glass transition of polyethylene: Volume relaxation,** *J. Appl. Phys.* **44,** No. 10, 4274-4281 (Oct. 1973).

Key words: Dilatometer; isothermal volume change; polyethylene; specific volume; superposition; thermal expansion; volume relaxation, WLF.

Data are presented to show that when linear polyethylene is quenched from room temperature to temperatures below 273 K, it exhibits a volume decrease for times long compared with that required to establish temperature equilibrium. The time, temperature, and density dependence of this decrease is shown to be consistent with a relaxation occurring in the amorphous portion (lamella boundary layers) of the samples. The data can be superposed and the shift factors follow the WLF formalism. Analysis by this method yields a T_g of 231 ± 9 K but the uncertainties preclude any correlation with specific volume over the range $1.01 - 1.05$ cm^3 g^{-1}. The data indicate the absence of any comparably strong time dependence of the volume near 150 K. This method of detecting a glass transition in partially crystalline polymers is relatively freer of subjective judgment than most.

Dellepiane, G., Gussoni, M., Hougen, J. T., **Hamiltonian, symmetry group, and vibrational coordinates for the nonrigid molecule $CXY_2 - C \equiv C - CXY_2$,** *J. Mol. Spectrosc.* **47,** No. 3, 515-530 (Sept. 1973).

Key words: Double-valued presentation; free internal rotation; Hamiltonian energy operator; non-rigid molecules; permutation-inversion group; vibrational coordinates.

A vibration-torsion-rotation Hamiltonian is derived for a molecule of the type $CXY_2 - C \equiv C - CXY_2$ exhibiting nearly free internal rotation. The Hamiltonian obtained preserves many of the features of the ordinary Wilson-Howard vibration-rotation Hamiltonian and is based qualitatively on the idea of a slowly varying torsional reference configuration from which the atoms make rapid vibrational displacements. The appropriate molecular symmetry group for this molecule

is found to be a double group of the simple Longuet-Higgins permutation-inversion symmetry group. The indeterminacy of symmetry species (single-valued vs double-valued) for coordinates used to describe the small amplitude vibrations is illustrated and clarified using a simple model for the skeletal bending vibrations.

Dewitt, D. P., Richmond, J. C., **Theory and measurement of the thermal radiation properties of metals,** Chapter 1 in *Measurement of Physical Properties: Some Special Properties*, E. Passaglia, Ed., **VI,** Part 1, 1-90 (Interscience Publ., New York, N.Y., 1972).

Key words: Absorptance; electromagnetic theory; emittance; measurement techniques; metals; reflectance; surface effects; thermal radiation properties.

This is a general review of the thermal radiation properties of metals, and includes (1) description and definition of the properties, and a discussion of their interrelationships, (2) a brief review of the physical laws relating to blackbody radiation, (3) discussion of the theory of the interaction of electromagnetic waves with electrical conductors, (4) the effect of surface condition—profile and surface films— on thermal radiation properties of metals, and (5) a review of methods of measuring thermal radiation properties of metals.

Dibeler, V. H., Walker, J. A., McCulloh, K. E., **Observations on hot bands in the molecular and dissociative photoionization of acetylene and the heat of formation of the ethynyl ion,** *J. Chem. Phys.* **59,** No. 5, 2264-2268 (Sept. 1, 1973).

Key words: Ethynyl ion; heat of formation; ionization threshold; mass spectrometry; vacuum ultraviolet.

Photoion yield curves in the vicinity of threshold are obtained for the molecular and the ethynyl ions of acetylene and acetylene-d_2 at ion source temperatures of 360, 298, and 130 K. Weak ionization below the adiabatic threshold for $C_2H_2^+$ and $C_2D_2^+$ is ascribed to the ionization of molecules excited by one quantum of the bending vibrations, ν_4 and ν_5. Consideration of selection rules suggests a change in symmetry from the linear ground state molecule to a bent ground state ion. The 0 K curves for C_2H^+ and C_2D^+ are estimated from the observed 130 K data. Satisfactory agreement is obtained when the 298 K data are compared with a curve calculated from the 0 K curve by convolution with vibrational and rotational distributions. The 0 K thresholds corrected for kinetic energy are used to calculate $\Delta Hf°_0(C_2H^+) = 17.47 \pm 0.01$ eV (402.8 ± 0.2 kcal mol^{-1}) and $\Delta Hf°_0(C_2D^+) = 17.43 \pm 0.02$ eV (402.0 ± 0.5 kcal mol^{-1}). The ionization energy of the ethynyl radical is estimated to be 11.96 ± 0.05 eV.

Diller, D. E., Sarkes, L. A., **Properties data for LNG,** *Amer. Gas Ass. Mon.* **55,** No. 9, 27-28 (Sept. 1973).

Key words: Calculation methods; densities; ethane; liquefied natural gas mixtures; methane; pure components; propane; properties data.

The need for new physical and thermodynamic properties data for liquefied natural gas mixtures at low temperatures is discussed. A plan is given for calculating properties data for liquid mixtures at temperatures well below the critical temperature. The National Bureau of Standards Cryogenics Division's program to provide accurate input data for calculating properties data for LNG is described.

Ederer, D. L., **Cross-section profiles of resonances in the photoionization continuum of krypton and xenon (600-400 Å),** *Phys. Rev. A* **4,** No. 6, 2263-2270 (Dec. 1971).

Key words: Autoionization; configuration interaction; inner shell excitation; photoionization cross section; resonance profiles; uv absorption spectroscopy.

The cross-section profiles in krypton and xenon have been measured for one- and two-electron excitations of the type $ns^2np^6(^1S_0) \rightarrow nsnp^6(^2S_{1/2})mp$ or $ns^2np^6(^1S_0) \rightarrow ns^2np^4(^3P, ^1D, ^1S)\, mlm'l'$. These cross sections were assumed to have the form

$$\sigma(E) = C(E) + \sum_i \frac{(E-E_i)(\Gamma_i/2)a_i + (\Gamma_i/2)^2 b_i}{(E-E_i)^2 + (\Gamma_i/2)^2},$$

where the adjustable parameters $C(E)$, b_i, a_i, E_i, and Γ_i were determined by a least-squares unfolding process which separated the smearing effect of the monochromator slit from the true optical density. Parameter values and cross-section curves are given for 12 krypton resonances and 11 xenon resonances.

Ederer, D. L., Lucatorto, T., Madden, R. P., **Resonances in the photoionization continuum of lithium I (55 to 70 eV),** *J. Phys.* **32,** Supplement to No. 10, C4-85—C4-87 (Oct. 1971).

Key words: Absorption; heat pipe; K-edge; lithium; resonances; spectrum.

Resonances in the photoionization continuum of lithium have been observed by absorption spectroscopy in the region of 55 to 70 eV. These resonances are associated with configurations of the type (1 s 2 snl) and (1 snln'l') and lie more than 50 eV above the ionization potential; the lowest lying most prominent of these can be idenitified with configurations of the type (1 s 2 snp) ^{2}P. A multiconfiguration calculation for the first five members of the series (performed by A. Weiss) has yielded values for the energies which agree with experimental results to within 2 eV.

The design of the lithium vapor absorption furnace was based on the heat-pipe principle. Argon, which has very little structure in the region from 55 to 70 eV, was used as a buffer gas and was contained inside the furnace by thin film aluminum windows. The light source was the 180 MeV NBS synchrotron.

Ely, J. F., Hanley, H. J. M., Straty, G. C., **Analysis of the pressure virials and Clausius-Mossotti function for polyatomic gases,** *J. Chem. Phys.* **59,** No. 2, 842-848 (July 15, 1973).

Key words: Clausius-Mossotti function; dielectric virial coefficients; m-6-8 potential; polarizability; polyatomic gases; pressure second virial coefficients; quadrupole moment; statistical mechanics.

Statistical mechanical equations for the second pressure virial coefficient and the second and third dielectric virial coefficients for quadrupolar molecules are evaluated using the *m*-6-8 potential function. The results are compared with experimental data for nitrogen and fluorine. An approximate value for the quadrupole moment of fluorine is estimated. Agreement between theory and experiment is generally good.

Etz, E. S., Robinson, R. A., Bates, R. G., **Dissociation constant of protonated tris(hydroxymethyl)aminomethane in N-methylpropionamide and related thermodynamic quantities from 10 to 55 °C,** *J. Solution Chem.* **2,** No. 4, 405-415 (1973).

Key words: Acidic dissociation; dissociation constant; emf measurements; ionization processes; N-methylpropionamide; solvation; tris(hydroxymethyl)aminomethane.

The dissociation constant of protonated tris(hydroxymethyl)aminomethane (tris · H^+) in the solvent *N*-methylpropionamide (*NMP*) has been determined at intervals of 5°C from 10 to 55 °C by measurement of the emf of cells without liquid junction using hydrogen and silver-silver chloride electrodes. At 25 °C, pK_a was found to be 8.831, as compared with 8.075 in water. The standard changes in Gibbs energy, enthalpy, and entropy for the dissociation process have been evaluated from the dissociation constant and its change with temperature. By comparison with similar data for the dissociation of tris · H^+ in water, thermodynamic functions for the transfer from water to *NMP* have been derived. The dissociation process is isoelectric, and the solvent dielectric constant is high (ϵ =

176 at 25 °C). Consequently, electrostatic charging effects are expected to be minimal, and the change in dissociation constant depends primarily on solute-solvent interactions. The results, combined with transfer energies for *HCl*, tris, and tris · *HCl* from emf and solubility measurements, demonstrate that the decreased acidic strength of tris · H^+ in *NMP* is attributable in large part to the fact that *NMP* is less effective than water in stabilizing tris and its salts.

Evans, A. G., **Strength degradation by projectile impacts,** *J. Amer. Ceram. Soc.* **56,** No. 8, 405-409 (Aug. 1973).

Key words: Ceramics; fracture; impact; projectiles.

The impacting of ceramic components by small projectiles can lead to strength degradation caused by the formation of Hertzian cracks. The conditions which produce degradation are analyzed in terms of the momentum and elastic properties of the projectile. A critical momentum must be exceeded before strength loss can occur, and the critical condition depends on the surface condition of the ceramic. Comparison of the analytical predictions with data for SiC confirms the reliability of the analysis.

Falge, R. L., Jr., Swartzendruber, L. J., **Influence of clustering on the paramagnetic behavior of a Cu-Ni alloy,** *Phys. Lett.* **44A,** No. 4, 285-286 (June 18, 1973).

Key words: Clustering; critical phenomena; Cu-Ni alloy; heat treatment; magnetism; susceptibility.

The equation usually reserved for the critical behavior of a ferromagnet just above T_c also describes the susceptibility of $Cu_{0.47}Ni_{0.53}$ over a very large temperature range. The parameters, which vary with heat treatment suggest lamellar clustering.

Fatiadi, A. J., **Facile coupling of sterically hindered 2,6-dialkylphenols with periodic acid,** *Synthesis Commun. No. 6,* 357-358 (June 1973).

Key words: Coupling; dialkylphenols; dimethylformamide; hindered; oxidation; periodic acid.

A procedure has been developed by which sterically hindered phenols can produce coupling products (diphenoquinones) in 60 to 94 percent yield when treated with periodic acid in an aqueous N,N-dimethylformamide.

Fatiadi, A. J., **Mechanism of formation of tris(phenylhydrazones) on treatment of cyclohexane-1,3-diones with phenylhydrazine,** *Chem. Ind.*, pp. 38-40 (Jan. 6, 1973).

Key words: Cyclohexane-1,3-dione; formation; free-radical; ionic; mechanism; phenylhydrazine.

The e.s.r. studies show that the formation of the 2-oxo-1,3-bis(phenylhydrazones) and tris(phenylhydrazones) from cyclohexane-1,3-diones, and of bis(phenylhydrazones) from cyclohexane-1,2-diones, following treatment with phenylhydrazine in polar solvents most likely proceeds by a concerted process, involving both ionic and free-radical pathways.

Feldman, A., Horowitz, D., Waxler, R. M., **Laser damage in materials,** *NBSIR 73-268,* 44 pages (Aug. 1973). (Available as AD 768-303 from the National Technical Information Service, Springfield, Va. 22151.)

Key words: Absorption coefficient; calcite; damage threshold; deuterated potassium dihydrogen phosphate; electrostriction; electrostrictive self-focusing; inclusion damage; Kerr effect; laser damage; lithium niobate; nonlinear index of refraction; potassium dihydrogen phosphate; self-focusing; thermal self-focusing; thoria:yttrium oxide ceramic; yttrium aluminum garnet.

Neodymium:glass laser induced damage is observed in lithium niobate ($LiNbO_3$), calcite ($CaCO_3$), potassium dihydrogen phosphate (KDP), and deuterated potassium dihydrogen phosphate (KD*P). The damage at the lowest power levels is caused by inclusions. At higher power levels, filamentary damage, which is indicative of self-focusing, is observed in $LiNbO_3$. An analysis of self-focusing data in yttrium aluminum garnet shows that the Kerr effect is the dominant self-focusing mechanism, with some contribution from the thermal effect. Bulk and surface damage thresholds in neodymium-doped thoria:yttrium oxide ceramic are obtained relative to bulk damage thresholds in several optical materials. For solid materials relationships are obtained between the stress-optic coefficients and the electrostrictive coefficients under different geometric boundary conditions.

Fickett, F. R., **Magnetoresistivity of copper and aluminum at cryogenic temperatures,** *(Proc. 4th Int. Conf. on Magnet Technology, Brookhaven National Laboratory, Upton, N.Y., Sept. 19-22, 1972),* pp. 539-541 (Atomic Energy Commission, Washington, D.C., 1972).

Key words: Aluminum; copper; electrical properties; magnetoresistance.

Results of recent measurements of the magnetoresistance of polycrystalline wires of aluminum and copper are presented. The measurements were made in the temperature range 4 K to 35 K and in magnetic fields to 100 kOe. The aluminum wires ranged in purity from RRR = 1000 – 30 000 and the copper wires from RRR = 200 – 7000. RRR = R(273 K)/R(4 K).

Field, R. W., Tilford, S. G., Howard, R. A., Simmons, J. D., **Fine structure and perturbation analysis of the $a^3\Pi$ state of CO,** *J. Mol. Spectrosc.* **44,** No. 2, 347-382 (Nov. 1972).

Key words: $a^3\Pi$ state; CO; electronic spectra; rotational analysis; vibrational analysis.

The Cameron absorption bands of CO($v' = 1 - 8$; $v'' = 0$) have been photographed at high resolution. The analysis of these bands along with a reanalysis of the $a^3\Pi$, $v = 0$ level and an analysis of the perturbations of the $a^3\Pi$ state by levels of the $a'^3\Sigma^+$, $e^3\Sigma^+$, $d^3\Delta_i$ and $I^1\Sigma^-$ states will be presented. Deperturbed molecular constants for the $a^3\Pi$ state and accurate perturbation parameters for the interactions of $a^3\Pi$ with nearby states have been determined by a last-squares matrix diagonalization technique. The input data included: (i) earlier measurements from triplet-triplet emission transitions, (ii) the new measurements of the Cameron bands, (iii) rf measurements of $a^3\Pi$ lambda doubling transitions, and (iv) measurements of absorption to the neighboring perturbing states.

Field, R. W., Wicke, B. G., Simmons, J. D., Tilford, S. G., **Analysis of perturbations in the $a^3\Pi$ and $A^1\Pi$ states of CO,** *J. Mol. Spectrosc.* **44,** No. 2, 383-399 (Nov. 1972).

Key words: $a^3\Pi$, $A^1\Pi$ states; CO; configuration interaction; electronic perturbation parameters; matrix element; perturbation analysis.

The results of an analysis of perturbation of the CO $a^3\Pi$ and $A^1\Pi$ states of the...$(\pi 2p)^4(\sigma^2 p)(\pi^* 2p)$ electronic configuration by states of the ...$(\pi 2p)^3(\sigma 2p)^2(\pi^* 2p)$ configuration provide evidence for the following conclusions: (i) For perturbations between vibronic levels of a given pair of electronic states, the perturbation matrix element is the product of a vibrational factor and a constant electronic factor. (ii) Simple single configuration arguments successfully predict that all the electronic factors for the perturbations between levels of each pair of states can be related to two constants which are joint properties of the two electronic configurations $\sigma\pi^*$ and $\pi^3\pi^*$.

Finkel, P. W., Miller, T. R., **A proficiency test assessment of clinical laboratory capability in the United States,** *NBSIR 73-163,* 147 pages (May 1973). (Available as COM-73-11190/8 from the National Technical Information Service, Springfield, Va. 22151.)

Key words: Accuracy; clinical chemistry; hematology; medical usefulness; microbiology; proficiency testing.

The proficiency of a representative sample of physician, hospital and independent laboratories was assessed with respect to their ability to analyse clinical chemistry and hematology samples and to identify microbiological organisms. For the assessment of clinical chemistry and hematology proficiency, the laboratories were grouped, and determinations of group accuracy and group precision were made. Further analyses were performed to determine relative accuracy and precision of the techniques presently applied by these groups. There was no significant difference at the 95 percent confidence level in the accuracy achieved by the various laboratory groups involved in clinical chemistry and hematology analysis. In clinical chemistry, the Medicare-Certified Independent Laboratories, CDC Tested Laboratories and JCAH-Members generally proved more precise than Physician's Office and Medicare-Certified Hospital Laboratories. However, none of the laboratory groups were sufficiently accurate to permit the monitoring over time of variation in an individual patient's constituent concentrations. It would appear that poor selection of techniques was an important contributor to this low performance level. In hematology the Physician's Office Laboratories proved to be the least precise of the groups. There was no noticeable difference in precision between participants in the CDC proficiency testing program and nonparticipants. With respect to microbiology, 76 percent of the identifications by laboratories participating in the CDC testing program were incorrect, while 19.4 percent of all other identifications were incorrect.

Finkel, P. W., Miller, T. R., **A proficiency test assessment of clinical laboratory capability in the United States: Appendix Volume,** *NBSIR 73-163*, Appendix, 48 pages (May 1973). (Available as COM-73-11193/2 from the National Technical Information Service, Springfield, Va. 22151.)

Key words: Accuracy; clinical chemistry; hematology; medical usefulness; microbiology; proficiency testing.

Appendices of NBS Report 73-163 which was abstracted as follows: The proficiency of a selected sample of physician, hospital and independent laboratories was assessed with respect to their ability to analyze clinical chemistry and hematology samples and to identify microbiological organisms. For the assessment of clinical chemistry and hematology proficiency, the laboratories were grouped and determinations of group accuracy and group precision were made. Further analyses were performed to determine relative accuracy and precision of the techniques presently applied by these groups. There was no significant difference at the 95 percent confidence level in the accuracy achieved by the various laboratory groups involved in clinical chemistry and hematology analysis. In clinical chemistry, the Medicare-Certified Independent Laboratories, CDC Tested Laboratories and JCAH-Members generally proved more precise than Physicians' Office and Medicare-Certified Hospital Laboratories. However, none of the laboratory groups were sufficiently accurate to permit the monitoring over time of variation in an individual patient's constituent concentrations. It would appear that poor selection of techniques was an important contributor to this low performance level. In hematology the Physicians' Office Laboratories proved to be the least precise of the groups. There was no noticeable difference in precision between participants in the CDC proficiency testing program and non-participants. With respect to microbiology, 7.6 percent of the identifications by laboratories participating in the CDC testing program were incorrect, while 19.4 percent of all other identifications were incorrect.

Finnegan, T. F., Witt, T. J., Field, B. F., Toots, J., **Measurements of $2e/h$ via the AC Josephson effect,** (Proc. 4th Int. Conf. on Atomic Masses and Fundamental Constants, Teddington, England, Sept. 6-10, 1971), Paper in *Atomic Masses and Fundamental Constants* **4,** J. H. Sanders and A. H. Wapstra, Eds., pp. 403-410 (Plenum Press, New York, N.Y., 1972).

Key words: Josephson junction; standard cell; voltage comparison.

Recent sub-part-per-million determinations of $2e/h$ have been reported by several groups. The accuracies of these determinations have been limited to a large extent by uncertainties in the local voltage standard (i.e., standard cells). The present state of agreement between the various $2e/h$ determinations will be reviewed by using the results of the triennial international volt comparisons at BIPM, as well as the results of direct volt comparisons between NBS and other national laboratories, to relate the various national as-maintained units of voltage.

Progress on the NBS project to maintain a unit of emf via a Josephson junction device will also be reported. The results of a series of $2e/h$ measurements made at the site of the NBS reference group of standard cells will be presented. The implications of these measurements on the stability of the NBS reference group of standard cells, and on the fundamental physical constants (i.e., the fine structure constant) will be discussed.

Flynn, J. H., **Instrumental limitations upon the measurement of temperature and rate of energy production by differential scanning calorimetry,** (Proc. 3d Int. Conf. on Thermal Analysis, Davos, Switzerland, Aug. 23-28, 1971), Paper in *Thermal Analysis*, H. G. Wiedemann, Ed. **1,** 127-138 (Birkhäuser Verlag, Basel, Switzerland, 1972).

Key words: Cooling curve temperature calibration; differential scanning calorimetry; evaluation of thermal apparatus; temperature calibration; thermal analysis.

Instrumental time constants for rate of energy production response, temperature-programming response and temperature-averaging network response, time constants for a wide variety of conditions for interfacial conductivity between the sample and the calorimeter cup, and for the thermal conductivity of the sample are catalogued for the differential scanning calorimeter. Assessment of the effects of these factors upon the net rate of power production sensitivity and the temperature calibration results in the establishment of limits of precision in the measurement of temperature, specific heat and heats and rates of enthalpy change during chemical and physical transformations. The vulnerability of these calibrations to instrumental readjustment and variation in experimental techniques is also quantitatively evaluated.

Frederikse, H. P. R., Hosler, W. R., **Electrical conductivity of coal slag,** *J. Amer. Ceram. Soc.* **56,** No. 8, 418-419 (Aug. 1973).

Key words: Electrical conductivity; slag; transfer.

The electrical conductivity of natural and synthetic slags (containing 14 to 36 wt% Fe) was measured from 1200 to 1700 K at O_2 pressures from 1 to 2×10^{-6} atm. The conductivity is relatively high ($\approx 10^{-2}\ \Omega^{-1}\ cm^{-1}$ at 1700 K) and stems from the transfer of electrons between Fe^{2+} and Fe^{3+} ions. Anomalies in the conductivity around 1600 K are the result of devitrification of the glass samples.

Freeman, D. H., Kuehner, E. C., **Laser detection of small particles in liquids,** *Annals N.Y. Acad. Sci.* **158,** Article 3, 731-740 (June 20, 1969).

Key words: Air pollution; laser; light scattering; liquid pollution; particulate matter; water pollution.

A 0.3 milliwatt He-Ne laser is used with a photomultiplier to survey the light scattered by particulate matter suspended in small (7 ml) samples of liquids. Estimates of weight compositions are inferred by calibration against reference solutions of suspended polystryrene latex. A small size dependence is observed in the particle size range of 0.1 to 2.0 microns. The method is useful in the range of one part per million (PPM) to one part per billion (PPB). Results are reproducible with relative errors of approximately twenty percent.

Samples of solid chemical reagents dissolved in distilled water have been examined. The results show variable contamination levels up to 1 ppm. A sample of NBS pond water indicated 1 ppm. The ef-

fect of ultra filtration is easily demonstrated. As a side benefit, the scattered laser beam is easily inspected in liquids to show gross presence or absence of suspended matter.

Fribush, S. L., Bowser, D., Chapman, R., **Estimates of vehicular collisions with multistory residential buildings,** *NBSIR 73-175*, 72 pages (Apr. 1973). (Available as COM 74–10395 from the National Technical Information Service, Springfield, Va. 22151.)

Key words: Collisions of vehicles with buildings; multistory buildings; progressive collapse of buildings; residential buildings; vehicular impact.

Through analysis of data from Oklahoma and Illinois along with national statistics, estimates are made of the number of vehicular collisions with buildings on an annual, nationwide basis. The best estimate is on the order of tens of thousands. However, since the impetus for the study was on multistory buildings and the likelihood of their being subject to progressive collapse the calculations have been refined to apply to substantial damage to multistory residential buildings. In 1970, such accidents were only on the order of 40, hence the probability of a given building being so affected in a single year is approximately one in 10,000. Some discussion is provided on improvement for data collection for the future.

Fried, C., Ramsburg, R., Butler, S., **A survey of the sanitary conditions of migrant labor camps,** *NBSIR 73-248*, 81 pages (Aug. 1973). (Available as COM 74–10474 from the National Technical Information Service, Springfield, Va. 22151.)

Key words: Health standards; migrant labor camps; questionnaire construction; regulations; survey design.

The Community Health Service (CHS) of the Department of Health, Education, and Welfare has been assigned the responsibility of providing health care services to migrant farmworkers. Since poor sanitation can be a major factor in the health of migrants, CHS requested NBS' Technical Analysis Division (TAD) to perform a field survey of the current state of the sanitary conditions of migrant housing.

A survey form was developed by TAD as an aid in evaluating migrant housing. The form was derived from the checklist procedure employed by sanitarians to determine whether migrant housing meets state and local housing regulations.

Field visits were made to migrant labor camps in five different regions of the United States. These regions were selected because they contained a large number of camps open at the time of the visits. Within each region, camps were selected on a modified random basis.

A description of the findings of the survey is provided in both tabular and narrative form. A discussion of the limitations in the procedures used in conducting the survey is also included, and changes are suggested which could be incorporated into future surveys.

Fuller, E. G., **Photonuclear Physics 1973. Where we are and how we got there,** (Proc. Int. Conf. on Photonuclear Reactions and Applications, Pacific Grove, Calif., Mar. 26-30, 1973), Paper in *International Conference on Photonuclear Reactions and Applications*, B. L. Berman, Ed., pp. 1201-1224 (Ernest O. Lawrence Livermore Laboratory, University of California, Livermore, Calif., 1973). (Available as CONF-730301 from the National Technical Information Service, Springfield, Va. 22151).

Key words: Data; experimental facilities; history; photonuclear reactions; research programs; survey.

A brief history is presented of the study of photonuclear reactions from the time of the first measurements in 1934 through the most recent measurements in 1972 and early 1973. Trends are indicated both for the specific types of measurements carried out, as well as for the geographic areas of the world active in the field. A review is given of the data obtained since 1955 as a function of element and isotope and the areas where data are missing are pointed out. Finally, the results of a survey made in early 1973 are given. This survey covered the existing experimental facilities, as well as the research programs directed toward the study of the interaction of electromagnetic radiation with nuclei.

Fung, F. C. W., **Evaluation of a pressurized stairwell smoke control system for a 12 story apartment building,** *NBSIR 73-277*, 53 pages (June 1973). (Available as PB 225–278 from the National Technical Information Service, Springfield, Va. 22151.)

Key words: Analysis; basic correlation formulas; computer calculations; high-rise building fire; operation BREAKTHROUGH; pressurized stairwell; quantitative experiment; smoke control; smoke simulation.

An NBS study to evaluate the effectiveness of a pressurized stairwell smoke control system in a high rise apartment building is summarized and discussed in the light of experimental results, analysis, and computer prediction. A quantitative experimental technique of smoke simulation and smoke movement measurement is described, supplemented by basic physical laws necessary for correlation with small fires, and illustrated by the results of an actual field experiment. Experiments were conducted in a 12 story apartment building constructed on the Operation BREAKTHROUGH prototype site in St. Louis, Missouri. The experimental results are then further extended to a wider range of ambient weather conditions by way of computer prediction calculations. General conclusions and relevant recommendations as a result of the study are also presented.

Furukawa, G. T., Reilly, M. L., **Application of precise heat-capacity data to the analysis of the temperature intervals of the international practical temperature scale of 1968 in the region of 90 K,** (Proc. 5th Symp. on Temperature, Its Measurement and Control in Science and Industry, Washington, D.C., June 21-24, 1971), Paper in *Temperature, Its Measurement and Control in Science and Industry*, H. H. Plumb, Editor-in-Chief, **4,** Part 1A, 27-36 (Instrument Society of America, Pittsburgh, Pa., 1972).

Key words: Heat capacity; specific heat; temperature intervals; temperature scale.

Precise heat-capacity data were employed to analyze the temperature intervals or smoothness of the International Practical Temperature Scale of 1968 (IPTS-68) between 15 and 380 K, particularly in the region of 90 K, as it is maintained at the National Bureau of Standards. Results show that there are no local irregularities in the temperature scale within the precision ($\pm$ 0.02 percent) of the heat-capacity data between 40 and 380 K. Below 40 to 15 K the uniformity of the temperature scale is less certain because of the lower precision of the heat-capacity data in the temperature range.

Gadzuk, J. W., Plummer, E. W., **Field emission energy distribution (FEED),** *Rev. Mod. Phys.* **45,** No. 3, 487-548 (July 1973).

Key words: Chemisorption; electronic properties of metals; field emission; surface physics.

The technique of measuring the energy distribution of electrons which have been field emitted from a cold cathode is considered. The general historical and introductory theory is presented. A survey of the experimental techniques and existing energy analyzers is given. Specific studies on clean metal surfaces in which work functions, band structure effects, surface states, thermal effects, and many-body effects have been studied are reviewed from both the experimental and theoretical points of view. Field emission energy distributions have been particularly valuable in studies of atoms chemisorbed on surfaces. Several theories of enhanced resonance tunneling due to chemisorbed atoms are discussed. Specific systems studied experimentally are reviewed. Inelastic adsorbate enhanced tunneling is also treated.

Giarrantano, P. J., Hess, R. C., Jones, M. C., **Forced convection heat transfer to subcritical Helium I,** *NBSIR 73-322*, 43 pages (May 1973). (Available as COM 73-11464-AS from the National Technical Information Service, Springfield, Va. 22151.)

Key words: Centrifugal pump; critical heat flux; film boiling; forced convection; heat transfer; helium; nucleate boiling; subcritical; supercritical.

Preliminary results of an experimental investigation of heat transfer to liquid helium under forced flow conditions are reported for a 0.213 cm i.d. × 10 cm long test section subject to the following range of operating conditions:

System pressures 1.1 – 2.1 atm

Mass velocities 4 – 64 g/s-cm²

Heat fluxes 0.04 – 0.53 W/cm²

Inlet subcooling 0.03 – 0.10 K

The effect of the above system parameters on the heat transfer and critical heat flux is discussed; a comparison of forced convection boiling with other modes of heat transfer (pool boiling and supercritical) and the performance of a centrifugal pump used for circulating the liquid helium are also included in the report.

Gilman, F. J., Kugler, M., Meshkow, S., **Pionic transitions as tests of the connection between current and constituent quarks,** *Phys. Lett.* **45B,** No. 5, 481-486 (Aug. 20, 1973).

Key words: Baryon decays; constituent quarks; current quarks; pionic transitions; su(3); $su(6)_w$.

A proposed connection between current and constituent quarks is discussed and tested through comparison with the magnitudes and signs of amplitudes for pionic transitions between hadrons.

Greenspan, M., **Transducer measurements: Use of the current probe,** *J. Acoust. Soc. Amer. Tech. Notes and Res. Briefs* **53,** No. 4, 1186-1187 (Apr. 1973).

Key words: Current probe; impedance measurements; piezoelectric transducer measurements; transducer measurements; ultrasonic instruments.

It has been found that various measurements commonly made on piezoelectric transducers are simplified by use of the current probe, a commercially available instrument. Examples are impedance, ultrasonic interferometry, and power.

Greifer, B., Taylor, J. K., **Survey of various approaches to the chemical analysis of environmentally important materials,** *NBSIR 73-209*, 237 pages (July 1973). (Available as COM 74–10469 from the National Technical Information Service, Springfield, Va. 22151.)

Key words: Air pollution; atomic absorption; electron microprobe; emission spectroscopy; environmental analysis; industrial effluents; ion-selective electrodes; nuclear activation analysis; particulate analysis; polarography; spark source mass spectrometry; spectrophotometry; trace elements; water pollution; x-ray fluorescence.

Various approaches to the chemical analysis of heavy industry process materials and effluents for trace element constituents that might contribute to environmental pollution are summarized.

The capabilities and costs of nuclear methods, spark source mass spectrometry, x-ray fluorescence and electron microprobe spectrometry, atomic absorption spectrometry, absorption spectrophotometry, atomic emission spectroscopy, voltammetry (polarography) and potentiometry (ion-selective electrodes) for determining traces (less than 100 parts per million) of mercury, beryllium, cadmium, arsenic, vanadium, manganese, nickel, antimony, chromium, zinc, copper, lead, selenium, boron, fluorine, lithium, silver, tin, iron, strontium, sodium, potassium, calcium, silicon, magnesium, uranium, and thorium in such matrices as fly ash, coal, oil, ores, minerals, metals, alloys, organometallics, incinerator particulates, slurry streams, and feeds to and from sedimentation processes have been assessed.

The report includes a critically selected bibliography of the current literature.

Haar, L., **The ideal gas-calorimetric thermometer,** *Science* **176,** 1293-1296 (June 23, 1972).

Key words: Ammonia; calorimetry; flow calorimeter; heat capacity; ideal-gas; temperature; thermodynamic temperature; thermometer.

A new thermometer is suggested for probing the difference between the thermodynamic temperature scale and a practical scale, say the International Practical Temperature Scale – 1968. The method is based on the fact that the fractional difference of the heat capacity as measured on two scales is very nearly equal to the temperature derivative of the difference in hotness between the scales. Now, the heat capacity on the thermodynamic scale is by definition that of the ideal gas calculated from the molecular structure using statistical mechanics. This we compare with the analogous quantity measured calorimetrically and extrapolated to the ideal gas limit. The feasibility of the method is illustrated using very accurate data for gaseous ammonia.

Hallowell, P. L., Bertozzi, W., Heisenberg, J., Kowalski, S., Maruyama, X., Sargent, C. P., Turchinetz, W., Williamson, C. F., Fivozinsky, S. P., Lightbody, J. W., Jr., Penner, S., **Electron scattering from ^{19}F and ^{40}Ca,** *Phys. Rev. C* **7,** No. 4, 1396-1409 (Apr. 1973).

Key words: Electron scattering; inelastic; ^{19}F; ^{40}Ca; transition strengths.

Electron scattering form factors were measured for the low-lying levels of ^{19}F and ^{40}Ca for momentum transfers between 0.55 and 1.00 fm^{-1}. Elastic scattering from ^{19}F yields an rms charge radius of 2.885 ± 0.015 fm. Transition strengths and transition radii are obtained for the lowest $5/2^+$, $5/2^-$, and $3/2^+$ states in ^{19}F. A deformed rotational model gives a very good fit to the form factors for the positive-parity levels with ground-state deformation parameters of $\beta_2 = 0.41$ and $\beta_4 = 0.17$. The form factors for excitation of the 3^- and 2^+ states in ^{40}Ca are analyzed by phase-shift analysis, and transition strengths and transition radii are also obtained for these levels.

Hampson, R. F., Garvin, D., Herron, J. T., Huie, R. E., Kurylo, M. J., Laufer, A. H., Okabe, H., Scheer, M. D., Tsang, W., **Chemical kinetics data survey VI: Photochemical and rate data for twelve gas phase reactions of interest for atmospheric chemistry,** *NBSIR 73-207*, 127 pages (Aug. 1973). (Available as AD 769266 from the National Technical Information Service, Springfield, Va. 22151.)

Key words: Atmospheric chemistry; chemical kinetics; data evaluation; gas phase reaction; optical absorption cross section; photochemistry; quantum yield; rate constants.

Photochemical and rate data have been evaluated for twelve gas phase reactions of interest for the chemistry of the stratosphere. The results are presented in data sheets, one for each reaction. For each reaction the data are summarized. A preferred value is given for the rate constant or the primary quantum yield and photoabsorption cross section.

Hartman, A. W., Rosberry, F. W., Simpson, J. A., **A non-contacting length comparator with 10 nanometer precision,** *Opt. Eng.* **12,** No. 3, 95-101 (May/June 1973).

Key words: Dimensional metrology; displacement measurement; microscope; non-contact sensing; optical surface probe; surface detection.

530-326 OL - 74 - 14

A non-contacting length comparator utilizing two specially designed photo-electric microscopes has been constructed. Performance tests of this comparator, using lapped and polished steel surfaces demonstrate a resolution of ~ 1 nanometer, a precision of ~ 10 nanometers, and a linear range in excess of 50 micrometers.

Hastie, J. W., **Mass spectrometric analysis of 1 atm flames: Apparatus and the CH_4-O_2 system,** *Combust. Flame* **21,** 187-194 (1973).

Key words: CH_3; flames; H; mass spectrometry; OH; radicals.

A mass spectrometric system is described for the measurement of reactive intermediates in 1 atm flames. The system has been tested on $CH_4 - O_2$ and $CH_4 - O_2 - N_2$ flames and provides for the first time a complete analysis of such flames for species in excess of 10^{-5} mole fraction concentration.

Hjortenberg, P. E., McLaughlin, W. L., **Use of radiochromic dye systems for dosimetry,** (Proc. Regional Conf. on Radiation Protection, Jerusalem, Israel, Mar. 1973), Paper in *Radiation Protection*, Y. Feige and T. S. Schlesinger, Eds., **1,** 122-140 (Israel Atomic Energy Commission, Yavne, Israel, 1973).

Key words: Accelerator; blood irradiators; dosimetry; electron beams; gamma rays; radiochromic dyes; x-rays.

Radiochromic dye systems have been developed at the U.S. National Bureau of Standards and have been further investigated at the Accelerator Department, The Danish Atomic Energy Commission Research Establishment Riso. Measurable absorbed doses range from 10^2 to 10^8 rads, depending on the particular system. Some characteristic properties are as follows: long shelf life, dose rate independence, low atomic number constituents (C, H, N, O), small temperature dependence, sensitivity to ultraviolet light, linear dose response, rather insensitive to organic impurities. In this paper a liquid system with a useful dose range of 10^2-10^5 rads is described. Results demonstrate its capabilities for calibration of radiation fields including isotope irradiators and electron accelerators. Intercomparisons were made with Fricke- and thermoluminescence dosimetry.

Hord, J., **Cavitation in liquid cryogens. III – Ogives,** *NASA CR-2242*, 235 pages (National Aeronautics and Space Administration, Washington, D.C., May 1973).

Key words: Cavitation; cryogenics; hydrofoil; nucleation; ogives; pumps; venturi.

This document constitutes the third of four volumes to be issued on the results of continuing cavitation studies. Experimental results for three, scaled, quarter-caliber ogives are given. Both desinent and developed cavity data, using liquid hydrogen and liquid nitrogen, are reported here. The desinent data do not exhibit a consistent ogive size effect, but the developed cavity data were consistently influenced by ogive size—B-factor increases with increasing ogive diameter. The developed cavity data indicated that stable thermodynamic equilibrium exists throughout the vaporous cavities. These data were correlated using the extended theory derived in Volume II of this report series. The new correlating parameter, MTWO, improves data correlation for the ogives, hydrofoil, and venturi and appears attractive for future predictive applications. The cavitation coefficient, $K_{c,min}$, and equipment size effects are shown to vary with specific equipment-fluid combinations. A method of estimating $K_{c,min}$ from knowledge of the noncavitating pressure coefficient is suggested.

Hougen, J. T., **Tabulation of hyperfine splittings in rotational F_1 and F_2 levels of the ground vibrational state of $^{12}CH_4$, for $J \leq 20$,** *J. Mol. Spectrosc.* **46,** No. 3, 490-501 (June 1973).

Key words: Computer tabulation; ground vibrational state; hyperfine splittings; methane; quantum mechanical Hamiltonian; rotational levels.

To a good approximation, hyperfine splittings for F_1 and F_2 rotational levels of the ground vibrational state of $^{12}CH_4$ depend linearly on three hyperfine interaction parameters. Coefficients in these linear expressions have been computed in a relatively simple manner and tabulated for levels with $1 \leq J \leq 20$. The hyperfine pattern for the $J = 7$ $F_2^{(2)}$ level computed from these expressions using values for the three hyperfine interaction parameters reported recently by Yi, Ozier and Ramsey [1] agrees well with the pattern obtained from new He-Ne laser measurements of Hall and Bordé [2] on the $P(7)$ $F_2^{(2)}$ line of the ν_3 band of methane.

Hummer, D. G., Kunasz, C. V., Kunasz, P. B., **Numerical evaluation of the formal solution of radiative transfer problems in spherical geometries,** *Comput. Phys. Commun.* **6,** 38-57 (1973).

Key words: Early-type stars; model atmospheres; radiative transfer; spectral line formation; spherical geometry.

If the source function and opacity are specified numerically on a grid of radius and frequency points in a spherically symmetric atmosphere, the program described here calculates the formal solution of the radiative transfer equation, that is, the intensity of radiation on the corresponding grid, and evaluates the first three angular moments of the radiation field. Extensive use of cubic splines in the analysis has made possible an extremely rapid and compact procedure for this calculation. This program has been used extensively in the solution for line formation problems in spherically symmetric atmospheres.

Issen, L. A., **Report of fire tests on flexible connectors in HVAC systems,** *NBSIR 73-267*, 67 Pages (July 1973). (Available as COM 73-11955 from the National Technical Information Service, Springfield, Va. 22151.)

Key words: Aluminum; ductwork; fabric; fiberglass; fire tests; high rise buildings; HVAC systems; steel; terminal units.

The contemporary high rise building with its control air conditioning system and high content of synthetic materials presents a higher hazard than those erected prior to 1950. The ability of the duct work to resist fire breaking into it and spreading through the duct system is an important factor affecting the integrity of the building. Since they penetrate fire barriers, the flexible connectors between the main ducts and the terminal units are important elements in maintaining the desired fire resistance. Flexible connectors made of four different materials (aluminum, galvanized steel, felted fiberglass and woven fiberglass fabric) and two attachment techniques were subjected to fire tests in accordance with ASTM E119. The results show that the materials of the connectors must withstand the fire exposure, the connectors must remain tightly attached to the main duct, and the penetrations through the fire barrier must be suitably blocked in order to prevent fire from breaking into the duct system. The tests also showed that rubber and plastic materials in the terminal units can produce significant amounts of irritating smoke.

Judd, D. B., Eastman, A. A., **Prediction of target visibility from the colors of target and surround,** *Illum. Eng.* **66,** No. 4, 256-266 (Apr. 1971).

Key words: Color; contrast; detection; tritanopia; visibility; vision.

The target visibilities of each of 266 combinations of target and surround colors have been measured by means of the Eastman contrast-threshold visibility meter. The targets and surrounds were Munsell papers, and the targets were of such size and distance from the observer (AAE) that they subtended 10 minutes of arc. Analysis of these data shows that a modification of the 1964 CIE uniform color space applied to the fluxes leaving target and surround accounts for two-thirds of the observed variation in visibility among the 266 combinations. This modification for 10-minute targets consists of neglecting the violet-greenyellow component of the color differences entirely

and of counting the red-green component less than one-tenth that proper for 60-minute targets. By taking into account the fact that the lens system of the human eye, because of chromatic aberration, causes some of the flux leaving the surround to fall on the retinal image of the target, this modified color space has been shown to account for four-fifths of the observed variations in visibility.

Kartaschoff, P., Jarvis, S., Jr., **Notes on infrared absorption experiments in a methane molecular beam,** *NBSIR 73-312*, 32 pages (May 1973). (Available as COM 73-11893/7AS from the National Technical Information Service, Springfield, Va. 22151.)

Key words: Frequency standard; methane resonance; molecular beam; Ramsey resonance; saturated absorption; stabilized laser; transition probability.

The problem of calculating the transition probability of methane molecules in a molecular beam interacting with an infrared (3.39 μ) radiation beam is discussed. Contrary to the usual microwave molecular beam experiments, first-order Doppler frequency shifts cannot be neglected. This makes the solution of the wave-equations more difficult. Weak field approximations to the transition probability have been calculated. Single optical beam experiments analogous to the Rabi-type interaction result in a Doppler-broadened absorption line with an estimated half-power width of a few MHz. For separated multiple field experiments analogous to the Ramsey-type interaction, no observable response is predicted, the expected sharp resonance pattern being smeared out by the random Doppler shifts due to the spread of the molecular beam trajectories. Further investigations are required in order to predict the resonance line shapes for strong fields, i.e., saturated absorption.

Kaufman, V., Sugar, J., **One-electron spectrum of singly ionized ytterbium (Yb II),** *J. Opt. Soc. Amer.* **63,** No. 9, 1168-1172 (Sept. 1973).

Key words: Energy levels; spectrum; ytterbium.

The spectrum produced by the hollow-cathode discharge was measured from 2107 to 1377 Å. With these new data and the previously published observations of Yb II at longer wavelengths, new $4f^{14}nl$ series terms were found, including $1\,6s$, $7p$, $7-11d$, $5-14f$, and $5-6g$. A value of 98 269(50) cm^{-1} was deduced for the ionization energy.

Kidnay, A. J., Hiza, M. J., Miller, R. C., **Liquid-vapour equilibria research on systems of interest in cryogenics—A survey,** *Cryogenics* **13,** No. 10, 575-599 (Oct. 1973).

Key words: Annotated bibliography; binary systems; cryogenic fluid mixtures; liquid-vapour equilibria; multicomponent systems; survey.

This survey provides a convenient summary of available data on liquid-vapour equilibria for systems of interest in cryogenics. An annotated bibliography of 392 references has been compiled, current to January 1973. These references have been scanned individually with few exceptions, and cross-indexed by system with notation of extent of data and other significant features. The systems included are those made up of the possible combinations of H_2(D_2, HD), N_2, O_2, F_2, CO, H_2S, He(He^3), Ne, Ar, Kr, Xe, and the saturated and unsaturated hydrocarbon through the C_4s.

Klein, W., **Perturbation solution of the Kirkwood-Salsburg equation,** *J. Math. Phys.* **14,** No. 8, 1049-1059 (Aug. 1973).

Key words: Asymptotic behavior at large cluster separations; Banach space; Kirkwood-Salsburg equation; perturbation expansion; product property; strip operator approximation.

A formal series solution to the Kirkwood-Salsburg equation and its radius of convergence are derived. This solution leads naturally to the establishment of an approximate hierarchy of equations for the distribution functions which needs no closure. The asymptotic behavior of the solutions to this approximate hierarchy is studied as well as the behavior of the derivatives of the pair function with respect to the interparticle distance.

Krauss, M., Julienne, P. S., **Dissociative recombination of $e+CH^+$ ($X^1\Sigma^+$),** *Astrophys. J.*, **183,** L139-L141 (Aug. 1, 1973).

Key words: CH, CH^+; dielectronic recombination; electron-ion recombination; energy curve; Rydberg excited state; valence excited state.

The ratio of the dissociative recombination rate for $e+CH^+$ to the dielectronic recombination rate is calculated to be of the order of 10^8. These rates place a serious constraint on homogeneous gas-phase production of interstellar CH^+ and CH from ground-state atoms.

Kruger, J., Ambrose, J. R., **The role of passive film growth kinetics and properties in stress corrosion and crevice corrosion susceptibility,** *NBSIR 73-244*, 75 pages (July 1973). (Available as AD 767326 from the National Technical Information Service, Springfield, Va. 22151.)

Key words: Chloride; crevice corrosion; dissolved oxygen; ellipsometry; nitrates; pH; repassivation kinetics; stainless steel; stress corrosion cracking; titanium alloys.

Repassivation kinetics of an AISI 304 stainless steel have been determined in 1.0N NaCl solutions using the triboellipsometry technique which permits measurement of film growth and total reaction rates following removal of the surface film by abrasion. Although deoxygenation of the solution resulted in little change in either film growth kinetics or the ratio of total change to film thickness (R_p), changing the solution pH affected both the mechanism and rate of film growth which resulted in increased rates of metal dissolution in acidic (pH3) and basic (pH11) solutions.

The triboellipsometry technique was also used to determine repassivation kinetics and stress corrosion cracking (SCC) susceptibility for Ti-8Al-1Mo-1V alloy. Repassivation transient behavior in a 1.0N NaCl solution, where cracks have been found to propagate, was compared to that in a 1.0N $NaNO_3$ solution where SCC susceptibility has never been detected. Susceptibility was found to be related to film growth kinetics in the two solutions.

The early stages of crevice corrosion of AISI 304 stainless steel in 1.0N NaCl solution have been detected using the ellipsometer to measure changes in optical properties occurring within the crevice between a polished metal surface and a glass plate. Changes in the ellipsometer parameters Δ and ψ begin almost immediately upon creation of the crevice and can be interpreted as resulting from a build-up of soluble species within the crevice solution, followed by an overall thinning of the protective film and general corrosion attack.

LaFleur, P. D., Thompson, B. A., **Gamma-ray spectroscopy,** Paper in the *Encyclopedia of Chemistry, Third Edition*, C. Hampel and G. G. Hawley, Eds., pp. 1032-1033 (Van Nostrand Reinhold Co., New York, N.Y., 1973).

Key words: Activation analysis; gamma-ray spectroscopy; Ge(Li) detectors; group separations; instrumentation.

This article has been prepared for the third edition of the Encyclopedia of Chemistry. It is a revision of an article which appeared in the previous edition, published by Reinhold Publishing Company in 1966.

Leasure, W. A., Jr., Bender, E. K., **Tire-road interaction noise,** (Proc. 1973 International Noise Control Engineering Conference, Copenhagen, Denmark, Aug. 22-24, 1973), Paper in *Inter-Noise 73 Proceedings*, O. J. Pedersen, Ed., pp. 421-425 (Inter-Noise 73, Technical University, Lyngby, Denmark, 1973).

Key words: Acoustics; noise (sound); tire noise; transportation noise.

The important parameters influencing tire noise are discussed and the basic mechanisms of tire-noise generation are briefly described from a theoretical viewpoint. Areas for future research are identified—based on gaps in the existing data base and a rather primitive level of understanding of tire noise-generating mechanisms.

Levine, J., Stebbins, R. T., **Ultrasensitive laser interferometers and their application to problems of geophysical interest,** *Phil. Trans. Roy. Soc. London A* **274,** 279-284 (1973).

Key words: Earth tides; interferometer; normal modes; strainmeter.

A 30 m laser strainmeter is currently being operated in an unworked gold mine near Boulder, Colorado. The strainmeter consists of an evacuated Fabry-Perot interferometer illuminated by a 3.39 μm He-Ne laser. A second 3.39 μm laser is stabilized by means of saturated absorption in methane and its wavelength serves as the reference length for the system. We shall describe the instrument in some detail and present the latest results in our investigation of the Earth tides and the Earth normal modes.

Levine, J., Stebbins, R., **Upper limit on the gravitational flux reaching the earth from the Crab pulsar,** *Phys. Rev. D* **5,** No. 7, 1465-1468 (Apr. 1, 1972).

Key words: Crab pulsar; gravitational waves; laser strainmeter; precision interferometry.

A 30-m laser interferometer has been used in a search for gravitational radiation from the Crab pulsar. The minimum detectable signal would be produced by an incident gravitational flux of 10^9 ergs/sec cm^2 and we find no effect at this level.

Livingston, R. C., Rothschild, W. G., Rush, J. J., **Molecular reorientation in plastic crystals: Infrared and Raman band shape analysis of neopentane,** *J. Chem. Phys.* **59,** No. 5, 2498-2508 (Sept. 1, 1973).

Key words: Band shape analysis; diffusion models; infrared; jump diffusion; molecular reorientation; neopentane; phase transition; plastic crystal; Raman; and rotational diffusion.

An infrared and Raman band shape analysis of the broadened 924 cm^{-1} fundamental for neopentane in its liquid and plastic crystal phases is presented. Correlation functions and times for molecular reorientation derived from both the infrared and Raman data show the liquidlike behavior of the plastic phase of neopentane, with the molecules rotating "freely" through $\sim 10°$ (175 K) to $\sim 30°$ (300 K) around an inertial axis with the corresponding reduced intermolecular torques ($< L^2 >^{1/2}/kT$) decreasing from 8.2 to 3.8. Furthermore, the linewidth and correlation time results show no indication of a change in rotational behavior in passing through the plastic crystal-liquid phase transition. Theoretical fits of our experimental infrared and Raman correlation function with Gordon's M and J diffusion models, as extended by McClung for spherical molecules, show that the experimental results lie between the functions predicted by these two models. The time between rotational "collisions" (angular momentum correlation time) varies continuously from 0.4×10^{-12} sec for the room-temperature liquid to 0.2×10^{-12} sec at the lowest temperature in the plastic phase. Activation energies for molecular reorientation of 4.1 and 3.6 kJ/mol are obtained, respectively, from the experimental half-widths and from the angular momentum correlation times, in good agreement with previous NMR and neutron scattering results. The results prove that neopentane melts in two stages: near 140 K, the rotational degrees of freedom of the (rigid) molecule are liberated, whereas near 253 K the translational degrees of freedom are liberated without observable change of the characteristics of the rotational motion.

Llewellyn, L. G., Peiser, C., **NEPA and the environmental movement: a brief history,** *NBSIR 73-218,* 40 pages (July 1973). (Available from the National Technical Information Service, Springfield, Va. 22151.)

Key words: Environment; environmental impact statement; environmental movement; National Environmental Policy Act (NEPA); politics and the environment.

This paper traces some of the critical events leading up to the National Environmental Policy Act (NEPA) of 1969. The opening section spotlights the rapid growth of an environmental ethic in this country, the impact of some highly visible ecological disasters, and the subsequent pressure for environmental reform exerted by opinion leaders and the mass media. The Federal Government's response to perceived changes in public priorities is the focal point of the second section. The activities of Congress and the Nixon Administration are charted in a two-year chronology spanning the 1968 and the 1970 elections, a key period in the development of environmental policy. The final section provides a critique of NEPA with special attention devoted to the controversial requirement for environmental impact statements. The paper concludes with a brief discussion of some of the challenges facing the environmental movement today.

Lovejoy, R. W., Olson, W. B., **Ground state rotational constants for $^{28}SiH_3D$,** *J. Chem. Phys. Letters to Editor* **57,** No. 5, 2224-2225 (Sept. 1, 1972).

Key words: Infrared spectrum; monodeuterosilane; perturbation allowed transitions; rotational constants; stretching vibrations.

The infrared spectrum of the ν_1 and ν_4 stretching vibrations of SiH_3D have been recorded with high resolution. The ground state rotational constants have been determined with much greater precision than has previously been reported. Observed perturbation allowed transitions have also made possible the determination of A_o-$B_o5D_o^K$.

Lyndon, R., McDonough, T., Newman, M., **On products of powers in groups,** *Proc. Amer. Math. Soc.* **40,** No. 2, 419-420 (Oct. 1973).

Key words: Free groups; powers.

In this note we show that a product of Nth powers in a group cannot in general be expressed as a product of fewer Nth powers. This extends a result of Lyndon and Newman.

Mabie, C. P., **Petrographic study of the refractory performance of high-fusing dental alloy investments: II. Silica-bonded investments,** *J. Dent. Res.* **52,** No. 4, 758-773 (1973).

Key words: Alloy; casting; chromium; investment; mold.

Petrographic study of the refractory performance of silica-bonded investments revealed that recrystallized silica bonds consisting of tridymite and cristobalite are formed during burnout. The major reaction product created during casting is eskolaite. Liquefaction and sintering in the investment at and near its interface with the casting plugs pores and may lower permeability.

Maki, A. G., **Infrared spectra of CS_2: Measurement of "hot" bands associated with the 2325 cm^{-1} and 2962 cm^{-1} bands,** *J. Mol. Spectrosc.* **47,** No. 2, 217-225 (Aug. 1973).

Key words: Absorption spectra; carbon disulfide; energy levels; high resolution; infrared; molecular spectra.

The $12^01 - 00^00$ and $02^01 - 00^00$ transitions of CS_2 have been measured with a resolution of 0.025 cm^{-1}. The following "hot" bands associated with these transitions were also measured $13^11 - 01^10$, $22^01 - 10^00$, $14^01 - 02^00$, $14^21 - 02^20$, $03^11 - 01^10$, $12^01 - 10^00$, $04^01 - 02^00$, $04^21 - 02^20$, $13^11 - 11^10$, and $22^01 - 20^00$. Improved rotational constants are given for the ground state and the first bending state. A consistent set of band constants is given for all the above vibrational transitions.

Maki, A. G., Johnson, D. R., **Microwave spectra of carbonyl sulfide: Measurements of ground state and vibrationally excited $^{16}O^{13}C^{32}S$, $^{18}O^{12}C^{32}S$, and other isotopic species,** *J. Mol. Spectrosc.* **47,** No. 2, 226-233 (Aug. 1973).

Key words: Bond distances; carbonyl sulfide; microwave spectra; molecular parameters; rotational transitions; spectra.

Microwave measurements have been made on isotopically enriched samples of ^{13}C-carbonyl sulfide and ^{18}O-carbonyl sulfide. Centrifugal distortion constants and l-type doubling constants have been determined for these isotopically substituted molecules. Rotational constants have been measured for all vibrational states below 2150 cm^{-1} and B_e values have been determined. The equilibrium bond distances calculated from different pairs of isotopes are compared and a substitution equilibrium structure is given. Some new measurements are also reported for the isotopic species $^{18}O^{13}C^{32}S$, $^{18}O^{13}C^{34}S$, $^{18}O^{12}C^{34}S$, and $^{16}O^{13}C^{34}S$.

Mandel, J., **Structure analysis in two-way tables of measurement data,** *Proc. 39th Session of the International Statistical Institute, Vienna, Austria, Aug. 20-30, 1973,* **2,** 697-705 (International Statistical Institute, Vienna, Austria, 1973).

Key words: Analysis of variance; interaction; principal components; structure; two-way tables.

A general procedure is presented for the elucidation of the structure of a two-way table. The method is based on a partitioning of the row by column interaction into a sum of multiplicative terms. To this partitioning corresponds a breakdown of the sum of squares of interaction and of the corresponding degrees of freedom in the analysis of variance table.

By studying the interrelationships of the parameters occurring in the model, the internal structure of the data can generally be ascertained. An illustrative example taken from an actual study is discussed.

Martin, W. C., Sugar, J., **Classifications of the resonance lines of europium** III, *Astrophys. J.* **184,** 671-674

Key words: Atomic ions; atomic spectra; classified lines; energy levels; europium; ionization energy; stellar spectra.

A first analysis of Eu III by Russell *et al.* in 1941 yielded classifications of seven lines (2350-2523 Å) as transitions from the $4f^7\ {}^8S^0_{7/2}$ ground level to upper levels identified only as belonging to the $4f^6\ 5d$ configuration. We have diagonalized a truncated energy matrix for $4f^6(^7F)5d$, using parameter values appropriate for Eu III. Comparison of the results with available data for the lines allows identifications of the seven experimental upper levels. These show that the seven lines include the three lines of the basic $4f^7\ {}^8S^0 - 4f^6(^7F)5d\ {}^8P$ multiplet, the strongest resonance lines of Eu III, and account for most of the oscillator strength of the $4f^7\ {}^8S^0 - 4f^6\ 5d$ group.

Masters, L. W., Wolfe, W. C., Rossiter, W. J., Jr., Shaver, J. R., **State of the art on durability testing of building components and materials,** *NBSIR 73-132,* 128 pages (Mar. 1973). (Available as PB222300 from the National Technical Information Service, Springfield, Va. 22151.)

Key words: Accelerated aging; aging of buildings; building components; climate; criteria; deterioration; durability; materials; mechanisms; nondestructive testing; testing.

This report is a summary of the present knowledge pertaining to durability predictions for building components and materials which are subjected to the effects of outdoor exposure. The various chapters of the report include discussions of the nature of aging, the measurement of properties to predict durability, nondestructive evaluation techniques, outdoor exposure techniques, accelerated aging techniques, techniques for applying testing data to durability predictions and difficulties which arise in predicting durability. Conclusions and recommendations are also included.

An appendix, which summarizes ASTM Standards for durability testing of building components and materials, is included.

McNeil, M. B., **Report to AID on an NBS/AID workshop on standardization and measurement services in industrializing economics,** *NBSIR 73-275,* 64 pages (May 4-18, 1973). (Available as COM 74-10126 from the National Technical Information Service, Springfield, Va. 22151.)

Key words: AID; assistance; economics; foreign relations; industrializing nations; LDC's; measurement services; standardization.

On May 4-18, 1973, a Workshop was held at the National Bureau of Standards (Gaithersburg), under the sponsorship of AID, whose object was to give standards officials of industrializing nations insight into the standards and measurement systems in the United States and the role of the National Bureau of Standards, so that these officials might consider what parts of the U.S. system might usefully be adapted to conditions in their home countries. The report contains copies of speeches and presentations by representatives of both the U.S. and the industrializing nations, in addition to a general agenda of talks, presentations, and tours of laboratories both of NBS and of other organizations.

Meinke, W. W., **Is radiochemistry the ultimate in trace analysis?,** *Pure Appl. Chem.* **34,** 93-104 (1973).

Key words: Accuracy error limits; activation analysis; atomic absorption; instrument biases; isotope-dilution; method biases; nuclear track technique; practical samples; radiochemistry; trace analysis techniques.

Proponents of widely-used analysis methods such as atomic absorption, spark source mass spectrometry, polarography, activation analysis, etc. often give the impression that their methods alone can solve a large fraction of the problems of trace analysis. In addition, from time to time new, specialized trace methods are reported and sometimes find use in solving special analytical problems. However, the trace analyst deceives himself and, worse yet, gives false impressions to others unless he is able to understand the biases of his methods and instruments in relation to other possible methods and instruments,—and in addition express these biases quantitatively as accuracy error limits. Our experience at NBS in certifying trace element Standard Reference Materials in matrices as diverse as glass, orchard leaves, gold, zinc, beef liver, tuna fish and coal has given us an insight into the optimum contributions which can be made of these methods. The advantages and disadvantages of activation analysis as well as of several other types of radiochemical methods will be discussed in relation to other trace analysis techniques, based on our NBS experience in practical trace analysis. It is concluded that activation analysis ranks high among the methods for trace analysis of real samples.

Mielenz, K. D., Eckerle, K. L., Madden, R. P., Reader, J., **New reference spectrophotometer,** *Appl. Opt.* **12,** No. 7, 1630-1641 (July 1973).

Key words: Beam geometry; high accuracy; optical design; spectrophotometer; systematic errors; transmittance.

A new single beam spectrophotometer is described in which transmittance is measured by placing samples normal to a parallel beam of light. Collimation and focusing of the main beam are achieved by means of off-axis parabolic mirrors. The wavelength at which the transmittance is to be measured is selected by a plane grating monochromator having off-axis parabolic mirrors and circular holes as entrance and exit apertures. The instrument has an inherent *accuracy* estimated to be 0.0001 transmittance unit. Its *precision* is characterized by a repeatability of 0.00004 transmittance units for neutral-density filters with transmittances between 10 and 30 percent. The design philosophy used to achieve these results is presented. A discussion of some systematic errors commonly

neglected in routine spectrophotometric measurements is given. Systematic errors such as detector nonlinearity and stray radiant energy are measured.

Miller, G. K., Goodman, K. M., **The Shirley Highway Express-Bus-on Freeway demonstration project—first year results,** *DOT/UMTA* **2,** 120 pages (Urban Mass Transportation Administration, Department of Transportation, Washington, D.C., Nov. 1972). (Available as PB 214333 from the National Technical Information Service, Springfield, Va. 22151).

Key words: Bus fringe parking; bus priority lanes; bus priority lanes in District of Columbia; bus transit operation; exclusive bus lanes; express-bus-on-freeway technology; Shirley Highway Corridor in Northern Virginia; urban mass transit demonstration project.

The purpose of the Shirley Highway Express-Bus-On exclusive freeway lane demonstration project is to determine the effectiveness of this technology in easing urban traffic congestion and improving the urban environment. This project, jointly sponsored by the Urban Mass Transportation Administration and the Federal Highway Administration, Department of Transportation, is comprised of three elements—exclusive bus lanes, new feature buses, and park-ride lots coordinated with the express bus service.

The objectives of this demonstration project are: (1) Determine the magnitude of the modal shift (auto-to-bus) in the Shirley Highway Corridor and develop an effective planning tool that may be used to transfer the knowledge gained from the Bus-on-Freeway experiment to other geographic areas; (2) Promote economic viability of transit operation; (3) Reduce traffic congestion during peak periods; (4) Increase people-moving efficiency of Shirley Highway; (5) Reduce vehicle-related air pollution; (6) Reduce travel times for motorists and transit users; (7) Improve reliability of transit service; (8) Increase perceived value of transit; and (9) Improve mobility of young, old, physically handicapped, and low income travelers.

The Technical Analysis Division, National Bureau of Standards is evaluating the demonstration project by monitoring performance in terms of attaining the project objectives, and by determining the contributions of project features to increases in the percentage of commuter trips by bus.

This report presents the results of the evaluation at the end of the first eighteen month period (June 1972) of this multi-year demonstration project.

Miller, G., **The Shirley Highway Express-Bus-on Freeway demonstration project—Project description,** *Report DOT/UMTA* **1,** 87 pages (Urban Mass Transportation Administration, Department of Transportation, Washington, D.C., Aug. 1971). (Available as PB 218983 from the National Technical Information Service, Springfield, Va. 22151).

Key words: Bus fringe parking; bus priority lanes, bus priority lanes in District of Columbia; bus transit operation; exclusive bus lanes, express-bus-on freeway technology; Shirley Highway Corridor in Northern Virginia; Urban Mass Transit Demonstration Project.

This report describes the three major demonstration project elements: (1) the busway, including the exclusive lane on Shirley Highway and the bus priority lanes in the District; (2) the bus transit operation, involving new buses (with special features) on new routes and schedules; and (3) the residential fringe parking, with shopping centers and new lots providing free parking for bus riders. The existing roadway and bus operations are documented and the improvements planned for 1971-72 are presented. The Shirley Highway Corridor where the bus and auto commuters live is described, as is the major employment destination areas. Data are also presented on bus and auto travel volumes for 1970-1971, before the busway was completed and the new buses placed into operation.

Milligan, D. E., Jacox, M. E., Guillory, W. A., **Infrared spectrum on the NO_2^- ion isolated in an argon matrix,** *J. Chem. Phys.* **52,** No. 8, 3864-3868 (Apr. 15, 1970).

Key words: Alkali metal reactions; electron attachment; infrared spectrum; matrix isolation; NO_2^-; photodetachment; photoionization.

The molecular ion NO_2^- has been stabilized in an argon matrix in sufficient concentration for detection of its antisymmetric stretching fundamental, ν_3, at 1244 cm^{-1} by electron bombardment or photoionization of matrix-isolated NO_2 and by the interaction of an alkali-metal atomic beam with NO_2 in an argon matrix. In contrast to the position of this fundamental in an inert, nonionic environment, a value of approximately 1275 cm^{-1} is characteristic of the crystalline material. Isotopic data are consistent with a 115° valence angle for NO_2^-, independent of environment. Irradiation of the sample with light of wavelength near 3150 Å leads to the destruction of the NO_2^- absorption in the studies of the electron bombardment and photoionization of NO_2, but not in the experiments in which the alkali metal atoms provide a reservoir of photoelectrons.

Milligan, D. E., Jacox, M. E., **Infrared and ultraviolet spectroscopic studies of a number of small free radicals and molecular ions in a matrix environment,** (Proc. Symp. on Spectroscopic Methods in Cryochemistry and of the Chemistry of High Temperature Species, Minneapolis, Minn., Apr. 1969), Paper in *Advances in High Temperature Chemistry*, Leroy Eyring, Ed. **4,** 1-42 (Academic Press, Inc., New York, N.Y., 1971).

Key words: Free radicals; infrared spectrum; matrix isolation; molecular ions; photolysis; ultraviolet spectrum.

The development of the matrix isolation technique is summarized, and the principles which have been found to be important for the *in situ* photoproduction of free radicals trapped in inert solid matrices in sufficient concentration for direct infrared and ultraviolet spectroscopic observation are considered. A survey of the small free radical species heretofore studied using these techniques is given. Examples of the successful application of the technique are drawn from recent studies of the vacuum-ultraviolet photolysis of matrix-isolated methane and silane and of their chloro- and fluoro-derivatives. Results of experiments designed to permit the trapping in inert, nonionic matrices of negatively charged molecular ions are presented.

Molino, J. A., **Pure-tone equal-loudness contours for standard tones of different frequencies,** *Perception Psychophysics* **14,** No. 1, 1-4 (1973).

Key words: Loudness; noise; psychoacoustics; psychophysics.

Six Ss made judgments of equal loudness by adjusting the intensity of comparison tones of 10 different frequencies. The comparison tones were presented diotically alternately with standard tones. Each standard tone remained fixed at one frequency (125, 1,000, or 8,000 Hz) and one intensity (10, 20, 40, or 70 dB sensation level) while collecting the data for any single equal-loudness contour. In this manner, families of equal-loudness contours were generated for each of the three standard frequencies. The contours for the 1,000-Hz standard were compared with those in the literature. The families of contours for the 125- and 8,000-Hz standards, determined by the same algorithm, differed in the spacing of the contours from the 1,000-Hz standard family as well as from each other. Implications for the reflexive, symmetric, and transitive properties of the equal-loudness relation are discussed.

Mopsik, F. I., Broadhurst, M. G., **Grüneisen constants of polymers,** *J. Appl. Phys.* **44,** No. 10, 4261-4264 (Oct. 1973).

Key words: Bulk modulus; Grüneisen constant; infrared; lattice vibrations; polyethylene; polymers.

One result of recent interest in Grüneisen constants, $\gamma = -d \ln \nu / d \ln V$, of polymers is a considerable spread of reported γ's for solids like polyethylene. From elasticity data (bulk modulus or sound velocities for example) one finds $\gamma \approx 6$ for linear polymer solids. Values of γ from thermal data are much lower than 6 because the relationship usually employed, $\gamma = \alpha BV/C_v$, is not valid for polyatomic solids. Measurements of the shifts in lattice frequencies with volume strains are the most direct way of measuring γ. However, the results for pressure-induced strains differ from those for temperature-induced strains, and both differ from the results from elasticity data. In this paper we consider vibrations in a simple anharmonic well and show how the apparent shifts in vibrational frequency with pressure and temperature can be derived from changes in force constants.

Morris, J. C., Walker, J. H., **Electron-neutral transport cross section of mercury,** *J. Appl. Phys.* **44,** No. 10, 4558-4561 (Oct. 1973).

Key words: Arc mercury; conductivity; cross section; electrical conductivity of mercury; electron-neutral; electron-neutral transport cross section of mercury; mercury arc.

The electron-neutral transport cross section and the electrical conductivity of Hg have been determined using a constricted dc Hg arc. This arc has a novel configuration which permits the precise measurement of the pressure, the voltage gradient, the temperature profile, and the total current. For the temperature range 5000-6500 K, the electron-neutral transport cross section was found to be 1×10^{-14} cm^2 with a precision of ± 6 percent and an absolute accuracy of ± 20 percent. A description of the apparatus and technique is presented as well as a comparison with other existing data.

Morrissey, B. W., Powell, C. J., **Interpolation of refractive index data,** *Appl. Opt.* **12,** No. 7, 1588-1591 (July 1973).

Key words: Cubic-spline interpolation; cyclohexane; interpolation; polystyrene; refractive index; sapphire.

A comparison of the interpolation of index of refraction data for Czochralski sapphire, cyclohexane, and polystyrene dissolved in cyclohexane using a three-term Sellmeier equation, the Lorentz-Lorenz equation with six terms, third and fifth order polynomials, and a cubic-spline technique indicates that the cubic spline method is extremely valuable for simple interpolation. Not only were the magnitudes of the rms and average absolute residuals the smallest, but the fits showed no systematic errors.

Mosburg, E. R., Jr., **A study of the CW 28-μm water-vapor laser,** *IEEE J. Quantum Electron.* **QE-9,** No. 8, 843-851 (Aug. 1973).

Key words: Infrared laser; vibrational excitation; water vapor discharge; water vapor laser.

The low signal gain of a CW water-vapor laser at 28 μm was measured as a function of the discharge current and pressure. Together with the measurement of other quantities such as the axial electric field and the concentration of OH, a partial interpretation of the mechanisms involved in pumping the 28-μm transition was possible.

Thermal equilibrium between the ν_0, $2\nu_2$, and n_3 vibrational levels will result in a large absorption at the elevated gas temperatures observed (800-1000 K). The strong dependence of gain on the electron temperature strongly suggests that the vibrational excitation proceeds through electron-impact excitation. Only the electron-impact excitation of H_2O is quantitatively capable of overcoming the large thermally induced absorption. Although vibrational-excitation transfer from H_2 to H_2O seems insufficient, by itself, to overcome this absorption, it may provide appreciable additional gain. Pumping of the 28-μm line through electron-ion recombination and by reactions involving OH can be ruled out.

Mulholland, G. W., **Line of symmetry for the classical equation of state,** *J. Chem. Phys.* **59,** No. 5, pp. 2738-2741 (Sept. 1, 1973).

Key words: Classical equation of state; coexistence curve; critical phenomena; diameter of coexistence curve; line of symmetry; liquid-vapor phase transition.

The existence and properties of the Widom-Stillinger line of symmetry are examined for the "classical" equation of state, that is, an equation of state in which the chemical potential is expressed as a power series in density and temperature. In doing this, the chemical potential is shown to be an analytic function of temperature in the two phase region. This analyticity has been anticipated for a number of years.

Mullen, L. O., **High and ultra-high vacuum by pumping with cryocooled surfaces,** (Proc. American Institute of Chemical Engineers, Symp. Series on Cryogenic Pumping, Denver, Colo., 1971), Paper in *Vacuum Technology at Low Temperatures,* **125,** No. 68, 24-30 (1972).

Key words: Cryopumping; cryosorption; gettering; vacuum pump; vapor pressures.

This presentation reviews the principles of pumping with cryogenically-cooled surfaces to produce high and ultra-high vacuum. The theory of cryopumping and entrapment by cryopumping, as well as some advantages and limitations are discussed.

Myers, V. W., **Klein-Gordon equation for a charged particle interacting with an electromagnetic wave,** *J. Franklin Inst. Brief Commun.* **295,** No. 6, 497-499 (June 1973).

Key words: Expectation values; Klein-Gordon equation; plane electromagnetic wave.

A solution of the two-component Klein-Gordon equation is obtained from a solution of the corresponding one-component equation for the example of a charged particle interacting with a plane electromagnetic wave. Expectation values for momentum components and the total energy of the particle are calculated.

Negas, T., Roth, R. S., Parker, H. S., Brower, W. S., **Crystal chemistry of lithium in octahedrally coordinated structures. I. Synthesis of $Ba_8(Me_6Li_2)O_{24}$(Me = Nb or Ta) and $Ba_{10}(W_6Li_4)O_{30}$. II. The tetragonal bronze phase in the system BaO-Nb_2O_5-Li_2O,** *J. Solid State Chem.* **8,** No. 1, 1-13 (1973).

Key words: $Ba_8Nb_6Li_2O_{24}$; BaO-Nb_2O_5-Li_2O systems; $Ba_8Ta_6Li_2O_{24}$; $Ba_{10}W_6Li_4O_{30}$; close-packed oxides; crystal growth; tetragonal bronzes.

The preparation, single crystal growth, and crystallographic properties of a close-packed, eight-layer, hexagonal ($a = 5.803$ Å, $c = 19.076$ Å) modification having the stoichiometry $Ba_8Nb_6Li_2O_{24}$ and of a close-packed, ten-layer, hexagonal ($a = 5.760$ Å, $c = 23.742$ Å) phase with $Ba_{10}W_6Li_4O_{30}$ stoichiometry are discussed. The isostructural $Ba_8Ta_6Li_4O_{24}$ form of the eight-layer phase was also prepared ($a = 5.802$ Å, $c = 19.085$ Å). Proposed crystal structures involve the pairing of lithium and metal (Nb, Ta, or W) octahedra to yield face-sharing units. The relationship of this phenomenon to other known close-packed phases containing Li is demonstrated. An investigation of the $Ba_8Nb_6Li_2O_{24} - Ba_{10}W_6Li_4O_{30}$ system is reported.

A tetragonal bronze phase homogeneity region was delimited at 1200 °C in the $BaO - Nb_2O_5 - Li_2O$ system. A new orthorhombic phase ($a = 10.197$ Å, $b = 14.882$ Å, $c = 7.942$ Å) was prepared with the stoichiometry $Ba_4Li_2Nb_{10}O_{30}$.

Nelson, J. D., Blair, W., Brinckman, F. E., Colwell, R. R., Iverson, W. P., **Biodegradation of phenylmercuric acetate by mercury-resistant bacteria,** *Appl. Microbiol.* **26,** No. 3, 321-326 (Sept. 1973).

Key words: Atomic absorption; biodegradation; mercury-resistant bacteria; mercury transformations; phenylmercuric acetate, Pseudomonas.

Selected cultures of mercury-resistant bacteria degrade the fungicide-slimicide phenylmercuric acetate. By means of a closed system incorporating a flameless atomic absorption spectrophotometer and a vapor phase chromatograph, it was demonstrated that elemental mercury vapor and benzene were products of phenylmercuric acetate degradation.

Newbury, D. E., Yakowitz, H., Myklebust, R. L., **Monte Carlo calculations of magnetic contrast from cubic materials in the scanning electron microscope,** *Appl. Phys. Lett.* **23,** No. 8, 488-490 (Oct. 15, 1973).

Key words: Contrast mechanism; electron backscattering energy filtering; iron; magnetic domains; Monte Carlo methods; scanning electron microscopy; transformer steel.

Monte Carlo calculations confirm that contrast observed in the scanning electron microscope from magnetic domains in materials of cubic anisotropy is due to the alteration of electron trajectories within the specimen. Results are presented for the effects of electron accelerating potential, specimen tilt, and rotation. The contrast arises mainly from the high-energy portion of the back-scattered electron distribution.

Newell, A. C., Baird, R. C., Wacker, P. F., **Accurate measurement of antenna gain and polarization at reduced distances by an extrapolation technique,** *IEEE Trans. Antennas Propagat.* **AP-21,** No. 4, 418-431 (July 1973).

Key words: Antenna gain; antenna polarization; extrapolation technique; 3-antenna technique.

A new technique is described for determining power gain and polarization of antennas at reduced range distances. It is based on a generalized three-antenna approach which, for the first time, permits absolute gain and polarization measurements to be performed without quantitative *a priori* knowledge of the antennas. The required data are obtained by an extrapolation technique which includes provisions for rigorously evaluating and correcting for errors due to proximity and multipath interference effects. The theoretical basis provides a convenient and powerful approach for describing and solving antenna measurement problems, and the experimental method employed illustrates the utility of this approach. Examples of measurements are included which exhibit errors in gain as small as ± 0.11 dB (3σ).

O'Connell, J. S., **Electromagnetic sum rules,** (Proc. Int. Conf. on Photonuclear Reactions and Applications, Pacific Grove, Calif., Mar. 26-30, 1973), Paper in *International Conference on Photonuclear Reactions and Applications*, B. L. Berman, Ed., pp. 71-94 (Ernest O. Lawrence Livermore Laboratory, University of California, Livermore, Calif., 1973). (Available as CONF-730301 from the National Technical Information Service, Springfield, Va. 22151).

Key words: Effective interaction; electron scattering; nucleon-nucleon correlations; photoabsorption; photon scattering; sum rules.

A survey of total and partial nuclear cross section sum rules for photoabsorption and electron scattering is presented. The sums are derived from closure or the dispersion relation and are compared with available data and discussed in the context of the single particle shell model. A few of the rules are model-independent or relate observables, but most are influenced either by the form of the effective two-nucleon interaction or by nucleon-nucleon correlations in the nuclear ground state. The relation of electron scattering sums in the low momentum transfer region to photo sums is emphasized. A new sum rule for elastic photon scattering is given.

O'Connell, J. S., **Neutrino disintegration of the deuteron,** (Proc. Int. Conf. on Few Particle Problems in the Nuclear Interaction, Los Angeles, Calif., Aug. 28-Sept. 1, 1972). Paper in *Few Particle Problems in the Nuclear Interaction*, I. Slaus, S. A. Moszkowski, R. P. Haddock, and W. T. H. van Oers, Eds., pp. 906-909 (North Holland Publishing Co., Amsterdam, The Netherlands, 1972).

Key words: Carbon; deuteron; interaction neutrino; neutron.

The cross section for the reaction $D(\nu_e,e^-)2p$ averaged over the neutrino spectrum expected from the beam stops of high-intensity proton accelerators is given. Calculations were carried out using a multipole expression for the neutrino-nucleus interaction and the effective-range theory for the electromagnetic breakup of the deuteron.

Ogburn, F., Johnson, C. E., **Banded structure of electroless nickel,** *Plating Technical Brief*, pp. 1043-1044 (Oct. 1973).

Key words: Electroless nickel; electroless plating; nickel phosphorus.

The cross section of an electroless nickel deposit was scanned for phosphorus with an electron probe. The variations in phosphorus content corresponded inversely with the degree of etching with the usual nitric-acetic acid etchant, which develops the striations characteristic of electroless nickel deposits.

Ogburn, F., Johnson, C. E., **Effects of electroless nickel process variables on quality requirements,** *NBSIR 73-240*, 34 pages (June 1973). (Available from the National Technical Information Service, Springfield, Va. 22151.)

Key words: Chemical nickel; coatings; electroless nickel; metal coatings; nickel; nickel-phosphorus.

Deposition rate, phosphorus content, hardness, appearance, and metal distribution are reported for deposits from two acid, hypophosphite type electroless nickel baths, one proprietary and one nonproprietary. The baths were operated under a variety of conditions with variations of composition. Extensive data is given on the relation of deposit hardness to phosphorus content and to heat treatment at 100, 200, and 400 °C.

Okabe, H., Dibeler, V. H., **Photon impact studies of C_2HCN and CH_3CN in the vacuum ultraviolet; heats of formation of C_2H and CH_3CN,** *J. Chem. Phys.* **59,** No. 5, 2430-2435 (Sept. 1, 1973).

Key words: Acetonitrile; cyanoacetylene; C_2H; heat of formation; photodissociation; photoionization; vacuum ultraviolet.

A photodissociation process to produce CN $B^2\Sigma$ from C_2HCN and CH_3CN has been studied as a function of incident wavelength. Threshold photon energies required for the production of CN $B^2\Sigma$ from C_2HCN and CH_3CN are 9.41 ± 0.04 and 8.52 ± 0.03 eV, respectively, from which $D_0(C_2H - CN) \leq 6.21 \pm 0.04$ eV and $D_0(CH_3 - CN) \leq 5.32 \pm 0.03$ eV are obtained. The photoionization yield curves have been measured for the C_2HCN^+ and C_2H^+ ions. Threshold photon energies obtained for the production of CN $B^2\Sigma$, C_2HCN^+, and C_2H^+ from C_2HCN lead to the following thermochemical values; I.P.$(C_2HCN) = 11.64 \pm 0.01$ eV, I.P.$(C_2H) = 11.96 \pm 0.05$ eV, $\Delta Hf_0°(C_2HCN) \geq 85 \pm 1$ kcal mol^{-1} (355 ± 4 kJ mol^{-1}). $\Delta Hf_0°(C_2H) = 127 \pm 1$ kcal mol^{-1} (531 ± 4 kJ mol^{-1}) and $D_0(C_2H - H) = 5.38 \pm 0.05$ eV. $\Delta Hf_0°(C_2H)$ obtained is in good agreement with the recent value obtained directly from a study of the high temperature reactions of graphite with hydrocarbons. $\Delta Hf_0°(CH_2CN) \geq 14 \pm 1$ kcal mol^{-1} (59 ± 4 kJ mol^{-1}) derived from $D_0(CH_3 - CN)$ agrees within the stated error limit with the value obtained recently by bomb calorimetry. The fluorescence efficiency vs incident wavelength curves for C_2HCN and CH_3CN show several peaks corresponding to Rydberg states indicating that the process is predissociative. The absorption coefficient of C_2HCN has been measured in the vacuum ultraviolet. The photoionization yield curve for C_2HCN^+ shows at least two Rydberg series converging to vibrationally excited C_2HCN^+ ions.

Olf, H. G., Fanconi, B., **Low frequency Raman-active lattice vibrations of *n*-paraffins,** *J. Chem. Phys.* **59,** No. 1, 534-544 (July 1, 1973).

Key words: *n*-paraffins; polyethylene phonon dispersion curves; Raman spectroscopy-lattice vibrations.

Raman spectra in the frequency range 5 – 200 cm^{-1} have been measured for a series of crystalline *n*-paraffins from *n*-C_5H_{12} to *n*-$C_{26}H_{54}$ and also *n*-$C_{32}H_{66}$, *n*-$C_{35}H_{72}$, and *n*-$C_{36}H_{74}$. It is found that the spectral data may be grouped consonant with crystal structures exhibited by *n*-paraffins. The data are used to map out portions of the transverse acoustical phonon dispersion curves of the orthorhombic polyethylenelike lattice and of one triclinic crystalline form. A band whose frequency is independent of chain length is observed for the orthorhombic *n*-paraffins and is assigned to the B_{3g} rotatory lattice mode of polyethylene.

Olson, W. B., **A precision photoelectric azimuthal polarimeter,** *Opt. Eng.* **12,** No. 3, 102-105 (May/June 1973).

Key words: Instrument; polarimeter; polarimetry quartz; signal-to-noise ratio; throughput.

A high precision photoelectric azimuthal polarimeter has been designed and constructed. The instrument is designed to determine the angle of rotation with an accuracy (3σ) of better than 1 part in 10^4. The instrument is of a relatively compact design and quite simple in construction.

Ordman, E. T., **Convergence and abstract spaces in functional analysis,** *J. Undergraduate Math.* **1,** No. 2, 79-96 (Sept. 1969); **2,** No. 1, 25-36 (Mar. 1970).

Key words: Convergence; filter; function space; limit space; linear topological space; net; topological space.

This paper is an expository survey of the theory of limit spaces, discussing and contrasting approaches by way of nets and filters and considering a number of the extant ways of axiomatizing such a structure. Applications are given to a number of common notions of convergence of functions and to the topology of function spaces linear topological spaces.

Ott, W. R., Fieffe-Prevost, P., Wiese, W. L., **VUV radiometry with hydrogen arcs. 1: Principle of the method and comparisons with blackbody calibrations from 1650 Å to 3600 Å,** *Appl. Opt.* **12,** No. 7, 1618-1629 (July 1973).

Key words: Continuum emission coefficient; hydrogen arc; radiometry; vacuum ultraviolet.

A method is described that utilizes the continuum emission from a wall-stabilized arc discharge as a radiometric standard in the vuv. Ultimately, this standard will cover the wavelength range from 500 Å to 3600 Å. Results of a first experiment comparing this method to two other calibration methods in the region above 1650 Å are presented. A calibrated tungsten strip lamp is used between 2500 Å and 3600 Å; the method of blackbody limited lines is applied at two wavelengths in the vuv. The hydrogen arc method depends upon the fact that the continuum emission coefficient for a hydrogen plasma at typical arc temperatures of about 14,000 K is calculable to within a few percent since the essential spectroscopic constants, continuum absorption coefficients, and transition probabilities are exactly known. The accuracy of the method depends primarily on the capability of spatially resolving in an end-on measurement the nearly homogeneous plasma layers near the axis of the cylindrically symmetric arc column.

Ott, W. R., Wiese, W. L., **Far ultraviolet spectral radiance calibrations at NBS,** *Opt. Eng.* **12,** No. 3, 86-94 (May/June 1973).

Key words: Calibrations; deuterium lamp; far ultraviolet; hydrogen; Krefft-Rössler lamp; spectral radiance; transfer standards; wall-stabilized arc.

The range of NBS radiometric calibration services has been extended into the far ultraviolet region of the spectrum where a dc high power hydrogen wall-stabilized arc is used as a primary standard of spectral radiance. A capability in the range 130 nm to 360 nm (overlapping conventional tungsten strip lamp radiometry) is presently available with estimated uncertainties between 5 and 10 percent depending upon wavelength. The status of radiometric source standards in the far ultraviolet is briefly reviewed and the hydrogen arc and NBS calibration facility are described in detail. The use of commercially available mercury Krefft-Rössler lamps and deuterium arc lamps as transfer or secondary standards is discussed and the spectra of these lamps calibrated with the hydrogen arc standard are presented.

Paabo, M., **Analytical methods for the detection of toxic elements in dry paint matrices—a literature survey,** *NBSIR 73-251,* 49 pages (July 1973). (Available as PB 224688 from the National Technical Information Service, Springfield, Va. 22151.)

Key words: Analytical methods; antimony; arsenic; cadmium; lead; mercury; review; selenium; toxic elements in paints.

This report is a summary description of the chemical procedures currently available for the analysis of selected toxic elements in dried paint. The elements included in this report are lead, mercury, cadmium, antimony, arsenic, and selenium. The literature search upon which this report is based was directed primarily toward references pertaining to the analysis of dried paint. A bibliography of 57 references to wet chemical analysis, colorimetry, atomic absorption spectroscopy, electrochemistry, neutron activation analysis, and x-ray emission analysis is presented.

Page, C. H., **Logarithmic quantities and units,** *Proc. IEEE Letters* **61,** No. 10, 1516-1517 (Oct. 1973).

Key words: Decibel; logarithm.

Recent letters on *decibel* are commented upon, and standardization proposed by the International Electrotechnical Commission (IEC) is mentioned.

Parrish, W. R., Hiza, M. J., **Calculated liquid phase thermodynamic properties and liquid-vapor equilibria for fluorine-oxygen (FLOX) mixtures,** *NBSIR 73-338,* 30 pages (Sept. 1973). (Available as COM73-11660 from the National Technical Information Service, Springfield, Va. 22151.)

Key words:; Calculated thermophysical properties; compressed liquid phase, fluorine-oxygen mixtures, hard-sphere model; liquid-vapor equilibria.

Liquid phase thermodynamic properties and liquid-vapor equilibria of fluorine-oxygen mixtures, for which no experimental data exist, have been calculated. The results are based on excess properties predicted from the Snider-Herrington equations, with an adjusted combining rule, and the corresponding data for the pure fluids. Mixtures considered are 0.6, 0.7, 0.8, 0.88, and 0.9 weight fraction of fluorine from 55 to 90 K up to 70×10^5 Pa. In the compressed liquid, molar volumes, enthalpy, entropy, and constant pressure specific heat were determined. Along the saturation boundary, coexistent vapor compositions and solution vapor pressures were determined as well. Corresponding properties of pure fluorine from experimental data have also been included. Results are tabulated in both British and S.I. units.

Pella, P. A., DeVoe, J. R., **Internal standardization in Mössbauer spectrometry,** *Appl. Spectrosc.* **25,** No. 4, 472-474 (July/Aug. 1971).

Key words: Beta-tin; internal standardization; Mössbauer spectroscopy.

The concept of internal standardization is applied in quantitative analytical studies using the Mössbauer spectrometric technique. The

ratio of the absorption intensity of SnO_2 (analyte absorber) to that of β—Sn (internal standard absorber) is measured using $BaSn^{119m}O_3$ as the source. The results demonstrate that the systematic error which arises because of differences in the chemical composition between the analyte samples and standards can be eliminated by using an internal standard.

Penn, D. R., **The concept of the surface molecule in chemisorption,** *Surface Sci.* **39,** 333-340 (1973).

Key words: Density of states at the adsorbate; energy levels; S state adsorbate; surface molecule; tight binding calculation; W substrate.

Under certain circumstances the binding of an adsorbate to a metal surface may be thought of as the formation of a surface molecule composed of the adsorbate and the metal. This point of view is reasonable if the metal density of states at the adsorbate resembles that of an atom, i.e., exhibits a small number of well defined peaks as a function of energy. The width of these peaks must be small compared to the metal band width. Within the context of a simple tight binding model for the metal we find that for an S state adsorbate on W there are certain adsorbate positions for which the surface molecule concept should be valid.

Petersen, F. R., McDonald, D. G., Cupp, J. D., Danielson, B. L., **Rotational constants for $^{12}C^{16}O_2$ from beats between Lamb-dip-stabilized lasers,** *Phys. Rev. Lett.* **31,** No. 9, 573-576 (Aug. 27, 1973).

Key words: Accurate rotational constants; carbon dioxide ($^{12}C^{16}O_2$); Josephson junction; Lamb-dip-stabilized lasers.

New experimental measurements of the frequency separations of 30 pairs of $^{12}C^{16}O_2$ laser lines in the 10.4-μm band and 26 pairs in the 9.4-μm band have been made with Lamb-dip-stabilized lasers. The use of a Josephson junction as the frequency-mixing element simplified the measurements. Uncertainties in existing rotational constants for the laser vibrational levels were reduced 20 to 30 times and an additional rotational constant H_v was determined for the first time.

Phelan, R. J., Jr., Cook, A. R., **Electrically calibrated pyroelectric optical-radiation detector,** *Appl. Opt.* **12,** No. 10, 2494-2500 (Oct. 1973).

Key words: Calibration; detector; infrared; pyroelectric; radiometers; ultraviolet.

An electrically calibrated optical detector has been developed using a pyroelectric response of the plastic, polyvinylfluoride. An in-depth look at the modulation frequency response was performed to substantiate the equivalence of the optical and electrical inputs, indicate the optimum structure and allow for a clearer understanding of the device limitations. The experimental results of the dynamic range, linearity, uniformity, and detectivity confirm the device's utility.

Piganiol, M. P., Balke, S., Branscomb, L. M., Hamada, S., Hookway, H. T., Tell, B. V., **Ad Hoc Group on Scientific and Technical Information OECD, INFORMATION for a changing society, some policy considerations,** *Organisation for Economic Co-operation and Development*, 46 pages (OECD Publications, Paris, France, 1971).

Key words: Information packages; information policy; information systems; information users; OECD; technical information.

Early in 1969 the Secretary General of OECD established an Ad Hoc Group on Scientific and Technical Information, requesting the Group to "explore the nature, magnitude, and implications of the needs for scientific and technical information and data in science, the economy and society, and how these needs may be met through changes in the structures, technologies and policies, and management concepts." The Ad Hoc Group reached 13 conclusions and recommendations dealing with the scope of action of OECD, the usefulness and applicability of scientific and technological information systems, quality control of content and procedure of information systems, education for information system needs, and international cooperation. The report describes the observations and arguments leading to the conclusions and recommendations.

Powell, C. J., **Semiautomated data-recording and control system for an electron energy analyzer,** *Rev. Sci. Instrum.* **44,** No. 8, 1031-1033 (Aug. 1973).

Key words: Auger-electron spectra; characteristic electron energy-loss spectra; digital data-recording and control system; electron energy analyzer; liquid aluminum; tungsten.

A description is given of a digital data-recording and control system that has been used with a high resolution low energy electron scattering apparatus for the measurement of characteristic electron energy-loss spectra and Auger-electron spectra of solids (at room and elevated temperatures) and liquids. This system is based on a multichannel analyzer and has the following features: (a) Specimens can be prepared many times with data accumulated in arbitrarily short times after preparation (prior to specimen contamination), and final spectra of high precision can be obtained by summation of individual runs; (b) the voltage sweep applied to the electron energy analyzer can be calibrated dynamically; and (c) data can be accumulated and the target heated by electron bombardment in a cyclic manner with variable accumulation and heating periods. Characteristic loss spectra of tungsten at 800 °C and of liquid aluminum are presented as examples of operation of the system.

Prince, E., Donnay, G., Martin, R. F., **Neutron diffraction refinement of an ordered orthoclase structure,** *Amer. Mineral.* **58,** 500-507 (1973).

Key words: Aluminum silicate; feldspar; neutron refinement; orthoclase, silicate minerals; silicon aluminum ordering.

The crystal structure of a pegmatitic monoclinic potassium feldspar, $(K_{0.86}Na_{0.10}\square_{0.04})(Si_{3.00}Al_{1.00})[0_{7.96}(OH)_{0.04}]$, from the Himalaya mine in the Mesa Grande pegmatite district, Calif., has been refined with 3-dimensional neutron-diffraction data to an unweighted R value of 0.031 for 721 symmetry-independent observed reflections. Atomic coordinates differ by no more than 3 estimated standard deviations from those of Spencer B adularia, yet the specimen does not have the adularia morphology, and no diffuse reflections with $(h+k)$ odd have been observed. Direct refinement of the tetrahedral cation distribution shows that the Al content of the $T(2)$ sites is not significantly different from zero (actually -0.016 with an e.s.d. of 0.029); in other words the Al-Si ordering in the tetrahedral sites is essentially complete. The mean Si-O distance in the $T(2)$ sites is 1.616 Å, appreciably greater than the values predicted by various regression lines relating bond distance to aluminum content. This indicates that the observed mean $T_1(m)$-O, $T_2(O)$-O, and $T_2(m)$-O bond lengths reported for low albite and maximum microcline are consistent with full Si occupancy. This ordered orthoclase occurs in gem pockets in a microcline-bearing pegmatite. The association suggests stable growth of ordered orthoclase above the field of stability of microcline and metastable persistence to lower temperatures. Perhaps because of more rapid crystal growth, the bulk of the pegmatitic K-feldspar ordered to common orthoclase, then transformed to maximum microcline.

Quindry, T. L., Flynn, D. R., **On a simplified field measurement of noise reduction between spaces,** (Proc. 1973 International Noise Control Engineering Conference, Copenhagen, Denmark, Aug. 22-24, 1973), Paper in *Inter-Noise 73 Proceedings*, O. J. Pedersen, Ed., pp. 199-207 (Inter-Noise 73, Technical University, Lyngby, Denmark, 1973).

Key words: Absorption coefficient; acoustics; airborne sound insulation index; frequency; noise reduction; transmission loss.

This paper investigates the relationships between ratings based on the 1/3-octave band data and more easily obtained ratings of isolation based on A-weighted or C-weighted sound level data. The effects of the source room sound power spectrum, source and receive room absorptions and other parameters on the correlation obtained are discussed.

Reader, J., Epstein, G., **Zeeman effect and revised analysis of singly ionized rubidium (Rb II),** *J. Opt. Soc. Amer.* **63, No. 9, 1153-1167 (Sept. 1973).**

Key words: Rubidium; spectra; ultraviolet; wavelengths; Zeeman effect.

The spectrum of Rb II has been observed in a sliding-spark discharge with the NBS 10.7-m normal-incidence vacuum spectrograph and in an electrodeless discharge with the NBS 10.7-m Eagle spectrograph in air. The Zeeman effect was observed from 2200 to 5200 Å with an electrodeless lamp in a magnetic field of 31 000 G. The analysis has confirmed all ten of the previously known levels of the $4p^5 5p$ configuration. The $4p^5 4d$, $4p^5 5s$, $4p^5 5d$, and $4p^5 6s$ configurations have been considerably revised and extended. Almost all levels of these configurations are now known, as well as those of $4p^5 6d$, $4p^5 7s$, and $4p^5 4f$, which were newly located. All configurations have been theoretically interpreted, with configuration interaction included. The energy parameters determined from a least-squares fit to the observed level values are compared with Hartree-Fock calculations. The ionization energy as derived from the $4p^5 ns$ series, $n = 5, 6, 7$, is 220 070 ± 25 cm^{-1} (27.285 ± 0.003 eV).

Roberts, J. R., Andersen, T., Sørensen, G., **Determination of atomic lifetimes and absolute oscillator strengths for neutral and ionized titanium,** *Nucl. Instrum. Methods* **110,** 119-125 (1973).

Key words: Absolute transition probabilities; arc; beam foil; experimental; lifetimes; titanium.

Measurements of atomic lifetimes by the beam-foil technique and branching ratios by use of a gas-flow stabilized arc have led to an experimental determination of absolute oscillator strengths of Ti II. Some lifetimes of Ti I, Ti III and Ti IV are also presented.

Robertson, A. F., **Tests indicate venting increases smoke from some polymerics,** *Fire Eng.* **126,** No. 9, 97-98 (Sept. 1973).

Key words: Buildings; cellulosics; fires; polymers; smoke; venting.

The problem of voluminous smoke production during burning of plastic or polymeric materials is considered. Experimental data on smoke density resulting from both smouldering and flaming pyrolysis of cellulosic and polymeric sheet and foam materials are presented and compared. It is concluded that in general, although exceptions occur for specific materials, cellulosics produce much less smoke than polymerics under flaming exposure. The smoke production under smouldering exposure is roughly comparable for the two classes of materials. However, the polymeric materials show a marked increase of smoke production for flaming vs. smouldering while the converse is true for cellulosics. It is suggested that the fire fighting ventilation tactics developed and used for fires involving cellulosic materials may aggravate rather than ameliorate the problem of fighting fires involving polymeric materials.

Rowe, J. M., Livingston, R. C., Rush, J. J., **Neutron quasielastic scattering study of SH^- reorientation in the cubic phases of cesium and rubidium hydrosulfide,** *J. Chem. Phys.* **58,** No. 12, 5469-5473 (June 15, 1973).

Key words: Alkali hydrosulfides; hydrosulfide ion; ion reorientation; neutron scattering; phase transition; quasielastic scattering.

The orientational disorder of the hydrosulfide ions in CsSH (CsCl phase) and RbSH (NaCl phase) has been investigated by quasielastic neutron scattering with high energy resolution ($\Delta E_{1/2max} = 0.25$ meV). The experimental results provide a clear demonstration of the theoretically predicted separation of the quasielastic neutron peaks for rotating groups or molecules into unbroadened and broadened components which reflect, respectively, the geometric and time behavior of the rotation. Jump reorientation of the ions between equilibrium directions is established as the dominant mechanism creating the rotational disorder in the hydrosulfides, and both small-step rotational diffusion and quasifree rotation are clearly ruled out. Average residence times between reorientation jumps are derived from comparisons of the experimental results with theoretical calculations based on jump reorientation models, but it is not possible to determine the equilibrium orientation of the SH^- ions. Mean-square vibrational amplitudes for the hydrogen atoms are also obtained from the observed integrated intensities of the elastic peaks. The present results are compared in detail with previous lower-resolution neutron results on NaSH and CsSH. It is concluded that in most cases measurements using single crystals will be necessary to establish the details of orientation disorder in solids.

Rush, J. J., de Graaf, L. A., Livingston, R. C., **Neutron scattering investigation of the rotational dynamics and phase transitions in sodium and cesium hydrosulfides,** *J. Chem. Phys.* **58,** No. 8, 3439-3448 (Apr. 15, 1973).

Key words: Cesium hydrosulfide; hydrosulfides; ion reorientation; libration; neutron scattering; phase transition; quasielastic; residence time; sodium hydrosulfide.

The rotational motions of the hydrosulfide ions in the trigonal and fcc phases of NaSH and in the pseudo-bcc (CsCl) phase of CsSH have been studied by quasielastic and inelastic neutron scattering. NaSH and CsSH are members of a broad group of compounds $M^+(XY^-)$ which have cubic symmetry in the solid phase just below the melting point and a lower symmetry in lower temperature crystal phases. The measured inelastic neutron spectra above and below the trigonal to cubic phase transition in NaSH show that SH^- ion "librations" about equilibrium orientations persist in passing through the transition. The maximum of the broad librational bands for both NaSH and CsSH occurs near 400 cm^{-1}. A temperature and momentum-transfer (Q) dependent broadening is observed, however, in the quasielastic peaks in the cubic phases of the hydrosulfides, which indicates a rapid reorientation of the SH^- ions. The experimental quasielastic scattering results are compared with theoretical calculations of quasielastic scattering behavior based on the assumption of instantaneous reorientational jumps between a limited number of quasiequilibrium orientations. The widths of the measured quasielastic peaks plotted vs Q show an oscillatory behavior as predicted by the theoretical calculations. An isotropic reorientation model is ruled out, and the differences in the rotational disorder in NaSH and CsSH are discussed. Relaxation times (τ) for the SH^- motions are derived from the theoretical analysis. The τ values for fcc NaSH vary from 0.4 t0 0.15 psec between 103 and 212 °C, while the values for pseudo-bcc CsSH vary from 2.0 to 0.75 psec between 23 and 140 °C.

Saks, T. H., Yates, R. F., Goodman, K. M., **The Shirley Highway Express-Bus-on-Freeway demonstration project-users' reactions to innovative bus features,** *NBSIR 73-265,* 53 pages (June 1973). (Available as COM 73-11453 from the National Technical Information Service, Springfield, Va. 22151).

Key words: Attitudinal survey; bus-on-freeway; exclusive bus lanes; importance assessments; interior bus features; mass transit technology; satisfaction assessments; transit service features.

The Shirley Highway Express Bus-on-Freeway Project demonstrates the application of a new mass transit technology. The elements tested in this demonstration project include: an exclusive bus

lane in the median of a freeway and bus priority lanes in the downtown distribution area; fringe parking facilities which are coordinated with the bus service; new-look/new-feature buses; and extension of service to additional residential areas in an overall systems approach to the improvement of mass transit. As part of the evaluation of this demonstration project, a survey of commuters on board these buses was undertaken in order to obtain users attitudes concerning the special interior bus features as well as transit service features.

The results obtained from this study should be of interest to persons considering how to allocate expenditures for new bus vehicles and transit service improvements.

Bus commuters perceptions of the relative importance of various bus interior features (i.e., carpeting, special lighting, etc.) and transit service features (i.e., reliable schedules, assurance of a seat, etc.) are analyzed in this report, along with their relative satisfaction assessments of the special bus interior features. Analyses were conducted to determine if marginal improvements in interior comfort and aesthetic features proved significantly more appealing to bus commuters. The relative impact of various project marketing and promotional techniques is also presented.

Sanchez, I. C., Colson, J. P., Eby, R. K., **Theory and observations of polymer crystal thickening,** *J. Appl. Phys.* **44,** No. 10, 4332-4339 (Oct. 1973).

Key words: Annealing; comonomer inclusion; copolymers; lamella thickness; theoretical and experimental; thickening; unit cell.

The thickening of polymer crystals during isothermal annealing is usually observed to be an irreversible process. Phenomenological laws that govern such processes take the form of simple proportionalities—flux being proportional to force. For polymer crystals, a thermodynamic force capable of driving the thickening phenomenon arises from the unequal free energies of the fold and lateral surfaces. By analogy with other irreversible phenomena, the rate of crystal thickening is taken to be proportional to the derivative of the surface free energy with respect to crystal thickness. After certain assumptions, integration yields an equation in which three parameters characterize the system: an initial thickness l_0, an equilibrium thickness l^*, and a relaxation time τ which is a function of the "undercooling." The theory provides a basis for considering the effects of parameters such as time, temperature, thermal history, pressure, and liquids on the thickening rate. In particular, the theory adequately describes the time and temperature dependence of crystal thickening in random copolymers of tetrafluorethylene and hexafluoropropylene which exhibit thickening behavior completely analogous to that of homopolymers. During thickening, the unit cell dimensions of *these quenched-crystallized copolymers* decrease in a manner that is consistent with the concept of complete comonomer inclusion upon crystallization.

Santoro, A., Mighell, A. D., **Coincidence-site lattices,** *Acta Crystallogr.* **A29,** Part 2, 169-175 (Mar. 1973).

Key words: Crystal aggregates; crystals; grain boundaries; lattices; sublattices; superlattices.

Coincidence-site lattices are characterized mathematically, in the general case, by a method that can be applied to a pair of original lattices of any symmetry, either metrically identical or metrically different, does not involve inspection and is readily adaptable to computer calculations. The procedure is illustrated by several numerical examples. The proposed characterization of coincidence-site lattices is based on the theory of derivative lattices and makes extensive use of the concepts of superlattice and sublattice. Appended is a simple procedure for determining the transformation matrices needed to generate superlattices and sublattices of any multiplicity.

Santoro, A., Mighell, A. D., **Properties of crystal lattices: The derivative lattices and their determination,** *Acta Crystallogr.* **A28,** Part 3, 284-287 (May 1972).

Key words: Crystallography; lattices; sub-lattices; super-lattices.

Derivative lattices are classified as super, sub and composite, on the basis of the properties of the transformation matrices relating them to the lattice from which they are derived. A method for obtaining the transformation matrices generating these lattices is given. The method has been applied to derivation of the unique super and sublattices in a few important cases.

Seltzer, S. M., Berger, M. J., Rosenberg, T. J., **Auroral bremsstrahlung at balloon altitudes,** *NASA Spec. Publ. 3081,* 25 pages (National Aeronautics and Space Administration, Washington, D.C., 1973).

Key words: Atmosphere; auroral electrons; balloon experiment; bremsstrahlung; energy spectrum; transport calculation.

Data from a Monte Carlo calculation of the transport of electrons and secondary bremsstrahlung are presented in tabular and graphical form. These data describe bremsstrahlung flux spectra at various atmospheric depths between 3.0g/cm^2 and 15.0 g/cm^2 caused by a wide-area uniform precipitation into the atmosphere of electrons with energies between 30 and 2000 keV. The angular distribution of the incident electrons has been assumed to be isotropic over the downward hemisphere. A basic set of results is given for incident monoenergetic electron beams, which can be used to treat incident electron beams with any spectrum of interest. A comprehensive set of results, in the form of differential and integral bremsstrahlung flux spectra, has been obtained for the case of electron beams with exponential energy spectra, for e-folding energies between 5 and 200 keV.

Shives, T. R., Willard, W. A., **MFPG detection, diagnosis, and prognosis,** *NBSIR 73-252,* 266 pages (Sept. 1973). (Available as AD 772-082 from the National Technical Information Service, Springfield, Va. 22151.)

Key words: Condition monitoring; failure detection; failure diagnosis; failure prevention; failure prognosis; diagnostic systems.

These proceedings consist of a group of sixteen submitted papers and discussions from the 18th meeting of the Mechanical Failures Prevention Group which was held at the National Bureau of Standards on November 8-10, 1972. Failure detection, diagnosis, and prognosis represent the central theme of the proceedings. Bearing condition monitoring, diagnostic systems technology and applications, and new approaches in sensing and processing are discussed.

Shirley, J. H., **Semiclassical theory of saturated absorption in gases,** *Phys. Rev. A* **8,** No. 1, 347-368 (July 1973).

Key words: Gas laser theory; lamb-dip; saturated absorption.

A three-dimensional theory for the resonant interaction of electromagnetic waves with a gas of two-level atoms is formulated in terms of macroscopic variables. The theory is utilized to find the steady-state attenuation of a plane wave in the presence of another plane wave running in the opposite direction with different amplitude. Contributions are included from the reflection of the oppositely running wave by an induced standing-wave inhomogeneity in the population inversion of the medium. The resulting attenuation and reflection coefficients are expressed as velocity integrals of continued fractions. Correspondence is made with existing gas-laser theories, yielding the formulation of a high-intensity ring-laser theory. Analytic approximations for the coefficients are presented for the Doppler-limit cases of both waves weak, one wave weak, and negligible reflection (rate-equation approximation). More-general cases have been calculated numerically. The attenuation coefficients exhibit a Lamb-dip feature. The relative depth of the dip increases rapidly with power at low saturation levels, slowly at high saturation, and is greater in the attenuation of the weaker wave. The width of the dip is nonlinearly power broadened. The shape of the dip is very nearly

Lorentzian, except for one special case at high power in which the line splits. The propagation equations for the two waves are integrated over long absorption paths. A large resulting attenuation increases the relative size of the dip while decreasing the power broadening.

Simmons, J. D., Keller, R. A., **Interferometric effects on the output of organic dye lasers,** *Appl. Opt.* **12,** No. 9, 2033 (Sept. 1973).

Key words: Dye laser continua; high resolution; interferometric effects; optical components; organic dye lasers; wedged optical surfaces.

This note illustrates the necessity of using wedged optical components in organic dye laser systems to avoid interferometric effects.

Siu, M. C. I., **Equations for thermal transpiration,** *J. Vac. Sci. Technol.* **10,** No. 2, 368-372 (Mar./Apr. 1973).

Key words: Anomalous Knudsen limit; diffuse scattering; irreversible thermodynamics; specular scattering; thermal transpiration.

A formalism for analytically obtaining an expression for the thermal transpiration pressure ratio R is presented. An experimental parameter σ, which is associated with the type of molecule-solid surface collisions, is introduced. A completely diffuse scattering and a completely specular scattering from a solid surface correspond to $\sigma = 0$ and $\sigma = 1$, respectively. A known distribution function is used to derive a practical formula for R in the case of long tubes and very low pressures. Quantitative results obtained from this formula indicate that deviations from completely diffuse scattering of molecules from solid surfaces give rise to an anomalous Knudsen limit.

Smith, M. W., Martin, G. A., Wiese, W. L., **Systematic trends and atomic oscillator strengths,** *Nucl. Instrum. Methods* **110,** 219-226 (1973).

Key words: Atomic oscillator strengths; homologous atoms; isoelectronic sequences; regularities; spectral series; systematic trends.

A number of newly established or significantly improved systematic trends of atomic oscillator strengths in isoelectronic sequences and spectral series are presented. For most of these trends, beam-foil experiments have played a prominent role in supplying critically needed points. Of particular interest are the changes in several transitions of the Be and C sequences brought about by improved beam-foil results and more refined theoretical calculations. Also of significance are newly detected trends in the Li and Al isoelectronic sequences. An example will be given where the analysis of the f-value dependence along a sequence, coupled with an understanding of the changes in the energy level structure, points out areas where future beam-foil experiments would be desirable in clearing up discrepancies. The n^{*3} dependence of oscillator strengths for perturbed series will be illustrated with another interesting example.

Son, B. C., **Fire endurance tests of unprotected wood-floor constructions for single-family residences,** *NBSIR 73-263,* 65 pages (July 1973). (Available as PB225-284 from the National Technical Information Service, Springfield, Va. 22151.)

Key words: Fire endurance; fire test; flame through; full scale; housing; operation BREAKTHROUGH; single family residence; small scale; thermal resistance; wood floor; wood joist.

Fire endurance tests were performed on two full-scale and twelve small scale wood floor constructions. The fire endurance ratings on unfinished wood joist and plywood subfloor constructions varied from 10 to 13 minutes and were mainly determined by the time to "flame through." In small-scale tests, the addition of carpeting with a hair pad delayed the time of "flame through" approximately 8 minutes. Time to "flame through" may be estimated from the thermal resistance of the construction, and may be modified by the effects of applied load or construction details such as gaps, joints, and penetrations.

Son, B. C., Fang, J. B., **Fire spread on exterior walls due to flames emerging from a window in close proximity to a reentrant wall corner,** *NBSIR 73-266,* 35 pages (Apr. 1973). (Available as PB225-286 from the National Technical Information Service, Springfield, Va. 22151.)

Key words: Exterior wall; fire spread; fire test; ignition; operation BREAKTHROUGH; reentrant corner.

As a part of the research program concerning the recommended criteria for fire safety in Operation BREAKTHROUGH, two full scale fire tests were performed on a mockup of a reentrant corner, i.e., the interior corner formed at the intersection of the exterior walls of adjacent buildings, such as townhouses and garden apartments.

In each test, two wall specimens representing exterior walls were erected perpendicular to a wall containing a window opening into a fire room. One wall was located 1 foot east and the other one 5 feet west of the edges of the window. The objective of the reentrant corner fire test was to study the potential ignition and spread of fire from the room to an adjacent exterior combustible wall.

In the first test, charring on the east wall, but no surface ignition was observed during the test. The peak temperature measured did not exceed 350 °C (660 °F). In the second test, surface ignition occurred on the east wall 9 minutes after the wood crib, representing the combustible contents of the room, was ignited. No significant changes were observed on the west wall during either test.

The instantaneous heat flux incident on the east wall just prior to ignition and the total heat energy absorbed were estimated to be on the order of 1.0 W/cm^2 and 175 Joules/cm^2 respectively.

Sparks, L. L., Powell, R. L., **Calibration of capsule platinum resistance thermometers at the triple point of water,** (Proc. 5th Symp. on Temperature, Its Measurement and Control in Science and Industry, Washington, D.C., June 21-24, 1971), Paper in *Temperature, Its Measurement and Control in Science and Industry,* H. H. Plumb, Editor-in-Chief, **4,** Part 2, 1415-1421 (Instrument Society of America, Pittsburgh, Pa., 1972).

Key words: Resistance thermometers; temperature measuring instruments; triple point; water.

Temperature determinations by means of a platinum resistance thermometer, both above and below the triple point temperature of water, depend upon an accurate value for the resistance at the triple point, 0.01 °C. A good general methodology for making such a determination was described by H. F. Stimson at the 1955 Temperature Symposium. However, several aspects of the method must be refined or modified for accurate measurements on capsule thermometers. After a series of development tests, we were able to isolate and correct for several types of systematic experimental errors that were significant, but not immediately obvious. Some of the effects that must be carefully controlled in order to guarantee high precision are (1) thermal resistance between the thermometer and the freezing interface; (2) thermal conductance down to the thermometer from the ambient environment; (3) high-resistance electrical leakage between leads in the heat exchange fluid; and (4) freezing conditions in the triple point cell itself. Using the procedures developed during the test program, we have been able to obtain reproducibilities and statistical imprecisions of about 10 $\mu\Omega$ or 100 μK.

Spurgeon, J. C., **Response characteristics of a portable x-ray fluorescence lead detector: Detection of lead in paint,** *NBSIR 73-231,* 37 pages (June 1973). (Available as PB 224645 from the National Technical Information Service, Springfield, Va. 22151.)

Key words: Lead paint detection; portable x-ray fluorescence lead detector; portable x-ray fluorescence lead calibration standards.

The objective of this investigation was to obtain an indication of the validity of the field data resulting from the use of portable x-ray fluorescence lead detectors by local lead paint detection programs. This report is intended to provide guidance in the use of portable x-ray fluroescence lead detectors by housing and/or health authorities who are responsible for the collection and interpretation of field data as part of lead paint control programs.

The response characteristics of such an instrument to conditions that are related to those encountered in the field have been investigated and the results are presented in this report. The effects of calibration standards, state of charge, paint overlayers, substrate, and distance on instrument response are discussed, in addition to the limit of detection and precision. The accomplishment of these tasks required the development of panel-type lead calibration standard. These standards encompass the concentration range from 0.1 mg/cm^2 to 9.0 mg/cm^2.

Stabler, T. M., **National program of metrology for Ecuador,** *NBSIR 73-157*, 33 pages (Apr. 1973). (Available as COM 74–10394 from the National Technical Information Service, Springfield, Va. 22151.)

Key words: Calibration and testing; Ecuadorian Institute of Standardization (INEN); field inspections; mass, length, and volume standards; metrology laboratory; model law and regulations; technical education; U.S. AID.

At the request of the Ecuadorian Institute of Standardization (INEN) the U.S. AID made arrangements for a weights and measures advisor to assist in the development of a program for scientific and legal metrology, including the design of a metrology laboratory, inspection system, a training program, and other essential features. A four week survey by an NBS representative has resulted in recommendations for a metrology laboratory, physical standards, an Ecuadorian weights and measures law, regulations, and control program.

Considered also were the Ecuadorian National Standards of mass, length, and volume; precision balances, and other laboratory instruments. A program of technical education was recommended for an INEN engineer (Program Administrator) and for other members of the INEN laboratory staff.

Stephenson, J. C., **Vibrational energy transfer in NO,** *J. Chem. Phys.* **59,** No. 3, 1523-1527 (Aug. 1, 1973).

Key words: Infrared lasers; laser pumping of molecules; nitric oxide; vibrational energy transfer.

Laser-excited vibrational fluorescence measurements have been used to obtain rate constants at room temperature for vibrational relaxation of the $V = 1$ state of NO in collisions with He, Ar, H_2, CO, NO, N_2, and CO_2. Pulses from a CO_2 laser, frequency doubled in a tellurium crystal, provided the excitation source. The rate for the $V - V$ exchange NO(1) + NO(1) → NO(0) + NO(2) was obtained.

Stillman, R. B., **The concept of weak substitution in theorem-proving,** *J. Ass. Comput. Mach.* **20,** No. 4, 648-667 (Oct. 1973).

Key words: Associative processing; first-order predicate calculus; resolution; subsumption; theorem-proving; unification.

Many of the centrally important predicates which occur within theorem-proving programs involve, in their computation, a subcalculation aimed at determining whether or not a substitution exists satisfying certain constraints. Some of the principal difficulties in achieving efficient theorem-proving programs are traceable to the amount of computation required by this "substitution-existence analysis." In this investigation, the concept of "weak substitution" is introduced and its utility and applicability in the subsumption and unification computations are examined. The main motivation for considering weak substitutions is this: the existence of a *weak* substitution having certain properties is relatively easy to detect, whereas the existence of a substitution proper having the same properties is not. Furthermore, the absence of such a weak substitution is a sufficient condition for the absence of the substitution proper. Using the concept of weak substitution, a particularly efficient implementation of the subsumption and unification computations on an associative processor is presented.

Straty, G. C., Younglove, B. A., **Some sound velocity measurements on liquid fluorine,** *J. Chem. Phys.* **58,** No. 5, 2191-2192 (Mar. 1, 1973).

Key words: Compressed liquid; fluorine; saturated liquid; sound velocity.

Some sound velocity measurements on liquid fluorine at 110 K and 130 K at pressures to 21 MN/m^2 are reported. Data were acquired prior to a destructive reaction in the cell which prevented further measurements.

Sugar, J., Reader, J., **Ionization energies of doubly and triply ionized rare earths,** *J. Chem. Phys.* **59,** No. 4, 2083-2089 (Aug. 15, 1973).

Key words: Cerium; dysprosium; erbium; europium; gadolinium; hafnium; holmium; ionization energy; lanthanum; lutetium; neodymium; praseodymium; promethium; samarium; terbium; thulium; ytterbium.

Values for the ionization energies of the doubly and triply ionized rare earth atoms have been derived from interpolated spectroscopic properties of the $4f^N ns$ series, and from interpolated energy intervals relating the first series member, $4f^N 6s$, to the ground state. The results in eV are

La III	19.1774(6)	
Ce	20.198(3)	IV 36.758(5)
Pr	21.624(3)	38.98(2)
Nd	22.14(30)	40.41(20)
Pm	22.32(36)	41.09(32)
Sm	23.43(30)	41.37(38)
Eu	24.70(32)	42.65(32)
Gd	20.63(10)	44.01(35)
Tb III	21.91(10)	IV 39.79(20)
Dy	22.79(30)	41.47(20)
Ho	22.84(10)	42.48(32)
Er	22.74(10)	42.65(21)
Tm	23.68(10)	42.69(20)
Yb	25.03(2)	43.74(20)
Lu	20.9596(10)	45.19(2)
Hf		33.33(2)

The values for the doubly ionized atoms agree to within ~ 1 percent with those deduced from thermodynamic measurements on lanthanide oxides. A value for the ionization energy of Gd II of 12.09(8) eV was determined by using new spectroscopic data for Gd II Gd III.

Trechsel, H. R., **Swiss building and housing research activities,** *NBSIR 73-288*, 63 pages (Aug. 1973). (Available as COM73-11861 from the National Technical Information Service, Springfield, Va. 22151.)

Key words: Building research; buildings; cooperation; housing; international; Switzerland.

Following up earlier contacts of CBT management with representatives of Swiss building research organizations, the author visited Switzerland in the Fall of 1972 for two weeks.

This report discusses the results of meetings with representatives of the Swiss Federal Commission for Housing Research (FKW), major educational and research establishments, architects, contractors, builders, and local building officials. Topics covered in the

discussions included building economics, modular coordination, pre-evaluation of performance of housing projects, pre-evaluation of research projects, building design, land use and planning, transportation, and building laws, codes, and standards.

It appears that cooperative programs in any or all of these areas could be profitable to NBS, and to the corresponding Swiss organizations.

Treu, S., **Characterization and testing of interactive graphics for computer-aided design and engineering,** *NBSIR 73-289*, 36 pages (June 30, 1973). (Available as COM 74–10475 from the National Technical Information Service, Springfield, Va. 22151.)

Key words: Characteristics; computer-aided design; interactive graphics; man-machine interaction; performance measurement.

This report presents material developed as part of a long-term "Interactive Computer-Aided Techniques Study." The report outlines the stages of development in the utilization of interactive graphics as a tool for Computer-Aided Design and Engineering (CAD/E). A series of characteristics are presented which are of significance to the designers and users of such systems and a series of questions of evaluative interest posed. These questions are intended to delineate the extent to which a system under examination achieves its stated design objectives. The characteristics are grouped in accordance with the nature and complexity of the experiments which would need to be conducted to establish values for them. The report suggests selected characteristics of particular interest and suggests the design of experiments for examining them in detail. The report makes specific reference to the MEDEA design terminal concept under development within the Graphical Systems and Technology Branch of ECOM.

Verdier, P. H., **Fluctuations in autocorrelation functions in diffusing systems,** Chapter in *Stochastic Processes in Chemical Physics*, K. E. Shuler, Ed., **15,** 137-148 (John Wiley & Sons, Inc., New York, N.Y. 1969).

Key words: Autocorrelation; correlation; diffusion; fluctuations; relaxation; time correlation.

The relative rates of relaxation of the autocorrelation function and the fluctuations in its sampled values are derived for several simple diffusing systems. It is found that in general, the autocorrelation function and its fluctuations relax at rates which are different, but of the same order of magnitude. In the cases studied, the ratio of the relaxation time for the fluctuations to that for the autocorrelation function varies from about 1/2 to about 1 1/6.

Waterstrat, R. M., Manuszewski, R. C., **The chromium-iridium constitution diagram,** *J. Less-Common Metals* **32,** 79-89 (1973).

Key words: Chromium alloys; constitution diagram; equilibrium diagram; iridium alloys; phase diagram.

The Cr-Ir alloy system has been investigated over the entire composition range by metallography, x-ray diffraction and electron microprobe studies. There are two intermediate phases in this system. The β phase possesses a Cr_3Si ($A15$)-type crystal structure and is stable from about 73 to 82 at.% Cr. The ϵ phase has a hexagonal close-packed crystal structure and is stable between 30 and 68 at.% Cr. The face-centered cubic iridium terminal solid solution can dissolve about 28 at.% Cr. Atomic ordering occurs within this solid solution, beginning at about 16 at.% Cr and forming a Cu_3Au type structure up to the limit of solid solubility. Iridium is soluble in the body-centered cubic chromium terminal solid solution to the extent of about 12 at.% Ir at 1680 °C but the solubility decreases at lower temperatures. Two peritectic reactions were observed at 1750 ± 10 °C and at 2200 ± 50 °C. A eutectic reaction is indicated at 1680 ± 10 °C.

Waterstrat, R. M., **The chromium-platinum constitution diagram,** *Met. Trans.* **4,** 1585-1592 (June 1973).

Key words: Alloys; chromium; constitution diagram; equilibrium diagram; phase diagram; platinum.

The system Cr-Pt has been investigated over the entire composition range by metallography, x-ray diffraction, and electron microprobe studies. There is only one intermediate phase and it has a Cr_3Si(A15)-type crystal structure. The fcc platinum terminal solid solution extends to 71 at.pct Cr at 1530 °C and forms a congruent melting maximum at about 1790 °C. Atomic ordering within this solid solution range begins at about 17 at.pct Cr and there is a continuous change from the Cu_3Au-type structure to the CuAu-type structure with increasing chromium content. Two eutectic reactions at 1530 ± 10 °C and 1500 ± 10 °C were indicated and there is evidence of a syntectic reaction at 1580 ± 10 °C. Platinum is soluble in the bcc chromium terminal solid solution up to about 10 at.pct Pt at 1500 °C but the solubility decreases rapidly at lower temperatures.

Wiederhorn, S. M., **Environmental stress corrosion cracking of glass,** (Proc. Int. Conf. on Corrosion Fatigue, Chemistry, Mechanics and Microstructure, University of Connecticut, Storrs, Conn., June 14-18, 1971), Paper in *Corrosion Fatigue*, **NACE-2,** 731-742 (National Association of Corrosion Engineers, Houston, Texas, 1972).

Key words: Cracked propagation of glass; glass; glass fibers; hardness of glass; static fatigue of glass; strength of glass; stress corrosion cracking of glass; structure of glass.

A review is presented on the effect of environment on the strength of glass. The structure of glass and its strength in the absence of environment are discussed briefly. Experimental results on environmental cracking of glass are presented. Finally, theroretical treatments are given and discussed with respect to available experimental data.

Woolley, M. L., **Bibliography of the electromagnetics division June 30, 1972 to June 30, 1973,** *NBSIR 73-320*, 22 pages (June 1973). (Available as COM73–11971 from the National Technical Information Service, Springfield, Va. 22151.)

Key words: Antenna parameters; attenuation; current; electromagnetic measurements; field strength; impedance; waveguide theory.

This bibliography lists the publications of the NBS Electromagnetics Division between June 30, 1972 and June 30, 1973.

Wyly, R. S., Rorrer, D. E., **Field test of hydraulic performance of a single-stack drainage system at the operation BREAKTHROUGH prototype site in King County, Washington,** *NBSIR 73-161*, 66 pages (May 1973). (Available as PB225–310 from the National Technical Information Service, Springfield, Va. 22151.)

Key words: Crossflow; field testing, plumbing; performance criteria, plumbing; performance, functional; single-stack drainage; siphonage, induced; siphonage, self; test loads, hydraulic; trap-seal reduction detector; trap-seal retention.

A procedure for measuring the hydraulic performance of drain-waste-vent (DWV) systems in the field is described, and the results obtained with this procedure in a field demonstration of the hydraulic performance of a single-stack DWV system are presented.

Among the most important criteria for hydraulic performance of drain-waste-vent systems are the following: (1) Trap-seal retention in idle fixtures; (2) Ability of the system to resist the rejection of suds, sewage, or foul gases due to hydrostatic or pneumatic pressures in the DWV system; (3) Absence of cross flow between fixtures; (4) Absence of self-siphonage in the individual fixture traps.

Considering the needs for minimization of maintenance in service and for the continuation of venting during cold weather, the following additional criteria can be identified: (5) Ability to maintain adequate

hydraulic performance over a long period of service without excessive maintenance of branch piping; (6) Adequacy of performance under climatic conditions conducive to frost closure of vent terminals.

The procedures for selection and application of hydraulic loads, based on state-of-the-art guidelines, are described as applied to the soil and waste stacks evaluated for conformance to criteria (1) through (4) above.

The results show adequate performance in relation to criteria (1) through (4), with a single example of non-conformance on criterion (3), subject to the limiting condition that some uncertainty exists as to the degree of leak resistance of the DWV systems made available for the tests.

Recommendations are offered concerning further work that could provide information to confirm estimated conformance to criteria (5) and (6).

Yates, J. T., Jr., Madey, T. E., Dresser, M. J., **Adsorption and decomposition of formaldehyde on tungsten (100) and (111) crystal planes,** *J. Catal.* **30,** No. 2, 260-275 (Aug. 1973).

Key words: Carbon dioxide; catalytic; chemisorption; decomposition; formaldehyde; methane; tungsten.

The chemisorption of formaldehyde at ~ 100 K has been investigated on two single crystal planes of tungsten, W(100) and W(111). At low H_2CO coverages, only H_2 and CO are observed as thermal desorption products. At higher H_2CO coverages both CH_4 and CO_2 are observed as additional desorption products. Work function and flash desorption measurements indicate that the dissociative adsorption of H_2CO into H(ads) and CO(ads) is accompanied at higher surface coverages by the formation of other surface complexes.

A detailed comparison of W(100) with W(111) indicates that crystallographic differences play a minor role in the surface catalyzed decomposition of H_2CO by tungsten.